SUBSIDENCE-UPLIFT HISTORY AND PETROLEUM SOURCE ROCK STUDY OF CENOZOIC FORELAND BASIN OF NW HIMALAYA, H.P., INDIA

A THESIS

Submitted in fulfilment of the requirements for the award of the degree of

DOCTOR OF PHILOSOPHY

in

EARTH SCIENCES

By

BAHMAN SOLEIMANI

DEPARTMENT OF EARTH SCIENCES
UNIVERSITY OF ROORKEE
ROORKEE–247 667 (INDIA)

MARCH, 1999

Gratis.

CANDIDATE'S DECLARATION

I hereby certify that the work which is being presented in the thesis entitled **"Subsidence-Uplift History and Petroleum Source Rock Study of Cenozoic Foreland Basin of NW Himalaya, H. P., INDIA"** in fulfilment of the requirement for the award of the degree of Doctor of Philosophy and submitted in the Department of Earth Sciences of the University of Roorkee is an authentic record of my own work carried out during a period from November, 1994 to March, 1999 under the supervision of Prof. A. K. Awasthi, Prof. A. K. Jain and Prof. Nand Lal.

The matter presented in this thesis has not been submitted by me for the award of any other degree of this or any other University.

B. Soleimani
Signature of the Candidate

This is to certify that the above statement made by the candidate is correct to the best of my (our) knowledge.

Date: March, 12 , 1999

Supervisors

Dr. Nand Lal	**Dr. A. K. Jain**	**Dr. A. K. Awasthi** 12/3/99
Professor of Geophysics	Professor of Geology	Professor of Geology
Deptt. of Earth Sciences	Deptt. of Earth Sciences	Deptt. of Earth Sciences
Univ. of Kurukshetra	Univ. of Roorkee	Univ. of Roorkee
KURUKSHETRA	ROORKEE	ROORKEE

The Ph.D. Viva-Voce Examination of ..Sri. B. Soleimani....., Research Scholar, has been held on ..11.10.1999.....

Signature of Supervisors 11/10/99 Signature of H.O.D. 11/10/99 Signature of External Examiner

Lal
11.10.99

Ajain 11/10/99

ACKNOWLEDGMENTS

I wish to express my heartfelt gratitude to my supervisors Prof. A. K. Awasthi, Prof. A. K. Jain, and Prof. Nand Lal for their valuable guidance throughout the course of this work. Without their encouragements, guidance and constructive criticisms, it would not have been possible for me to complete this thesis. I owe them my sincere gratitude. Finally, special thanks are to Prof. A. K. Awasthi, Head, Earth Sciences Department, University of Roorkee, for extending all facilities.

The assistance of faculty members, other staff and specially Dr. Surya Parkash, teachers of Earth Sciences Department, University of Roorkee, in the completion of this work is sincerely acknowledged.

I have to thank to Prof. K. Chandra, Director University Science Instruments Center (U.S.I.C.), Roorkee University for his cooperation in the results of X-Ray diffractograms of clay minerals slides.

I express my thanks to Dr. Ashok Kumar, and Mr. Devender Kumar (research scholar) and all teachers of Departments of Earth Sciences and Physics, Kurukshetra University, Kurukshetra for their help while working in the laboratory of fission track dating, and also to the Head, Geology Department, Kurukshetra University for allowing the use of the counting digital instrument for petrographic modal analysis.

I am extremely thankful to Mr. K. Chandra, Director, Keshav Dev Malviya (KDM) Institute of Petroleum Exploration, Dehra Dun, for the permission to avail the laboratory and library facilities and the helps provided by Dr. U. Samanta and Mr. V.N. Sharma to measure the Vitrinite Reflectance and Mrs. Thomas for help in measuring the Total Organic Carbon (TOC).

My sincere thanks are to the Indian Council of Cultural Relations (I.C.C.R.), New Delhi, to give permission, admission and also the scholarship and also to the Iran Government and Shahid Chamran University, Ahwaz, which allowed and sponsored me.

Lastly, indeed I am short of words to express my gratitude to my parents, my wife, Fereshteh, and daughters and son who could not receive my full attention due to my extensive involvement with this thesis.

Bahman Soleimani

March - 1999

ABSTRACT

The Sub-Himalayan Cenozoic foreland basin is one of the youngest features in the evolutionary history of this mountain running as foothill belt along the southernmost parts of the Himalaya. The Cenozoic sediments of the Himalayan foothills have been target area for oil exploration for more than a decade. Subsidence-uplift history of the basin affects the thermal maturation of organic matter to generate petroleum. The Cenozoic sediments occurring to the south of Main Boundary Thrust (MBT) were subjected to the present study. These sediments belong to the Early Cenozoic (Subathu, Dagshai, and Kasauli formations) and the Late Cenozoic Lower Siwalik Formation.

The Subathu Formation (Paleocene-Late Eocene) forms 1500 m thick sequence of sedimentary rocks dominated by shale, siltstone and limestone with minor intraformational conglomerate, quartz arenite, and arenites. Shale/siltstone sequence of the Subathu Formation breaks into lead pencil-type fragments. The Subathu sediments are deposited in a shallow marine environment at around 60 to 40 Ma. The contact between the Subathu and pre-Cenozoic rocks is a disconformity. The transition between the Subathu and the Dagshai formations may seem to be abrupt. Subathu is overlain by the Dagshai Formation (Late Eocene – Early Oligocene) which consists of 600 m thick sequence of gray and purple claystone/shale alternating with the fine grained, greenish, hard, impure sandstone. The Dagshai sediments are deposited in brackish, fresh water or distal alluvial fan and fluvial system. The deposition time of the Dagshai is ~30 Ma to 24 Ma. The overlying Kasauli Formation (Middle Oligocene – Early Miocene) is marked by 2100 m thick sediments characterized by massive pale gray to buff coloured micaceous sandstone alternating with the purple and gray shale. The lower contact of the Kasauli with the Dagshai is transitional, but the upper contact with the Lower Siwalik is a thrust. The Kasauli sediments are deposited in alluvial fan or fresh water at 23.8 Ma. The Kasauli Formation is overlain by the Lower Siwalik (Middle Miocene) Formation comprising 1700 m thick sequence of alternating sandstone-shale/ siltstone with minor amount of conglomerate. The Lower Siwalik Formation was deposited in alluvial plains in dry and wet seasons. Its depositional age is ca. 15

to 10 Ma. The paleocurrent patterns of the pre-Siwalik and the Lower Siwalik rocks are from north to south.

The Main Boundary Thrust has played important role in juxtapositioning of different older stratigraphic horizons and tectonic units with the Siwalik Group. Its activity started in Middle Miocene time (15-10 Ma) and reached its peak activity around 4-5 Ma.

Sandstone and shale samples were collected from stratigraphic sections of the Subathu, Dagshai, Kasauli and Lower Siwalik formations along different traverses in areas of Nahan-Sarahan, Kalka-Kasauli-Dharampur, Dharampur-Subathu, Dharampur-Kumarhatti and Kumarhatti-Solan of the foothills of the Himachal Pradesh (H.P.). The samples thus collected, were analysed for petrography, illite crystallinity, fission track analysis, total organic carbon (T.O.C.), vitrinite reflectance (VR_o), rock eval analysis and hydrogen indices etc. with a view to decipher the **subsidence-uplift history and the source rock evaluation** of these Cenozoic sediments for petroleum.

The modal analysis of sandstone samples when plotted on QFL are classified as quartzite–sublitharenite, sublitharenite-litharenite from the Subathu to Dagshai respectively, and litharenite for the Kasauli and Lower Siwalik formations. However, considering framework constituents and matrix classification (Pettijohn, 1975), sandstone samples may be classified as: quartz arenite, sublitharenite (Subathu), lithic graywacke (Dagshai), lithic graywacke and litharenite (Kasauli and Lower Siwalik formations). The petrographic studies also indicate that the sandstones of the various formations exhibit a vertical upward discernable pattern in these compositions. These upward patterns are (a) decrease in the amount of monocrystalline quartz, (b) increase though small of detrital feldspar and polycrystalline quartz %, (c) increase of lithic constituents (metamorphic, igneous and sedimentary), and (d) increase in higher grade metamorphic rock fragments. The QFL plot also suggests **recycled orogenic provenance** for these sediments. The paleocurrent patterns of pre-Siwalik and the Lower Siwalik rocks are mainly from north to south. In the early stage of continental collision, the detritus was largely derived from sedimentary and very low grade metamorphic rocks from the proto-Himalaya supracrustal Indian margin rocks which are mainly Late Proterozoic to Cambrian pelitic rocks. Towards the late stages of Cenozoic deposition, the diversity of source rocks is observed.

Lack of wackes in Subathu Formation indicates relatively quiet tectonic conditions with very low rate of erosion and uplift. After Subathu time, in younger rocks, continual increase in lithic fragments in the sandstones suggests relatively higher uplift rate.

The **X-ray** studies indicate that the dominant clay minerals in shales and matrix of sandstones are illite, kaolinite, mixed layer, chlorite, vermiculite and montmorillonite in order of decreasing abundance. The crystallinity of illite decreases with younging of sediments. The relation of sharpness ratio and crystallinity index (C.I) in pre-Siwalik and Lower Siwalik sediments is uniform and linear. The mean 2θ values of C.I. showed that the Subathu (0.37) and Dagshai (0.42) formations are both at the same stage of "late diagenesis", the Kasauli Formation (0.44) is at the "lower stage of middle diagenesis", and the Lower Siwalik Formation (0.53) is at the "middle stage" of diagenesis.

The most dominant clay minerals in the shale and matrix of sandstone samples are illite, kaolinite, mixed-layer, chlorite, vermiculite and montmorillonite in decreasing order of abundance. The illite peaks are sharp and well defined. The percentage of illite varies from 50 to 82 in Subathu, 73 to 99 in Dagshai, 77 to 89 in Kasauli and 67 to 70 in the Lower Siwalik shales. The percentage of kaolinite varies from 14 to 28% in Subathu, 8 to 26% in Dagshai, 6 to 19% in Kasauli and 24 to 28% in the Lower Siwalik shale samples. The percentage of chlorite in shales ranges from 20 to 30% in Subathu, 1 to 7% in Dagshai, 4 to 6% in Kasauli formations. The montmorillonite percentage is very less (<9.5) and is found only in the younger sediments. The clay matrix of sandstone samples shows variations similar to those found in shale samples. The mean illite intensity ratio (0.7 to 0.4) from Subathu to Lower Siwalik formations generally shows little recrystallization of illite.

The **zircon Fission Tracks (FT)** in all Cenozoic sediments have very wide age range with Gaussian peak width "W" more than 18 and thus suggest that (a) the FT in zircon grains are unreset, implying thereby that the FT in the zircon grains could not have been annealed and FT ages reveal exhumation ages of the provenance, and (b) the zircon grains were **derived from multi FT sources**. The FT ages of zircon grains range from 557 to 42 Ma for Subathu; 515-16 Ma for Dagshai; 529-12Ma for Kasauli, and 363-9 Ma for Lower Siwalik sediments.

The Cenozoic sediments have a wide distribution in zircon FT ages, and the distribution of peak widths (W≥19) is higher than that of reference sample (Fish Canyon, W=16). Thus, fission tracks in zircon grains of all samples are unreset. However, the FT in **apatite** grains are reset.

The χ^2-ages from clubbed samples of the Subathu, Dagshai, Kasauli, and the Lower Siwalik formations are 58.8, 26.2, 22.2-14.2 and 9.7 Ma respectively. The lag time between χ^2-ages and independently-determined depositional age is less than 5 Ma between cooling age of the youngest zircons and depositional time. The detected Gaussian peaks in all these formations show shifting towards younger ages indicating more and more contributions from younger sources of sediments.

The source area for the zircon grains, based on paleocurrent directions, appears to be north and northeastern Himalayan terrains. The distribution of zircon FT dates indicates Paleozoic and Mesozoic sediments/igneous rocks as source of sediments to the Himalayan foreland basin. The first indicator of Cenozoic Himalayan orogeny is identified in the Middle Subathu around 40.7 Ma.

Based on fission tracks (FT) in zircon grains the upper limit of depositional ages as estimated by youngest Gaussian peak age of individual formation are: Subathu ca. 39.1 Ma, Dagshai ca. 25.1 Ma, Kasauli ca. 25.2-15.2 Ma, and Lower Siwalik ca. 14.6 Ma. These ages are consistent with the ages determined by biostratigraphy (Arya, 1998), magnetostratigraphy (Sangode, 1997) and argon-argon methods (Najman, 1997; Harrison, 1992).

On applying the Gaussian Best Fit method on clubbed (bulk) samples of each formation, it is found that the percentage of grains of old FT ages continually decreases upward and the younger FT ages continually increases upward from the oldest Subathu Formation to Lower Siwalik Formation. This indicates continual rising up of the source (Himalaya) which contributed sediments to this Cenozoic foreland basin. The oldest age peaks are mostly characterized as static type in all the formations. The possible source area for the static peaks is unreset and / or reset terrains located on the northern side of the Cenozoic belt with the low rate of uplift. The absence of regular pattern in the age distribution of relatively younger age peaks may be related to the recycling of sediments which is also corroborated by petrographic

evidences in the form of sedimentary lithics, abraded quartz overgrowth and rounded zircon, tourmaline and garnet found in these sediments. These two types of peaks and "wide distribution" of FT ages in zircon grains in various formations of Cenozoic sediments show that the uplift rate in the provenance was not uniform .

Petroleum hydrocarbons are generated by the thermal degradation of sedimentary organic matter in the temperature limit of about 60°–180° C. The peak oil generation takes place at temperature of the order of 120° C. It is important to note the preserved fission tracks in apatite grains indicate that these sediments have attained temperatures required for generation of petroleum hydrocarbon. In view of this, petroleum source rock studies were conducted to estimate abundance of organic matter in terms of Total Organic Carbon (TOC) content, quality of organic matter in terms of type of kerogen and the thermal maturation of organic matter to generate the hydrocarbons. The TOC in shales varies from 0.09% to 0.3% (mean 0.2%) in the Subathu Formation, 0.07% to 0.37% (mean 0.15%) in the Dagshai Formation, 0.09% to 0.6% (mean 0.2%) in the Kasauli Formation and 0.06% to 0.17% (mean 0.1%) in the Lower Siwalik Formation. The kerogen is mainly of type III with major terrestrial component. This type of kerogen, which is prone to generate mainly gas but little oil, is found in all formations. The mean values of vitrinite reflectance (VR_o) are 1.2% for Subathu, 0.9% for Dagshai, 0.7% for Kasauli and 0.8% for the Lower Siwalik formations, indicating thereby that organic matter is matured to various levels to generate petroleum hydrocarbons.

Based on fission track analysis, illite crystallinity indices and vitrinite reflectance the maximum paleotemperature of various Cenozoic formations are estimated to be 100–120°C (110°C) for Lower Siwalik, 120-130°C (125°C) for Kasauli, 130–140°C (135°C) for Dagshai and 140–160°C (150°C) for Subathu formations.

Analysis of fission tracks on zircon using External Detector Method (EDM) indicates that sediments of all the formations of the Cenozoic foreland basin have not **subsided** to the depth level corresponding to the closure temperature of fission tracks in zircon (240±25°C). The basin subsided maximally to the depth level corresponding to temperatures of the order of 160° C. The fission tracks preserved in the apatite grains in the sandstone of various formations appear to be

reset. This resetting is also indicated by the ages of FT in apatite, which are younger to their depositional ages (8 Ma in Dagshai, 13 Ma in Kasauli and 10 Ma in Lower Siwalik Formations).

Spatially and temporally, the rate of subsidence in all parts of the foreland Cenozoic basin has not been uniform. Subsidence history shows breaks (40-30 Ma and 6.5-5 Ma) in the continuous trend in the region of Surinsar, Jammu hills.

The present data indicate that the Kasauli sediments exhumed 1 km before 13 Ma. The Dagshai sediments were exhumed at least 0.5 km since 13 to 8 Ma, i.e. 0.1 km/Ma. The exhumation of sediments in the foreland basin is estimated to be about 2.5 to 3.0 km in the present area, i.e. 0.3-0.4 km/Ma since 8 Ma to present time. Thus, the total exhumation of the sediments is around 4.0-4.5 km since the beginning of exhumation. Thus, the rate of exhumation of foreland sediments from early to end of Middle Miocene (from 13-8 Ma) is very low (0.1 km/Ma) but from the Upper Miocene to present is high (~0.3-0.4 km/Ma).

The history of the northern margin of the foreland basin may be different from the southern part. The northern margin of foreland basin between Nahan Thrust and MBT started uplifting, due to MBT activation >13 Ma ago according to apatite FT results, and contributed detritus for the younger sediments as additional source.

The subsidence curve of the Subathu sediments indicates that they are within petroleum "window zone" stage of maturation. The petroleum hydrocarbon generation started at ~25 Ma (Middle Miocene) when the Subathu reached a burial depth of ~2500 m and continued till to about 13 Ma back when these sediments reached a depth ~4500 m, i.e. the time of inception of *uplift*. For all formations, the hydrogen indices (HI) are below ~150 mg CO_2/gTOC, indicating low prospects of liquid hydrocarbon. The Subathu shales with the VR_o%~1.2 and T_{max}>470°C indicates late stage of metagenesis; the Dagshai Formation with the VR_o%~ 1 and T_{max} of 450° C and the Kasauli (Murree) sediments with the VR_o%~ 0.9 and T_{max} between 450°-430°C indicate initial to middle stage (catagenetic) of maturation of organic matter; and the Lower Siwalik Formation with the VR_o%~ 0.8 and T_{max} 445° C indicates that it is in the gas stage catagenetic maturation to generate petroleum hydrocarbons. These results indicate that the shales of the Cenozoic sediments are matured enough to generate petroleum hydrocarbons. The kerogen type-III indicates that the principal organic matter is prone to gas generation. The source rock of

the Cenozoic sediments is, thus, matured to generate mainly gas. These results are supported by the gas seepage and live oil shows in the Siwalik foreland basin. However, since the TOC is generally less than 0.5%, the chance of generation of commercial quantities of petroleum hydrocarbons is less, and it is important to note in this regard that the exploration efforts of Oil and Natural Corporation during the past have not met with success as yet.

CONTENTS

Chapter-3 Petrographic studies

Chapter 4-Himalayan foreland basin: Application of fission track dating

List of Figures

List of Tables

CHAPTER- 1

INTRODUCTION

1.1 PREAMBLE

The Himalaya has always been considered as the highest and youngest mountain range. Its evolutionary history started since Early Cenozoic time. At that time the oceanic lithosphere (Neo-Tethys), which was a part of the Indian Plate, was being subducted beneath the southern margin of Eurasian plate (Condie, 1997). In fact, the presence of ophiolitic belt in the Himalayan range corresponds to an Andean subduction environment, which has occurred ~ 55 Ma ago. The collision caused vigorous changes in the structural features of the Himalaya. The occurrence of different tectonic trends and change of tectonic activity from north to south through time are the crucial results of the collision (Misra, 1979; Valdiya, 1979 a, b; Searle et al., 1987). This collision is still active today (Edelman, 1991), thus indicating that the Himalaya is very unstable belt and still rising. One of the important features produced by the collision process is the Cenozoic foreland basin in the southernmost parts of the Himalaya. Study of paleohistory of sediments of this basin in terms of their petrography, fission track study and organic matter maturity is important to understand the thermal history, subsidence /uplift and petroleum prospects of this basin.

The Cenozoic sedimentary basin of the Northwestern Indian Himalaya includes outer foothill belt of Jammu, Himachal Pradesh (H. P.), Uttar Pradesh (U. P.) and the adjoining Indo-Gangetic Plains. The foothills extend from Nainital (29°N, 80°E) through Mandi (31°43′N, 76°56′E) to west of Muzafarabad (34°30′N, 73°27′E) and continue further to the west in Pakistan (Fig. 1.1). It covers an area of ~40,000 km^2 and occurs as a belt which is ~800 km long and ~20-100 km wide. Geographically, it extends from the Jhelum river in the west to Sapt Kosi river in the east. Tectonically, the basin is bounded by the Delhi-Sargodha subsurface ridge in the west and by the Monghyr-Saharsa ridge in the east, which are the extensions of the Indian Peninsular shield. The northern limit of this basin is approximately marked by the Main Boundary Thrust

(MBT), which separates the Cenozoic from the pre-Cenozoic outcrops. Therefore, this belt within the *Sub-Himalaya* of the Cenozoic sedimentary zone is made up of the early Cenozoic Subathu, Dagshai, Kasauli (Murree) formations and the late Cenozoic-Quaternary Siwalik Group. The thickness of sediments of pre-Siwalik Group is estimated ~6000m (Raiverman, 1964) and that of the Siwalik Group is ~ 6000 m (Tripathi and Saxena, 1987). As almost all the sedimentary components of the Sub-Himalayan belt are derived from the rising Himalaya, it is important to discuss them.

Lesser Himalaya: The Lesser Himalaya consists of a thick continental margin deltaic and turbiditic prism (Brookfield, 1986) of late Precambrian. This unit is tangled confusion of stratigraphy and structure (Valdiya, 1980). The large part of this old and geomorphically mature zone is made up of the Riphean sedimentaries occurring in the lowest structural level. In the central sector, they are tightly folded and repeatedly faulted, and have been thrust southward over the Siwalik zone. Divisible into three litho-stratigraphic formations, the succession begins with a flysch and flyschoid assemblage known as the Sundernagar Formation in Himachal, the Rautgara in Kumaun, the Kunchha in Nepal, the Sinchula-Jainti in Sikkim, the Phuntsholing in Bhutan and Bichom in western Arunachal. The flyschoid sediments are normally succeeded by the Middle Riphean stromatolitic-carbonates designated the Jammu (=Sirban =Great) Limestone in the northwestern sector, the Shali in Himachal, the Deoban in Kumaun, the Buxa in Bhutan and the Dedza in western Arunachal. The carbonates grade into an argillocalcareous assemblage called the Basantpur in Himachal, the Mandhali in Kumaun and the Saleri in Arunachal.

The autchthonous Precambrian sediments are overlain by a succession of three large thrust sheets, made up of Paleozoic sediments, epimetamorphic and mesometamorphic crystallines, respectively. In the extreme southern belt the Precambrian sediments are overthrust by a thick succession of Paleozoic sedimentary rocks divisible into the Mandhali, Chandpur (flysch), Nagthat (quartzarenite with contemporaneous basic volcanics), Blaini (flyschoid assemblage with diamictites), Krol (carbonates) and Tal (diamictites, phosphatic rocks, sandstones and limestones). The Tal is locally capped by the Subathu of lower Eocene age. Constituting the Krol nappe unit and confined in the very southern belt in the central sector, this

Krol nappe unit is represented in the eastern Himalaya by a narrow strip of the Gondwana rocks (Valdiya, 1980).

Epimetamorphic rocks, with characteristically sheared and mylonitized porphyroids throughout, have been thrust over the sedimentaries, Precambrian of Paleozoic, known as the Chail in Himachal. These rocks (Table 1.1) extended eastward as the Ramgarh sheet in Kumaun, the Lower Midland Formation in western Nepal, the Daling in the Sikkim Himalaya, the Samchi or Shumar in Bhutan and the Tenga in western Arunachal Pradesh.

The uppermost thrust sheet is made up of medium–grade metamorphics intruded by granite-granodiorite of the trondhjemitic suite. This unit is called the Salkhala in Kashmir, the Jutogh in Himachal, the Munsiari-Almora (the former being the root of the later) in Kumaun, the Upper Midland Formation in west Nepal, the Kathmundu in central and east Nepal, the Paro in the Sikkim Himalaya and the Bomdila in Arunachal. In the central sector the crystallines have suffered considerable erosion and denudation so that the once-continuous sheet is now represented by synclinal klippen and nappes. In the northwestern and eastern sectors the crystalline rocks have been thrust southwards considerably so that they have reached the proximity of the foothills. The MBT forms the southern boundary of the Lesser Himalaya (Valdiya, 1980).

The Lesser Himalaya has been affected by three main generation of folding, exhibited by the crystallines of the nappes, normal Himalayan fold, and younger structures which have been influenced by the older structure and superimposed on the 2nd generation (Valdiya, 1979 a).

Great Himalaya: It is made up of Central crystallines or high-grade katazonal metamorphism including migmatite and forming the basement of the Tethyan sediments. As a result of folding, it is bifurcated into southern Pir Panjal in Kashmir and the northern Zanskar ranges. This lithotectonic zone is built up of older Precambrian high grade metamorphics known as the Vaikrita Group in Himachal and Kumaun. The Central Himalayan gneisses in Western Nepal are intruded by young Cenozoic granites. The high grade metamorphic rocks occupy the structurally and topographically highest positions within the Great Himalaya, while lower grade rocks occur below, due to (a) thrust imbrication or recumbent folding of a normal metamorphic

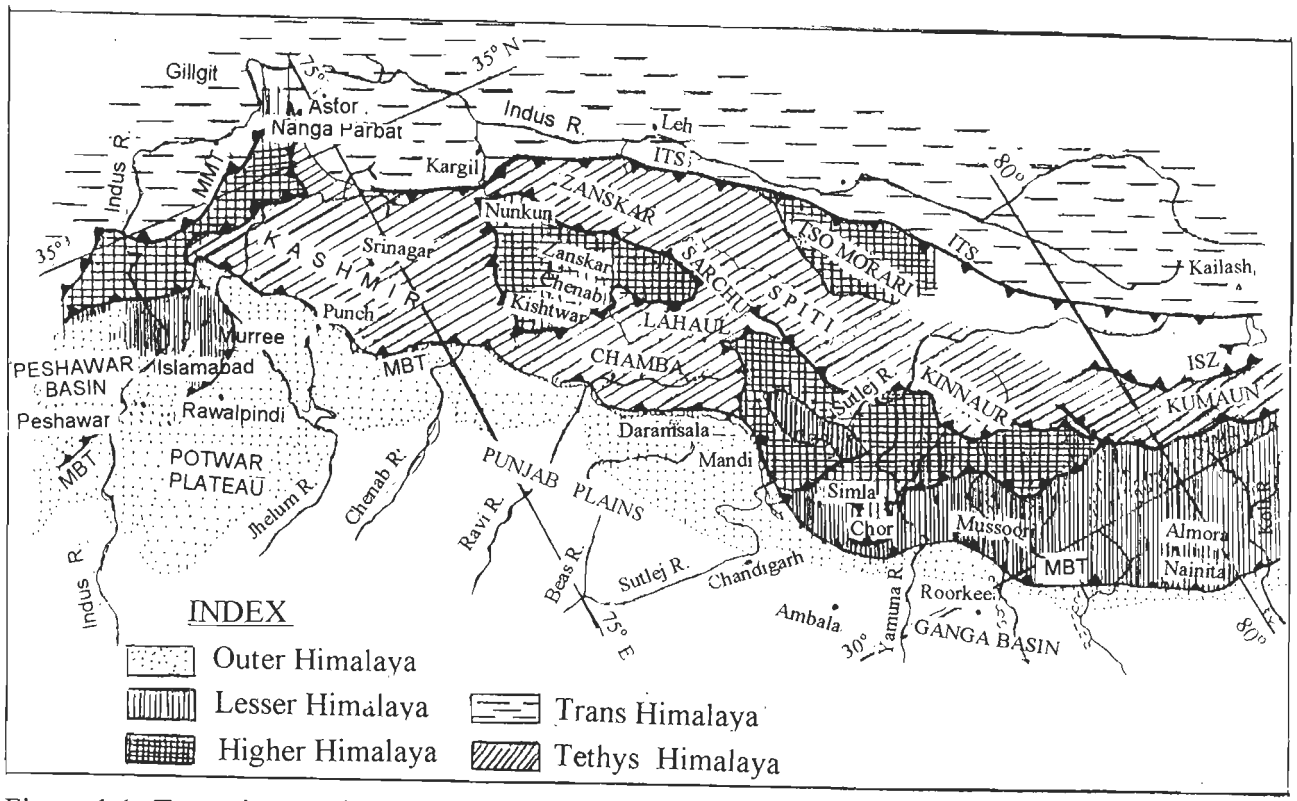

Figure 1.1- Tectonic zonation map of western Himalaya (Thakur, 1993)

Table 1.1 Tectonic succession in the Himalaya (Valdiya, 1980)

Kashmir	Himachal	Kumaun	Nepal	Darjeeling	Bhutan	Kameng
Tethys sediments	Tethys sediments	Tethys sediments	Tethys sediments		Tethys sediments	
	"Central Gneiss"	Vaikrita	Up Cryst/Tibetan Slab	Darjeeling	Thimpu (Chasilakha)	Sela
	MC (Vaikrita) T	**MC (Vaikrita) T**	**MCT**	**T**	**T**	**T**
Salkhala	Jutogh	Munsiari (+ Almora)	Lr Cryst/Up Midland	Paro	Paro	Bomdila
Panjal T	**Jutogh T**	**Munsiari T**	**Thrust**	**T**	**T**	**T**
Ramsu	Chail	Ramgarh (Bhatwari Unit)	Chail-2/Lr Midland	Daling	Samchi (Shumar)	Tenga
Duldhar T	**Chail T**	**Bhatwari-Ramgarh T**	**Thrust**	**T**	**T**	**T**
	Jaunsar	Berinag	Chail-3/Birethanti			
	Jaunsar T	**Berinag T**	**Thrust**			
Parautochthon	Parautochthon Autochthon	Autochthon	Parautochthon Autochthon	Parautochthon	Parautochthon	Autochthon
	Tons T	**Srinagar T**		Tansen		
	Krol	Krol				
Murree T	**Krol T**	**Krol T**	**K- Thrust-MBT**	**MBT**	**MBT**	**MBT**
Murree	Dharmsala	Siwalik	Siwalik	Siwalik	Siwalik	Siwalik

sequence (Heim and Gansser, 1939; Bordet, 1961), (b) local heating of the structurally highest parts of the sequence by granitic injection (see Auden, 1935; Hodges et al., 1988) and thermal pertubation responsible for prograde metamorphism during movement on the MCT, (c) shear heating along the thrust (Le Fort, 1975), (d) ductile shear displacements along ubiquitous, closely spaced S-C shear planes causing metamorphic inversion (Jain and Manickavasagam, 1993; 1994).

Rapid thrust culmination of the High Himalaya during the Miocene also resulted in dorsal culmination collapse with normal faulting down throwing the shelf sediments to the north and juxtaposing the Lower Paleozoic sediments against high grade metamorphic rocks and leucogranite of the High Himalaya (Searle et al., 1987). The presence of east-west striking, gently north-dipping normal faults (post-collision, probable Miocene) in the Higher Himalaya and southern Tibet during late stage metamorphism and igneous activity in the crystalline zone may be genetically related to the shortening strain (Burchfiel and Royden, 1985). These relations give a time for their formation between 20-15 Ma.

Tethys Himalaya: It is extending to the north of the Great Himalaya. It comprises predominantly fossilferous sediments ranging in age from Late Proterozoic to Cretaceous or even Eocene (Valdiya, 1980)

Trans-Himalaya: This unit includes the Indus-Shyok sutures and the Karakorum zone and constitutes the southern part of the Asian plate and Tibet Karakorum block (Thakur, 1993). A belt of granitoids crops out immediately northwards of the 2500km long Indus-Tsangpo Suture Zone from Kohistan to Assam. The Trans-Himalayan batholith ages span from 94-41 Ma (Searle et al., 1987). In fact, the Gangdise plutonic belt comprises numerous bodies of gabbro, diorite, granodiorite and granite, which have intruded from 95-40 Ma and interpreted as a mixture of mantle-derived component within the continental crust (Alleger et al., 1984). Extensive andesite, rhyolite, ignimbrite (Searle et al., 1987) and ophiolite are also observed together in association with the plutonic belt. Ophiolite complexes with the age of 120±10 Ma (Gopel et al., 1984) occur in two main tectonic settings: (i) in thrust sheets obducted southward on the northern

continental margin of Indian plate before 40 Ma (Tapponnier et al., 1981), and (ii) discontinuous, tectonically disrupted lenses within the Indus Tsangpo Suture Zone.

MCT and MBT: Main Central Thrust (MCT) is the boundary between the Great and Lesser Himalaya. Copeland et al. (1991) investigated the thermal history of the MCT by using $^{40}Ar/^{39}Ar$ and U-Pb methods. There is a marked asymmetry of ages between footwall and hanging wall of the MCT. In the footwall, there is a spectrum of ages from 400-1400 Ma, but in hanging wall, ages cluster at about 13 Ma (max.) in the Lesser and Great Himalaya respectively. Infiltration of hot fluids through the MCT zone appears to be the best hypothesis to explain these data (Copeland et al., 1991). The movement of hot fluids and shear heating along the MCT are two possible mechanisms of thermal pulses. The thermal disturbance appears to have occurred at ~ 5-4 Ma. Late fluid phases, which were derived by underplating thrust slices and inducing melting in the MCT slices, played an important role in the crystallization of the melt rich in B, P, Li, F, and H_2O (Searle et al., 1987). If the amount of fluid liberated from the rocks thrust beneath the MBT is 5%, approximately $3x10^{10}$ kg of fluid will be available for each metre along the MCT (Copeland et al., 1991). The similarities in the structural orientation of these faults favor a common mechanism for the fluid events. Therefore, if this hydrothermal phenomenon is widespread, the thermal denudation rates are of the order of ~1 mm/yr, with this assumption that their temperature is at least ~525°C when fluids reach the rock currently exposed (Copeland et al., 1991). It is generally accepted that the movements may have begun in the Late Oligocene and most workers assume that displacement on the MCT effectively ceased when the structurally lower MBT become active (Copeland et al., 1991). As a deep crustal fracture, the MCT appeared within Indian plate in Oligocen-Miocene, and continental subduction developed by underthrusting of the Indian block along this fracture. Finally, a similar mechanism seems responsible for the MBT (Hamet and Allegre, 1976; Allegre et al., 1984) and more probably for southward thrust faults, i.e., the Foothill Frontal Thrust (FFT). The amount of underthrust Indian continental lithosphere under the MCT may be up to 1000 km, and also the transported amounts should be greater in the eastern Himalaya as compared to NW India to the extent of ~200-300 km (Klootwijk et al., 1985). At the present time, it seems that the MCT is no longer an active

thrust but the tectonic activity has jumped southward, with a new continental thrust. The MBT is presently active at the rate of ~2 cm/yr (Allegre et al., 1984; Valdiya, 1980). Therefore, when the suture became blocked (~45 Ma), motion transferred to the MCT and then to the MBT (Besse et al., 1984). The MBT activity started >10 Ma ago and reached to its peak ~5 Ma (Meigs et al., 1995). Peak activity of the Nahan thrust with the foreland basin is at ~1.75 Ma (Sangode, 1997). Therefore, the Lesser Himalayan formations were thrusted over the Cenozoic sediments by the MBT at ~10 Ma.

Indus Suture Zone: It is a major tectonic divide which has been described as the original site of the lithospheric subduction by Gansser (1973), and is the only constant structural element all along the Alpine-Himalayan belt (Gansser, 1980). This zone, in fact, is strongly tectonized along the 2500 km length. It separates the highest known mountain range (Himalayan) from the largest and highest landmass on our globe, the Tibet.

The process of continental collision of the Indian and Eurasian plates during the Cenozoic time (Verma et al., 1977; Rai, 1982; Edelman, 1991) or ~50±5 Ma (Patriat and Achache, 1984; Besse et al., 1984; Searle et al., 1987; Dewey et al., 1989; Klootwijk et al., 1979; Copeland et al., 1991; Edelman, 1991) resulted in the origin and evolution of the Himalaya, which is one of the best outstanding physiographic features on earth.

1.2 CENOZOIC FORELAND BASIN

If more attention is focused on the distribution of the Cenozoic sediments (Fig. 1.1) in the *Sub-Himalaya,* one would find that these sediments have much less width in the east than in the west. Many parametres could have played the role in producing this feature, such as:

(i) The pre–collisional diamond-shape of the Indian plate (Treloar and Coward, 1991) has exerted a fundamental control on the Himalayan thrust stack, and also in the distribution of the Cenozoic sediments of the Himalayan foreland basin.

(ii) Change in the direction of stresses between Indian and Eurasia plates. This factor certainly resulted in moving and thrusting some large parts of these sediments due to

different thrusts. Therefore, at present time, they are covered by different formations and do not crop out at the surface.

(iii) The slope of foreland basin of the Sub-Himalaya is not unique in width and depth.

Extensive geological and geophysical surveys have been carried out over the Cenozoic foreland basin of the NW Himalaya since the last century (see, Raiverman and Seshavataram, 1970) and have resulted in maps of the Cenozoic sediments. These investigations, however, were particularly intensified during the last three decades for hydrocarbon exploration by the Oil and Natural Gas Commission (ONGC) (Raiverman et al., 1983).

Till recent years, commercial generation of petroleum was thought mainly to be of marine origin from many parts of the world (Demaison and Murns, 1984), but the continental sediments have, of late, also became attractive for their hydrocarbon prospects. During the past 3-decades, geologists have increasingly turned to thermal maturation studies of organic matter as a tool to estimate the hydrocarbon generation-preservation stage of the sedimentary strata as well as to reconstruct the thermal histories of sedimentary basins and orogenic belts (Guthrie et al., 1986).

In the present study, in order to gain insight into the thermal history and evaluation of source rock, the following methods were used on a segment of the Cenozoic foreland basin of the NW Himalaya: petrographic studies, illite crystallinity index, fission track (FT) method, total organic carbon (TOC), vitrinite reflectance and rock eval pyrolysis.

Petrographic studies– It includes petrographic studies, modal analysis of sandstone, and identification of clay minerals of shale and the matrix of sandstone using X-ray diffractograms to determine the probable provenance of the Cenozoic sediments.

Illite crystallinity index– It is a useful and simple method in classifying the diagenesis stage and to separate the boundary of diagenesis and metamorphism. Diagenesis stage is terminated when the width of half peak of 10A° illite reaches to 3.7 mm. Therefore, it is an indicator of paleotemperature.

Fission Track Dating Method– Fission tracks are linear damage in a crystal lattice by nuclear fragments from the spontaneous fission of ^{238}U. Once tracks are formed, they begin to

anneal in a process that appears to be first order of a function of temperature and time (Naeser et al., 1989; Green et al., 1989; Naeser et al., 1990). Annealing also providing the tracks the potential for defining localized temperature anomalies in sedimentary basins, such as related to intrusions or the passage of high-temperature fluids through the rocks. The annealing temperatures of zircon and apatite are 240±25°C (Brandon, 1992) and 100°C (Naeser and Forbes, 1976; Zimmermann and Gains, 1978; Zimmermann, 1977; Naeser, 1981) respectively, and span the mean temperature range for oil generation. Most petroleum generation begins at about 50°C and ends at about 200°C (see Hunt, 1979). More recently, Quigley and McKenzie (1988) stated that most oil forms between 100° and 150°C and most gas between 150° to 220°C.

Fission track method can be a good tool to understand the thermal and depositional histories of sedimentary basins (Naeser, 1979; Naeser et al., 1989). Fission track analysis of detrital apatite or zircon grains has already been used to reconstruct the provenance and thermal or exhumation history of sedimentary basins (see Zeitler et al., 1982; 1986; Hurford et al., 1984; Johnson, 1984; Baldwin and Harrison, 1985; Yim et al., 1985; Baldwin et al., 1986; Cerveny, 1986; Cerveny et al., 1986, 1988; Lonergan and Johnson, 1998). Typically, most thermal information is provided by apatite, because many sedimentary rocks have not been related to temperatures sufficiently high to anneal zircon. Therefore, unannealed zircon or annealed zircon can be useful. However, the ages of individual unannealed detrital zircon grains are also valuable to determine the sediment accumulation rate (Kowallis and Heaton, 1987). Zircon has also been used extensively to date the volcanic ashes and their altered equivalents (Naeser and Naeser, 1988).

In the present study, it should be noted that the fission track method is used to evaluate thermal history and provenance of the sediments of the Cenozoic foreland basin of NW Himalaya, in India for the first time.

Total Organic Carbon (TOC) Measurement and Rock Eval Pyrolysis– These are useful to asses the abundance of organic matter in sediments and its maturity respectively.

Vitrinite Reflectance (VR_o) Method– Vitrinite is one of the macerals in sedimentary rocks. It is relatively easy to concentrate from bulk rock sample and yields a quantitative measure of thermal maturity. Vitrinite has also been concentrated with stages of hydrocarbon

generation and preservation and can be used, therefore, as a reliable tool for evaluating the hydrocarbon potential of sedimentary basin (Tissot and Welte, 1978; Waples, 1981). VR_o data are used in two basic ways. Firstly, VR_o as an index of the degree of thermal maturation is an important factor to kinetically model the petroleum generation (see Sweeney and Burnham, 1990). Secondly, VR as a peak geothermometer, because maturity in organic matter rapidly increases and stabilizes after a geologically short duration of heating at peak temperature under the conditions of moderate to high temperature diagenesis in partially open fluid-rich system (Barker, 1991).

VR_o has the advantage over other maturation techniques in covering the entire temperature range from early diagenesis to metamorphism. It is the most useful subsurface prospecting tool for determining the present and past stages of maturation (Hunt, 1979). VR_o data can be used as a check on the paleogeothermal gradient indicated by FTD. Therefore, the combination of FTD and VR_o data allows definition of the major facts of thermal history (Bray et al., 1992) and is more powerful than alone (Duddy et al., 1991; Duddy and Green, 1992; Green et al., 1993).

1.3 AREA OF STUDY

In the present investigations, the Cenozoic sediments of foothill belt of the NW Himalaya between the longitude 77°20′E and 76°56′E and latitudes 30°59′N and 30°32′N and having the type sections of the Subathu, Dagshai, Kasauli and Lower Siwalik (=Nahan) formations were selected. The present study covers an area between Nahan to Solan, Subathu, and Kalka. The most important reason for this selection was the existence of type sections of the Paleogene rocks. The available geological maps were prepared by Chaudhri (1969 a) and Raiverman et al. (1983).

1.4 PHYSIOGRAPHY AND DRAINAGE

The Outer or Sub-Himalaya comprises the Siwalik Hills, with altitudes varying from 250 m to 800 m and width between 25 to 100 km and is characterized by flat-floored structural valleys. The southern slopes of the main Siwalik ranges, facing the Indian Plains are steep, while

the northern slopes are gentle, descending gradually into flat-floored linear basins called the 'Duns'. The best known of them is the Dehra Dun valley of Garhwal.

The Outer Himalaya consists of about 9500 m thick Cenozoic and Quaternary sedimentary pile, ranging in age from Paleocene to Upper Pleistocene. Its northern boundary is delimited by the Main Boundary Thrust (MBT), which separates the Cenozoic belt from the pre-Cenozoic Lesser Himalayan formations. To the south, the generally prominent topographic break of the Outer Himalaya against the alluvial plains of Ganga basin is expressed as a fault called the Himalayan Foothills Fault, which has been designated as the Main Frontal Thrust (MFT). Geophysical data together with subsurface drilling for oil revealed that the Cenozoic rocks, similar to the Outer Himalaya, also occur in the Ganga basin.

The general drainage pattern of the area under study was shown in Figure 1.2. The most important rivers of the east-northeastern and west-southwestern parts terminate to the Yamuna and the Satluj rivers, respectively.

In the western Himalaya, the Indus system and its tributaries such as the Jhelum, the Chenab, the Ravi, the Beas and the Satluj drain the mountains, while the Yamuna, the Ganges, the Ramganga, and the Kali (Sarda) belong to the Gangetic System in the eastern sector. Of these, the Indus, the Satluj and the Ganges and Bhagirathi traverse across the great Himalaya range and are believed to be older than the mountains (Thakur, 1993).

1.5 OBJECTIVES

With the above premise, it is proposed to take up the Cenozoic sediments of the Northwestern part of the Himalaya for this study, keeping in view the general optimism that the pre-Siwalik sediments form the source rock for petroleum–gas hydrocarbons.

The main objectives of the present investigations of the Cenozoic foreland basin of the NW-Himalaya are:

i) To asses the timing of subsidence and uplift

ii) To investigate petrography of sediments and their provenance

iii) To work out thermal history of this part of Sub-Himalayan basin using fission track technique, vitrinite reflectance and illite crystallinity.

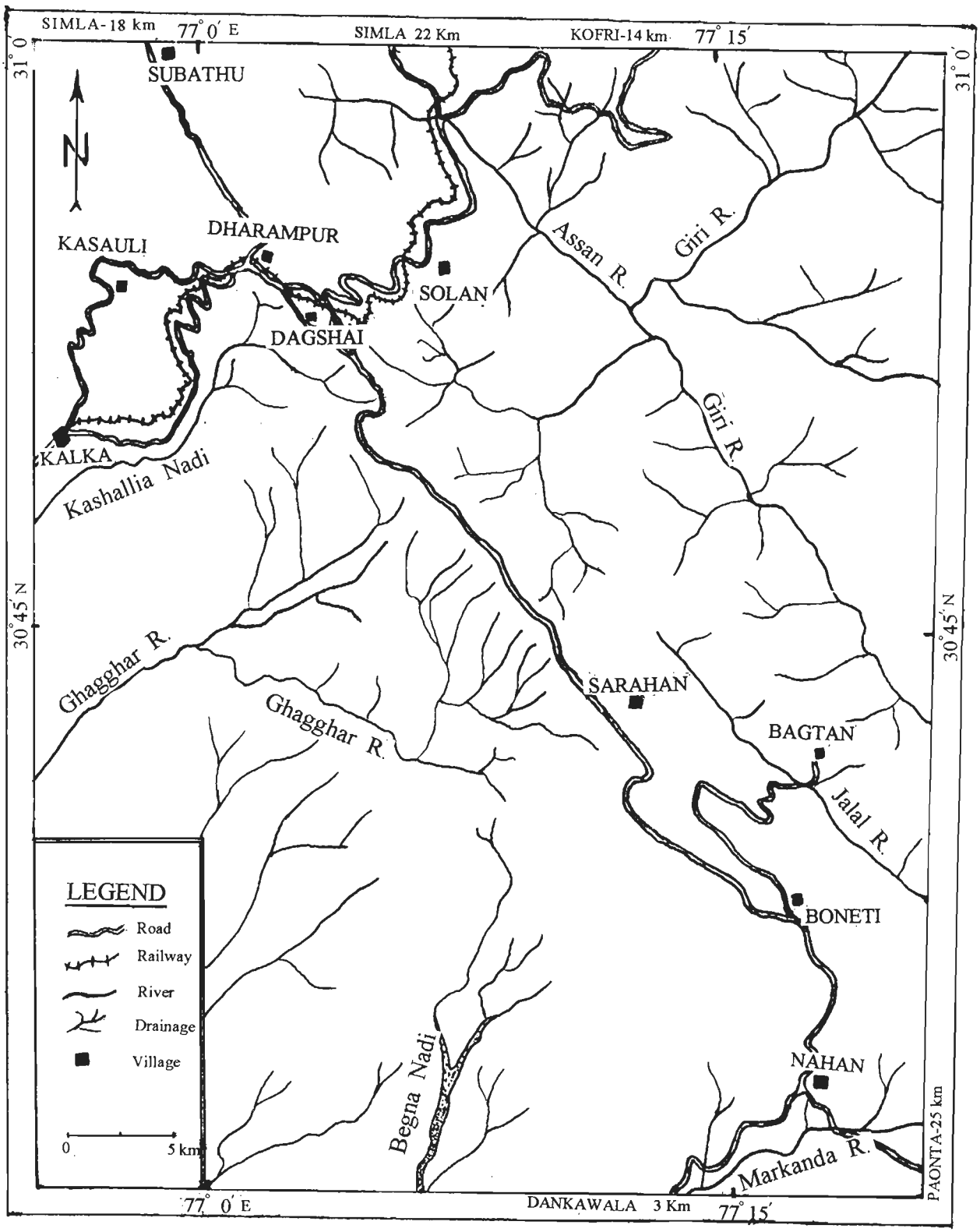

Figure 1.2- Sketch map showing the general drainage pattern of area understudy.

iv) To asses the petroleum prospects.

1.6 EXISTING LITERATURE

The history of the geological investigations in this area began with the work of Medlicott (1864), who introduced the term of Subathu. The sedimentological, petrographic and petrochemical studies of the Cenozoic sediments of NW Himalaya have been carried out by a number of workers including McMahon (1883), Ganju and Srivastava (1961, 1962), Kharkwal (1964, 1966, 1969), Raiverman (1964, 1968), Chaudhri (1966 a, b; 1969 b, c, d, e; 1970 a, b, c; 1971 a, b, c; 1972 a, b, c; and 1975), Raju (1967), Bhattacharya (1970), Raiverman and Seshavataram (1970), Bhattacharya and Raiverman (1973), Bhushan (1973), Najman et al (1993, 1994, 1997), Mehta et al. (1993) and others.

While Datta (1970) and Mahandroo (1972) confined their studies to the Paleogene sediments, Krynine (1937), Babu and Dehadrai (1958), Misra and Valdiya (1961), Sikka et al. (1961), Cummins (1962), Raju and Dehadrai (1962 a, b, c), Saxena et al., (1968), Sinha (1970), Dass and Vanshnarayan (1971), Tandon (1971; 1972 a, b) emphasised more on the Neogene sediments. A very brief account of more important of these publications is given here.

Petrographic studies- Raiverman et al. (1961), Chakraborty et al. (1962) and Raman and Ravi Shankar (1963) correlated the Lower Dharmsala with the entire Dagshai-Kasauli sequence of the Simla Hills, whilst the Upper Dharmsala is absent in this region. Raiverman (1964) studied the clay minerals and trace element components of some clay samples from the Subathu and the Dharmsala rocks. Based on V/Ni ratio, he suggested a brackish water environment for the Subathu and Upper Dharmsala sediments. Raiverman and Seshavataram (1970) suggested that the typical Dharmsala sea was somewhat deeper than the Subathu sea, but the sea had shallowed again during the last phase of the Dharmsala deposition.

Many certain trends and cyclic patterns have been reported since long within the Cenozoic sequence in H.P., by Medlicott (1864), Krishnan (1960), Wadia (1966) and Sahni and Mathur (1964) in view of grain size of the clastic component, proportion of constituents of sandstones, colours of sediments and degree of in duration of the sediments.

Dayal and Chaudhri (1967) reported Dicotyledonous leaf–impressions from the Nahan beds of the Kalka area.

Raju (1967) used heavy mineral distribution of the Cenozoic foothill sediments to make stratigraphic zonations and correlation, but with limited success in the subsurface.

Chaudhri (1969 c) investigated sedimentology of the Lower Cenozoic rocks of the Punjab Himalaya in detail. He concluded that the Subathu (Upper Paleocene–Upper Eocene) were deposited in shallow marine water, the Dagshai (Upper Eocene–Lower Oligocene) in fresh water, and the Kasauli (Upper Oligocene-Lower Miocene) in a shallow fast sinking basin. He also suggested, based on the shape analysis, that the sediments have not travelled far from the source rocks. The provenance of the Cenozoic sediments was discussed by Chaudhri (1972 d). He believed that the Subathu sediments were derived largely from the sedimentary veneer (low and medium grade metamorphism and plutons) of the Himalaya. The Dagshai had an origin in low and medium grade metamorphites and plutonic rocks of the rising Himalaya, and the Kasaulis have been derived mostly from slightly higher grade metamorphites (garnetiferous mica schist).

Bhattacharya (1970) studied clay mineralogy and trace element geochemistry of the Subathu, Dharmsala and Siwalik sediments from Dharmsala to Kalka area. This study showed that dominant clay minerals are moderately degraded illite and chlorite; degraded illite, vermicullite and expanded mixed layers; montmorillonite, kaolinite, highly degraded illite and chlorite, respectively.

Raiverman and Seshavataram (1970) discussed the petrographical, paleontological and palynological of the Subathu-Dharmsala groups and ruled out the possibility of unconformity between the Subathu and Dharmsala.

Raiverman and Raman (1971) suggested facies relations in the Subathu sediments of Simla Hills and believed that three stratigraphic units, i.e., Subathu, Dagshai and Kasauli, have intertonguing relation, as green, gray and red facies based upon the dominant shale color.

Chaudhri (1972 a) studied the heavy minerals of the Siwalik formations. He identified the opaque fraction, which included magnetite, hematite, limonite, illmenite, rarely pyrite and

sporadic chromite as a sizable proportion of the heavy mineral. Staurolite is the marker for the Lower Siwalik Formation.

Raiverman (1972) recognized 8-mega-cycles based on the changes in grain size of sediments representing successive impulses of uplift and subsidence related to the Himalayan orogeny. The eight energy sequences named as En-Seq 8 are characterized by their typical association of rocks, color, stratification, texture, structure and mineralogy.

Bhattacharya and Raiverman (1973) studied the clay mineral distribution in the Dharmsala sediments over a region extending from Palampur to Mandi and Sarkaghat. In the Lower Dharmsala, the relatively fresh illite and chlorite indicate that sediments were deposited in a marine environment and presumably by slow sedimentation in a shallow sea or in large saline lakes. The Upper Dharmsala sediments were supposed to be non-marine (probably continental) origin. The sediments exhibit very slight diagenetic changes.

Chaudhri (1975) discussed the sedimentology and genesis of the Cenozoic sediments by petrographic analysis (Fig. 1.3). Further, he reported the presence of rhythmic nature of the Paleocene-Eocene sequence (three sedimentary rhythms in Paleocene, Early Eocene and Middle Eocene epochs) resulted from the eustatic sea level, during the Subathu deposition (Chaudhri, 1976).

Chaudhri and Gill (1983) studied clay mineralogy of the Siwalik Group of Simla Hill. The mineral assemblage comprises kaolinite, illite, chlorite, vermiculite, montmorillonite and mixed layers. The sediments were deposited in mildly subsiding fresh water basin. They attributed the variation in clay mineral assemblage of the Siwalik Group exposed in different regions to the variation in the character of source rocks, weathering intensity, sediment transport, drainage and topography.

Raiverman et al. (1983) identified two time-dependent geological processes: (i) the energy-sequence concept, and (ii) the stability order in heavy minerals. The pulses of uplift and subsidence have been synchronous throughout the NW- Himalaya and have left their imprint in the sediments. The eight En-Seq. with their individual lithological associations, gross field characteristics, heavy mineral assemblages, and also biostratigraphy are described.

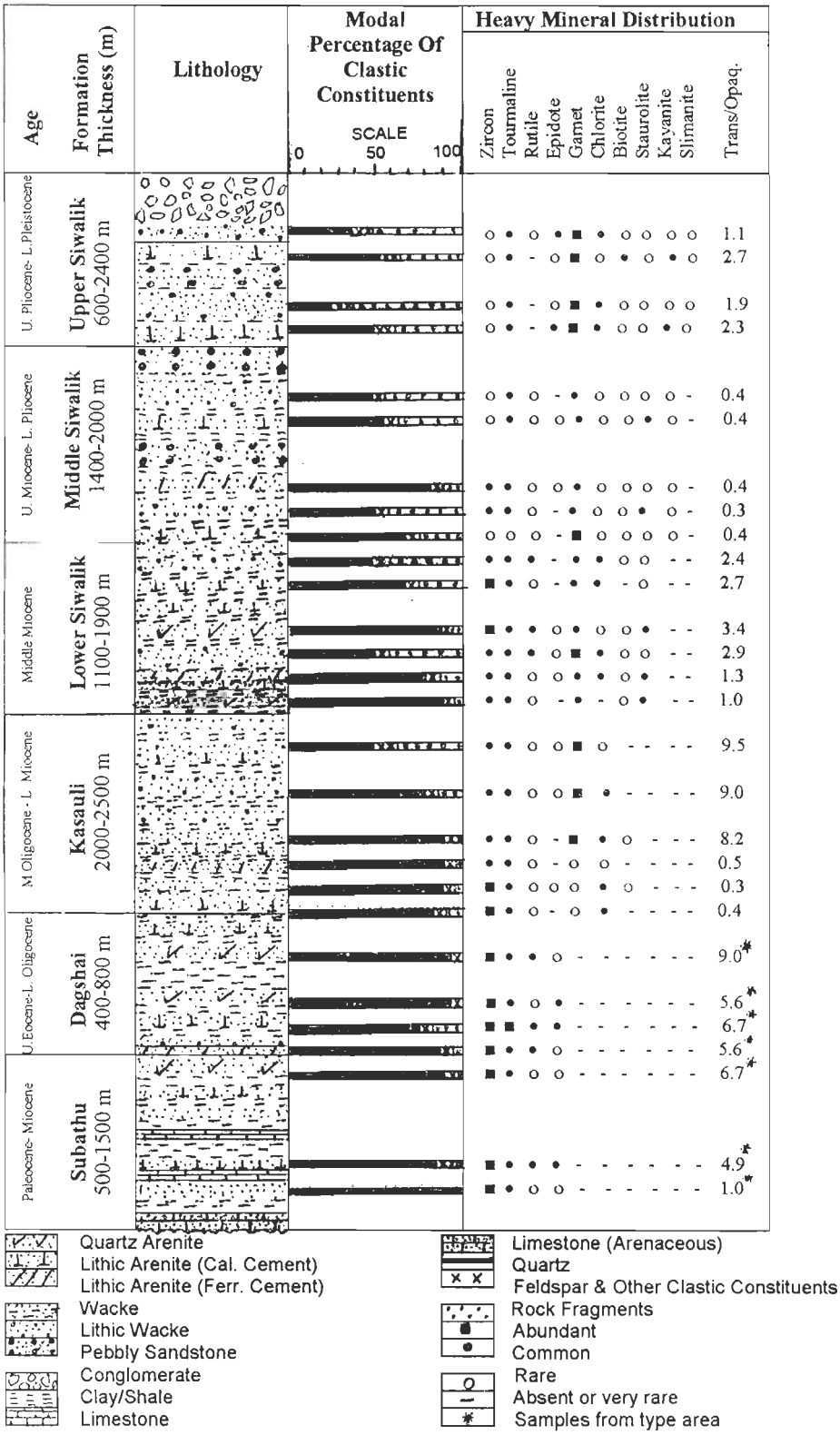

Figure 1.3- Generalized section of the Cenozoic formations of Northwestern Himalayas showing the variations in lithology, modal composition and heavy mineral distribution (Chaudhri, 1975).

Bagati and Kumar (1994) studied the clay mineral distribution of the Middle Siwalik sequence in the Mohand area (Dehra Dun) with its application to climate and source area.

Provenance studies- Tripathi and Saxena (1987) suggested that the Siwaliks and the inception of the Main Boundary Thrust are directly related to the Lower-Middle Miocene orogeny. The nature and thickness of the Siwalik sediments clearly indicated that the basin subsided gradually along with sedimentation. The nature of Siwalik sediments shows major changes from Lower to Middle and upward to Upper Siwalik, and also indicate periodic and continuous changes in the provenance. This suggests respective movements of positive and negative areas.

Critelli and Garzanti (1994) found that detrital modes of sandstones of the Lower Cenozoic Murree red beds (=Daghshai) of N-Pakistan testify a provenance from the proto-Himalayan chain with a comparison between the overall petrographic affinity of the Murree supergroup and younger orogenic sandstones with the High Himalaya which evolved during the Cenozoic from lower to higher grade metamorphic rocks. Slight increase of detrital feldspar and polycrystalline quartz through time points to progressive deepening of erosion into crystalline rocks, until in the Early Miocene a huge hot wedge of the Indian crust was rapidly uplifted and carried hundred of kilometers southward along the Main Central Thrust (MCT). Rise of the Himalaya at that time is indicated by isotopic data on the High Himalaya crystalline rocks (Le Fort, 1989; Hodges et al., 1992) and by progressive composition of the Siwalik foreland basin sandstones (Chaudhri, 1972 a; Parkash et al., 1980; Abid et al., 1983).

Dating studies- Srikantia and Bhargava (1967) reported the occurrence of an exclusive Paleocene horizon (Kakra series) in a tectonic setting in the Sub-Himalaya. The fossil assemblage within the Kakra limestone is the complete absence of typical Subathu fossils.

Barry et al. (1982) proposed interval zones of Middle and Upper Siwalik formations are bounded by five important faunal events: (1) 9.5–7.4 Ma; (2) 7.4–5.3 Ma; (3) 5.3–2.9 Ma; (4) 2.9–1.5 Ma B.P., and (5) 1.5 Ma to present.

Johnson et al. (1982 a) reported nominal age of stratotype section ranges of 13.1–10.1 Ma, 10.1–7.9 Ma, and 7.9-5.1 Ma for Siwalik formations. Mean sediment accumulation rates range from 13 to 52 cm/10^3yr in Potwar plateau, Pakistan. Johnson et al. (1982 b) reported a FT

age of the bentonitized tuffs from Jhelum area (Pakistan) ~2.4±0.2 Ma, and from the Nagri Formation ~9.46±0.59 Ma.

Srivastava and Casshyap (1983) proposed two systems of paleocurrents for the pre-Siwalik Cenozoic rocks in Himachal Pradesh: (i) across the delta plain complex, and (ii) long shore-currents operating parallel to shore line. They suggested that the bulk of the clastic debris was derived from the Infra-Krol and Krol-sequences and only a minor contribution of the Simla Group and no contribution from the crystalline zone of the Central Himalaya.

Rao (1989) discussed the boundary of Neogene and Quaternary. He believed that it is controversial and largely related to the choice of criteria; climate, vertebrate fauna and magnetostratigraphy. He used FT dating of bentonite beds to solve this problem. This technique yielded an age of 2.8±0.56 Ma in the Paramandal–Utterbeni area.

Appeal et al. (1991) investigated magnetostratigraphy of the Miocene - Pleistocene of Siwalik in Surikhola region, West Nepal. Opdyke et al. (1979), Johnson et al. (1982 a), Tauxe and Opdyke (1982), Johnson et al. (1983), and Burbank and Johnson (1983) have made magnetostratigraphic investigations in other areas of the Siwalik range. Recently, Sangoda (1997) used this technique in the area between Dehradun and Nahan. He ascribed the age of 18.7-10.7 Ma for the Lower Siwalik part.

Harrison et al. (1993) determined the depositional ages of 10.0 Ma and 8.25 Ma for the Lower Siwalik in Bakiya Kohla, Southern Nepal, by paleomagnetic analysis and $^{40}Ar/^{39}Ar$ dating, respectively.

Using fission track method, Mehta et al. (1993) dated the zircon grains, from the Upper Siwalik subgroup of Chandigarh and Jammu sections, and reported cogenetic ages of 2.14±0.5 Ma, and 1.56±0.32 Ma respectively with the ash fall events.

Najman et al. (1994) dated the Dagshai formation at 35.5±6.7 Ma using paleomagnetic method; this age was interpreted as the time when embryonic Himalaya began to be strongly eroded and regionaly uplifted.

Mehta (1995) reported the apatite fission track age of ~8 Ma for the Dagshai samples collected near Mandi area. This age indicates a reset age which is showing that Dagshai samples passed through the closure temperature of apatite and started to uplift before/ or near 8 Ma ago.

Meigs et al. (1995) suggested that the activity of the MBT started >10 Ma, but it reached to its peak activity ~5 Ma.

Najman et al. (1997) reported a $^{40}Ar/^{39}Ar$ dating of individual detrital white micas from the Dagshai and the Kasauli formations. This dating method has provided maximum depositional ages of <28 Ma and <25 Ma for different localities of the Dagshai, whereas <28 Ma and <22 Ma for the Kasauli formations. They believed that these ages are related to the depositional age of Dagshai and Kasauli. They also criticized the previous paleomagnetic data of the Dagshai Formation (Najman et al., 1994). They concluded that the paleotemperature should be <200°C, which is insufficient to reset the micas.

Sangode (1997) studied magnetostratigraphy and sedimentation history of the Siwalik foreland basin in Dehra Dun-Nahan sector. He increased the age of Siwalik deposition to 18.7 Ma instead of 14.8 (18.7-10.1 Ma). This difference in age with previous authors is related to account the Kamlial Formation as a part of Lower Siwalik Formation.

Tectonic studies- Singh (1964) gave a short discussion about geology of the Simla Hills. This area is very complicated and the rocks having been very much folded, faulted and thrust; some of the thrust sheets having travelled long distances from their places of origin.

Najman et al. (1993) believed that the intercalation of the Subathu and Dagshai sediments is due to post-depositional tectonics, rather than primary intertonguing, as described in some previous reports. The relative abundance of sandstones greatly increased in the Upper Dagshai time continuing into Early–Mid–Miocene (30–10 Ma). The marine Subathu Formation is interpreted as having been deposited between initial and terminal India–Eurasia continental collision, with the overlying fluvial/or flood plain Dagshai (Late Eocene-Oligocene) and Kasauli (Miocene) formations as southward prograding foreland basin successions related to progressive stages of India–Eurasia continental collision.

Doglioni (1994) in a classification of foredeeps, suggested that the foredeep of Himalaya is placed in the foredeep group associated with east-or northeast dipping subduction related accretionary wedges. This type of foredeep is characterized with the high relief and broad outcrops of metamorphic rocks, and the low rate of subsidence. The foreland basin associated with the east or northeast dipping subduction is shallower than other type (west dipping).

Based on deep drilling and a few seismic profiles, Raiverman et al. (1994) believed that neither the model of down to basement faults nor thin- skin tectonics applies uniformly all over the basin.

Virdi (1994) suggested that the Cenozoic basin exhibited the influence of pre-existing topography as well as structural grains in the basement rocks and also southward-migrating Himalayan thrust sheets; MCT, MBT and HFT. He believed that Delhi–Sargodha ridge (DSR) as a young feature and possibly post collision played an important role in differentiating the basin into two contrasting sectors during Late Eocene. Early Oligocene when the Cenozoic and older rocks if any were eroded away. However, the frontal basin in front of the Himalaya continued to receive sediments from the rising orogen, though the facies changed from marine to brackish water and then finally to fresh water. Thus, we have a nearly complete Cenozoic succession in the Outer Himalaya while, to the South, the basement is succeeded by successively younger members of the sequence and finally by the alluvial and district sediments.

Petroleum prospects- Agarwal et al. (1994) studied hydrocarbon potential of the Siwalik basin. Their study revealed that the Upper and Lower Siwalik sediments are too poor in organic matter content with an average TOC of ~0.12–0.33 and 0.41% respectively, with the exception of some samples which indicate marginal to fair organic matter richness. Similarly, the Upper Murree/or Upper Dharmsala sediments indicate an overall poor organic matter carbon with TOC in the range of 0.01–0.34%. The TOC data on Lower Dharmsala samples and Lower Murree formations have also indicated poor organic matter content. They have also drawn the maturation subsidence curves of the sediments of the Siwalik basin, based on Waples (1980) time temperature index (TTI) method.

Biswas (1994) discussed about the status of exploration for hydrocarbons in the Siwalik basin, and future trends. Pyrolysis characterization of a good number of samples of basal Dharmsala sequence indicated marginal to good hydrocarbon generating potential and organic matter of kerogen type-II in a majority of the samples indicating oil and gas generating potential. VR_o of the basal Dharmsala samples is ~0.49% and thermal alternation index (TAI) values range from 2.5 to 2.75. All these data suggest that the basal Dharmsala has reached an early stage of

maturation. In spite of the exploratory input during the last three decades, no success in exploration could be achieved.

Berry (1994) recorded rich humic organic matter in the Lower Dharmsala/or Lower Murree and Subathu formations. The Siwalik sediments, in general, contain poor organic matter. The pre-Siwalik sediments possess source potential for hydrocarbons.

Samanta et al. (1994) recorded coals and coaly shales in the Cenozoic and Gondwana sediments of the Ganga basin and in the Subathu Formation of the Siwalik basin. The Siwalik and Dharmsala formations are poor source rocks because of low total organic carbon content. The Cenozoic sediments near the MBT may offer good source potentials.

1.7 SCOPE OF STUDY

An appraisal of published geological literature indicates that though the Cenozoic foothill belt of NW-Himalaya has received attention by geologists since long, very few studies were carried out on subsidence-uplift history (thermal history) and petroleum source rock evaluation, and, thus, it has left enough scope for detailed and comprehensive investigations of these rocks. The present work is an endeavor in this direction.

This study is based on detailed laboratory investigations, which include petrographic studies of sandstone, clay mineralogical studies of shale and sandstone matrix using X-ray technique, illite crystallinity, zircon and apatite fission track studies using external detector method, total organic carbon, virtinite reflectance and rock eval pyrolysis. The results of the investigations which form the frame of the present thesis are presented in the following chapters.

***Chapter* 1: Introduction**– It presents the general scope of the area understudy, the techniques which are used in the present investigations very brief, and available published literature.

***Chapter 2*: Geology of the Area**– A geological description of the Cenozoic stratigraphic units, which are exposed in the area in view of their facies, environments, and paleocurrent directions.

***Chapter 3*: Petrographic Studies**– It presents the petrographic description of different Cenozoic sediments including the Subathu, Dagshai, Kasauli, and Lower Siwalik formations, using modal analysis and X-ray diffractograms of the collected samples. The provenance of the sediments based on present data is also discussed.

***Chapter 4:* Himalayan Foreland Basin: application of fission track dating-** The definitions and different FTD methods with special attention to the External Detector Method has been discussed. Amongst the different FT methods, EDM has been used due to its advantages over others. The interpretation of the FT results of >750 individual grains of zircon and apatite (mostly zircon >700 grain) has been made using two basic methods: (i) χ^2 -age and (ii) Gaussian Best Fit. The FT results are significant regarding the depositional age of the Cenozoic sediments and the provenance of the grains.

***Chapter 5*: Petroleum Source Rock Evaluation**– It presents the source rock evaluation of Cenozoic sediments of the present area using techniques to determine the amount of organic matter which has undergone optimal thermal maturation. The basic parameters to evaluate the source rock are discussed as: (i) determination of Total Organic Carbon (TOC) as a measure of abundance of total organic matter in sediments, (ii) use of chemical and optical methods to determine organic matter to generate oil or gas or oil and gas, and (iii) measurement of Vitrinite Reflectance, T_{max}, and Illite Crystallinity Indice for finding out the degree of maturity of organic matter. These methods, when used conjuntively, help in evaluating the source rock objectively. In this chapter, the existing data about other areas of the Cenozoic foreland basin of the NW Himalaya have also been compared with the data of the present study to extend the results further to elucidate the petroleum potential of the Cenozoic sediments.

***Chapter 6:* Paleotemperature, Subsidence and Exhumation History-** The paleotemperature estimated by different inorganic and organic indicators are collated and utilized

to reconstruct the subsidence history and exhumation of the sediments. The results also compare with the available data for other parts of the Cenozoic foreland basin.

Chapter 7: **Summary and Conclusions**- It summarizes and integrates the results of different chapters. The salient findings of the investigations are brought out and important conclusions are drawn.

CHAPTER - 2

GEOLOGY OF THE AREA

2.1 INTRODUCTION

The area under study is a part of the southernmost Himalayan foreland basin of the Cenozoic sedimentary rocks. It is made up of early Cenozoic formations (Subathu, Daghshai and Kasauli) and the late Cenozoic Lower Siwalik (=Nahan). These are thrown into Jura-type folds and affected by faults (Valdiya, 1980) that increase in number towards the Main Boundary Thrust (MBT) in the north. The area under investigation is shown in Figure 2.1. The stratigraphic measurements of the Cenozoic formations exposed in the area and the sample locations are shown in Figures 2.2 and 2.3, respectively. A brief description of the various formations is given herewith and summarized in the Table 2.1.

2.2 EARLY CENOZOIC SEQUENCE

2.2.1 Subathu Formation

The term of Subathu was introduced a century ago by Medlicott (1864), named after the Subathu town. The Subathu Formation includes intra formational conglomerate, quartzite, quartz arenite, arenite with calcareous and ferruginous cement, shale/siltstone and limestone. This formation is marked by the absence of lithic wacks (see Chapter 3). The width of exposure of the sediments varies from 100 m (in the Nahan area) to 1500 m (in the Dharampur area), which is attributed to thrusting and folding.

Based on the colour of shale associated with this formation, three distinct lithofacies, termed as green, gray and red are recognized. The top of green facies is marked by a white quartzose sandstone, which is considered as a marker bed between Subathu and Dagshai formations. The areal repetition of green and red facies of Subathu was described by Raiverman and Raman (1971) as stratigraphic intertonguing of Subathu and Dagshai. However, this view

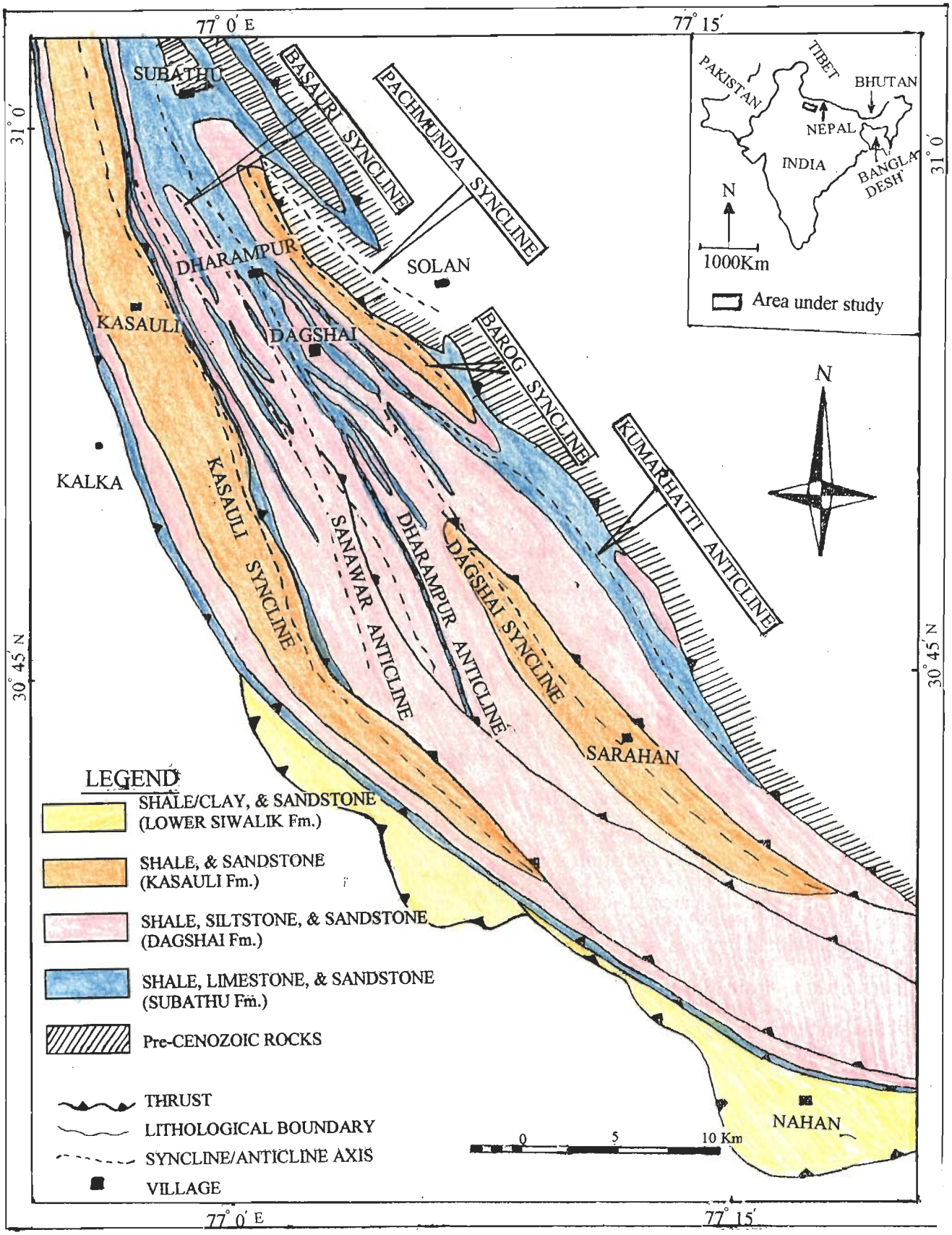

Figure 2.1- Geological map of Nahan-Subathu-Solan-Kalka area of the Sub-Himalaya (after Chaudhri, 1969 a).

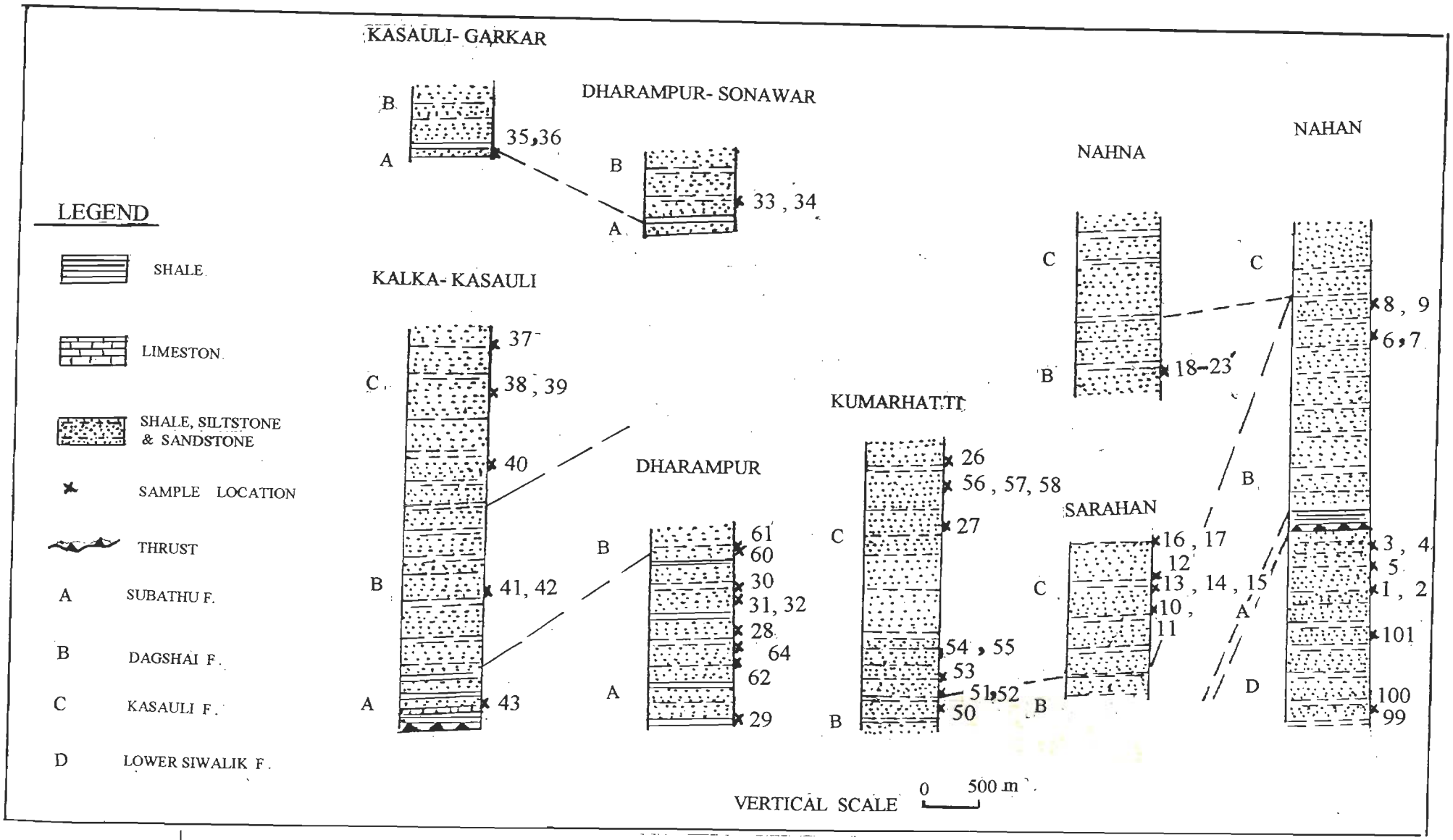

Figure 2.2- Stratigraphic columns of the Subathu, Dagshai, Kasauli and Lower Siwalik formations in various geologic sections in present area understudy. The numbers showing sample reference no.

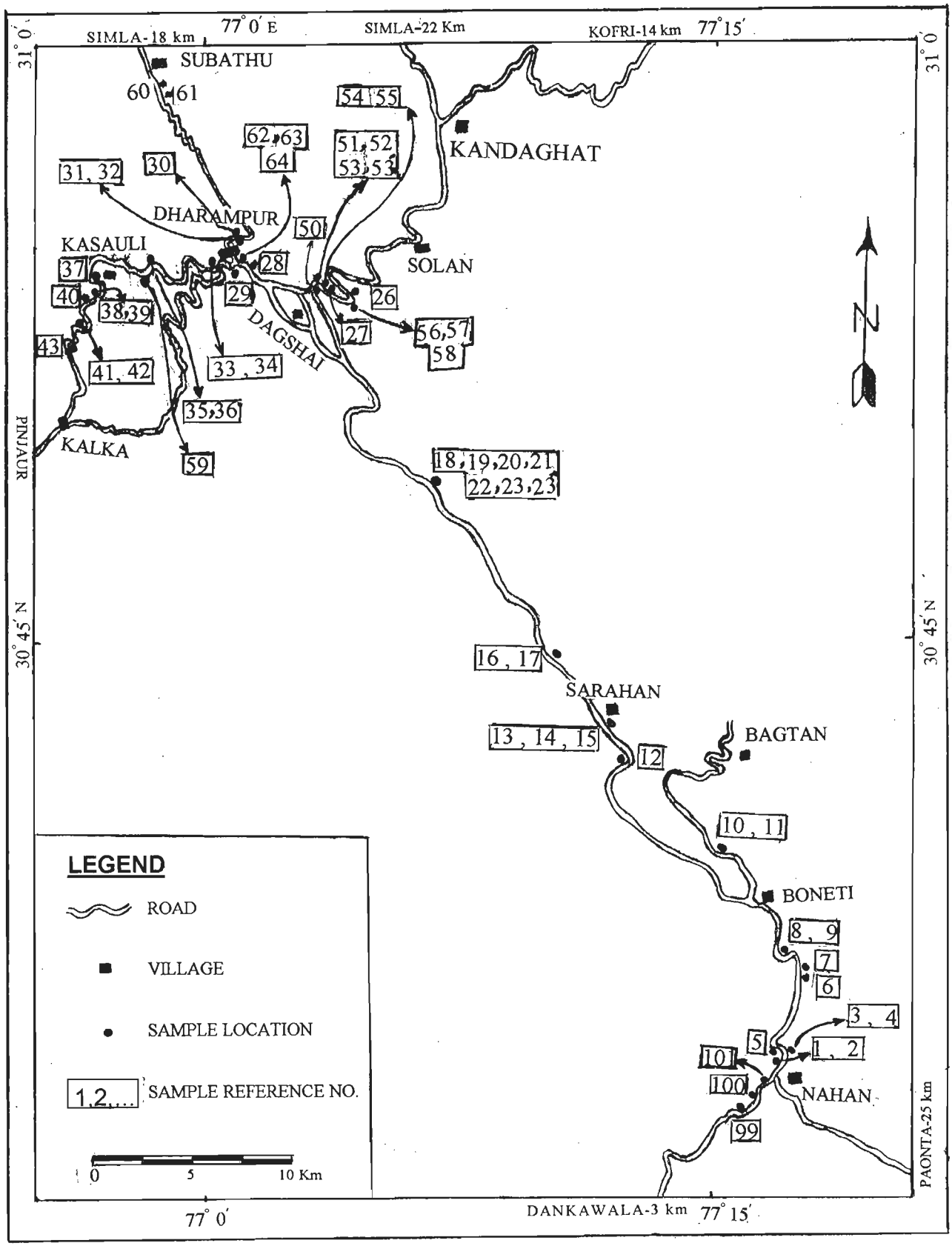

Figure 2.3 - Sample location map of the different sections of the present investigation.

Table 2.1 The Cenozoic sedimentation (pre-Middle Siwalik) in the Himalaya

Formation	Approx. Age Ma)	Lithology	Events
Lower Siwalik (= Nahan)	15-10	Greenish-gray, coarse grained, hard sandstone, red and purple shale	Initiation of MBT activity >10 Ma and subsequent upliftment in the north front of the Himalayan foreland
Kasauli	24 -15	Gray sandstone, siltstone,Mudstone and woody material and shale	Peak of MCT at ca.20 Ma
Dagshai	40-24	Red sandstone, siltstone, mudstone, and caliche	Initiation of MCT after 30 Ma. Start of thrust- stacking and crustal thickening after collision
Subathu	65-40	Green sandstone, mudstone, shale and limestone	Collision of Indian-Asian Plates ~50 ± 5 Ma

point was not accepted later on by Batra (1989) and Kumar (1992) as they believed that these intertonguing are due to folding and faulting.

In the type area, the Subathu Formation consists of green shale, gray marl, thin lenticular limestone and occasional white sandstone. The marl and limestone contain mollusca, foraminifera and other fossils (Raiverman and Raman, 1971). The Subathu Formation comprises three lithologically distinct facies from base to top as a basal black–gray facies, a middle green facies and a topmost red facies. The basal black-gray facies yields typical marine vertebrates including sharks, rays, pycnodonts and tetraodonts, etc. (Sahni et al., 1981; Kumar and Loyal, 1987). Nine biostratigraphic zones have been established in the Subathu succession (Mathur, 1969). The green facies yields more or less similar vertebrate fauna as the black gray facies, but in less abundance. The red facies constituting the upper most part of the Subathu Formation is transitional and yields Middle Eocene land mammal (Sahni, 1979). Kumar et al. (1997) report the Eocene rodents from Himachal Pradesh, which can be correlated with the Eocene rodent-yielding horizons at the top of the Subathu Formation in Jammu, Kashmir and the Kuldana

Formation in Pakistan are in the same timeframe. On weathering, the shale-siltstone sequence of the Subathu Formation break into millimetre to centimetre wide and a few cm long pieces, similar to that of lead pencil.

The age of deposition was considered to be 65-40 Ma Late Paleocene-Upper Eocene (Chaudhri, 1969 c; Mathur, 1978; Kumar, 1992).

2.2.2 Dagshai Formation

It was adopted from the name of Dagshai town, and comprises ~600 m thick alternating sequence of gray/red shale and hard, fine grained green/red impure sandstone and siltstone. It is also characterized by caliche and absence of limestone. Mudstone is dominant in the lower part, while upper part of the sequence is more arenaceous. The more common rock fragments in sandstone, which makes up to 30 % of the sequence, include of chlorite schist, siltstone, chert, quartzite and plutonic rocks. The rocks whose fragments are encountered in the Dagshai rocks are traceable in the adjacent Himalayan region (Chaudhri, 1971 b). Some of the pebbles occurring in the basal conglomerate of the Dagshai succession were derived by erosion of locally uplifted parts of the basin of deposition (Chaudhri, 1968). The purple colour in shale is mainly due to ferric oxide. The transition between the Subathu and the Dagshai is somewhat abrupt and is marked by pisolitic marl, purple shale and white sandstone with ferruginous concretion. The transition of the Dagshai Formation to the overlying Kasauli Formation is gradual and conformable.

The depositional age of the Dagshai Formation, due to very rare/lack of fossils is ambiguous, till recently. Some attempts were made to determine its age by paleomagnetic studies and other dating methods. Najman et al. (1994) ascribed an age of 35.5±6.7 Ma, which was revised by Najman et al. (1997) using $^{40}Ar/^{39}Ar$ dating of single detrital muscovite grains. They reported maximum depositional ages of <28 Ma.

2.2.3 Kasauli Formation

Named after a hill station in southeastern H.P., this formation consists of about 2100 m thick alternating massive pale/gray to buff micaceous sandstone and purple and gray shale.

Sandstone is classified as litharenite (see, Chapter 3) and is of fine to medium in grain size. The sandstone is generally softer, coarser and more micaceous than the Dagshai sandstone. Petrographically, rock fragments of slate, phyllite, garnet mica schist, granitic/gneissic and sedimentary rocks are observed. In comparison to the Dagshai Formation, the percentage of rock fragments has increased in this formation. Considerable abundance of certain minerals like mica and garnet is mentionable. In the lower parts near Kumarhatti, plant impressions in sandstone and ripple marks in the shale were observed. The rock formation of the NW-Himalaya that have been correlated with the Dagshai and Kasauli formations have been grouped into the Dharmsala and Murree groups, respectively (Gansser, 1964; Kumar, 1982).

An early Miocene age is generally assumed for the Kasauli depositional age, on the basis of the occurrence of Early-Middle Miocene plant remains (Fiestmantel, 1982). In a new finding of plant fossil, Arya (1998) ascribed the age of 23.8 Ma for the base of Kasauli Formation. Based on laser $^{40}Ar/^{39}Ar$ dating of single detrital muscovite grains, Najman et al. (1997) reported an age of 28 and 22 Ma in different localities of this area.

2.2.4 Lower Siwalik (=Nahan) Formation

The succession is named after the Siwalik Hills near Hardwar, but is best exposed in the Tawi valley of Jammu region and Hartalyangar area in H.P. The base of these sediments is generally not exposed. The Nahan Formation of southeastern H.P., has been correlated with the lower most unit of the Siwalik Group (Sen, 1981; Kumar, 1982; Kumar et al., 1991). It is generally accepted that the Siwalik Group is divisible into three parts: the Lower, the Middle and the Upper Siwalik Formation.

The Lower Siwalik Formation consists of 1700 m of alternating sandstone and shale/siltstone, and a few beds of conglomerate in the upper part. The detritus is poorly sorted. Sandstone is medium to coarse grained in size and greenish to yellowish in colour. Its hardness towards the upper section part of the Nahan area decreases. Lithologically, these sediments are unconsolidated to semi consolidated in character. The rocks occasionally bear fossil vegetable matter, which is mainly leaves and stems. The Lower Siwalik sandstone includes of 30-35% rock fragments (metamorphic, igneous and sedimentary rocks). They are classified as litharenite.

More significant is the presence of garent, staurolite, epidote and flaky minerals. Clays are less frequent in this formation. The lower contact of Lower Siwalik Formation with the Subathu Formation is determined by the Nahan Thrust. Elsewhere, upper part was thrust over by the Middle/Upper Siwaliks.

The age of Lower Siwalik is poorly constrained at around 15 Ma (Lyon-Caen and Molnar, 1985). In Pakistan, the base of Lower Siwalik *sensu stricto* (i.e. the base of the Chinji Formation) has been dated as 14.3 Ma (Johnson et al., 1985). The Kamlial Formation, which underlies the Chinji Formation, is dated as 18.3–14.3 Ma. However, the confusion exists as to whether this part should be assigned to the Lower Siwalik or is a correlative with the Kasauli Formation. Nevertheless, recently Sangode (1997) ascribed an age of 18.7–10.7 Ma to the Lower Siwalik, while considering the Kamlial Foramtion as a part of the Lower Siwalik. In the southern part of Nepal, Harrison et al. (1993) determined the initial depositional age of 10.8 and 8.25 Ma for the Lower Siwalik Formation using the paleomagnetic and $^{40}Ar/^{39}Ar$ methods, respectively.

2.3 PALEOENVIRONMENT

Considerable difference of opinions exist on the stratigraphic nomenclature and mode of deposition of the Subathu and Dharmsala sediments. However, most geologists agree at least that the Siwalik sediments are deposited in brackish water to continental environment (Bhattacharya, 1970).

The pre-Siwalik rocks grouped as the Subathu, Dagshai, and Kasauli formations of Himachal Sub-Himalaya have been interpreted as of marine brackish or lagoonal origin (Srivastava and Casshyap, 1983). They are grouped into five distinct lithofacies.

1. Fossiliferous green shale with lenses of limestone interpreted as tidally influence shelf deposits.
2. Clean-white sandstone, as coastal barrier bar.
3. Red mudstone with lenses of gray sandstone as lagoonal and tidal flat deposits.
4. Gray sandstone with channel lag and red mudstone and siltstone as distributary channel and inter-distributary plains of fluvio-delta.

5. Gray-white sandstone and mudstone, as mixed of assemblage of fluvio-delta and coastal barrier facies.

Srivastava and Casshyap (1983) proposed two systems of currents: (i) across the delta plain complex, and (ii) long-shore currents operating parallel to shore-line.

The distribution and paleocurrent patterns of pre-Siwalik Cenozoic rocks in Solan-Nahan area (H.P.) have been presented in Figure 2.4. Figure 2.5 is a map showing paleocurrent directions and centres of sediments supply of Dharmsala sediments for comparison.

2.3.1 Subathu Sediments

The Subathu Sediments were deposited in a shallow marine with the transgressive and regressive phases with partial reworking from shelf (Chaudhri, 1969 c; Bhattacharya, 1970; Raiverman and Raman, 1971). Chaudhri (1976) observed the rhythmic nature in these sediments and attributed it to the eustatic sea level changes accompanied by subsidence.

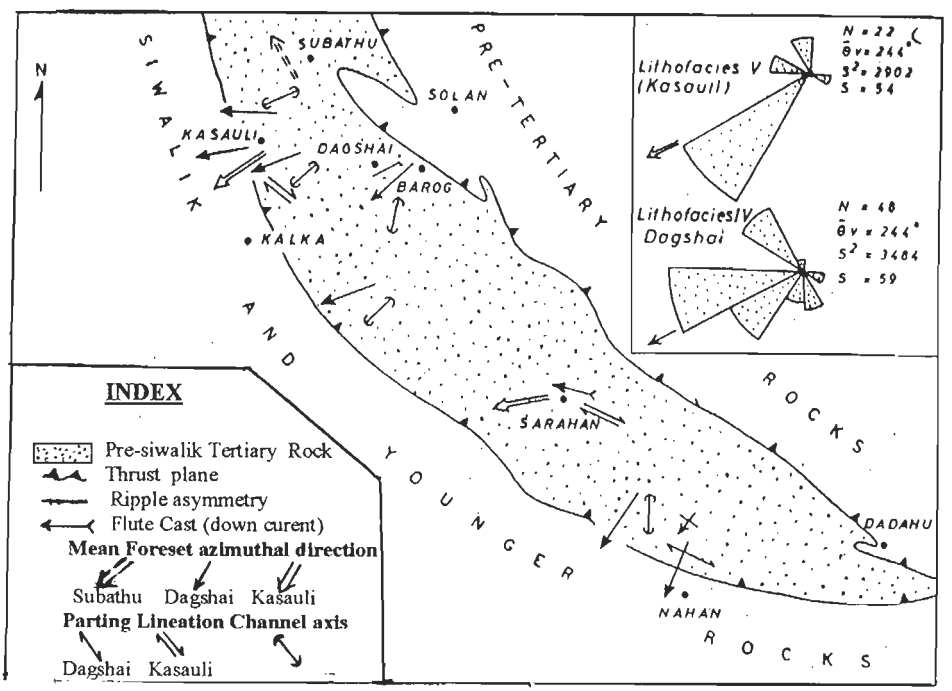

Figure 2.4- Paleocurrent patterns of Cenozoic rocks (Subathu, Dagshai, and Kasauli formations) in Solan-Nahan area (H. P.). Inset shows cross-bedding azimuthal distribution of Dagshai and Kasauli lithofacies (Srivastava and Casshyap, 1983).

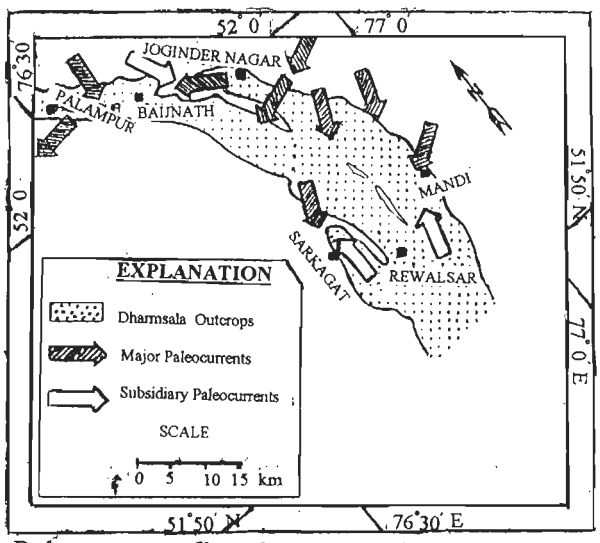

Figure 2.5- Paleocurrent directions and centres of sediment supply for Dharmsala sediments (Chaudhri and Gill, 1983).

2.3.2 Dagshai and Kasauli Sediments

The sediments of Dagshai and Kasauli sediments were deposited in brackish and fresh water, respectively (Krishnan, 1982). Bhattacharya (1970) suggested the Dagshai to be flysch sediments deposited in a geosyncline. Raiverman and Seshavataram (1970) suggested that the typical Dagshai sea was somewhat deeper than the Subathu sea, but the sea had shallowed again during the last phase of the Dagshai deposition.

Chaudhri (1969 c) has suggested that the Dagshai (Upper Eocene-Lower Oligocene) representing fresh-water deposits, while for the Kasauli (Upper Oligocene-Lower Miocene) a shallow fast sinking basin is considered. The former was the period of the most active erosion and deposition, perhaps a prelude to the further Himalayan upheaval. The sinking of the basin was at a very fast rate, and so was the erosion in the mountainous region as is evinced by the frequent occurrence of fragments of shale, schistose and gneissose rocks. The sediments carried by the rivers were deposited as such, and the clay and the sand fractions could not be separated. Therefore, argillaceous sandstone is much more in quantity than sandstone and clay/shale unit in the Kasauli Formation.

The organisms could not thrive due to muddy water condition prevalent during the sedimentation of the Kasauli. A few organic remains that might have been entombed in the

sediments were perhaps destroyed during the diagensis of these rocks. In spite of this, a few stratigraphically significant fossils have been found in the Dagshai and Kasauli formations apart from pollen spores in the former. Highest structural levels have been dated as Early Cenozoic by Oil & Natural Gas Corporation (Chakraborty et al., 1963), and plant remains in the Kasauli formation which have been dated as Early-Mid Miocene (Sahni, 1953; Fiestmantel, 1882; Arya and Awasthi, 1994). Nevertheless biostratigraphical dating of the Dagshai and Kasauli formations is still more problematical than Subathu Formation.

2.3.3 Siwalik Sediments

The Siwalik sediments were deposited as molasse in the zone of fore deep of the Himalaya. The lower part is deposited in brackish waters; the middle and upper parts are deposited in continental environment (Bhattacharya, 1970). The Miocene Siwalik Group in N-Pakistan records fluvial and lacustrine environments within the Himalayan foreland basin (Zaleha, 1997 a). Sedimentological variations of the Siwalik Group were evaluated with respect to local, regional and global controls on fluvial deposition and basin filling (Zaleha, 1997 b). Climate during deposition of the Siwalik Group was monsoonal. Although the deposits contain no direct evidence for climate change, independent evidence indicates global cooling throughout the Miocene and the possibility of glacial periods e.g. around 10.8 Ma. The shoreline was many ~100 km away during the Miocene (Khan et al., 1997). The frequent occurrence of current bedding, ripple marks, swash marks, logs of fossil wood and the association of cobble and pebble sized fragments with sand grade detritus are suggestive of shallow water condition (Chaudhri, 1971 b). Kumar (1982) expressed this opinion that the Middle Siwalik sediments were laid in marshy environments and high energy fluvial influence attained the predominance during the deposition of the Upper Siwalik. Based on clay mineralogy studies of Simla Hills by Chaudhri and Gill (1983), the source-rock bearing feldspar, micas, and ferro magnesian minerals suffered chemical decomposition and mechanical fragmentation in temperate climate. The sediments were deposited in rapidly subsiding fresh water basin. The mean paleocurrent directions for the Siwalik formation have been shown in Figure 2. 6.

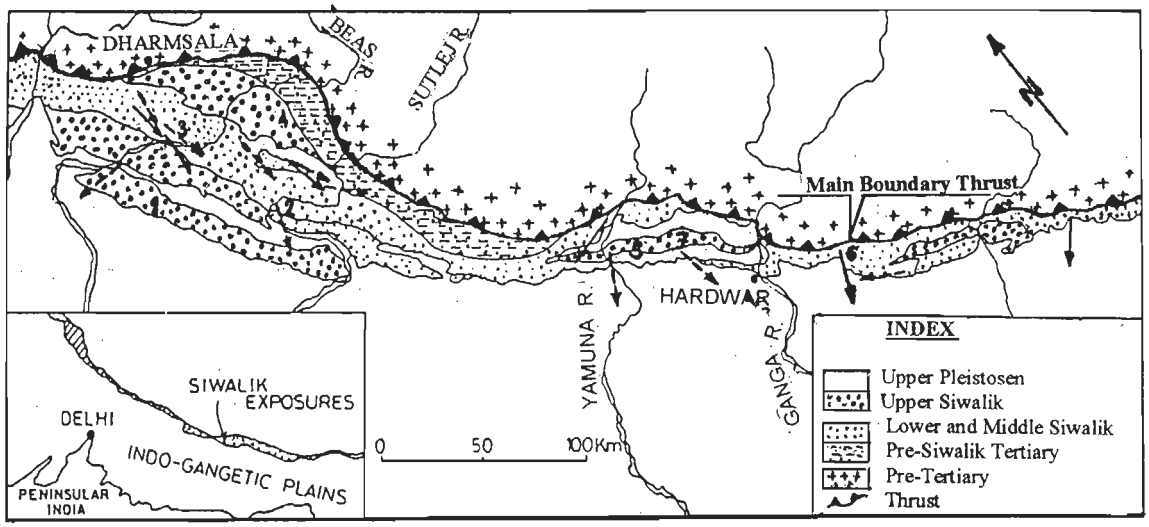

Figure 2.6- Geological map of a part of the Western Himalaya (after Gansser, 1964). Arrows indicate mean paleocurrent directions for the Lower (solid arrows) and Middle (broken) Siwaliks. 1= Januari section, 2= Bhakra-Nangal section, 3= Jawalamukhi section, 4= Sarkaghat section, 5= Saharanpur section, 6= Kotdwara section, and 7= Ramganga–Plain rivers section (Parkash et al., 1980)

2.4 MAIN BOUNDARY THRUST (MBT)

The Main Boundary Thrust (MBT) as the youngest of large tectonic features of the Himalaya has played an important role in juxtaposing of the different stratigraphic horizons and tectonic units with the Siwalik formations. The surface expression of the MBT is a steeply north-dipping fault that marks the contact between the Lesser Himalayan sequence and the underlying Cenozoic Sediments. It is reasonable to assume that movements of the MBT began in Middle to Late Miocene time, providing a source rock for the Siwalik foreland basins (Nakata, 1989). Geomorphology of the Himalayan front (Nakata, 1989) as well as fault-plane solutions for Himalayan earthquakes (Baranowaski et al., 1984) reveal that the MBT remains active today. Figure 2.7, presents some evidences of recent movements along the MBT.

The rate of underthrusting beneath the Himalaya over the past 20 Ma has been estimated 15±5 mm/yr (Molnar, 1987). The average rate of Quaternary movements inferred from the field observations, detailed mapping of Quaternary and active faults as well as microtectonic measurements between south of the Karakorum-Jiali fault zone and MBT is estimated to be ~1 cm/yr (Armijo et al., 1986). Therefore, the rate of underthrusting of India along the Himalaya is

as high as ~20±10 mm/yr. These rates imply that as much as 60-180 km of underthrusting could have occurred on the MBT since its inception in Middle Miocene time (18.7-11.7 Ma). The activity was at its peak at about 4-5 Ma (Meigs et al., 1995).

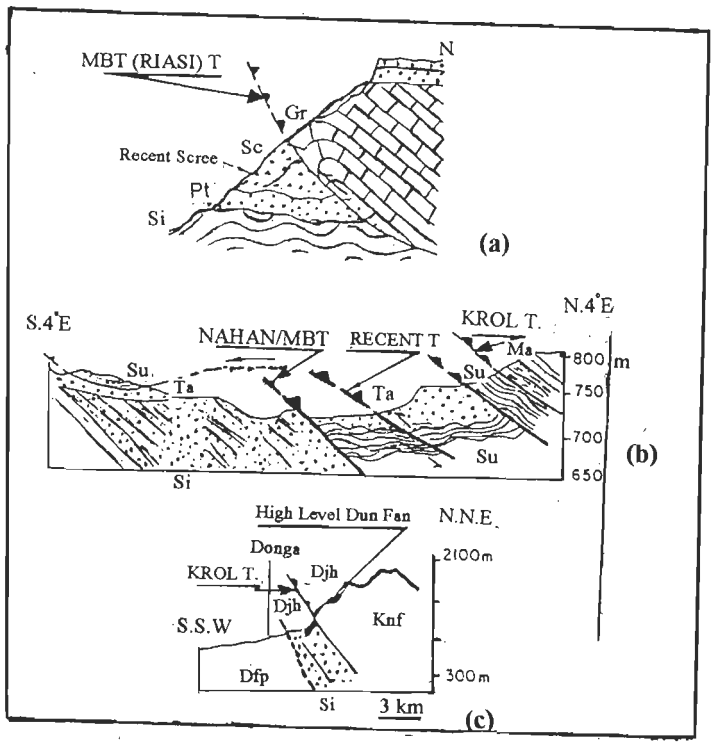

Figure 2.7- Evidence of recent movements along the MBT and what were originally known as MBT. a. Riasi, Jammu (after Krishnaswamy et al., 1970); b. Tons Valley, Western Kumaun (after Krishnaswamy et al., 1970); c. Dehra Dun (after Nossin, 1971), Sc =Recent scree; Pl =Upper Pleistocene; Si =Siwalik; Su =Subathu; Djh =High level Dun fan; Dfp =Principal Dun fan; Ma =Mandhali (Valdiya, 1980).

In the present area, the MBT is manifested as a zone of thrusting, as all the thrusts including the Paonta, Bilaspur, Bata, Sarauli, East Nahna, Surajpur and Main Boundary/Krol thrusts, which pass through the area under study, terminate into the MBT (Fig. 2.8).

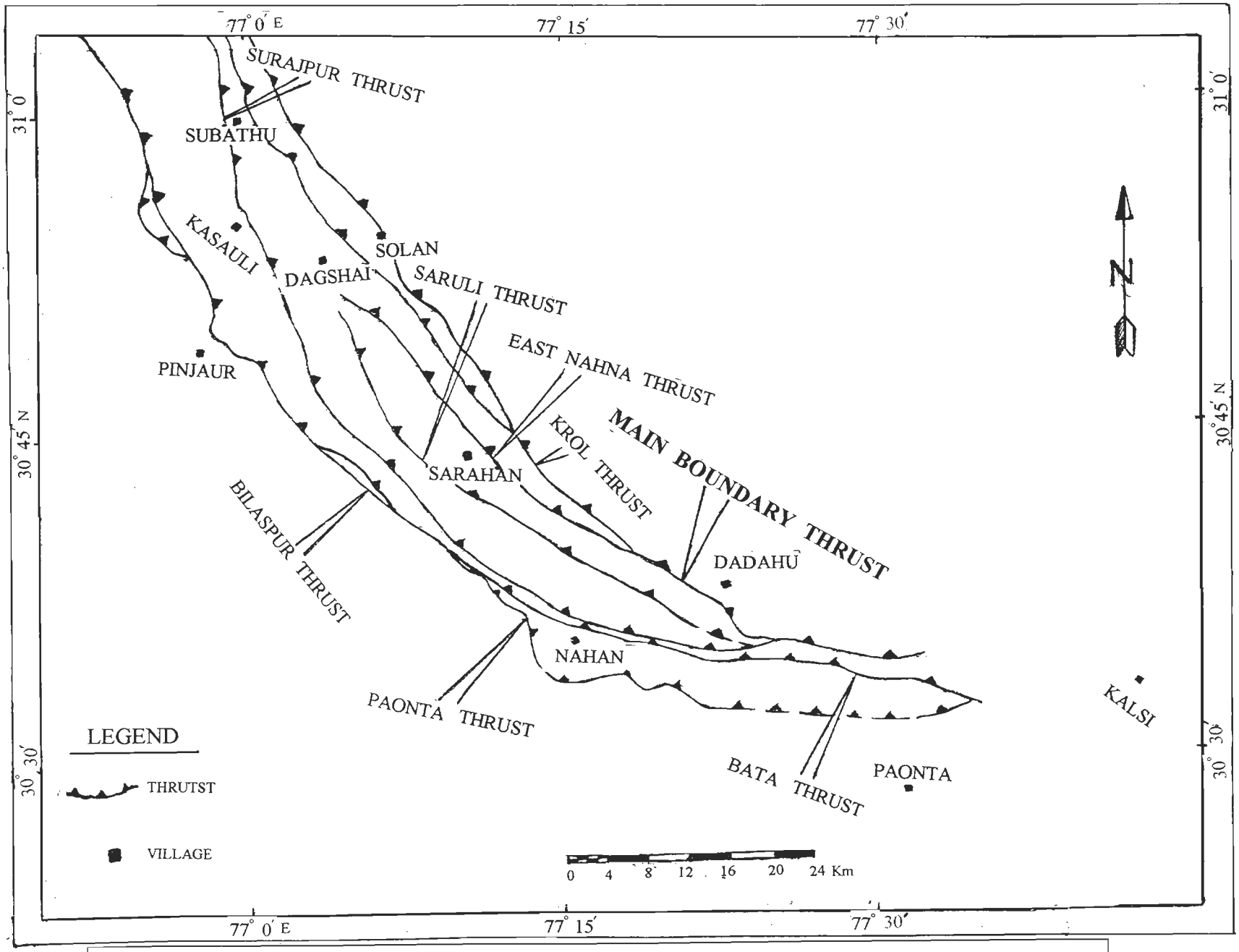

Figure 2.8- Structural map of area understudy (after Raiverman et al., 1983).

2.5 CONCLUDING REMARKS

The area understudy is the southernmost part of the Himalayan foreland basin. It is made of the following formations: the Subathu, the Dagshai, the Kasauli and the Lower Siwalik.

(i) The Subathu consists of green shale, gray marl, sandstone, limestone and occasional white sandstone. It shows three lithologically distinct facies, which are black-gray, green and red from bottom to top, respectively. Shale/siltstone sequence of the Subathu Formation breaks into lead pencil-type fragments. The Subathu Formation is deposited in a shallow marine at around 64 to 40 Ma. The contact between the Subathu and pre-Cenozoic rocks is disconformity. The transition between the Subathu and the Dagshai formations may seems to be abrupt but there is no discontinuity. The Dagshai Formation consists of thick alternative sequence of red shale, and hard, fine grained impure sandstone. The Dagshai sediments are deposited in brackish, fresh water or distal alluvial fan and fluvial system. The deposition time of the Dagshai is ambiguous ~30 Ma to 24 Ma.

(ii) The Kasauli Formation presents an alternation of massive gray to buff micaceous sandstone and purple/ gray shale. The lower contact of the Kasauli with the Dagshai is transitional, but the upper contact with the Lower Siwalik is a thrust. The Kasauli sediments are deposited in alluvial fan or fresh water at 23.8 Ma.

(iii) The Lower Siwalk sediments are unconsolidated to semiconsolidated in character and consist of alternating sandstone, shale/siltstone and a few conglomerate beds in the upper part. The Lower Siwalik Formation was deposited in alluvial plains in dry and wet seasons. Its depositional age is ca. 15 to 10 Ma. The paleocurrent patterns of the pre-Siwalik and the Lower Siwalik rocks is from north to south.

(iv) The Main Boundary Thrust has played an important role in juxtaposition of different stratigraphic horizons and tectonic units with the Siwalik Group. Its activity started in Middle Miocene time (18.7-11.7 Ma) and reached to its peak activity around 4-5 Ma.

CHAPTER - 3

PETROGRAPHIC STUDIES

3.1 INTRODUCTION

Lithologically, various stratigraphic units of Cenozoic consist of clastic sedimentary rocks. The Subathu Formation (Paleocene-Late Eocene) is mainly argillaceous (green, red and gray) with minor siltstone/sandstone. The overlying Dagshai Formation (Late Eocene-Early Miocene) mainly consists of gray to purple clay and purple/greenish sandstone followed by Kasauli Formation (Early-Middle Miocene) which mainly comprises of the pale/gray to buff micaceous sandstone and purple/gray shale in minor. The overlying Lower Siwalik forms alternations of shale/clay/siltstone and sandstone. The petrographic studies of these rocks in terms of their constituents are presented herewith.

3.2 SANDSTONE

The sandstone of the exposed sediments in the area under study have been studied mainly with a view to find their provenance and to differentiate various formations on the basis of light, heavy minerals and rock fragments. The investigations are also aimed at deciphering sandstone units which may provide samples for fission track studies.

In order to decipher the constituents and the provenance of arenaceous rocks, 22 samples of sandstone from the Subathu (6), Dagshai (6), Kasauli (6) and Lower Siwalik (4) units were subjected to detailed modal analysis following the Gazzi-Dickinson method (Ingersole et al., 1984). Grain parameters, quartz, feldspar, lithic, aphanitic grains are the same as those of Ingersole and Suczek (1979) and Critelli and Garzanti (1994) were investigated for 22 selected thin sections. 500-600 points were counted by the Swift-Point Counter, Model F and with the leech microscope (Leitz Labour Lux, 12 pols) for each thin section (Tables 3.1-3.4).

3.2.1 Subathu Formation

The sandstone of the Subathu Formation exhibits various colours varying from white (at the top, forming key bed) to greenish, to red in other parts. It alternates with the shales varying in colour from red, greenish and gray. These sandstones are very hard and medium to fine grained size. The petrographic constituents as studied under microscope are indicated in the Figures 3.1a, 3.1 b.

Light minerals- Quartz is the most dominant constituent of sandstone. It varies from 49% to 86%. Both monocrystalline and polycrystalline varieties of grains are found in these sandstones. The monocrystalline quartz is the major component which at times is replaced by calcite.

Feldspar grains vary from trace to 1.3%. Plagioclase occurs as the main component with the composition of oligoclase (An = 18%). Potash feldspar also is present as fresh grains in some samples.

Heavy minerals - Amongst the heavy minerals, zircon, tourmaline, epidote, glauconite, and oxides (mainly magnetite) are the main constituents (Figs.3.1c, 3.1d). The zircon and tourmaline occur both as euhedral to rounded grains. The zircon crystals are colourless to pinkish.

Mica, both biotite and muscovite and chlorite are also observed, besides serpentine and glauconite.

Rock fragments include fine to coarse grained lithic fragments. Fine grained lithic fragments are both the metamorphic lithics (slate and phyllite) and the sedimentary lithics (as chert). The coarse grained lithic fragments are quartzite and metamorphic lithic.

The *matrix* is generally less than 15% and consists of clay, sericite and quartz.

The *cement* in these sandstones is mainly siliceous and calcitic (sparite) forming negligible to about 29% of the bulk composition. There appears to be a definite order in which different types of cement were formed. Silica was initially precipitated, followed by siliceous (chert) and calcite cements, respectively.

Table 3.1 Modal Constituents (in %) of Sandstones of the Subathu Formation

Parameter	Sample no.					
	28	32	35	61	62	64
Qz – Monocrystalline	76.9	70.7	86.1	84.8	49.5	49.0
Qz – Polycrystalline	T	-	T	-	-	2.3
Plagioclase	T	T	-	-	T	1.3
Potash Feldspar	-	-	-	-	-	T
Metamorphic Fragment	5.5	5.7	-	-	-	3.1
Chert	T	-	-	-	-	-
Oxide (Iron)	T	2.7	T	T	4.5	1.8
Mica	T	11.8	-	-	-	1.3
Serpentine	-	0.3	-	-	-	-
Zircon	T	T	T	0.2	0.7	T
Glauconite	T	-	-	-	2.0	-
Zoisite	-	0.6	-	-	-	-
Tourmaline	-	-	T	-	T	-
Calcite Sparite (cement)	-	-	-	-	29.2	28.8
Clay + Sericite	14.5	8.1	12.8	14.8	13.6	12.0

Note: T= Trace

Table 3.2 Modal Constituents (in %) of Sandstones of the Dagshai Formation

Parameter	Sample no.					
	6	9	19	23	33	42
Qz – Monocrystalline	39.8	37.2	50.3	50.4	47.3	50.5
Qz – Polycrystalline	15.0	6.8	4.4	T	T	-
Plagioclase	1.9	1.4	1.5	1.3	2.7	T
Potash Feldspar	1.2	T	-	-	-	-
Metamorphic Fragment	7.5	9.2	18.1	19.4	17.6	10.8
Volcanic Fragment	-	T	-	-	-	-
Sedimentary Fragment	-	T	T	-	-	-
Chert	T	T	-	T	-	-
Oxide (Iron)	3.3	2.6	1.2	0.5	2.8	3.4
Mica	-	1.7	T	T	0.8	1.4
Serpentine	-	-	-	-	-	T
Apatite	-	-	-	T	T	-
Zircon	T	T	T	T	T	T
Tourmaline	T	T	T	T	T	T
Pyroxene	-	-	-	-	T	-
Calcite Sparite (cement)	1.0	16.1	-	0.7	1.7	0.6
Clay + Sericite	29.6	22.0	24.3	26.6	26.1	32.9

Note: T= Trace

Table 3.3 Modal Constituents (in %) of Sandstones of the Kasauli Formation

Parameter	Sample no.					
	11	12	26	27	37	40
Qz – Monocrystalline	39.2	52.9	52.8	47.2	53.1	37.0
Qz – Polycrystalline	4.2	0.7	2.2	-	T	-
Plagioclase	1.7	2.7	1.7	1.6	3.3	3.4
Potash Feldspar	0.9	0.9	-	-	-	-
Metamorphic fragment	21.0	19.2	17.0	18.2	21.5	20.0
Sedimentary fragment	-	-	-	T	-	-
Chert	-	-	-	T	-	-
Oxide (Iron)	T	5.6	1.5	T	6.0	T
Mica	2.4	1.1	1.0	1.8	1.9	4.2
Serpentine	-	-	T	-	-	-
Apatite	-	-	-	-	T	-
Zircon	T	T	T	T	T	T
Glauconite	T	-	-	T	-	-
Fe-mineral	-	-	-	-	-	T
Zoisite	-	-	-	-	T	-
Garnet	-	-	-	-	0.7	-
Tourmaline	T	T	T	T	T	T
Calcite Sparite (cement)	-	3.8	-	-	2.5	0.7
Clay + Sericite	30.2	13.1	23.4	30.0	10.7	33.6

Note: T= Trace

Table 3.4 Modal Constituents (in %) of Sandstones of the Lower Siwalik Formation

Parameter	Sample no.			
	99	101	1	5
Qz – Monocrystalline	31.0	31.6	40.2	48.6
Qz – Polycrystalline	6.9	3.9	6.3	3.6
Plagioclase	3.0	3.0	3.2	2.9
Potash Feldspar	1.8	1.8	1.7	1.9
Metamorphic Fragment	6.3	10.8	11.0	9.0
Volcanic Fragment	T	1.4	T	-
Sedimentary Fragment	6.7	14.4	6.5	-
Chert	T	T	-	T
Oxide (Iron)	3.6	2.0	-	-
Mica	1.8	2.5	8.0	9.0
Serpentine	T	-	-	-
Apatite	T	T	T	T
Zircon	T	T	T	T
Glauconite	-	T	-	-
Fe-mineral	-	-	T	-
Zoisite	-	T	-	-
Garnet	-	T	-	-
Tourmaline	T	T	T	T
Pyroxene	-	T	-	-
Calcite Sparite (cement)	27.5	28.2	21.6	T
Clay + Sericite	10.1	-	T	24.1

Note: T= Trace

Table 3.5 Re-Calculated Point Counted Data (Petrographic Parameters after Ingersoll and Suczek, 1979)

Sample no.	QFL (%)			QmFLt(%)			QmPK(%)			LmLvLs(%)		
	Qt	F	L	Qm	F	Lt	Qm	P	K	Lm	Lv	Ls
Subthu Fm.												
28	92.0	0.2	7.8	91.7	0.2	8.1	99.7	0.3	-	84.6	-	15.4
32	91.9	0.7	7.4	91.9	0.7	7.4	99.3	0.7	-	100.0	-	-
35	99.4	0.6	-	99.4	-	0.6	100.0	-	-	100.0	-	-
61	100.0	-	-	100.0	-	-	100.0	-	-	100.0	-	-
62	99.6	0.4	-	99.6	0.4	-	99.6	0.4	-	100.0	-	-
64	92.3	2.6	5.1	83.2	2.5	14.3	97.0	2.6	0.4	50.8	-	49.2
X	95.9	0.7	3.4	94.3	0.6	5.1	99.3	0.7	0.1	89.2	-	10.8
S.D.	4.2	0.9	3.8	6.7	1.0	5.8	1.1	1.0	0.2	19.8	-	19.8
Dagshai Fm.												
6	83.2	4.6	12.2	60.3	4.7	35.0	92.5	4.4	3.1	92.6	-	7.4
9	78.8	3.0	18.2	66.5	3.1	30.4	95.6	3.6	0.8	90.2	2.9	6.9
19	73.1	2.0	24.9	67.3	2.0	30.7	97.1	2.9	-	97.3	-	2.7
23	70.9	1.8	27.3	70.2	1.8	28.0	97.5	2.5	-	98.5	-	1.5
33	70.3	3.9	25.8	69.2	4.0	26.8	94.6	5.4	-	100.0	-	-
42	82.1	0.3	17.6	82.1	0.3	17.6	99.6	0.4	-	100.0	-	-
X	76.4	2.6	21.0	69.3	2.6	28.1	96.1	3.2	0.6	96.4	0.5	3.1
S.D.	5.7	1.6	5.9	7.2	1.6	5.9	2.5	1.7	1.2	4.1	1.2	3.3
Kasauli Fm.												
11	64.8	3.9	31.3	58.0	3.9	37.6	93.8	4.1	2.1	100.0	-	-
12	70.2	4.7	25.1	69.2	4.7	26.1	93.6	4.8	1.6	100.0	-	-
26	74.6	2.3	23.1	71.6	2.3	26.1	96.9	3.1	-	100.0	-	-
27	69.8	2.4	27.8	69.7	2.4	27.9	96.7	3.3	-	96.3	-	3.7
37	68.3	4.2	27.5	68.0	4.2	27.8	94.1	5.6	-	100.0	-	-
40	61.3	5.6	33.5	61.3	5.6	33.5	91.6	8.4	-	100.0	-	-
X	68.2	3.9	28.0	66.4	3.9	29.8	94.5	4.9	0.6	99.4	-	0.6
S.D.	4.6	1.3	3.8	5.2	1.3	4.7	2.0	2.0	1.0	1.5	-	1.5
L-Siwalik Fm.												
99	67.3	8.3	24.4	55.0	8.3	36.7	86.8	8.1	5.1	45.7	4.3	50.0
101	53.1	7.1	39.8	47.1	7.2	45.7	86.8	8.3	4.9	40.3	5.2	54.5
1	67.1	7.1	25.8	58.0	7.1	34.9	89.1	7.1	3.8	61.5	2.2	36.3
5	79.2	7.2	13.6	73.2	7.2	19.6	91.0	5.4	3.6	95.7	-	4.3
X	66.7	7.4	25.9	58.3	7.5	34.2	88.3	7.2	4.4	60.8	2.9	36.3
S.D.	10.7	0.6	10.8	10.9	0.6	10.8	2.2	1.3	0.8	24.9	2.3	22.7

Fm.- Formation, $\bar{X}$- means value, S.D.- standard deviation, Qt - total Quartz (Qm= monocrystalline, Qp= polycrystalline, including chert), F- total feldspar (P = plagioclase, K= feldspar), L- aphanitic lithics (Lm= metamorphic, Lv = volcanic; Ls = Sedimentary, including chert), Lt-total aphanitic lithic grains(= L + Qp) (Ingersoll and Suczek, 1979; Critelli and Garzanti, 1994).

3.2.2 Dagshai Formation

Sandstones of the Dagshai Formation vary in colours from olive to pale-red. They alternate with the red-shale. They are hard and medium to fine grained. The petrographic characteristics are given below.

Light minerals - Quartz grains form the main component of the bulk of composition, varying from 44% to 55%. The monocrystalline form (Figs. 3.1e, 3.1g) is the main type of quartz as compared to polycrystalline variety. These are at times replaced by calcite.

Amongst the feldspar, the palgioclase is the main feldspars in these sandstones. It ranges from trace to 3.1% and are mainly oligoclase in composition (An = 18%). Plagioclase crystals, in some cases, altered to sausurite. Orthoclase also, in some samples, is observed.

Heavy minerals - Quartz grains form the main component of the bulk of composition, varying from 44% to 55%. The monocrystalline form (Figs. 3.1e, 3.1g) is the main type of quartz as compared to polycrystalline variety. These are at times replaced by calcite.

Amongst the feldspar, the plagioclase is the main feldspars in these sandstones. It ranges from trace to 3.1% and are mainly oligoclase in composition (An = 18%). Plagioclase crystals, in some cases, altered to sausurite. Orthoclase also, in some samples, is observed.

The most important of other constituents is mica (biotite and muscovite) and chlorite. The main source of chlorite is due to alteration of biotite.

Heavy minerals- The dominant heavy minerals are zircon, apatite, zoisite, garnet and tourmaline as well as oxides (Fig. 3.1 h). Tourmaline and zircon crystal grains vary in shape as euhedral to rounded forms. The colour of zircon grains indicates a wide range from colourless to reddish.

Rock fragments- Fine grained lithic fragments are mainly metamorphic lithics which include slate and phyllite. Sedimentary fragments appear as chert. Also, the coarse grained lithic fragments form assemblages of quartz and mica with the plutonic or gneissic (metamorphic) sources.

Matrix - It mainly consists of clay, sericite and quartz. It varies from 22-30%. *Cement* in the sandstone consists of ferruginous, siliceous and calcite (sparite). It varies from 1% to 16%. Silica is the first phase of cement, which is followed by ferruginous, siliceous and then calcite cements.

3.2.3 Kasauli Formation

The Kasauli Formation is composed of hard, medium to fine grained greenish sandstones alternating with shale. Compositionally quartz is the main mineral followed by rock fragments, feldspar and calcite (Table 3.3).

Light minerals - It includes of quartz and feldspar. Quartz varies from 37 to 53% of the bulk composition. It occurs as the monocrystalline and polycrystalline types. The monocrystalline form of quartz is the main component. It occurs in rounded, subrounded and angular forms (Fig. 3.2 a, 3.2 b).

Plagioclase (An = 16%) with 1.7 to 3.4% is the main variety of feldspar. Its crystals occur generally in euhedral form. Orthoclase is the main type of potash feldspar. Microcline is also found to be in very small amounts. Most of feldspar crystals are fresh (Fig.3.2 b).

Amongst the other constituents, mica, biotite and muscovite, serpentine, chlorite and glauconite are found in minor amounts. Chlorite and serpentine, most probably, are due to alteration of biotite and Fe-Mg minerals, respectively.

Heavy minerals - Zircon, garnet, tourmaline and oxides are the main components of heavy minerals. The garnet grains are found as well formed and well developed crystals, pinkish in colour. Zircon and tourmaline vary from well developed crystals to rounded grains. Zircon grains show a wide spectrum of colours, varying from colourless to reddish colour (Fig. 3.2 c).

Rock fragments - They form two separate groups:

i) Fine grained lithic fragments in order of abundance are metamorphic lithics (slate, phyllite and garnet mica schist) and sedimentary fragments (chert and shale).

ii) Coarse grained lithic, represented by quartz assemblages and mica with the source from plutonic and metamorphic rocks.

Matrix consists of clay, sericite, quartz, which form about 12 to 30% of the total constituents. *Cement* forms up to 4% of the bulk composition of these sandstones. It is mainly calcite (sparite), ferruginous and siliceous. The first formed cement was siliceous followed respectively by, ferruginous, siliceous (chert) and calcite.

Figure 3.1- Photomicrographs of main framework grains, and some of heavy minerals of Subathu Formation (a, b, c, d) and Dagshai Formation (e, f, g, h). Monocrystalline Q_z (A), chert (C), polycrystalline Q_z (D), calcite spary (E), replacement of Q_z by calcite (F), matrix (M), tourmaline (T), zircon (Z), oxide (O), metamorphic lithic fragment (H), chloritization of biotite (I), plagioclase crystal (N),

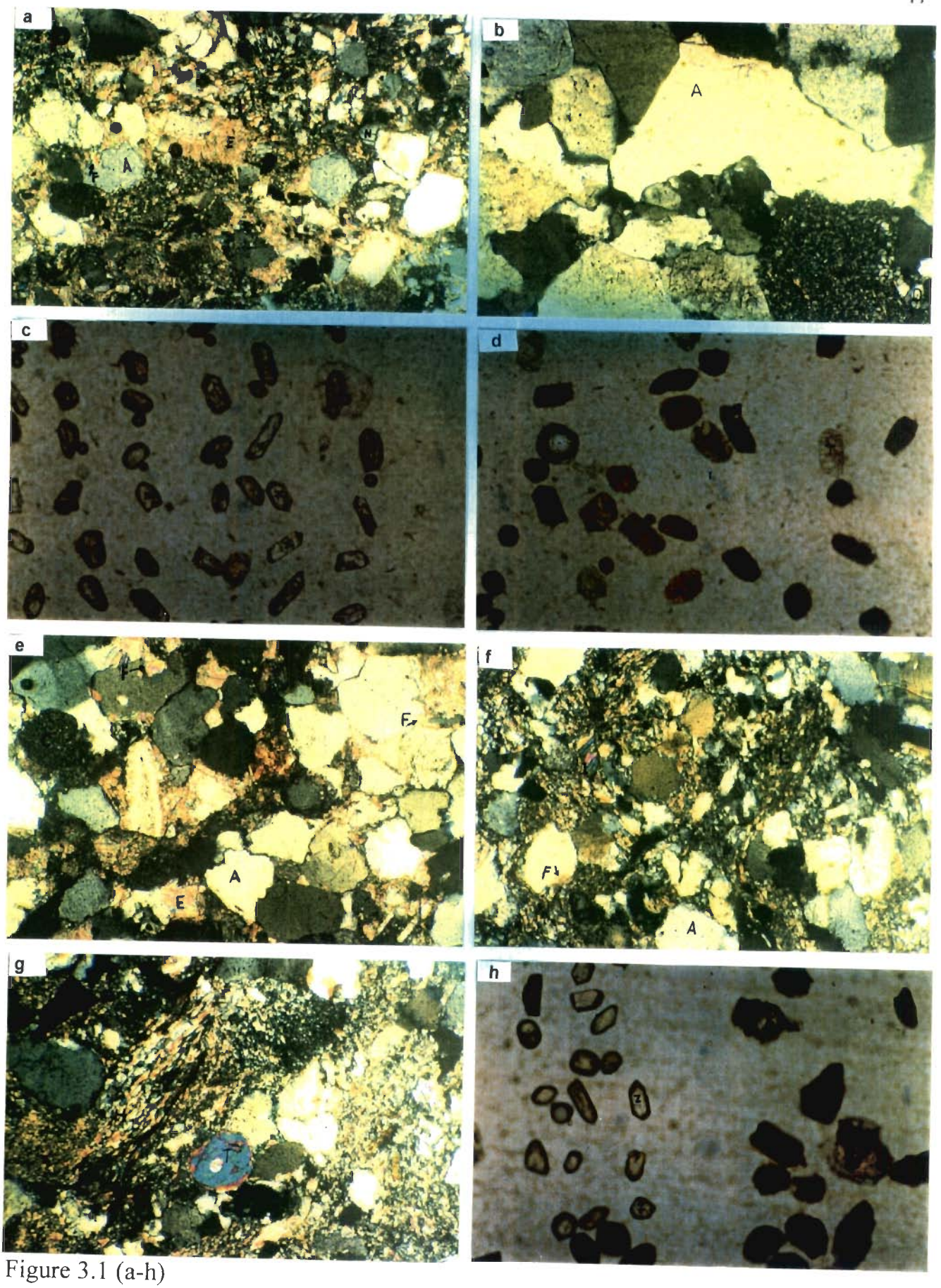

Figure 3.1 (a-h)

3.2.4 Lower Siwalik Formation

The Lower Siwalik sandstones are gray to yellowish with the coarse to medium grain size. The hardness of the sandstones decreases up section. The petrographic constituents as identified are given below (Figs. 3.2 d - 3.2 g).

Light fragments form the bulk of composition of the sandstones in thin section. Quartz is the most dominant mineral, followed by rock fragments, calcite, mica and feldspar.

Quartz grains occurring mainly as angular form ranges between 34 to 52% of the bulk composition. Though, both monocrystalline and polycrystalline quartz are observed, the monocrystalline variety is dominant. In some cases, it was replaced by calcite. Feldspars are common and vary from 5 to 8%. Plagioclases are more frequently encountered as compared to potash feldspars. The plagioclases are mainly sodic (Na% = 82-77). Orthoclase is the prominent variety of potash feldspar. Microcline is found to be in very small amounts.

Plagioclase grains are coarse and angular. Both fresh and altered grains of feldspar are observed. Commonly the alteration product of plagioclase is sausurite. Plagioclase crystals are replaced partially by calcite. Potash feldspars are altered to sericite and clayey mass.

Amongst the other constituents, mica, as biotite and muscovite, in the form of flakes and chlorite is observed. Biotite in a few cases bends around quartz grains, indicating compaction of sediments (Fig. 3.2 f). Biotite and chlorite, both are often altered to iron oxide. These minerals do not exceed 9% of the bulk composition.

Heavy minerals- Zircon, garnet, tourmaline and apatite were identified in the heavy fraction of these samples. Garnet occurs as well developed crystals. Zircon and tourmaline (Fig. 3.2 h) occur as well formed and preserved crystals as well as rounded grains. Zircon crystals show a spectrum of colours from colourless to reddish. Apatite is found in the elongated, well developed form. Besides these heavy minerals, oxides, staurolite, epidote, and glaunconite are also found.

Rock fragments - They are found as two types: (i) Fine grained lithic fragments which include, in order of abundance, low grade metamorphic fragments (slate, chlorite schist and sericitoschist), sedimentary fragments (chert, chloritic sandstones and micritic calcite) and volcanic fragments showing needle form of plagioclase in the glass mass (porphyry texture, Fig.

Figure 3.2- Photomicrographs of main framework grains, and the dominant heavy minerals of Kasauli Formation (a, b, c) and Lower Siwalik Formation (d, e, f, g, h). Monocrystalline Q_z (A), chert (C), polycrystalline Q_z (D), calcite spary (E), replacement of Q_z by calcite (F), matrix (M), tourmaline (T), zircon (Z), metamorphic lithic fragment (H), chloritization of biotite (I), oxide (O), slate fragment (I), sausuritization of plagioclase (M), plagioclase crystal (N), micritic limestone lithic (ML), lathwork volcanic fragment (V), biotite flake (R).

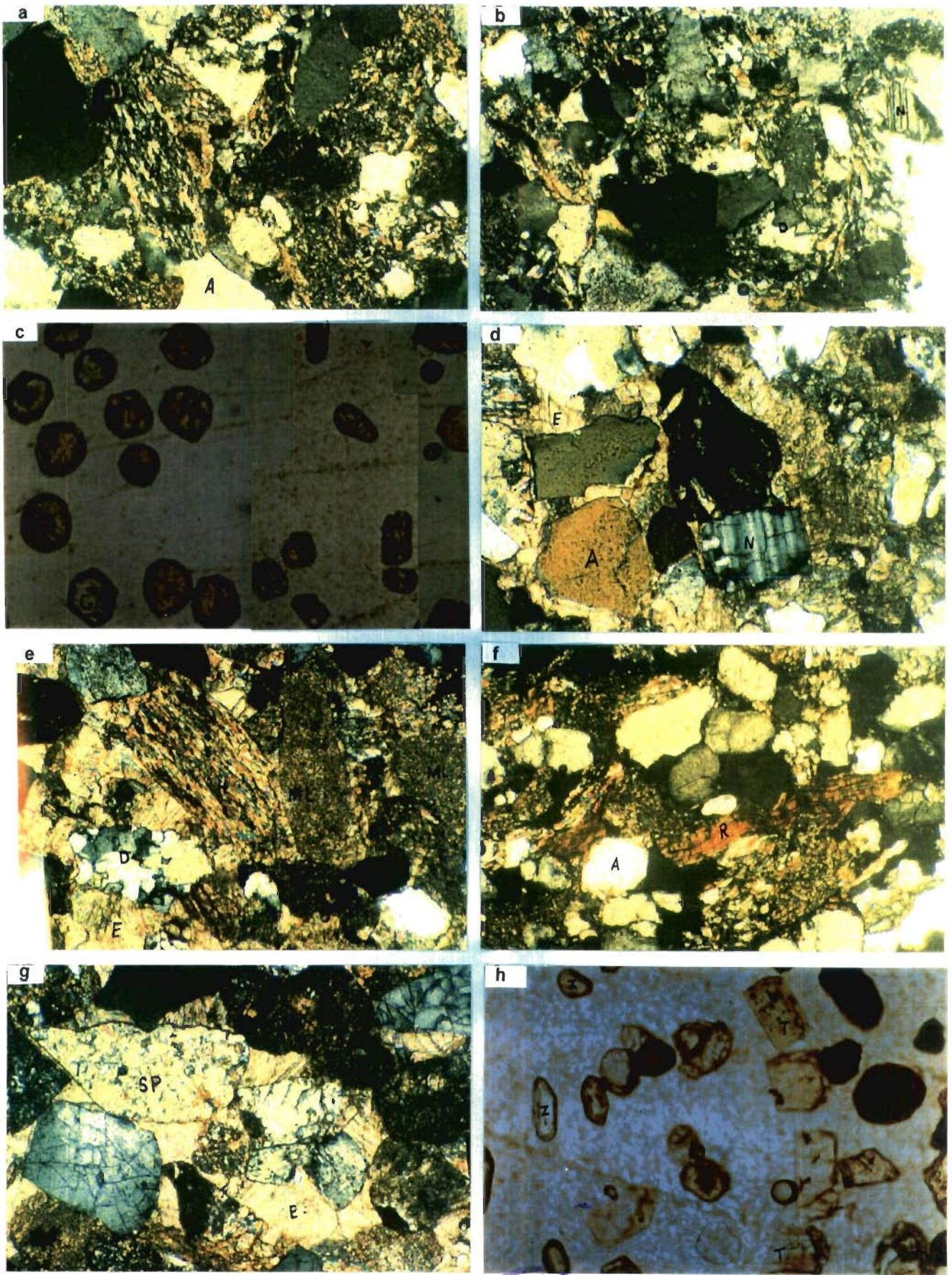

Figure 3.2 (a-h)

3.2 d). (ii) The coarse grained lithic fragments occur as plutonic and metamorphic lithics consisted of quartz and mica with the amigdal or granular texture.

Matrix consists of clay, sericite and calcite (Fig. 3.2 f). It occurs as trace at sections but may form up to 24% of the bulk composition.

Cement forming negligible to 28% of the bulk composition, is mainly calcitic and siliceous. Silica was the first to precipitate, followed by calcite cements.

3.3 CLASSIFICATION AND PROVENANCE OF SANDSTONE

3.3.1 Classification

A number of classifications of sandstone have been proposed from time to time. Some of the important classification diagrams that are in use, are the ones given by krynine (1948), Gilbert (1955), Mc Bride (1963) Pettijohn (1975), and Folk (1980).

In the present study the Folk's classification (1980) has been used to classify the sandstone. The data retrieved from the modal analysis of selected samples (Table 3.5) have been plotted in the triangular Q (quartz), F (feldspar) and RF (rock fragments) diagrams (Fig. 3.3). These plots indicate that the sandstones of Cenozoic formations of the area under study may be designated as quartzite and sublitharenite for the Subathu Formation. Sublitharenite and litharenite constitute the Dagshai Formation and sandstones of the Kasauli and Lower Siwalik formations are mainly the litharenite. With the younging of formations the metamorphic rock fragments increase. However, considering framework constituents and matrix classification (Pettijohn, 1975), sandstone samples may be classified as: quartz arenite, sublitharenite (Subathu), lithic graywacke (Dagshai), lithic graywacke and litharenite (Kasauli and Lower Siwalik formations).

3.3.2 Provenance

An attempt has been made to identify the source of sandstones of Cenozoic sedimentary grains using detrital constituents such as quartz, feldspar, heavy minerals and rock fragments as well as the QFL diagram.

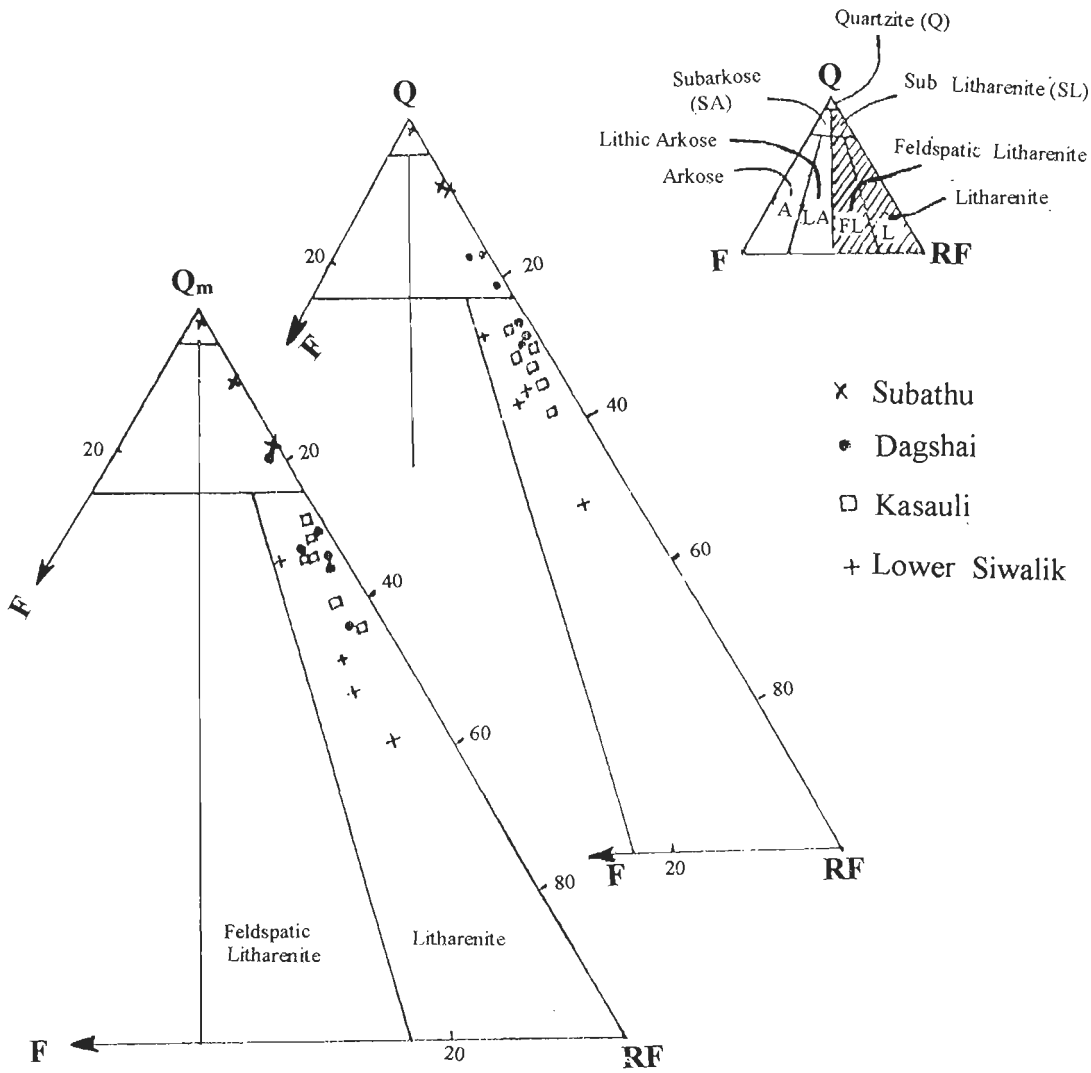

Figure 3.3- Folks (1980) subdivisions of lithic sandstones. Classification utilizing only framework grains. Main components are quartz (Q), feldspar (F), and rock fragments (RF).

Quartz- Amongst the lighter minerals, detrital quartz is found in almost all types of classic rocks. In view of its abundance and ubiquitous distribution in detrital rocks it can prove to be a useful indicator of provenance.

The undulosity of quartz together with the abundance of vacuoles, the composite nature of grains, the shape and the nature of the boundary of quartz grains and their overgrown part

have also been used to know about the probable source rock of these sediments. This line of approach suggests the following provenance:

(i) The occurrence of single crystal units showing more/less straight extinction and having very few vacuoles might have come from acid plutons (Krynine, 1940), both coarse grained igneous and recrystallized gneissic rocks. There are some quartz grains containing abundant vacuoles which suggest their origin from pegmatite and vein quartz.

(ii) Some polycrystalline quartz grains with crystal units having straight boundaries and showing straight to slightly undulose extinction, might have originated by recrystallization as a result of elevated temperatures and little shearing stress (Todd, 1964).

(iii) The occasional occurrence of polycrystalline quartz grains with crystal units having satured or crenulated borders and showing strong undulose extinction, are pressure metamorphic quartz. This type of quartz as Todd (1964) opines is the one which has been subjected to only shearing stresses and not the lithostatic pressure.

Feldspar- Detrital feldspars are subordinate, indicating very little contribution from infracrustal rocks. Orthoclase, microcline and plagioclase feldspar (sodic in nature) indicate mainly acidic igneous source rocks. Occurrence of perthite, though very rare, is suggestive of an acid igneous plutonic source rocks (Table 3.6).

Heavy minerals are the most useful indicators provenance. Amongst the heavy minerals, tourmaline, zircon, garnet and iron oxide as mentioned earlier, form the most dominant fraction.

The dark brown and green variety of tourmaline occurs most commonly and might have come from plutonic igneous rocks-granitic in nature (Krynine, 1946). This is also evidenced by the occurrence of zircon, rutil and sphen. The blue tourmaline is indicative of a pegmatite source rock (Krynine, 1946). Garnet, probably support this inference. The yellowish tourmaline points towards low grade metamorphism source rocks.

Table 3.6 Provenance From Petrographic Constituents

Petrographic Parameters	Stratigraphic Units			
	Subathu	**Dagshai**	**Kasauli**	**Lower-Siwalik**
Quartz	Single grains, straight and undulose extinction (very few crystals), straight contact, without vacuole Polycrystalline, undulose, with crenulated border, greater than 3-units	Single grains, straightand undulose extinction, coated with oxide, straight contact, crenulated, a few grains rich of epidote and mica. Poly crystalline, undulose & straight extinction greater than 3-units with crenulated orders	Single grains, Straight and Undulose extinction with vacuoles, over growth, contact straight. Polycrystalline, 3-units and higher, contact straight & crenulate.	Single grains, straight and undulose extinction, without vacuole and with vacuole, Hexagonal form. Polycrystalline, undulose, and straight extinction, straight & crenulated contact, 3-units & higher
Feldspar	Plagioclase (sodic) & Orthoclase (T)	Plagioclase (sodic) & Orthoclase	Plagioclase (sodic) & Orthoclase (pertite) & Microcline	Plagioclase (sodic), Orthoclase (pertite), & Microcline
Rock Fragments	Metamorphic (Slate, Phyllite, Gneissic/ granitic), Sedimentary (Chert, Quartzite)	Metamorphic (Slate, Phyllite), Sedimentary (Chert, shale, Quartzite), Igneous (Granitic)	Metamorphic (Slate, Phyllite, Garnet mica Schist), Igneous (Granitic/ Gneissic) Sedimentary (Chert, Quartzite),	Metamorphic (Slate, Phyllite, Staurolite & Sericito Schist) Plutonic (Granitic/ Gneissic) Sedimentary (Chert, Quartzite, Micritic Limestone) , Volcanic Porphyric (Andesite/Dacite)
Heavy Minerals	Tourmaline: Green, dark-brown, yellow, Rounded & well-developed Zircon: Well developed & rounded; Oxide: Well-developed (octahedral form) & amorphose	Tourmaline: Green, dark-brown, rounded & well-developed Zircon: Well developed & rounded Oxide: Coated grains & amorphose Apatite	Garnet: Well developed Tourmaline: Green dark-brown, yellow, Rounded & well-developed Zircon: Well developed & rounded Oxide Apatite	Garnet: Well developed & rounded; Staurolite, Epidote, Sphene (T), Tourmaline: Green, dark-brown, yellow, rounded & well-developed Zircon: Well developed & rounded; Oxide Apatite (elongate & rounded form)
(Provenance)	Acid igneous rocks & basic rocks Metamorphic (low-grade), Re-cycled sediments	Plutonic (Granitic), Metamorphic (low – grade), Re-cycled sediments	Plutonic (acid); Metamorphic (low – medium grade) Re-cycled sediments	Metamorhpic (low - high grade), Plutonic (acid), Sedimentary (re-cycled), Volcanic (andesitic/ dacitic

The occurrence of garnet indicates a relatively high rank metamorphic parent rock. The presence of magnetite is indicative of basic source rocks. The rounded tourmaline and zircon indicate that they might have come from preexisting sedimentary or meta sedimentary rocks.

Rock fragments provide a direct evidence of provenance of the sedimentary rocks. Amongst rock fragments, granite, schist, phyllite, slate, and quartzite, have been identified which may be considered as the source rock for sandstones of the Cenozoic sediments. These observations confirm the inference drawn about the provenance from the study of quartz and feldspar. Although the fragments of low grade metamorphic rocks, sedimentary rocks and plutonic igneous rocks are found in the entire Cenozoic sediments. Low grade metamorphic lithics (mainly phylites) are most abundant in the Kasauli Formation. In the Lower Siwalik sandstones contribution from new source rock in the form of volcanic fragments occurring as lathwork (andesitic-dacitic composition), is notable besides the above sources.

Summing up, therefore, it may be concluded that a variety of source rocks namely the low grade metamorphic rocks (slate, phyllite), sedimentary rocks, plutonic igneous rocks (granite) and high grade metamorphic rocks (gneiss) supplied sediments to the Cenozoic basin (Table 3.6). Further, the plots on QFL diagram (Fig. 3.4) of Critelli and Garzanti (1994) exhibit conspicuous patterns of these modal constituents from the Subathu to Siwalik formations in the re-cycled orogenic field in this plot. Similar observations have been made by other workers, e.g. Chaudhri (1971 b), Parkash et al. (1980), Critelli and Garzanti (1994) in other areas. Sandstone petrography testifies that in the earliest stage of continental collision, detritus was largely derived from low grade metamorphism. Towards, the later stages of collision (Siwalik time), it was associated with the higher grade of metamorphism and also increasing the amount of metamorphic particles, and decreasing of quartz grains. Increasing of detritus feldspar and polycrystalline quartz through time in the younger formations indicate progressive upliftment and erosion of source area resulting in exposure of and shedding from the infracrustal crystalline rocks.

3.4 CLAY MINERAL STUDIES

3.4.1 Introduction

In the present study an attempt has been made to identify clay minerals in the shales and the sandstones of various formations and work out the changes that they undergo due to the burial of sediments.

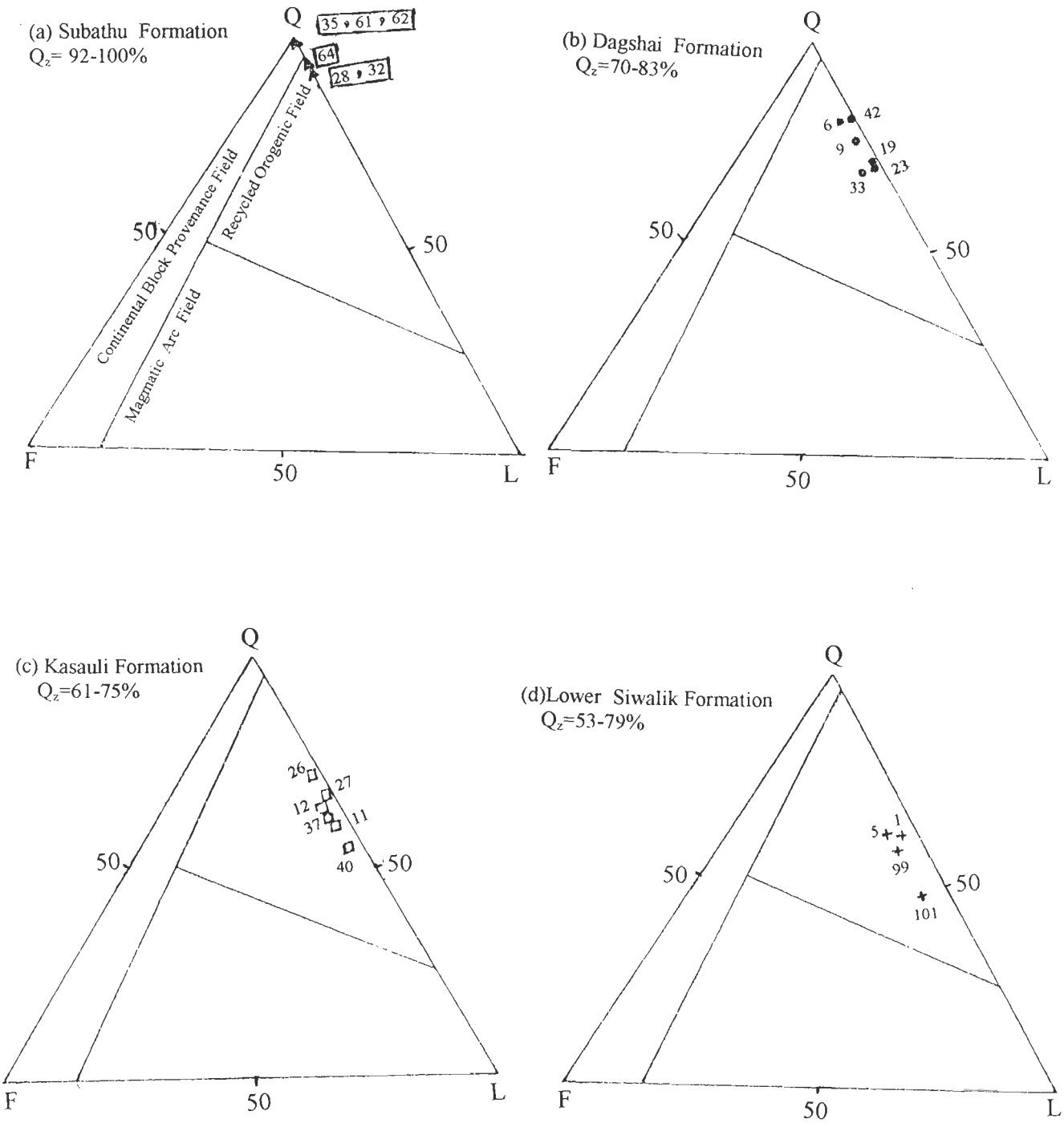

Figure 3.4- Detrital modes of Tertiary sandstones on QFL plot of Critelli and Garzanti (1994). (a) Subathu, (b) Dagshai, (c) Kasauli, and (d) Lower Siwalik formations. All of data are placed in the recycled orogenic field, with this characteristic that lithic fragments increase with decreasing age. It suggests the continuous rising up of Himalaya.

Amongst the various methods of study of clay minerals, the X-ray diffraction (XRD) provides the most satisfactory method for the analysis of clay minerals.

Before attempting to achieve the mentioned aims, the principles of clay mineral identification and their usefulness is discussed herewith.

3.4.2 Principles

Clay minerals consist of minute crystals, which are made up of ordered arrays of atoms. A monochromatic beam of X-rays passing through a mineral grain in scattered by the atoms that compose the mineral. At specific angles of incident, the scattered X-rays are in phase producing an intensified secondary beam. This phenomenon is known as diffraction.

Diffraction occurs when the distance traveled by one scattered beam is different (by a length equal to the X-ray wavelength) from the distance traveled by another scattered by an adjacent plane of atoms. This diffracted beam is called a *first-order reflection*. Diffraction also occurs when the difference in distance traveled by X-rays scattered from two adjacent layers of atoms equals two wavelengths. The resultant beam is called a *second order-reflection*. Higher-order reflections occur each time when the path difference is a whole-number multiple of the wavelength. The general relationship is expressed by the Bragg equation.

$$n\lambda = 2d \sin \theta \qquad \text{(Bragg's Law)}$$

Where n is whole number, λ is the X-rays wavelength, d is the distance between planes of atoms (A^{o}) and θ is the angle of incident.

When clay sample (slide) is placed in the diffractometer, the direction of the primary X-rays beam remains constant as the sample rotate around an axis normal to the primary beam. Diffracted beams that arrived at the detector tube, attached to a goniometer are recorded as peaks on a strip chart. The diffractometer is one scattered beam designed that the goniometer arm and the attached detector tube rotate at twice the rate of the sample. Thus, as the sample rotates through a angle of θ, the detector tube rotates through 2θ, which is the angle read on the goniometer (Fig. 3.5). The geometrical arrangement of the diffractometer is such that only mineral grains whose lattice planes are parallel to the surface of the specimen holder will contribute secondary beams that enter the detector tube.

Identification of major clay minerals types, using a sample, oriented on the (001) plane is relatively straightforward and satisfactory (Lindholm, 1987). Clay minerals are identified using the based spacing along the c-axis. It is often the characteristic of a mineral.

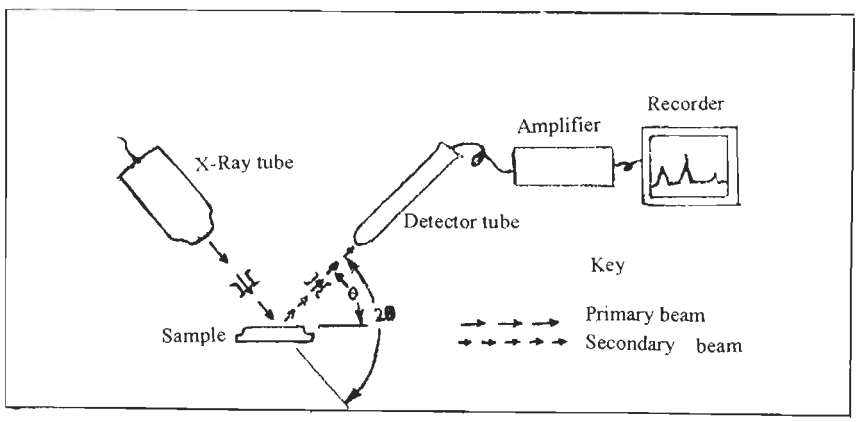

Figure 3.5- A schematic diagram showing the geometry of an X-ray diffractogram (Lindholm, 1987).

3.4.3 Methodology

Although, some clay minerals are evident in whole rock diffractograms, most satisfactory method is to extract and separately analyse the clay fraction (2 μm).

In the present study, 26 shale samples and 32 sandstone samples were crushed and then sieved with (200 mesh, ≤ 75 μ). Between 50 to 100 grams of sample poured in the measured cylinder (1000 ml) and adding the distilled water to reach the 1000 ml volume. This water-sample system is thoroughly stirred and then left for 24 hrs for sediments to settle through time, until the desired size fraction can be removed. The usual size fraction for routine clay analysis is <2 μm. Clay fraction will be in the upper section that should be decanted into the beaker with the helps of a pipett/pipe tube. In the next stage, the clay-water rich sample, thus collected, is evaporated at 50°-60°C, to make it in the form of slurry. This mixture, i.e., clay portion + distilled water is suitable for preparation of the slides, which are used in XRD analysis. In this study, for each sample, three oriented slides were prepared. Of these three slides, one was treated with glycol and the other heated to 550° C for 2-hrs for each sample.

3.5 CLAY MINERALS IN THE CENOZOIC SEDIMENT

Clay oriented mineral slides of shales and clay matrix of sandstones of the Subathu, Dagshai, Kasauli and Lower Siwalik Formation were subjected to X-rays studies, in the University Science and Instrumentation Center. The operating conditions are summarized below:

Radiation : K

Target : Cu

Filter : Ni

Scanning angle: 3° to 30° of 2θ

Current : 20 Ma

Voltage : 35 kv

Range : 4 kc/s

Chart speed : 1 cm per minute

Goniometer speed: 1° of 2 θ per minute

3.5.1 Identification of Clay Minerals

As discussed earlier, the oriented slides allow the identification of clay minerals by their basal reflection (Table 3.7). Figure 3. 6 indicates the X-ray diffraction patterns of major clay minerals, using oriented mounts. X-ray diffractograms representative samples of shale and clay matrix of sandstone from various formations are shown in Figures 3. 7, and 3. 8 (for detail see appendix-I). The major clay minerals, identified in the Cenozoic sediments, both shale and clay matrix of sandstone, are Illite, kaolinite, chlorite, mixed layer. Vermiculite and montmorillonite also in some cases were identified. Illite is the dominant mineral in samples (Tables 3.8, 3.9). It corresponds to peaks at 10 A° (8.8°), 5A° (17.7°), and 3.3 A° (26.6°) on all the diffrectograms (Figs. 3.7, and 3.8). Kaolinite shows reflections at 7A° (12.3°) and 3.5A (24.9°). Samples, in general, contain this mineral. Peaks of kaolinite on the diffractograms for all of the samples are sharp and well define, indicating probably its detrital origin. Chlorite is lesser than kaolinite and illite. It has been identified by its peaks at 14.2 A°(6.3°), 7.0 A°(12.4°) and 4.8 A°. Glycolation does not affect it. The peaks are broad, but well defined. Montmorillonite in some of the shale samples such as sample no. 3, 4, 100 (belong to Lower Siwalik Formation), 38

Table 3.7 Identification of Clay Minerals in an Oriented Mount Using X-ray Diffraction (based on Carroll, 1970).

Clay Minerals	Untreated	Ethylene Glycol	Heated to 550°C
Illite	Generally broad (001) reflection at approximately 8.8° 2θ (10 A°) with integral series of basal reflections including 17.7° 2θ (5 A°) and 26.75° 2θ (3.3 A°)	No change	(001) may be more intense
Montmorillonite	(001) reflection variable from 6.80 to 5.89° 2θ (13-15 A°); higher-order basal reflection irrational	(001) increases to approximately 5.2° 2θ (17 A°) with integral series of basal reflection including 10.4° 2θ (8.5A°) and 15.5° 2θ (5.7 A°)	(001) collapses to between 9.83° and 8.84° 2θ (between 9 and 10A°) with corresponding integral series of higher order basal reflections
Chlorite	(001) reflection at approximately 6.3° 2θ (14- A°) with an integral series of basal reflections including 12.62° 2θ (7A°), 18.92° 2θ (4.7A°) and 25.45° 2θ (3.5 A°)	No change	(001) reflection intensified; higher order basal reflections disappear
Kaolinite	(001) reflection at 12.38° 2θ (7.15A°) and (002) reflection at 24.94° 2θ (3.57 A°) higher order reflections generally too weak for recognition in samples composed of several clay minerals; disorder (poorly crystallized) Kaolinite shows broader and less intense basal reflections	No change	Structures collapses to an X-ray amorphous mineral metakaolin (peaks disappear)
Vermiculite	(001) reflection at 6.30° (14.2 A°) with an integral series of basal reflections including 19.42° 2θ (4.57A°) and 34.29° 2θ (2.6A°).	No change	(001) reflection intensified to 8.84° 2θ (10A°). The higher order basal reflection collapses to 17.72° 2θ (5A°)

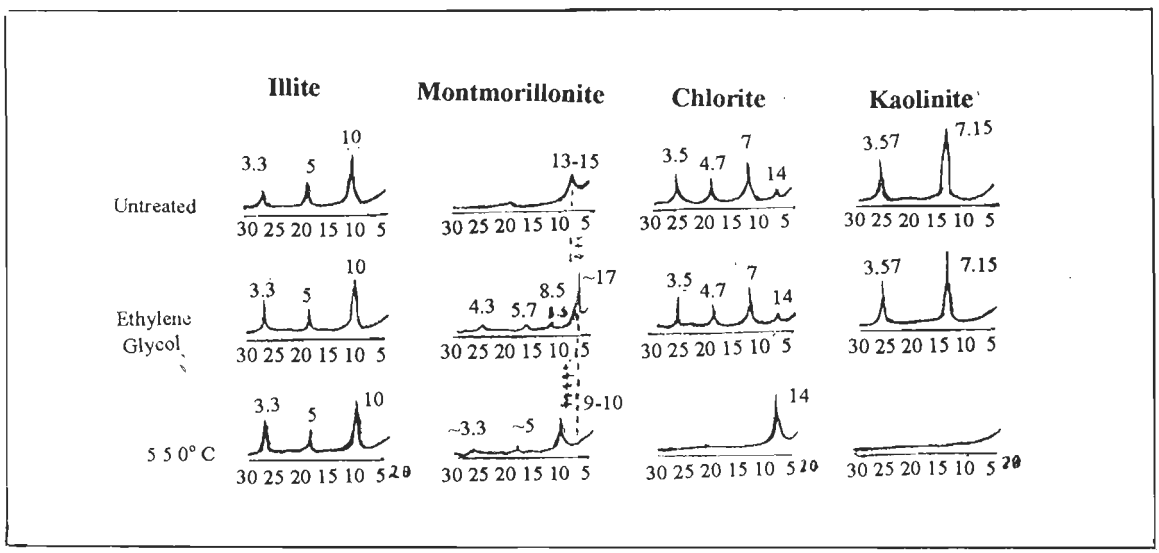

Figure 3.6- X-ray diffraction patterns for clay minerals (Lindholm, 1987).

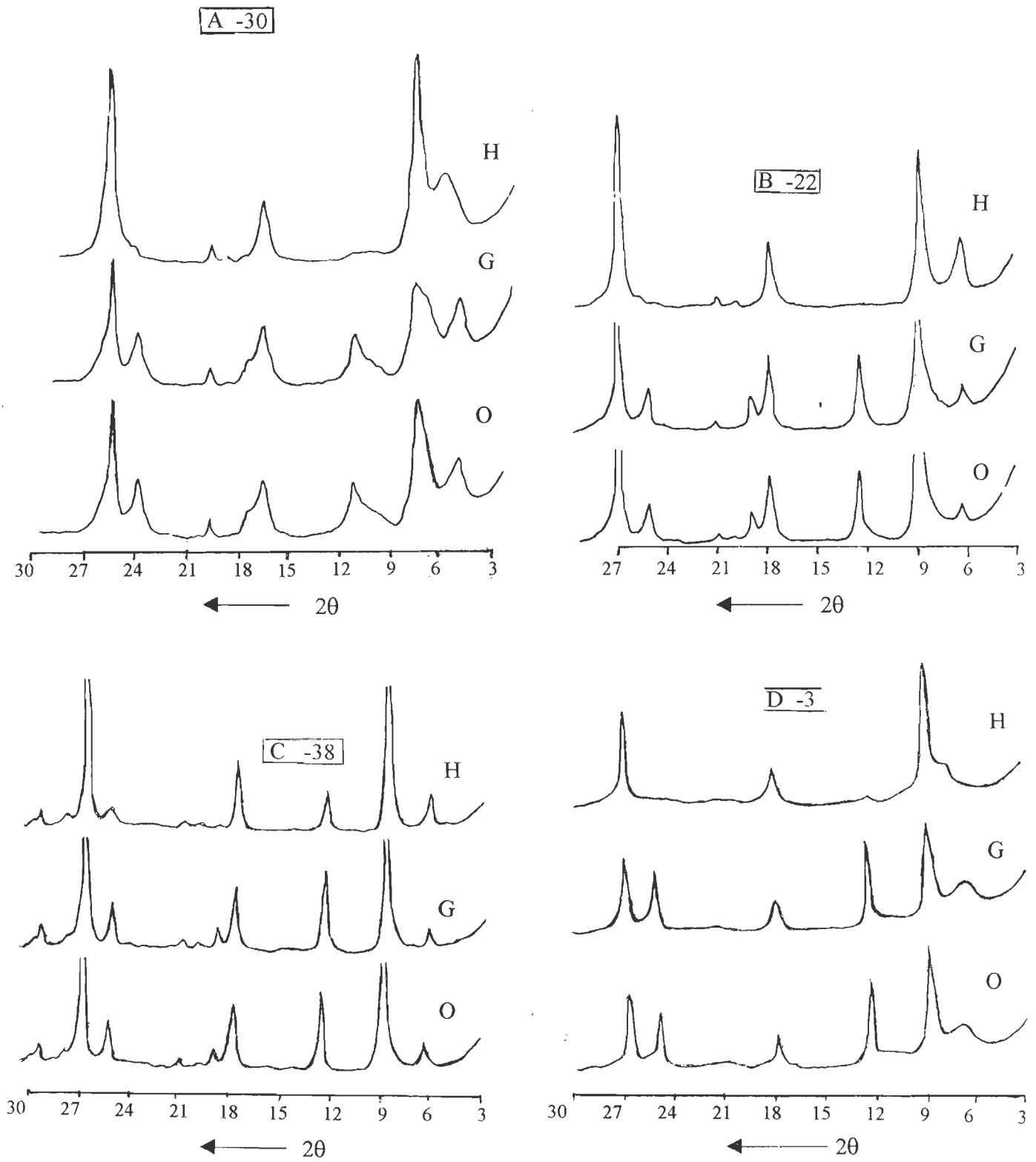

Figure 3.7- X-ray diffraction patterns of clay samples. O- ordinary, G- glycolated, and H- heated slides. A-Subathu, B-Dagshai, C-Kasauli, and D-Lower Siwalik samples. (Numbers are sample reference no.)

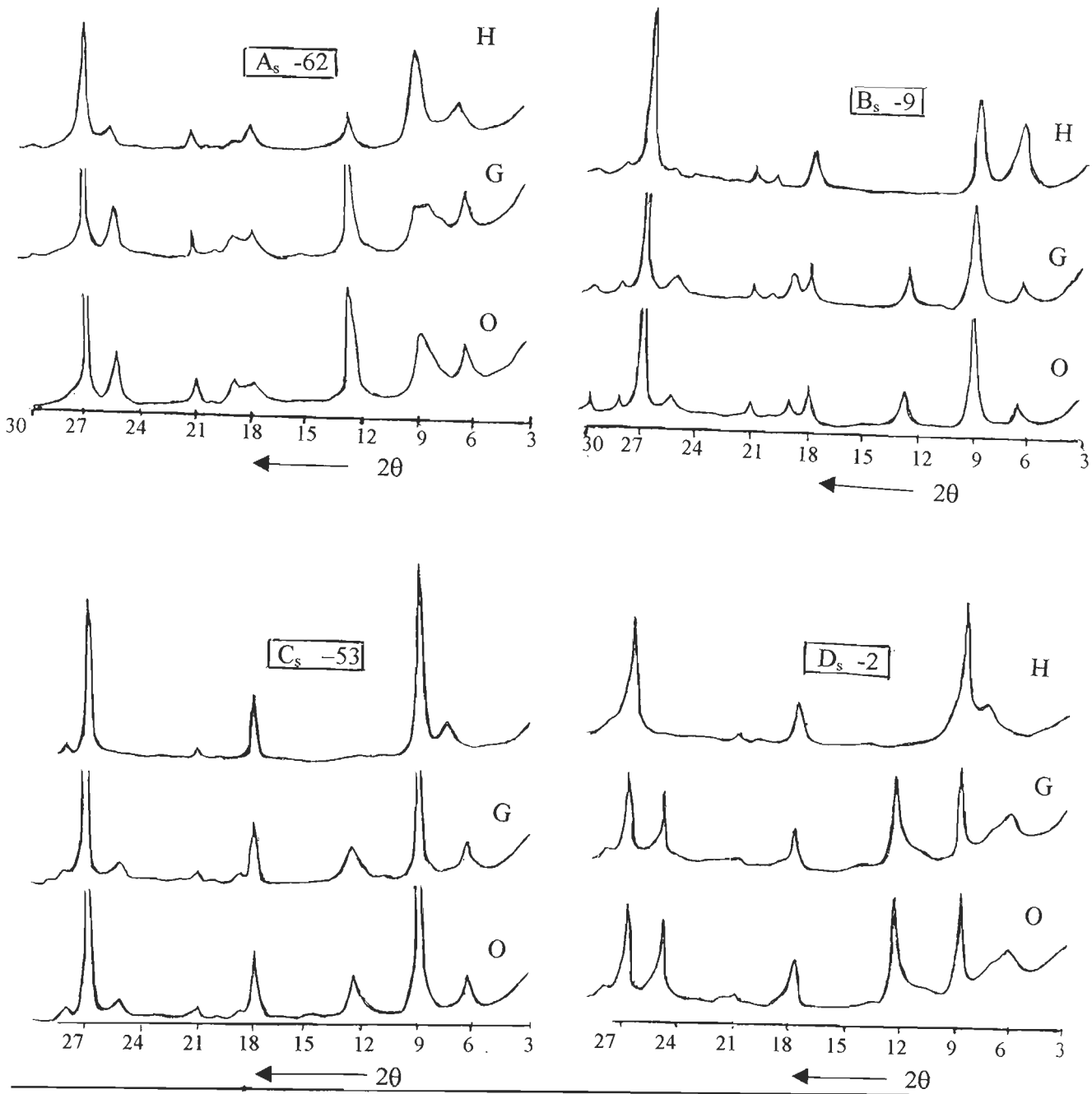

Figure 3.8- X-ray diffraction patterns of clay matrix of sandstone samples. O- ordinary, G- glycolated, and H- heated slides. A_s-Subathu, B_s-Dagshai, C_s-Kasauli, and D_s -Lower Siwalik samples. (Numbers are sample reference no.)

Table 3.8 Clay Mineral Composition of Shales (Based on Weir's Parameters, 1975)

Stratigraphic Formation	Sample No.	Clay Mineral Composition in Percentage			
		Illite	Kaolinite	Chlorite	Montmorillonite
Subathu	30	81.8	18.2	-	-
	36	78.1	21.9	-	-
	43	78.3	21.7	-	-
	60	60.4	14.5	25.2	-
	9	59.3	20.5	20.2	-
	29	72.2	27.8	-	-
	63	49.8	20.4	29.8	-
Dagshai	7	85.6	8.6	5.8	-
	8	83.9	10.8	5.3	-
	18	83.7	11.7	4.6	-
	20	80.5	12.3	7.2	-
	22	80.2	14.1	5.7	-
	23	83.6	10.2	6.2	-
	52	73.9	26.1	-	-
	34	81.2	12.3	6.5	-
	41	98.6	-	1.4	-
Kasauli	57	100.0	-	-	-
	38	76.3	14.8	5.0	3.9
	54	77.2	18.7	4.1	-
	52	93.8	6.2	-	-
	16	89.4	10.6	-	-
	15	84.4	15.6	-	-
	10	83.3	10.4	6.2	-
Lower Siwalik	3	69.7	25.3	-	5.0
	4	5.5	28.3	-	6.2
	100	6.4	24.8	-	8.8

(Kasauli Formation), and sandstone samples such as sample no. 39 (Kasauli Formation) and 2 and 5 (Lower Siwalik Formation) was detected. It gives a reflection peaks at 15A° (5.8°) corresponding to montmorillonite which expands to 17A° (5.2) on glycolation. Mixed layer clay minerals in 85% of shale and more than 95% of sandstone samples occurs with a 'd' spacing of about 19 A° (6.3°) and have a peak at 18.9°(d=4.7A°).This peaks are diffused and with heating completely vanish at 550°C (heated samples). The randomly interstratified illite-vermiculite and illite-vermiculite-chlorite are detectable by the major (001) basal reflection, which shows a series of peaks between 10A° and 14.3A°. This interstratified form is termed as mixed-layer of illite-vermiculite-chlorite. Most occurrence of this form is in Subathu samples, and a few cases in Kasauli and Lower Siwalik and only one case in the Dagshai Formation are detected, in both shale and sandstone samples. Vermiculite with the strong reflection at 14 A° (6.3°) and 4.57 A°

(19.4°) is characterized. In the heated samples, the (001) reflection is intensified to 8.84° (10 A°) and separated from the (001) reflection of chlorite. It is detected in some samples of Subathu (e.g. sample no. 30), Dagshai (e.g. sample no. 52), Kasauli (e.g. sample no. 57, 16) and Lower Siwalik (e.g. sample no. 100, 3) formations in both shale and sandstone.

Raiverman (1964), Bhattacharya (1970), Bhatacharya and Raiverman (1973), Shukla and Verma (1976), and Chaudhri and Gill (1983) have been identified these minerals in Cenozoic sediments in various sections, which they studied.

Table 3.9 Clay Mineral Composition of Matrix in Sandstone (Based on Weir's Parameters, 1975).

Stratigraphic Formation	Sample No.	Clay Mineral Composition in Percentage			
		Illite	Kaolinite	Chlorite	Montmorillonite
Subathu	31	49.5	50.5	-	-
	32	75.9	24.1	-	-
	35	74.4	16.9	8.7	-
	61	42.6	57.4	-	-
	28	87.0	13.0	-	-
	62	38.3	41.7	20.0	-
	64	79.0	6.8	14.1	-
Dagshai	6	80.1	13.0	6.9	-
	9	79.9	13.2	4.5	-
	19	84.0	10.9	5.1	-
	21	85.4	9.1	5.5	-
	23	82.8	13.1	4.1	-
	33	59.6	33.2	7.2	-
	42	7.9	6.6	5.5	-
Kasauli	56	90.0	10.0	-	-
	58	93.7	6.3	-	-
	37	51.9	37.0	11.1	-
	39	72.8	17.6	5.5	4.1
	27	84.4	15.8	-	-
	26	86.3	13.7	-	-
	11	92.6	7.4	-	-
	12	76.7	18.9	4.4	-
	13	90.5	9.5	-	-
	14	89.3	4.3	6.4	-
	17	64.0	27.9	8.0	-
	51	88.1	-	11.9	-
	53	91.6	8.4	-	-
	55	84.7	8.2	7.3	-
	40	80.1	16.0	3.9	-
Lower Siwalik	2	67.1	26.6	-	4.4
	5	63.1	13.4	15.4	9.4
	99	60.5	-	39.5	-

3.6 SEMI QUANTITATIVE ESTIMATES OF MAJOR CLAY MINERALS

Theoretically, the quantitative estimation of various clay mineral concentrations is based on the principle that the intensity of X-rays diffraction by a mineral is related to the amount of that mineral. But, there are many factors such as crystallinity, composition, impurities of clay minerals, orientation of clay mineral grains and the radiation set-up of X-ray machine, which affect such a relationship. These problems have been discussed at length by Johns et al. (1954), Schultz (1960), Bradley and Grim (1961), Hinckley (1963), Gibbs (1967) and Carrol (1970), etc. As such the relationship between X-ray diffraction intensity and the clay mineral concentration at best is semi-quantitative. In the present study, the sample mount conditions and the X-ray machine set-up were kept uniform for all the samples as far as possible to minimize the error of estimation to these factors.

3.6.1 Peak Height Versus Peak Area Methods of Estimation

Griffin (1962), Vemuri (1967), and Knuze and Scafe (1971) advocated the use of peak heights, whereas Brindley (in Brown, 1961, p.512) and Biscaye (1965) suggest that the peak areas in diffractograms give better estimates of clay mineral compositions. However, Hurley et al. (1963), Harlan (1966) and Awasthi (1979) concluded that for estimation of relative abundance of clay minerals either of the methods can be used. Accordingly the peak height method has been used in the present study. It helped in removing the subjectivity involved with shouldering peaks.

For rapid, reproducible semi-quantitative percent composition of clay mineral, in the present study the method proposed by Weir et al. (1975) was used, using the following equation:

$$\frac{I_{kaolinite}}{2.5} + I_{illite} + I_{smectite} + \frac{I_{chlorite}}{2.0} = 100\ \%$$

The divisors have the function of correcting for the relative greater X-ray responses of kaolinite and chlorite.

Following this approach the percentages of Illite, kaolinite, Chlorite, and montmorillonite were estimated in various formations (Tables 3.8, and 3.9). A brief description of these minerals is given below:

The illite peaks are sharp and well defined. The percentage of illite varies from 50 to 82 in Subathu, 73 to 99 in Dagshai, 77 to 89 in Kasauli and 67 to 70 in the Lower Siwalik shales. The matrix of 32 sandstone (Table 3.9) indicates the following range; 38 to 87% in Subathu, 59 to 89% in Dagshai, 52 to 94% in Kasauli and 60 to 67% in the Lower Siwalik. As an additional point, it should be noted that in some samples of Subathu and Dagshai formations most probably due to degradation of illite (muscovite) or mix-layering of illite with vermiculite/smectite, the 10A° peak of illite is not sharp. It seems stripped mica were deposited in sea water (Weaver, 1958, Weaver, 1989, p.179), and still the reaction of this stage has not get been completed to final illite. It may be shown by the following reaction:

$$\text{Illite (muscovite)} \xrightarrow[\text{Degradation}]{} \text{K-stripped illite (I/s, I/v)} \xrightarrow[\text{Aggregate}]{} \text{K- illite}$$

The percentage of kaolinite varies from 14 to 28% in Subathu, 8 to 26% in Dagshai, 6 to 19% in Kasauli and 24 to 28% in the Lower Siwalik shale samples. The matrix of sandstone samples indicate a wide range from 7 to 57% (in Subathu), 7 to 33% (in Dagshai), 4 to 37% (in Kasauli) and 13 to 27% (in the Lower Siwalik).

The percentage of chlorite in shales is a range from 20 to 30% in Subathu, 1 to 7% in Dagshai, 4 to 6% in Kasauli formations. The matrix in sandstone samples shows a short range. It varies from 8 to 20% in Subathu, 5 to 7% in Dagshai, 4 to 12% in Kasauli and 15 to 40%in Lower Siwalik formations.

The montmorillonite percentage is very less (<9.5).

3.7 CRYSTALLINITY INDEX AND ILLITE INTENSITY RATIO

Jacob (1974) measured crystallinity index of illite and kaolinite by determining the ratio of the width of (001) peak at mid height above the back ground to the peak height on XRD. The basis for such determinations is that a sharply resolved peak of high intensity indicating high crystallinity would have a small value. Crystallinity index was determined using Jacob's (1974) method for different minerals detected in shale samples (Table 3.10) and in matrix sandstone samples (Table 3.11). It is observed that crystallinity of illite and kaolinite is least in the Subathu Formation.

The crystallinity of illite is dependent on its chemical composition. Dunoyer De Segonzac (1970) and Esquevin (1969, in Gill et al., 1977) noted that a high AL/(Fe+Mg) ratio in the octahedral favoured the re-crystallization of illite. Esquevin (1969) suggested that Al/(Fe+Mg) ratio could be estimated by taking the ratio of 5A° (17.7°) and 10A° (8.8°) peaks corresponding to (002) and (001) reflections, respectively and called it "Intensity ratio". The mean of illite intensity ratio (Table 3.10, 3.11) from Subathu to Lower Siwalik formations is; 0.7>0.5>0.41 ≤ 0.43 (in shales) and 0.55 > 0.42 > 0.36 < 0.5 (in sandstones). With decreasing age the lower values of intensity ratio indicate little recrystallization of illite.

Table 3.10 Crystallinity Index and Illite Intensity Ratios in Shales.

Stratigraphic Formation	Sample No.	Crystallinity Index						Illite Intensity Ratio
		Ill.	Kaol.	Chl.	Verm.	M.L.	Mont.	
Subathu	30	0.10	0.30	-	0.30	0.40	-	0.70
	36	0.03	0.03	-	0.30	0.40	-	0.60
	43	0.04	0.08	-	0.10	0.30	-	1.10
	60	0.13	0.40	0.50	-	0.50	-	0.90
	59	0.18	0.20	0.30	-	0.60	-	0.40
	29	0.13	0.20	-	0.40	0.60	-	0.60
	63	0.10	0.10	0.10	-	0.30	-	0.70
	X =	0.10	0.19	0.30	0.27	0.44	-	0.70
Dagshai	7	0.04	0.10	0.20	-	0.20	-	0.50
	8	0.03	0.09	0.20	-	0.10	-	0.50
	18	0.03	0.08	0.30	-	0.20	-	0.60
	20	0.04	0.09	0.30	-	0.30	-	0.60
	22	0.05	0.09	0.40	-	0.20	-	0.40
	23′	0.03	0.09	0.20	-	0.20	-	0.40
	52	0.04	0.03	-	0.10	-	-	0.50
	34	0.04	0.10	0.30	-	0.40	-	0.40
	41	0.03	-	0.80	-	0.30	-	0.60
	X =	0.04	0.08	0.30	0.10	0.20	-	0.50
Kasauli	57	0.03	-	-	0.60	-	-	0.50
	38	0.04	0.06	0.20	-	0.20	0.40	0.40
	54	0.04	0.05	0.30	-	0.35	-	0.40
	52′	0.06	0.40	-	0.50	-	-	0.50
	16	0.05	0.20	-	0.30	0.60	-	0.40
	15	0.07	0.20	-	0.50	1.00	-	0.40
	10	0.06	0.20	0.35	-	0.80	-	0.30
	X=	0.05	0.18	0.28	0.47	0.59	0.40	0.41
Lower Siwalik	3	0.08	0.06	-	1.00	0.30	1.00	0.36
	4	0.04	0.02	-	0.50	-	0.40	0.43
	100	0.09	0.04	-	0.10	0.50	0.60	0.50
	X =	0.07	0.04	-	0.50	0.40	0.66	0.43

X- Mean value, Ill.- illite, Kaol.- kaolinite, Chl.- chlorite, Verm.- vermiculite, M.L.- mixed layer, Mont.- montmorillonite

Table 3.11 Crystallinity Index and Illite Intensity Ratios in Sandstone's Matrix.

Stratigraphic Formation	Sample No.	Crystallinity Index						Illite Intensity Ratio
		Ill.	Kaol.	Chl.	Verm.	M.L.	Mont.	
Subathu	31	0.30	0.07	-	0.40	0.70	-	0.70
	32	0.10	0.10	-	0.50	0.80	-	0.50
	35	0.10	0.20	0.70	-	0.60	-	0.40
	61	0.08	0.03	-	0.30	0.40	-	0.60
	28	0.04	0.08	-	0.50	0.30	-	0.50
	62	0.30	0.06	0.30	-	0.50	-	0.60
	64	0.07	0.70	0.30	-	0.70	-	0.40
	$\bar{X}$ =	0.14	0.17	0.40	0.40	0.57	-	0.55
Dagshai	6	0.06	0.10	0.40	-	0.20	-	0.50
	9	0.07	0.20	0.70	-	0.40	-	0.40
	19	0.03	0.10	0.30	-	0.30	-	0.40
	21	0.03	0.10	0.30	-	0.10	-	0.50
	23	0.03	0.06	0.40	-	0.20	-	0.40
	33	0.06	0.03	0.30	-	0.30	-	0.40
	42	0.07	0.30	0.60	-	0.40	-	0.40
	$\bar{X}$ =	0.05	0.13	0.40	-	0.30	-	0.42
Kasauli	56	0.05	0.50	-	0.40	1.00	-	0.40
	58	0.06	0.70	-	1.10	0.50	-	0.50
	37	0.10	0.06	0.40	-	0.60	-	0.20
	39	0.08	0.10	0.60	-	1.00	1.00	0.30
	26	0.08	0.20	-	0.60	1.00	-	0.40
	27	0.10	0.30	-	0.90	1.00	-	0.40
	11	0.07	0.40	-	0.40	1.30	-	0.40
	12	0.06	0.09	0.50	-	0.80	-	0.30
	13	0.06	0.30	-	0.60	1.00	-	0.40
	14	0.04	0.30	0.30	-	0.30	-	0.40
	17	0.07	0.07	0.50	-	0.80	-	0.30
	51	0.09	-	0.40	-	0.80	-	0.30
	53	0.04	0.30	-	0.30	1.30	-	0.40
	55	0.06	0.20	0.50	-	0.40	-	0.30
	40	0.05	0.09	0.50	-	0.60	-	0.40
	$\bar{X}$ =	0.07	0.25	0.46	0.60	0.80	1.00	0.36
Lower Siwalik	2	0.06	0.06	-	1.00	-	1.70	0.50
	5	0.06	0.12	0.50	-	1.30	0.60	0.50
	1	0.23	-	0.20	0.3	1.00	-	0.50
	$\bar{X}$ =	0.12	0.09	0.35	0.65	1.15	1.15	0.50

$\bar{X}$ - Mean value, Ill.- illite, Kaol.- kaolinite, Chl.- chlorite, Verm.- vermiculite, M.L.- mixed layer, Mont.- montmorillonite

Weaver and Kubler Indices- Weaver (1960, 1961), observed that the peak sharpness and peak width of the 10A° Illite peak change continuously with increasing metamorphic grade in Ouachita mountain region and Texas of USA. He suggested a measure of peak character (Fig. 3.9) which he called the sharpness ratio (SR) which is also called the weaver index (W.I.).

Weaver's sharpness ratio is defined as the ratio of diffractogram peak height at 10.0A° divided by peak height at 10.5A°.

Later, Kubler (1967, 1968) suggested using the peak-width at half height (in mm) as a measure of metamorphism or crystallinity. He called his measure "crystallinity index" (C.I.) which is also known as "Kubler index" (K.I.). Kublers' crystallinity index decreases with increasing illite crystallinity (Guthrie et al., 1986).

The following factors may have some effects on illite crystallinity:

i) Temperature is the principal factor controlling illite crystallinity but, the crystallinity of illite is also dependent on other factors such as, the composition of the sediment and the fluid phase, porosity and permeability. For examples sandstone and siltstone with high potassium and Aluminum contents may be expected to display enhanced crystallinity, whereas shale which also have high K and Al contents but low permeabilities, may show retarded illite crystallinities (Singh and Singh, 1994).

ii) Lithology influences crystallinity but in what way is not well established. Kubler (1968) found that the Illite in limestone had higher values than adjacent shale, where as Weaver et al., (1984) found the opposite relation.

iii) The presence of paragonite, with a basal reflection of 9.6-9.7 A° and mixed layer paragonite / phengite will broaden the 10 A° peak (Weaver, 1989).

iv) Illite associated with coal or other organic matter is less well crystallized than when it occurs without organic matter (Teichmuller et al., 1979).

v) Tectonic shear movements, besides temperature, pressure and time, have still to be demonstrated (Stach et al., 1982).

Numerous studies have been confirmed that the shape and width of the 10A° Illite-mica peak changes with increased depth of burial and grade of metamorphism (Weaver, 1989). Figure 3.10, shows the variations of 10A° peak of illite with increasing metamorhpic grade. Thus the illite crystallinty index is one of the principal parameters used in assessing the conditions of burial from diagenesis to low–grade metamorphism. Diagenesis is generally considered to include all changes which affect minerals. The boundary between diagenesis and metamorphism

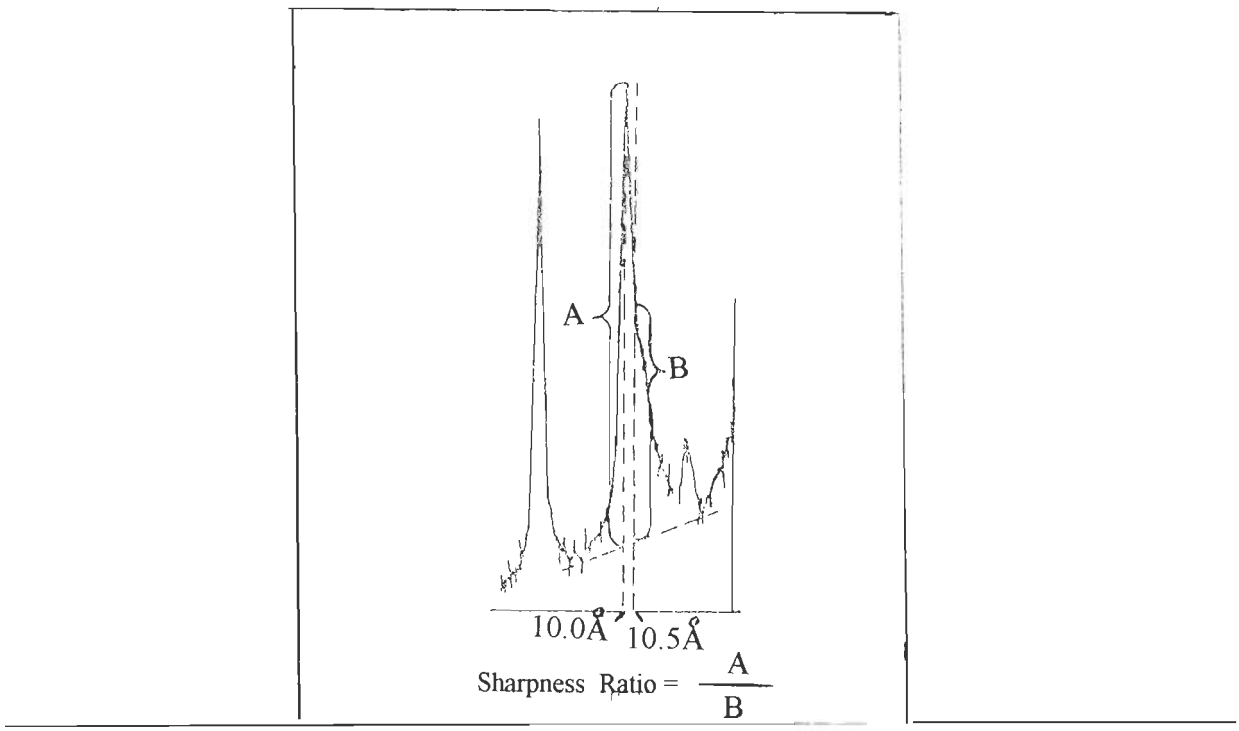

Figure 3.9- Method of measuring sharpness ratio, from Weaver, 1960, 1961, Copyright, 1969, Texas Bur. Econ. Geol. (Weaver, 1989).

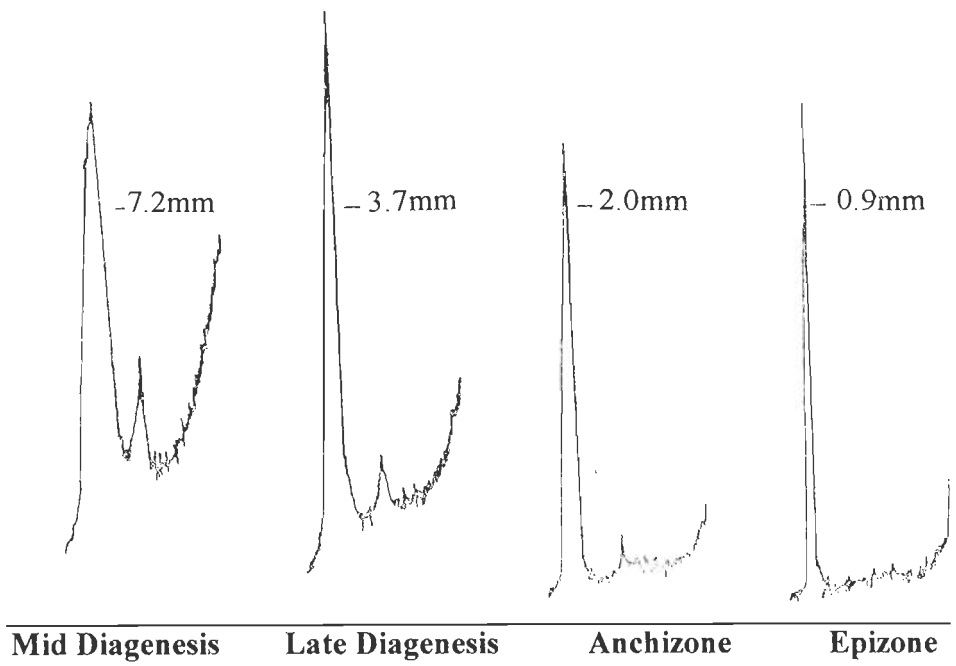

Figure 3.10- Sequence of 10 A° peaks showing decrease in peak width at half height (K.I.) with increasing grade of metamorphism (Weaver et al., 1984).

is a controversial problem, but commonly stated that the boundary occurs at ~200°C when recrystallization of clay minerals occurs. The temperature at which the boundary changes occur, varies with grain size. In order to standardize the boundary between diagenesis and very low grade metamorphism, it is best to use the <2 μm fraction (Weaver, 1989). Table 3.12, shows the variations of sharpness ratio and crystalinity values to identify the boundary between diagenesis, very low grade (anchizone) and low grade metamorphism (epizone; Weaver, 1989). The Table 3.12 indicates that the diagenetic stage is characterized by Sharpness Ratio less than 2.3, and Illite Crystallinity Index (Kubler Index) more than 3 (mm) or 0.42 (2θ). The Sharpness Ratio for Anchizone should be between 12.1 and 2.3, whilst the Illite Crystallinity index will be between 3.0 to 1.50 (mm) or 0.42 and 0.25 (2θ).

Illite crystallinity was determined from diffractogrms of glycolated samples using the technique of both Weaver (1960) and Kubler (1968). Illite Crystalinity Index (I.C.I.) and Weaver's index (W.I.) were determined for shale (Table 3.13). The average illite crystalinity index (I.C.I.) or Kubler Index (K.I.) of shales in Cenozoic sediments (Table 3.13) varies from 5.3 to 4.3 in shale.

i) Kubler Index (illite–crystallinity index) increases from Subathu, the oldest Formation, to Dagshai, Kasauli and Lower Siwalik formations, youngest one.

ii) The ralation of sharpnes ratio (SR) and crystallinity index (Fig. 3.11) in shale samples is uniform and linear.

iii) The sediments still are in the diagenetic stage, based on the three parameters calculated and presented in the data sets (Table 3.13). The mean values of C.I. (K.I.) in shale samples are as follows:

- Lower Siwalik with 5.7 (SR is 2), indicating the early middle stage of diagenesis (C.I. = 7.5).
- Kasauli with 5.00 (SR is 2.3) indicating the late of middle diagenesis (C.I.=5.3)
- Dagshai with 4.6 (SR is 2.4) showing the late of middle diagenesis, same as Kasauli Formation.
- Subathu with 4.3 (SR is 2.5) presenting the early stage of late diagenesis. It seems that some of the Subathu samples are in the end of diagenesis.

Table 3.12 Comparison of Sharpness Ratio, and Illite Crystallinity Index and Temperature (Weaver, 1989)

Zone	Sharpness Ratio (Weaver, 1960)	Illite Crystallinity Index		Temperature (° C)
		Degree 2θ Cu K (Kubler, 1978) 2θ	1°/min., 381 mm/hr (Weaver,1984) mm	
Diagenesis				
	---------2.3 -------	----------0.42----------	----------3.0----------	--------200-------
Anchizone				
	--------12.1-------	----------0.25----------	----------1.5 ---------	--------350-------
Epizone				

Table 3.13 Illite Crystallinity Indices of Shale

Stratigraphic Unit	Sample no.	Illite Crystallinity Index (Kubler Index)		Sharpness Ratio (W. I.)
		mm	2θ	
Lower Siwalik	100	6.5	0.55	2.0
	3	4.5	0.48	2.2
	4	6.0	0.55	2.0
	Average	5.7	0.53	2.0
Kasauli	10	4.0	0.37	2.5
	15	4.0	0.38	2.4
	16	46.0	0.44	2.5
	52′	5.0	0.48	2.0
	57	8.0	0.60	1.5
	38	4.0	0.38	2.8
	Average	5.0	0.44	2.3
Dagshai	7	5.2	0.50	2.7
	8	4.5	0.40	2.5
	18	5.0	0.45	2.0
	20	5.0	0.45	2.0
	22	4.5	0.40	2.3
	23′	4.2	0.40	2.6
	52	4.7	0.44	2.5
	34	4.0	0.35	2.3
	41	4.5	0.40	2.5
	Average	4.6	0.42	2.4
Subathu	29	3.5	0.35	2.8
	30	5.0	0.40	2.4
	36	4.0	0.32	2.4
	43	5.0	0.42	2.5
	63	4.4	0.40	2.5
	59	4.0	0.33	2.5
	60	4.0	0.35	2.6
	Average	4.3	0.37	2.5

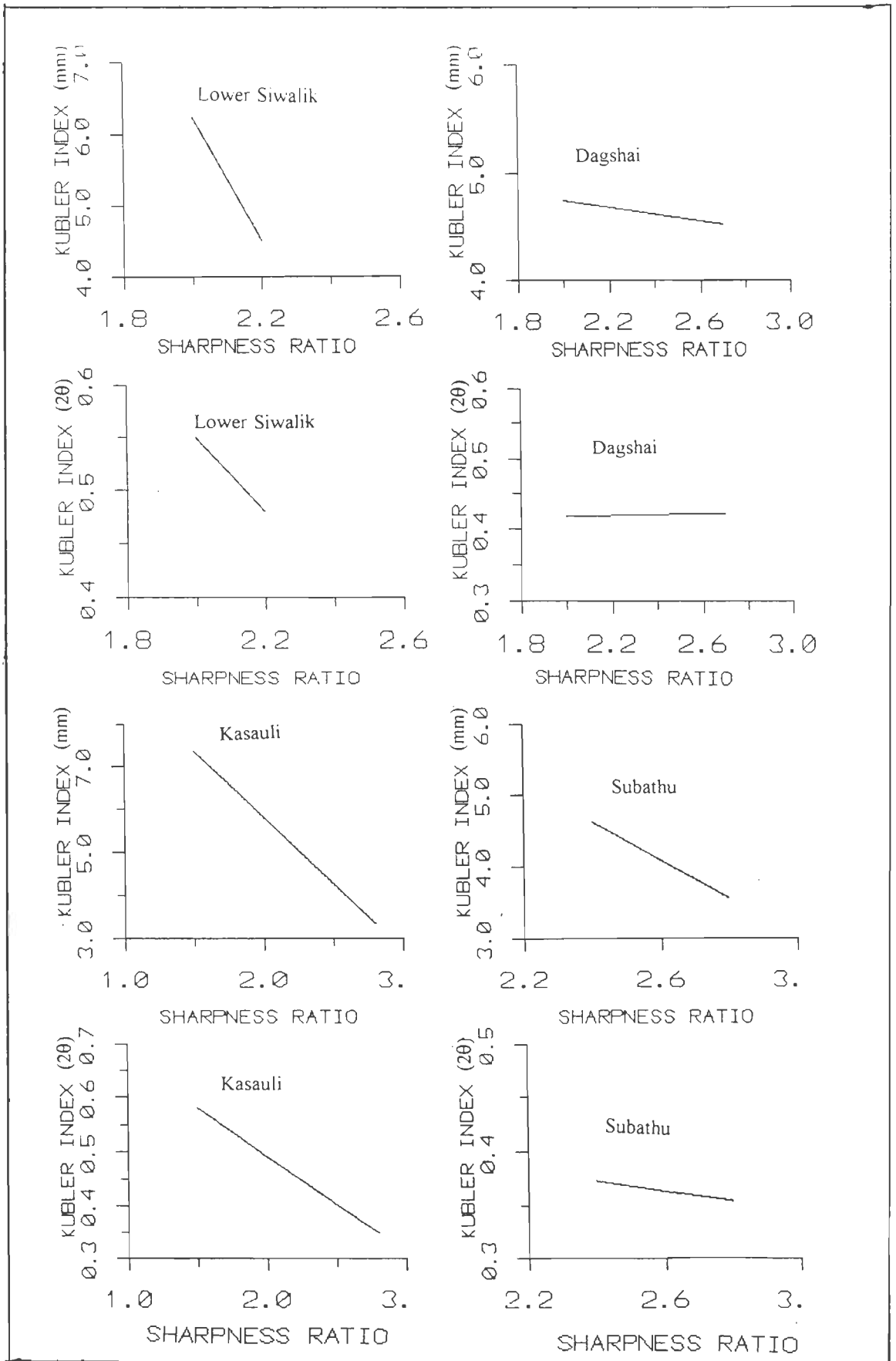

Figure 3.11 The relationship of sharpness ratio (SR) and crystallinity index (I.C.I) in shales of various Cenozoic formations.

3.8 GENESIS CLAY MINERAL

Illite is relative resistant to weathering and relatively intense weathering is required before it is appreciably altered. Illite owes its origin partly to the source rock and partly to the diagenetic process. The mineral is not affected during transport over relatively short distance. Weaver (1967) has suggested that most of illite is due to diagenesis of kaolinite and montmorillonite. Partial loss of structural potassium and hydration of micaceous minerals may be responsible for the genesis of a part of illite. According to Keller (1963), montmorillonite alters to illite by cations base exchange. Kulbicki and Millot (1963) suggest illitization of kaolinite by saline waters. Microorganisms, by concentrating K (potassium), may play a role in the formation of illite from feldspar (Weaver, 1989). Illite in sediments of Cenozoic may be detrital in part derived from pre-existing marine rocks, but its stability would have been affected if the environment was non marine (Raiverman, 1964). The Illite Crystallinity Indices exhibit very slight diagenetic changes. The sharp and well-defined peaks of illite along with kaolinite and chlorite indicating the relative fresh crystals were deposited in a marin environment, presumably by slow sedimentation in a shallow sea or at least in large saline lakes, esp. in the lower part of Dharmsala sediments. But for younger sediments a non-marine origin be considered (Raiverman, 1964).

Kaolinite owes its origin to weathering of granitic and basic rocks. During the weathering process Ca^{+2}, Mg^{2+}, Na^{+}, K^{+} and Fe^{2+} are leached out and H^{+} is added. Decomposition of feldspars and other constituents is aided by high porosity and permeability of the rocks and proceeds at a faster rate in fresh water environment (Keller, 1970). Murray (1954) also recorded that acidic to neutral pH-environment are more congenial for the formation of kaolinite. Under marine conditions, kaolinite is either dissolved or changed into illite or chlorite during diagenesis (Grim et al., 1949). Derivation of kaolinite from weathering of feldspars by the low feldspar content of the arenaceous rocks of the Siwalik group was also suggested (Chaudhri, 1970 c, 1975). Shukla and Verma (1976) also attributed the origin of kaolinite to feldspars rather than to mica. The minor occurrences of kaolinite are possibly the results of derivation from land areas (Raiverman, 1964).

Chlorite owes its origin to alteration of terrigenous minerals in an environment of less intense chemical weathering and temperate climate (Chaudhri and Gill, 1983). A part of chlorite may owes its origin to the alteration of montmorillonite on account of deep burial and easy accessibility to Mg^{2+} and K^{+} ions (Keller, 1963, 1970). Raiverman (1964) suggested the development of chlorite from kaolinite. In some samples the mixed layer of chlorite-kaolinite was identified.

Montmorillonite is highly sensitive to physical and chemical environments. The mineral might have been destroyed during denudation. The near absence to minor content of montmorillonite may as well be attributed to the accumulation of sediments in fresh-water environment. Keller (1970) recorded that in non-marine environment, montmorillonite is altered to illite. Weaver (1989) opined the conversion of montmorillonite into chlorite is diagenetic and the provenance of illite varies from terrestrial to marine environment.

Vermiculite owes its origin partly to the alteration of chlorite and illite (Bhattacharya and Raiverman, 1973) and partly to selective fixation of potassium during diagenesis (Weaver, 1958). The authigenic vermiculites commonly form in soils developed on basic igneous rocks (Walker, 1975).

During the process of alteration of non-expanded sheet structure minerals to vermiculite, an intermediate mixed-layer phase is commonly produced (Weaver, 1989). Most of these clays are formed by the removal of K from biotite, muscovite, illite or the brucite sheet from chlorite.

Artificial weathering of biotite (Ismail, 1969) showed that oxidation of ferrous iron was independent of PH; however, under neutral and alkaline conditions iron oxidation caused a large decrease in layer charge and a smectite formed. Under acid conditions the charged decrease due to the oxidation of ferrous iron, was balanced by the loss of octahedral Fe and Mg, and a highly charged vermiculite material was formed. Thus, in general, smectite would form in the more arid environments and vermiculites in the more humid environments (Weaver, 1989). It is possible some vermiculite layers are created by acid leaching during burial.

Based on clay mineral distribution and the environmental and climatic conditions (Table 3.14), an increasing weathering intensity is postulated in the source rocks from pre-Siwalik to Siwalik times. The depositional environment changed from epineritic to continental.

Table 3.14 Environmental, Climatic Conditions (after Kumar, 1992; Najman et al., 1994;) and the Nature of Clay Mineral of Cenozoic Sediments.

Parameter	Stratigraphic Formation			
	Subathu	**Dagshai**	**Kasauli**	**Lower Siwalik**
Environment	Regression and Transgression, Prolonged phase of tropical erosion, shallow marine/low energy	Meandring, fluvial regime	Braided fluvial regime	Alluvial plains
Climate	Tropical	Semi-arid	Humid	Dry season-Wet season
Type of Clay	Ill.,Kaol., Chl., (very less) and M.L.	Ill., Kaol., Chl., and M.L.	Ill., Kaol., Chl., M.L., and Verm.	Ill., Kaol., Chl. M.L., Verm., and Mont.

The abbreviations are: Ill.=Illite, Kao.=Kaolinite, Chl.=Chlorite, M.L.=Mixed Layer, Mont.= Montmorillonite, and Verm.=Vermiculite

3.9 CONCLUDING REMARKS

(i) Sandstones of Cenozoic sediments, petrographically, are classified as quartzite, sub litharenite (for Subathu), sub litharenite, litharenite (For Dagshai) and litharenite (for Kasauli and Lower Siwalik). However, they show variations in their characteristics with time. Some of these characteristics are; slight increase of detritus feldspar and polycrystalline quartz, decrease in the amount of monocrystalline quartz, abundance of metamorphic lithic, igneous rocks (plutonic/volcanic) and sedimentary rocks through time in younger and younger rocks.

(ii) In the early stage of basin formation, detritus was largely derived from sedimentary and very low grade metamorphic rocks of age mainly Late Protrozoic to Cambrian from the proto-Himalaya reliefs (supra crustal Indian margin rocks). Towards the latest stages of Cenozoic deposition, the diversity of source rocks is observed. The present data plotted in the QFL diagram support that the Cenozoic sediments source from the recycled orogenic materials.

(iii) Lack of wackes in Subathu Formation indicates relatively quiet tectonic conditions with very low rate of erosion and uplift. After Subathu time, in younger rocks, continual increase in lithic fragments in the sandstones suggests relatively higher uplift rate.

(iv) The most dominant clay minerals in the shale and matrix of sandsone samples are illite, kaolinite, mixed-layer, chlorite, vermiculite and montmorillonite in decreasing of abundance. The illite peaks are sharp and well defined. The percentage of illite varies from 50 to 82 in Subathu, 73 to 99 in Dagshai, 77 to 89 in Kasauli and 67 to 70 in the Lower Siwalik shales. The percentage of kaolinite varies from 14 to 28% in Subathu, 8 to 26% in Dagshai, 6 to 19% in Kasauli and 24 to 28% in the Lower Siwalik shale samples. The percentage of chlorite in shales is a range from 20 to 30% in Subathu, 1 to 7% in Dagshai, 4 to 6% in Kasauli formations. The montmorillonite percentage is less than 9.5 % and found only in the younger sediments. The clay matrix of sandstone samples shows the similar variations as shale samples.

(v) Based on Jacob's (1974) crystallinity index, it is observed that amongst all formations, the Subathu Formation has the least crystallinity of illite and kaolinite.The mean of illite intensity ratio from Lower Siwalik to Subathu formations generally shows little recrystallization of illite.

(vi) The ralation of sharpnes ratio (SR) and illite crystallinity index (I.C.I) in shale samples is uniform and linear. Kubler Index (illite crystallinity index) increases from Subathu to Lower Siwalik formations.

(vii) The sediments still are in the diagenetic stage. The mean values of C.I. (K.I.) in shale samples are as follows:

- Lower Siwalik with 5.7 (SR is 2), indicating the early middle stage of diagnesis (C.I. = 7.5).
- Kasauli with 5.00 (SR is 2.3) indicating the late of middle diagenesis (C.I.=5.3)
- Dagshai with 4.6 (SR is 2.4) showing the late of middle diagenesis, same as Kasauli Formation.
- Subathu with 4.3 (SR is 2.5) presenting the early stage of late diagenesis. It seems that some of the Subathu samples are in the end of diagenesis.

(viii) The depositional environment changed from epineritic (Subathu Formation) to continental fluvial (younger formations).

CHAPTER - 4

HIMALAYAN FORELAND BASIN: APPLICATION OF FISSION TRACK DATING

4.1 INTRODUCTION

The earth is a dynamic planet having signatures of its past activities in the crustal material. The identification of these events spatially and temporally has been a vital part for geosciences. The radioisotope-based geochronology has significantly contributed in determination of geological time spans of these events. The age spectrum, provided by the available dating methods, now covers the entire range of earth's history.

The evolution of the Himalaya is an important event in earth's history. While several geochronologic studies have already been made in various regions of the Himalaya, age data are further required from many more parts of the Himalaya to decipher the tectonic history using different geochronological methods.

Geochronology data from in-situ Himalayan rocks provide important constraints on the timing of events associated with the Himalayan orogeny, but are necessarily limited to rocks at the present-day erosional surface. The age data from the sediments, on the other hand, have an advantage over the data from the in-situ Himalayan rocks as it has an ability to provide an orogen averaged perspective of the cooling history of rocks, eroded from the Himalaya through time.

Besides the denudation information from the rocks of the foreland basin about the character and tectonics of the Himalayan highlands in the past, thermal evolution of these basins is also of utmost important. Among the various geological factors controlling the maturation of organic matters in sediments, temperature is the most important one. Apart from the maximum temperature, the thermal evolution of the sediments through geological time also influences the maturation process. By a fortunate coincidence, Fission Track Dating (FTD) has proved to be a unique tool for deciphering the thermal history of sediments at temperatures corresponding to the

oil windows. This coupled with the ability of FTD method to determine the ages of individual mineral grains within a detrital heavy mineral population has made the technique as a powerful tool for the study of thermal and provenance history of the sedimentary rocks. Several studies have used the FT dating of detrital minerals to address sediment provenance, stratigraphic correlation and age control of clastic sediments (Hurford et al., 1984; Baldwin et al., 1986; Kowalis et al., 1986; Cerveny et al., 1988; Brandon and Vance, 1992). Since FTD is an outcome of Solid State Nuclear Track Detector (SSNTD) technique, it will be apposite to describe briefly about the salient features of these detectors.

4.2 SOLID STATE NUCLEAR TRACK DETECTION TECHNIQUE

Solid State Nuclear Track Detectors (SSNTD's) are essentially the materials that are damaged by the energetic particles in such a way that the particle tracks can be developed by subsequent etching and observed microscopically. These materials include most of the insulating solids, such as minerals, glasses and polymers in the order of increasing sensitivity. A comprehensive review of this subject is available in various publications (Fleischer et al., 1975; Durani and Bull, 1987; Lal, 1991, 1992 a, 1992 b).

The passage of heavily ionizing particles through dielectrics creates narrow paths of intense damage primarily through coulomb interaction with the orbital electrons of the target materials atoms. The salient features of these damages are:

(i) The extent of these damages is less than 100 A° and that it is the damage within 50 A° of the particle trajectory, which is significant.

(ii) Tracks have been found to be consisting of atomic defects.

(iii) Latent tracks though stable at ambient conditions fade at elevated temperatures. The activation energies associated with the repair of damage trails are several electron volts. These energy values are typical of those involved in atomic diffusion and thus provide further evidence of the atomic nature of the defects.

(iv) TEM observations of tracks in diffraction contrast mode reveal that tracks are centers of strain.

(v) In the last few microns of the range of charged particle, the track is not revealed. This is called range deficit.

(vi) Metals and most semiconductors do not record tracks.

The track formation model, which is consistent with all the above experimental features of tracks in inorganic crystals, is known as Ion Explosion spike model. According to this model, tracks are the result of the defects created by the removal of electrons by the ionizing particle (Fleischer et al., 1965 a, 1975). A narrow cylindrical region of positively ionized atoms ~1 nm in diameter is produced behind the ion trajectory. These positive ions strongly repel one another and are ejected into interstitial positions surrounding a new-depleted core region. The repulsion will take place if and only if the electrostatic stress is greater than the mechanical strength. Subsequent processes include neutralization of the positive ions and relaxation of the surrounding lattice that produces long range strain fields (Fig. 4.1). This model explains all the experimental features of the tracks in minerals and glasses.

4.2.1 Chemical Etching Process

Chemical etching of radiation damages is the backbone of SSNTD technique in having its wide spread applications. The chemical etching transforms the latent track into an unerasable structure by supplying the required amount of energy for the enlargement process. The sensitivity of this chemical amplifier is comparable to very sensitive electronic amplifier (e.g. etched track of 100 μm diameter has a volume which is 10^8 times larger than the volume of the original track).

Etching takes place via rapid dissolution of the damaged region of the track core than the undamaged bulk material. The preferential chemical attack velocity V_t and bulk attack velocity V_g determine the size and shape of the resultant etched track. Each detector has a etching efficiency which is defined as the ratio of the number of observed etched tracks to the number of latent damage trails crossing a unit area of the original surface of the detector. Its value depends on V_t and V_g of the detector.

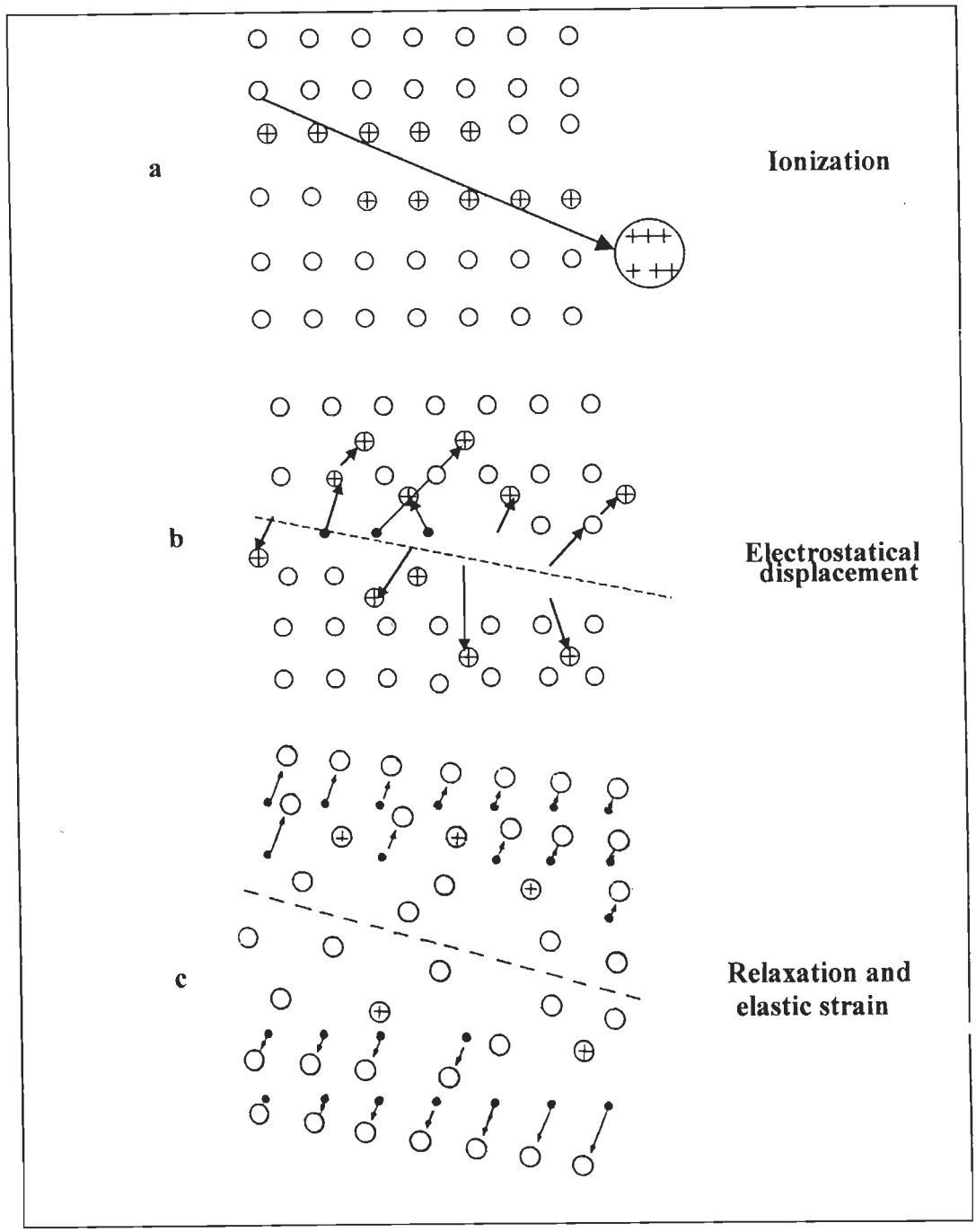

Figure 4.1- The ion explosion spike mechanism for track formation in inorganic solids. The original ionization left by passage of a charged particle (a) is unstable and ejects ions into the solid creating vacancies and interstitials (b). Later the stressed region relaxes elastically (c) straining the undamaged matrix (Fleischer et al., 1965 a, 1975).

4.3 FISSION TRACK DATING

4.3.1 Age Equation

Uranium is fairly ubiquitous trace element at ppm to ppb level in minerals and glasses. In the span of geologic time, ^{238}U is transformed in two different ways namely alpha decay and fission. Alpha particles are not sufficiently massive or energetic to make tracks in common minerals. About one out of every two million transformations in ^{238}U is by fission. As a result of fission, the nucleus breaks up into two lighter nuclei, one averaging about 90 amu and the other about 135 amu, with the liberation of about 200 MeV of energy. These two fission fragments recoil in opposite directions, and damage the crystal lattice along its path. The result is a zone of damage defining the **fission track** which is tens of angstroms in diameter and 10-20 μm in length. Tracks formed in the low-density minerals are longer than those formed in dense minerals. In terrestrial materials although other fissioning elements such as ^{235}U and ^{232}Th are also present, ^{238}U is the only significant producer of tracks due to its high rate of fission.

The total number of decay of ^{238}U, in a given volume of a mineral containing uranium atoms distributed evenly throughout its volume, during time T is

$$D_s = N_{238}(e^{\lambda_d T}-1) \qquad \text{....4.1}$$

Where D_s and N_{238} are the number of decay events/cc and the number of uranium-238 atoms/cc (at present) in the mineral sample respectively, λ_d is the total decay constant of ^{238}U.

Most of these decay events correspond to α-emission. The fraction of ^{238}U decays that are due to spontaneous fission, is λ_F/λ_d, and so the number of fission events F_s, per unit volume is given by

$$Fs = \lambda_F/\lambda_d\, N_{238}(e^{\lambda_d T}-1) \qquad \text{.....4.2}$$

The number density, ρ_s, of spontaneous fission tracks crossing a unit internal surface of the sample after etching is related to the volume density F_s by

$$\rho_s = \eta\, R\, F_s \qquad \text{.....4.3}$$

Where R is the range of a single fission fragment, and is the etching efficiency of the material.

Combining equations 4.2 and 4.3, we obtain

$$\rho_s = \lambda_F/\lambda_d \, N_{238} \, \eta \, R \, (e^{\lambda_d T} - 1) \qquad \text{.....4.4}$$

The determination of age T thus requires the measurement of ^{238}U concentration in the sample. Rather than measuring the ^{235}U content directly, it is more convenient to measure the ^{238}U content of the sample and to assume (as is always the case) that this stands in a constant ratio to the ^{238}U. The determination of ^{238}U content by fast-neutron fission is avoided as these neutrons would produce fission, also in the thorium content of the sample. If the sample is irradiated with a known fluence ϕ of thermal neutrons, then the number of induced fissions per unit volume is

$$F_i = N_{235} \, \sigma\phi \qquad \text{....4.5}$$

where σ is the thermal-fission cross-section of ^{235}U, and N_{235} is the number of ^{235}U atoms per unit volume. If we assume that the range and etching efficiency for spontaneous and induced fission tracks are the same, then the number of induced fission tracks per unit area is

$$\rho_i = R \, F_i \, \eta = \eta R \, N_{235} \, \sigma \, \phi \qquad \text{.....4.6}$$

Dividing equation 4.4 by 4.6 and re-arranging the terms we get

$$T = 1/\lambda_d \ \ln \left[1 + \frac{\lambda_d \sigma I \phi \rho_s}{\lambda_F \, \rho_i} \right] \qquad \text{....4.7}$$

One of the important assumptions in calculating the ages using equation 4.7 is that the material being dated has been a closed system with respect to fission tracks and uranium since its formation. This means that the only alteration in the ratio ρ_s/ρ_i is due to radioactive decay. Two aspects of this assumption need to be considered. Firstly, the fission tracks once formed must be stable over the life time of the material recording them. Secondly, there must be no migration of uranium.

4.3.2 Experimental Procedure

(i) Mineral Separation

FTD is a mineral dating technique and hence the separation of suitable minerals from the rock specimen is an essential step. In the present study the separation procedure relevant to

apatite and zircon is described as these are the only two minerals which have been used for dating work embodied in the present thesis.

Before starting the separation procedure, thin section of each rock specimen was examined and only those specimens were retained for mineral separation which showed the presence of suitable sized (≥ 100 μm) grains of either apatite and or zircon. This step also helped in assessing the quantity of the crop of apatite and/or zircon so as to get an idea of the amount of the rock specimen to be taken for processing. The flow chart showing all the steps involved in mineral separation is drawn in Figure 4.2 and discussed below.

(ii) Crushing

For sufficient crop of zircon and apatite in a given rock sample, about 1-5 kg of the sample was crushed, depending on the abundance of the minerals sought for dating. The sample was crushed with a jaw-crusher to get its powder. This stage was repeated (many times) to get satisfactory yield of the powder.

(iii) Sieving

The crushed rock powder was gently washed with water to remove clay and then sieved through 60-mesh sieve. The powder under 60-mesh was panned with water to remove any left-over clay and light minerals. While panning, the water flow was kept very slow. After panning, the powder was again sieved through a 200- mesh cloth sieve. During this step, water was continuously poured in the sieve. The grains between 60-200 mesh were dried in an electric oven for about 12 hours. The temperature of the oven was kept about 60°C so as to avoid the annealing of spontaneous track even in the most thermally sensitive mineral, apatite. Sample above 60-mesh was also dried and stored for a second use, if necessary. Before switching this process to the next sample, the 60-mesh sieve was thoroughly washed in an ultrasonic cleaner and the cloth of the 200-mesh sieve was changed to new one.

(iv) Magnetic and Heavy Liquid Separation

In order to increase the concentration of apatite and zircon, standard procedure of isodynamic magnetic separation and heavy liquid separation was adopted. Separation of ferromagnetic minerals from the rock powder was done with the help of a permanent magnet.

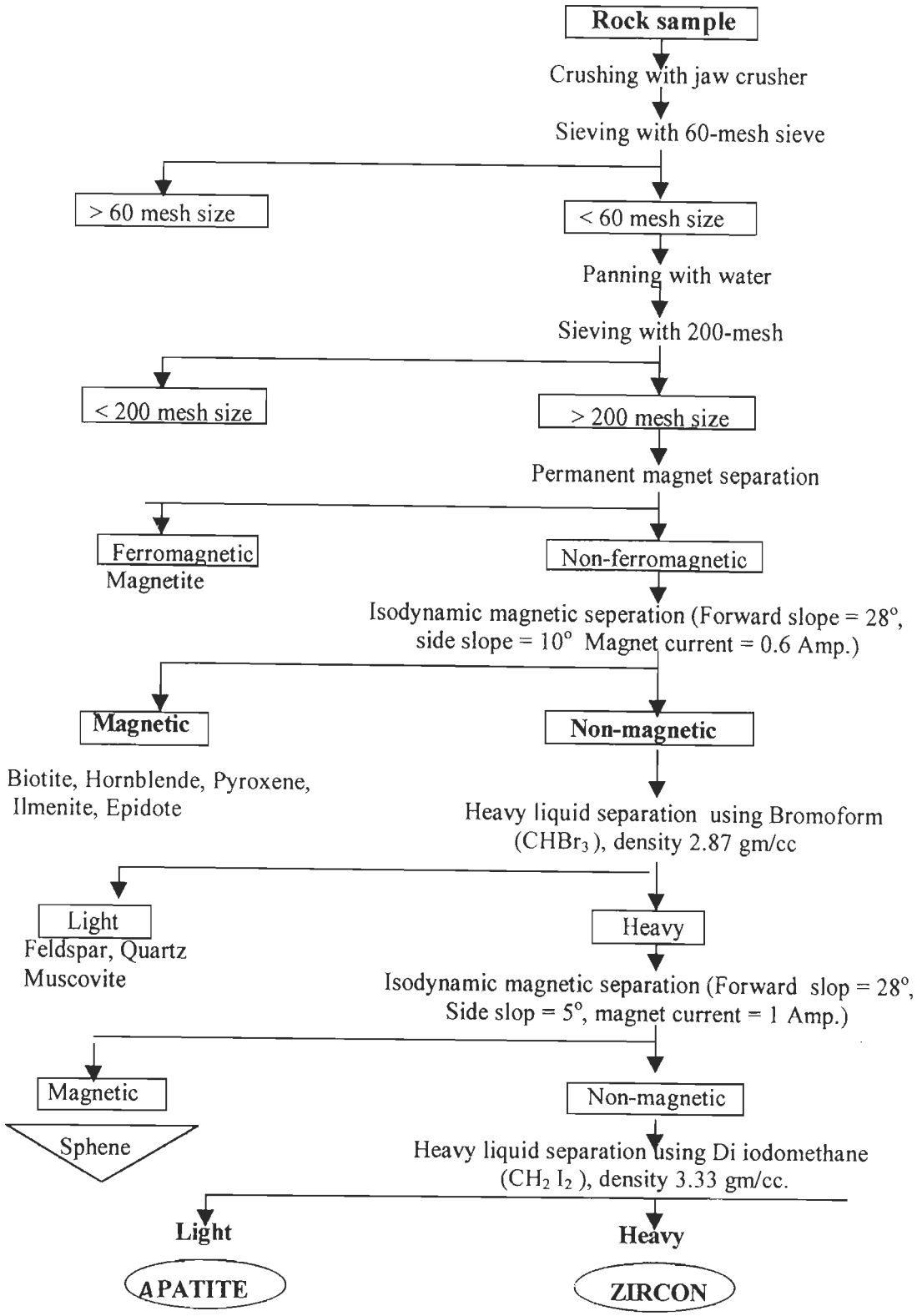

Figure 4.2 – Flow chart for mineral separation

Sample powder was then passed through isodynamic magnetic separator at constant forward slope of 28° and 10° side slope with 0.6 ampere magnet current.

Non-magnetic fraction containing the desirable minerals was then subjected to heavy liquid separation technique using bromoform. Its density (2.87 gm/cc) was confirmed with the help of standard density glass cubes. The heavy fraction was washed thoroughly with alcohol using ultrasonic cleaner then labeled and kept in an electric oven for few hours at 60°C for drying. The lighter fraction in the filter paper was also washed thoroughly with alcohol to extract the bromoform, absorbed by lighter fraction.

The mixture of bromoform and alcohol was poured in a separation flask of suitable size and mixed with distilled water. This arrangement was kept undisturbed for about 12 hours so that water absorbed the alcohol and, thus, bromoform got collected at the bottom of the flask.

The non-magnetic fraction was again was again passed through the isodynamic separator with forward slope at 13° and 1 amp magnet current. The non-magnetic fraction containing apatite and zircon was again subjected to the process of heavy liquid separation using di-iodomethane whose density (3.3 gm/cc) was checked before use. During di-iodomethane separation, the light fraction on the filter paper and heavy fraction in the beaker was washed with acetone. By storing the mixture for a long time, di-iodomethane is easily recovered as acetone evaporates into the air. Both fractions were labeled and dried in an electric oven at 60° C for about 1-2 hours. The heavy fraction containing zircon and the lighter containing apatite were separately stored in properly labeled plastic vials.

(v) Dating Methodology

As has been discussed in Section 4.3.1, the FT age calculation requires the measurement of ρ_s, ρ_i, and ρ_d. An ideal fission track dating method is one where spontaneous and induced tracks are measured with identical track registration, etching and counting conditions over areas having exactly same uranium concentrations. However, each laboratory was using its own procedure for the first fifteen years after the introduction of the technique by Price and Walker (1963). These different procedures are nothing but different methods of measuring ρ_i. A critical examination of these methods have been made by Gleadow (1981). Before describing the methodology adopted in the present study, it will be imperative to give a summary of the various

dating procedures and to see which method encompasses the conditions of ideality. The main source of this summary is the publication by Gleadow (1981). The dating strategies have been classified into two sub-groups namely the multi-grain and single-grain methods (Table 4.1).

(a) Multi-grain methods

These methods are used for sufficiently large population of small mineral grains (100 to 200 μm dia.) separated from their host rocks. The population is split into two aliquots to measure ρ_s and ρ_i. If the grains for ρ_i measurements are annealed to erase spontaneous tracks, then the method is called **Population Method** (PM). In the other case, it is **Subtraction Method** because spontaneous tracks are subtracted from the total tracks to get induced tracks. The errors in the two measured track densities combine to give a greater uncertainty in the ρ_i than if it were measured directly. The method is, therefore, less precise than PM, unless the ρ_i is much greater than ρ_s. Both these methods assume that two aliquots of the population have identical uranium distribution which may not be true. If the uranium is highly variable between grains, it may lead to an imprecise or even invalid age. Also, if some grains have a track density too high to count, or serious interference from artifacts, then both these methods become unworkable because they require a representative selection of grains to be counted.

The annealing of grains in some minerals (e.g. zircon and sphene with $\rho_s > 10^6$ cm^{-2}) cause a drastic change in the etching behavior of tracks (Gleadow, 1978, 1981) and hence for such minerals PM method will not be suitable.

Counting of spontaneous tracks on external surfaces, although not in common use, is found to be advantageous in some minerals such as zircon which have well-developed crystal faces with low bulk etch rate. Etching on external surface eliminates the need for polishing and can facilitate track identification and counting, because there are no short tracks produced on them. The danger in using external mineral surfaces is that they could be contaminated by tracks from adjacent high-uranium materials in the parent rock. Similarly, uranium-bearing mineral grains must not be in contact with each other during neutron irradiation if external surfaces are to be used for counting induced tracks.

In view of the merits and drawbacks of multi-grains methods discussed above, it appears that apatite is the most suitable mineral which can give precise ages by these procedures.

Table 4.1 Some Alternative of FT Dating Strategies (Gleadow, 1981)

Method	External surface	External detector	Internal surface	Annealing of spontaneous Tracks	Geometry correction
Multi-grain Methods					
Population (P1)	----------	----------	S, I	*	----------
Population (P2)	S, I	----------	----------	*	----------
Subtraction (S1)	----------	----------	S, S+I	----------	----------
Subtraction (S2)	S, S+I	----------	----------	----------	----------
Single grain Methods					
ExternalDetector(D1)	----------	I	S	----------	0.5
ExternalDetector(D2)	S	I	----------	----------	0.7-1.0
Re-Etch (RE1)	I	----------	S	----------	0.5-0.7
Re-Etch (RE2)	S, I	----------	----------	----------	----------
Re-Polish (RP1)	----------	----------	S, S+I	----------	----------
Re-Polish (RP2)	----------	----------	S, I	*	----------

Note: 'S' stands for spontaneous tracks, 'I' stands for induced tracks, * indicates applies to this method and, -----, indicates does not apply to this method.

(b) Single grain methods

Single grain methods allow ages to be measured on individual grains, even at very small grain size (about 100 μm). Thus, only the most suitable grains need to be selected for counting, and those with poorly developed or inhomogeneously distributed tracks, or interfering dislocations may be quite simply ignored. Besides this, single grain dating methods are the only ones that can be applied where all the grains of a mineral do not necessarily have the same age, such as in case of detrital minerals (Gleadow, 1980; Gleadow and Duddy, 1984; Duddy et al., 1984; Hurford et al., 1984; Kowallis et al., 1986). The various strategies adopted in these methods (Table 4.1) are discussed below.

I) Re-polish method

In the re-polish method, the grain mount is etched after polishing to reveal spontaneous tracks and then irradiated. Sometimes, when the spontaneous track density is high, the mineral grain mount is annealed to wipe out spontaneous tracks before irradiation. The mount is re-polished to remove the upper surface containing spontaneous tracks and re-etched to reveal induced tracks. This procedure, thus, not only destroys spontaneous tracks and makes the later

check impossible but also two track densities are not revealed and counted under identical conditions. Further, if the volume distribution of uranium is inhomogeneous, the method will lead to erroneous ages. In those cases where annealing before irradiation is necessary, all the difficulties which arise due to change in etching efficiency by annealing as discussed in the population method will be encountered in this method as well.

II) Re-etch Method

In this method, the grain mount is thoroughly washed and irradiated after etching. After irradiation, the spontaneous tracks are counted and the grain mount is again etched to reveal induced tracks. Due to re-etching, the spontaneous tracks get enlarged in size and hence the induced tracks due to their normal size are easily distinguished.

The reagents used for washing the grain mount should be uranium- free which, otherwise, will contribute some undesirable tracks to ρ_i. If the spontaneous tracks density is high, the normal-sized induced tracks in the vicinity of the over-etched tracks may be difficult to distinguish. Anisotropic etched can also cause problems in this method. As the induced and fossil tracks are distinguishing by their size and if bulk etch rate differs on various planes, then for the same etching time, tracks can be of such different size to one another that it may be difficult to distinguish the two sets of tracks.

III) External Detector Method (EDM)

In this method, spontaneous tracks are counted in the etched mineral grains while the induced tracks are counted on the same area in an external detector of low-uranium concentration.

Out of the various alternatives, EDM is considered to be the most reliable and useful due to its following advantages (Tagami et al., 1988).

(i) Range of age determination is generally wide.

(ii) Age is not affected by variation of uranium distribution within and between crystals.

(iii) Contamination effect of detrital crystals can be assessed for dating of volcanic ash layers.

(iv) Later check of sample is possible.

(v) Sample of small amount can be dated.

(vi) Precision of age determination is generally high.

In the minerals showing anisotropic behavior the etching efficiency is different for various crystallographic orientations and hence direct comparison of spontaneous tracks etched on surface having low-etching efficiency with induced tracks etched on an adjacent mica detector having approximately 100% etching efficiency will result in imprecise ages. But in minerals like zircon which is used in the present study, it is possible to select some surfaces with low bulk etch rate so as to have negligible effect of anisotropy on ages (Gleadow, 1981). Gleadow (1981), thus, has concluded that except for apatite where PM can also be used it is the EDM, which is most suited for age determination.

In India, FTD lab of Kurukshetra University is the only lab where EDM is being used. The procedure is similar to the one already described by Tagami et al. (1988). In the present study, zircon and apatite grains from sediments have been used for dating and the procedure for them is described below:

(a) Hand picking and mounting

In order to identify the mineral grains and corresponding replica in the external detector precisely, some arrangement of mineral grains is desired. As will be obvious during further discussions, this grain arrangement also facilitates the steps of pre-grinding and description procedure. The grains were arranged in an array and mounted as mentioned below. The size of the array was adjusted according to the requirements. The mounting of apatite and zircon was made in different materials because of their different track etching and fading conditions. Hence, their hand picking and mounting procedures are described separately.

(i) Zircon

Small fraction of the zircon grains was spread on a silica glass of size 5 cm x 5 cm. Using a sharp tipped needle the grains were picked one by one and arranged at a small place on the glass slide in such a manner that c-axis of all the grains was in one direction (Fig. 4.3).

In selecting the zircon grains, care was taken so as to hand pick large transparent euhedral crystals having well-defined c-axis, and crystals of approximately same size for a single mount. One of the corner grains was slightly displaced from the regular array as shown in Figure 4.3. The necessity of arranging the grains along their c-axis and the slight displacement of one grain will become clear during the discussion on grinding/polishing, etching of zircon and track

counting in mica detector respectively. The remaining grains were removed from the glass slide and stored in the vial. The silica glass slide was then shifted on to a hot plate having good temperature control. Zircon grains are mounted in PFA (Copolymer of tetrafluorethylene-perfluoro alkoxyethylene) teflon pieces (each of size 1.5 cm x 1.5cm x 0.5 mm), because of its stability against the etching of zircon. The temperature of the hot plate was maintained at 320°C. The teflon mount, was then slightly cut asymmetrically at its right top corner (Fig. 4.3). This asymmetric cutting makes it convenient to recognize the grain side of the teflon sheet by naked eyes. The sample code was written with a needle pen on the back side of the teflon mount.

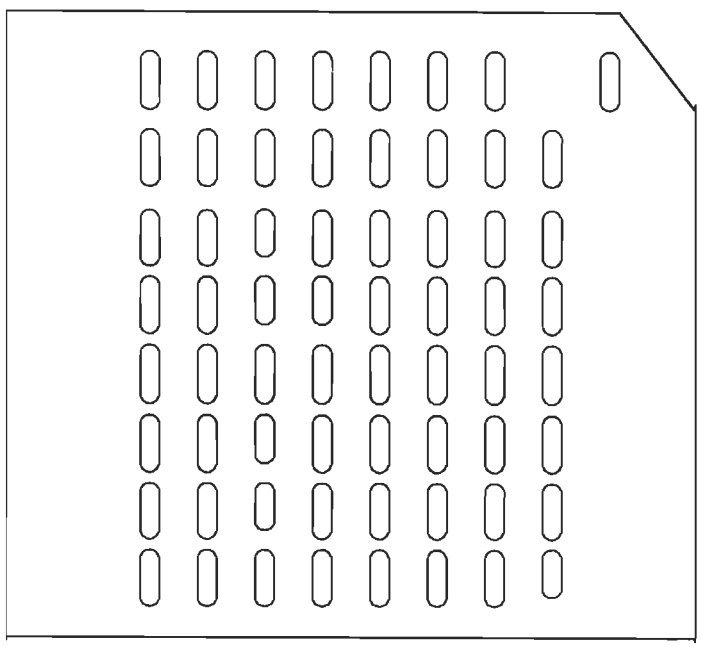

Figure 4.3- Zircon grains arranged in an array of 8 × 8 and mounted in PFA teflon piece of 1 × 1 cm^2

(ii) Apatite

Since fission tracks in apatite are very sensitive to thermal effects, its mounting in teflon is not possible. An alternative procedure, which does not involve high temperature treatment, was adopted. Epoxy is the best material for this purpose, as it gets solidify at room temperature. We have used the commercially available Araldite (AY-108 resin and HY-951 hardener) manufactured by M/S CIBATUL limited, Atul-396 020 Valsad. Resin and hardener were mixed in the ratio of 9:1 by volume respectively.

The epoxy resin mount after drying cannot be detached from the glass slide but can easily be removed from the teflon slide, which is, therefore, very useful for apatite mounting. The teflon slide was attached on the glass slide of the same size by means of bifacial tape (henceforth this combination of glass and teflon sheet will be called TG slide). TG slide is cleaned with alcohol and a little petroleum jelly was applied on the teflon side of the TG slide so that the apatite grains would stick to it. In the absence of the jelly the electrostatic effect could disturb the grain arrangement during hand picking. The hand picking of apatite grains was done similar to that of zircon but without any directional alignment of the grains.

All the TG slides containing apatite grains were arranged on a horizontal surface. On each slide, two small glass pieces of thickness 15 mm were placed as spacers. Then the epoxy resin of fixed amount was poured on the grains carefully so that the grain arrangement did not get disturbed during pouring of epoxy resin. The amount of the epoxy resin was adjusted in such a manner that when another TG slide was put on the glass spacers, the poured resin was made a flattened cylindrical form whose diameter was about 15 mm. The entire process is illustrated in Figure 4.4.

This arrangement was kept for about 24 hours at room temperature to allow the epoxy resin to solidify. After removing the mount from the TG slide, sample code was written with a needle pen parallel to one of the four sides of the grain arrangement on back side of the mount.

(b) Grinding and polishing

In order to expose the internal surface of crystals for measuring spontaneous track density, mineral grains were exposed by grinding and polishing.

For using internal surfaces of the minerals, it is essential to remove a certain thickness to expose 4π geometry. This thickness corresponds to half of a etchable track length, which varies from one mineral to another i.e., ~6 μm for zircon (Krishnaswami et al., 1974), ~8 μm for apatite (Gleadow et al., 1986) and ~7 μm for sphene (Gleadow and Lovering, 1977). If all the mineral grains are mounted so that the exposed crystal surface is equally flat, then the grains will be ground almost uniformly and the removal of the thickness, which satisfies 4π geometry, will be quite easy. However, in case mineral grains are inclined, eroded or have irregular shape or caves, all the surface area of each grain will not be ground equally, and hence the measurement of the

removed thickness for the 4π geometry condition will not be possible from the first grinding. In such a case, before measuring the thickness grinding should be continued till maximum possible area is exposed (from now onward this step will be called as "pre-grinding").

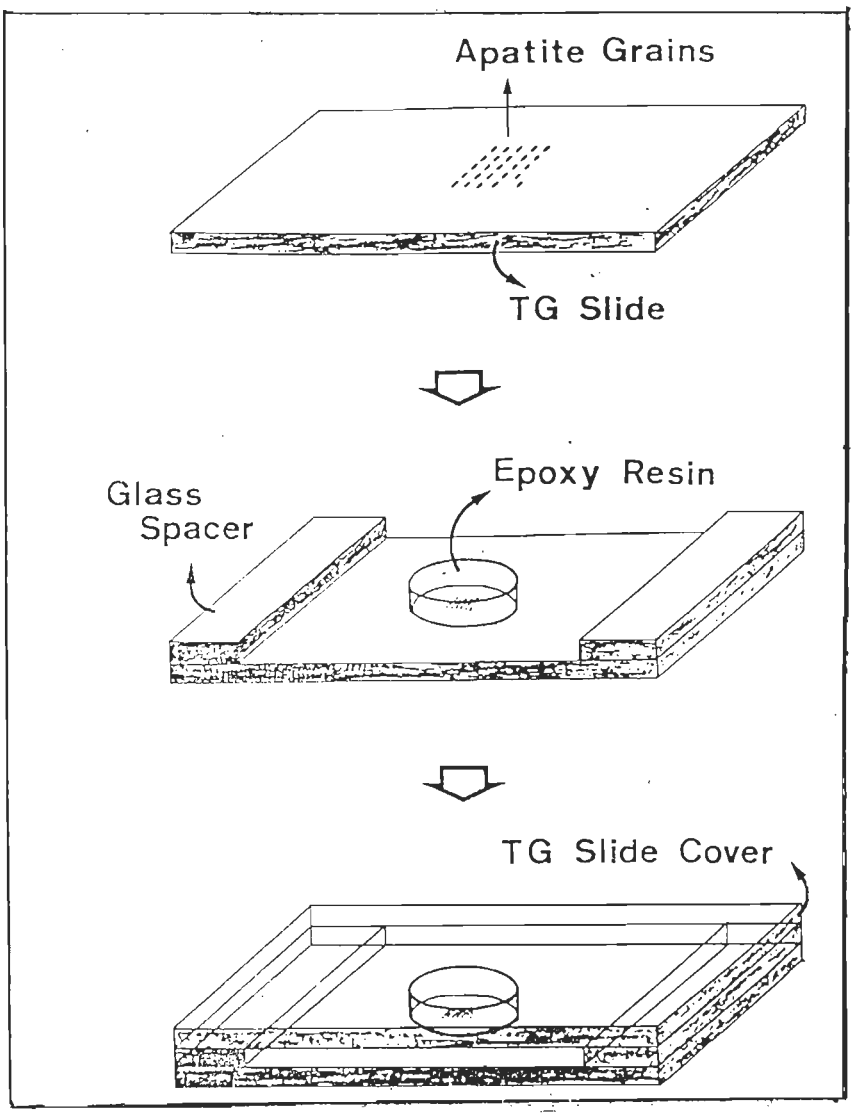

Figure 4.4 Mounting procdure for apatite grains in epoxy resin.

After pre-grinding, a brief description about the suitability of each grain is necessary. As discussed above, some part of the crystal might not have been exposed during pre-grinding and

will not satisfy the condition of 4π geometry. As it is impossible to judge such non-exposed area after finishing the grinding, all these areas were recorded at this stage in a notebook by labeling individual grain.

The next step was to grind the mount and remove a certain thickness peculiar to each mineral for exposing 4π geometry. After description, the mount was ground perpendicular to the direction of the pre-grinding (using 25 μm diamond paste) till all the preceding grinding scratches disappeared. Next step of grinding was carried out, using 14 μm diamond paste, again perpendicular to the direction of the previous grinding scratches and new scratches on all surface area were checked. This alternate grinding with 25 μm and 14 μm diamond paste resulted in the removal of ~1.75 μm thickness. While shifting from one grade of diamond paste to another, mount was washed with water using ultrasonic cleaner for about 8-10 minutes.

This process was repeated until the removed thickness reached half of etchable track length for each mineral. To be on the safe side, however, the thickness of the removed surface was kept more than 3/2 of the minimum depth for exposing 4π geometry. Thus, above step of grinding was repeated, in our routine, 5 times for zircon, and 7 times for apatite.

In case of zircon, the grinding procedure was slightly different from those of apatite. It is not advisable to grind zircon crystals along their crystallographic c-axis because it often produces deep cracks or damages on the surface. The cracks or damages are enlarged during chemical etching and sometimes disturb the track counting. Hence, the pre-grinding and grinding of zircon mounts should be carried out perpendicular to c-axis only, for which the arrangement of zircon crystals along c-axis is desired. After each step of grinding, all grinding scratches were erased by 8 μm diamond paste polishing parallel to c-axis so that next grinding scratches could be easily observed.

After grinding, the mount was polished successively with 8 μm, 3 μm, 1 μm, 0.25 μm diamond paste. At every step of polishing, the direction of polishing is changed by 90° from that of preceding polishing. The alternately changing of polishing direction made it easy to distinguish the disappearance of the preceding polishing scratches, thereby, ensuring the completion of each polishing step. Before switching from one diamond paste to another the

samples were washed under running water and ultrasonic cleaner to make them clean of the preceding grade diamond paste.

(c) Etching of Tracks

(i) Zircon

The determination of conditions for optimum etching in zircon requires a special care. As already mentioned that zircon show anisotropic etching behavior of fission tracks and all the tracks in various crystallographic directions do not have same etching rate (Gleadow, 1981; Sumii et al., 1987). Therefore, it is necessary to continue the etching until the tracks in all directions become visible. In case of zircon, isotropic distribution of etched tracks is characterized by the complete revelation of thin tracks parallel to c-axis.

The optimum etching time of zircon can vary even in one sample from grain to grain and area to area due to large variation of spontaneous track density. It is quite possible that some of the grains are optimally etched whereas others may require more etching for the appearance of tracks in a certain direction of low track etching rate. In such case, the decision for further etching can be taken on the basis of number of grains, which are under-etched. If the observer feels that further etching makes more grains available for dating than the number it spoils by over-etching, he can etch the sample further. In view of this, the progressive etching and counting experiment to determine the optimum etch time of tracks in zircon had to be made for one mount of every sample wherever this mineral was present. The etching procedure used for this mineral is described below.

For etching a large number of zircon mounts together, a specially designed etching bath with temperature controller (manufactured by NOVA Co. Ltd., India) as shown in the Figure 4.5 was used.

After obtaining the desired temperature (230°C) of the heater, the teflon beaker/beakers containing the eutectic mixture of NaOH:KOH etchant (Gleadow et al., 1976) was kept in the heater for 12 hours before putting the sample mounts in the beaker. In doing so, no air bubbles were left in the etchant. The mount after etching for a desired time was put in 5% HCl solution in an ultrasonic cleaner for 15-20 minutes and subsequently in water for 5-10 minutes using ultrasonic cleaner to remove the traces of the etchant sticking to the mount.

The etching time for zircons varies with the track density. Most zircons with average track density (10^6-10^7 tracks/cm^2) etch within a period of 18-24 hours, while those with high track density (>10^7 tracks/cm^2) may etch in 4-6 hours. Those with very low track density (<10^6tracks/cm^2) require much longer times (Naeser, 1978). A detrital suite of zircons, therefore, presents a problem in that it may contain zircons that require all of these etch times. A procedure, called the double-etch method (Cerveny et al. 1988), was used to overcome this problem.

Figure 4.5 Etching bath with temperature controller, used in the present study to etch zircon mounts

The double-etch method involved making two mounts of the detrital zircon suite from a given sample. This often meant splitting the sample in half in cases where zircons were not abundant. One of the mounts was etched to the point there were no grains underetched. This meant that the low track density grains were fully etched, while most of the high track density

grains were either overetched or dissolved (in the case of metamict grains). The second count was etched for roughly half of the time of the first, such that the high track density grains were properly etched. In this mount the middle track density grains ranged from fully etched to under etched and low track density grains were under etched. It is clear that by using this double-etch procedure the middle track density populations would be at varying stages of etch ranging from under etched to over etched. In making two mounts of each sample with two distinct etching sequences, it is hoped to cover all possible ages in the detrital zircon suites.

(ii) Apatite

The tracks in apatite were etched in 0.6% HNO_3 (by volume) at 30°C for 70 seconds.

(d) Packing and Irradiation

Before irradiating the samples in reactor with thermal neutrons, uranium-free fission track detectors were fixed firmly in contact with the mineral mounts. The Brazilian muscovite, which is almost free from uranium impurities, was used in the present study. It was cut into square pieces of size slightly larger than the area of the mounted grains and of suitable thickness (~0.1 mm).

In order to get reliable data, the external detector besides the internal contamination should also be free from any external contamination. For getting a contamination free and freshly cleaned surface of muscovite, one end of a small strip (~5 cm) of scotch magic tape was struck to the edge of a laboratory table and then, using tweezers the trimmed muscovite was stuck on it. Now a jerk was given with hand such that the muscovite was cleaved off from the lower flake sticking to the tape. This process was repeated until we get an even fresh internal surface of muscovite.

The sample code was written with a sharp needle on the back of the muscovite. To distinguish the surface fixed against mineral grains, one corner of it was cut asymmetrically such that when fixed against the grain arrangement in the teflon sheet, the cuts of both were in the same direction (Fig. 4.6). For epoxy resin mounts, the corner cut of muscovite detector was made in the same manner before putting detectors. All the mineral mounts were thoroughly washed with alcohol using ultrasonic cleaner. After keeping the mica detector on the grains, it was

covered with a clean plastic sheet (thickness 0.5 mm) of size slightly larger than the muscovite. The purpose of this plastic sheet was to avoid the sticking of the tape to the mica detector. The entire arrangement was then wrapped up firmly with scotch magic tape and the sample code written on the tape. The sample was thus ready for irradiation.

(e) Thermal Neutron Irradiation

IC2 thermal column of the CIRUS reactor at Bhabha Atomic Research Centre, Trombay, Mombay was used throughout the present study for thermal neutron irradiation. The dimensions of the aluminium capsule for sample irradiation in this reactor are 3.5 cm in length and 1.5 cm diameter. After fixing the muscovite detectors on mounts, the samples were stacked vertically and packed in the capsule. In order to measure thermal neutron fluence and to take into account dose gradient along the capsule, two uranium standard glasses (one on the top and another at the bottom of the capsule) were also packed along with the samples. Each dosimeter mount was made using two standard glasses, namely Corning 1 (CN1) and Corning 5 (CN5) prepared by Dr. J.W.H. Schreurs at Corning Glass Works Corning, New York, USA. The mounting, polishing and packing of these standard glasses was done similar to that of apatites. The muscovite

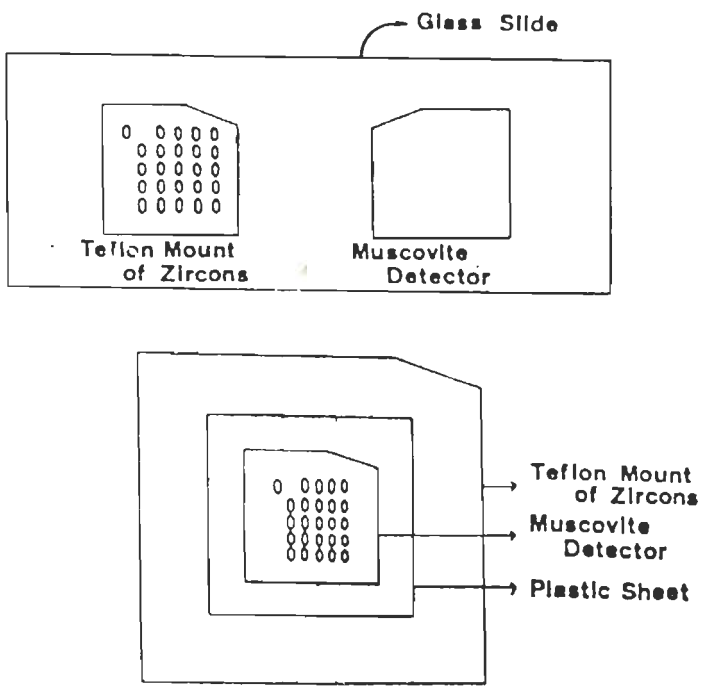

Figure 4.6 Packing of zircon mounts for thermal neutron irradiation.

detectors attached to these standard glass mounts were used for counting of the tracks. The track density ρ_d was calculated by taking mean of the counts of two dosimeter glasses. The Corning glass CN1 contain ~39 ppm undepleted uranium of natural isotopic abundance ($^{235}U/^{238}U$=0.7262%) and ~0.4 ppm thorium, without any interfering trace elements (J.H.W. Schreurs, personal communication).

(f) Counting of tracks

After thermal neutron irradiation of the samples, the muscovite detectors were separated from the mounts. In order to have a smooth and easy detachment of muscovite detectors, the mounts after irradiation were immersed in alcohol for 2-3 minutes. For etching the large number of muscovite detectors simultaneously, 10-12 small cuts were made in a rubber ring (O ring used in vacuum systems) of inner dia of 3 cm and thickness ~2.5 mm using a sharp blade. The muscovite detector was fixed in each of the cuts in such a manner that only its one side went inside the cut (Fig. 4.7). One muscovite detector got fixed in the ring due to the rubber ring's elasticity. This ring could be used repeatedly until the cuts became too wide to withhold the muscovite detectors.

The ring with muscovite detectors was transferred to a plastic beaker having holes all around on its lower half of the curved surface and bottom. This beaker was put into another plastic beaker having 48% HF maintained at 30°C. The optimum etch time, again determined by progressive etching and counting experiment, was found to be ~6 minutes.

After etching, the rubber ring with detectors was transferred to another beaker having holes only on the upper half portion of the curved surface. This beaker was washed under running water for about 4 to 5 hours and subsequently washed with water for few minutes using ultrasonic cleaner to remove any traces of HF sticking to the detector. After this detectors were dried for ~30 minutes.

The muscovite detectors and the sample mounts were fixed in the following manner. The sample mount and its corresponding mica detector were fixed on the glass slide using transparent manicure (Fig. 4.8). The mineral mount and its mica replica were fixed in such a way that the upper most line of the grains in both the mount and its replica hold almost the same horizontal position to make the track counting convenient. The transparent manicure is used because it dries

easily and is soluble in organic substances like benzene and alcohol, and hence the sample or muscovite detector could be easily removed from the glass slide, if necessary. On one side of the glass slide, a paper sticker was fixed on which the sample code was written. The sample and its corresponding mica detector, thus, became ready for the next stage, i.e. counting of fission tracks.

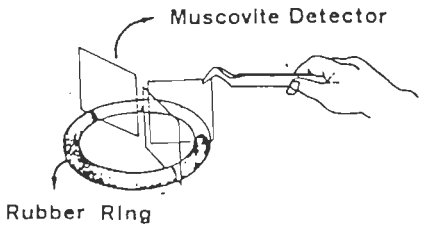

Figure 4.7 Fixing of muscovite detectors in a rubber ring.

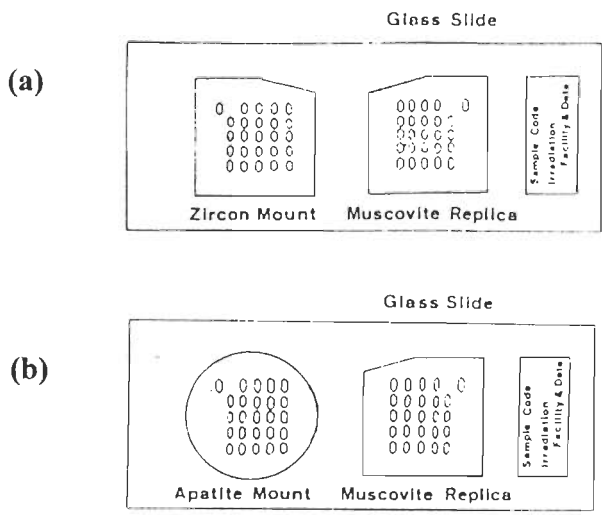

Figure 4.8- Fixing of irradiated mineral mount and corresponding muscovite replica on a glass slide for track counting: (a) for zircon, and (b) for apatite.

The counting of the fission tracks both, in the mineral grains (zircon and apatite) and muscovite was made under a Nikon-Optiphot microscope with 100X dry objective and 15X pair of eyepieces.

While counting the tracks in any of the mineral grains, the shape of the grain was drawn first on the paper and suitable area for counting was chosen according to the description of each grain as discussed in grinding and polishing. The counted area was also marked with the help of graticule fitted in one of the eye pieces of the microscope. After counting the tracks in the

mineral grain, the corresponding area in the muscovite replica of the grain was also scanned for counting the induced tracks. Due to the regular arrangement of grains and thus the corresponding muscovite replica, the scanning was quite easy. Systematic traverses were made, and all suitable grains were counted. Care was taken to count only properly etched grains, where the section was parallel to the c- crystallographic axis and where all tracks were clearly resolved. An effort was made to count grains with both low and high track densities to avoid systematic biases between young and old grains.

The criteria for discrimination of fission tracks from other etched features are well discussed by Fleischer and Price (1964). In case of zircon, only the grain surfaces of high etching efficiency which were easily judged by the existence of sharp polishing scratches and the optimally etched grains or areas which show isotropic angular distribution of etched tracks were used for counting.

For thermal neutron fluence measurement the muscovite replica of the dosimeter glass was uniformly scanned with the help of a scale attached on the mechanical stage of the microscope. A total of about 40 to 50 graticules were counted for each dosimeter glass.

4.3.3 Calibration of FTD System

In principle, since values for the constants λ_d, σ and I are well established, it remains only to determine the track density ratio ρ_s/ρ_i, to measure the neutron fluence and insert a value for the fission decay constant λ_f in order to determine a FT age. Unfortunately, there is a wide disparity in the determined values of λ_f (Thiel and Herr, 1976; Bigazzi, 1981) with results obtained in most post-1960 experiments grouping around either $8.46\times10^{-17}a^{-1}$ or $7.00\times10^{-17}a^{-1}$. The lower value is supported by track accumulation experiments and the dating of minerals and natural glasses of independently known age, the higher value by measurements made using rotating bubble chambers, ionisation chambers, radiochemical measurements and by the dating of man-made glasses of known date of manufacture. These two values of λ_f which are commonly used, differ by 20 per cent. In addition, the determination of absolute values for the neutron fluence, used to induce fission of ^{235}U in the sample, can be very complex. For FT dating,

fluence is usually monitored by the inclusion of a monitor glass, which produces a track density in an external mica detector (see above). The fluence ϕ is related to this track density ρ_d by:

$$\phi = B\,\rho_d \qquad \text{.....(4.8)}$$

where B is a fluence calibration factor which may be evaluated from an independent measurement of the fluence using neutron induced gamma activity in a metal activation foil of gold, copper or cobalt. Several lines of evidence indicate that there is poor consistency between different methods of dosimetry. With diverse values for both the fundamental decay constant λ_F and neutron fluence measurement systems, great variation in the calculated age can be obtained from the ρ_s/ρ_i track density ratio counted for a sample.

The ratio ϕ/λ_F is effective in giving "correct" FT ages. Since there is no agreed single value for λ_F and, for practical purposes, neutron fluences cannot be measured absolutely, it must be accepted that at the present time absolute values of these two parameters are not known independently of each other.

However, an empirical calibration approach suggested by Fleischer and Hart (1972) circumvents the need for selecting a λ_F value and for absolute neutron dosimetry. If equation (4.8) is substituted into equation (4.7), we obtain:

$$T = (1/\lambda_d)\ \ln\,[1+ (\lambda_d\,\sigma\,I\,\rho_s\,B\rho_d)/(\rho_i\,\lambda_F)] \qquad \text{.....(4.9)}$$

All of the constants, except λ_d, may be treated together as a single calibration constant zeta (ζ):

$$T_{UNK} = (1/\lambda_d)\ \ln\,[1+ \lambda_d\,\zeta\,(\rho_s/\rho_i)\,\rho_d] \qquad \text{.....(4.10)}$$

Zeta represents a calibration baseline for the specific dosimeter glass in which ρ_d is counted, and can be evaluated from a series of age standards by:

$$\zeta = [e^{\lambda_d\ T_{STD}} - 1]/[\,\lambda_d\,(\rho_s/\rho_i)_{STD}\,\rho_d] \qquad \text{.....(4.11)}$$

In each of equations (4.7, 4.9, 4.10 and 1.11) ρ_s and ρ_i are assumed to be counted on surfaces of similar registration geometry, or else, modified by a suitable geometry factor. Such a system calibration should be based on a series of age standards, not on a single measurement that is far from precise. The list of internationally accepted age standards is given in Table 4.2.

Table 4.2 Prominent reference samples used as age standards in fission track dating (Wagner and Van Den Haut, 1992).

Reference Material	Geological Specification	Region, Country	Age* (Ma)	Method and reference	Relevant fission-track publications
Zircon	Bishop volc. tuff	California, U.S.A.	0.734± 0.024	$^{40}Ar/^{39}Ar$ (sanidine) Hurford and Hammerschmidt (1985)	Hurford and Green (1983); Green (1985)
Zircon	Buluk Member volcanic tuff Bakata Formation	Bakata Valley, N. Kenya	16.4± 0.2	K-Ar (alkali feldspar) McDougall and Watkins (1985)	Miller et al. (1985) Hurford and Watkins (1987)
Zircon	Tardee rhyolite	Northern Ireland, U.K.	58.7± 1.1	K-Ar and $^{40}Ar/^{39}Ar$ (sanidine) Hurford et al. (unpub.)	Hurford and Green (1983); Green (1985) Hurford et al. (unpub.)
Zircon **Apatite**	Fish Canyon Volc. tuff	Colorado, U.S.A.	27.8± 0.2 (27.9±0.7)	$^{40}Ar/^{39}Ar$ (biotite) Hurford and Hammerschmidt (1985) (K-Ar of four mineral phases, Steven et al.,1967)	Hurford and Gleadow (1977); Naeser et al. (1981); Hurford and Green (1983); Green (1985); Miller et al. (1985)
Apatite	Durango mitite ore body in Carpintero volcanic group	Cerro de Mercado, Mexico	31.4± 0.6	K-Ar (average of Carpintero Group) Mc Dowell and Keizer (1977)	Naeser and Fleischer (1975); Hurford and Gleadow (1977); Green (1985)
Apatite Sphene Zircon	MountDromedary Intrusivecomplex	New South Wales, Australia	98.8± 0.6	Rb-Sr (biotite) Williams et al. (1982)	Green (1985) Miller et al. (1985)
Glass	Moldavite Tektite	S.Bohemia Czechoslovakia	15.21±0.15 (15.1±0.7)	K-Ar, Staudacher et al. (1982) (K-Ar, Gentner et al., 1967)	Wagner (1966) Gentner et al. (1967) Naeser et al. (1980)

* Recalculated with IUGS recommended constants (Steiger and Jager, 1977) where necessary.

(i) Zeta Calibration Constant

In the present FT work, the ages of zircons were calculated by using the value of zeta determined by Thakur and Lal (1993). This value for CN1 glass is 110.6± 2.6 (2σ). The apatite ages were determined using CN5 as the glass dosimeter. Zeta value for this glass as determined by Kumar (1999) using two apatite age standards namely, Fish Canyon volcanic tuff, and Mount Dromedary intrusive complex was used for age calculations.

4.4 THERMAL ANNEALING AND CLOSURE TEMPERATURES OF APATITE AND ZIRCON

In order to quantify the geothermal history using mineral ages, Dodson (1973, 1979, 1981) and Dodson and McClelland-Brown (1985) introduced the concept of **closure temperature** (T_C) of a radiometric clock such as minerals. The closure temperature of a mineral-isotopic system represents a critical threshold above which the radiogenic daughter product (stable isotopes or fission damages) is not retained against thermal disturbance and below which these are accumulated. The closure is not instantaneous and there exists a transitional temperature range in which the daughter product or radiationdamage is partially retained and partially lost. The rate of cooling also has some effect upon the closure temperature, the slower the cooling, the lower the temperature and vice-versa.

In fission track dating, the term **annealing** is used for the partial to complete erasure of tracks (Fleischer et al., 1965 b). The fading occurs when some of the ions that were displaced during formation of the track, diffuse back into the track and heal some of the broken bonds. The annealing process appears to slow the etching rate, and so the etchant takes longer and longer to etch out the track. After a certain amount of annealing, the track has been broken by diffusion so many times that it etches at the same rate as the crystal and therefore cannot be seen.

The studies of the effects of various environmental parameters on track stability in different mineral and glasses (see Fleischer et al., 1975; Wagner and Van Den Haute, 1992), indicate that ordinarily it is the temperature which has the predominant effect. Under geological condition, fading of fission tracks is a common phenomenon and the resulting loss of fission tracks tends to lower the apparent FT age. In that case, the time at which the FT clock was turned on and the time that is given by the clock is no longer the same. The apparent FT mineral ages lowered by partial or complete track fading have resulted in understanding the insights of the thermal history of the host rock.

Track fading is a time and temperature dependent process (Fleischer et al., 1965 b) and equivalent effects can be achieved by heating at low temperatures for prolonged periods and vice-versa. The available results of the fading properties for apatite and zircon are reviewed below in terms of their closure temperatures.

4.4.1 Annealing Characteristics of Apatite

Apatite [nominally $Ca_5 (PO_4)_3$ F,Cl,OH] is a common accessory mineral in most igneous rocks and in many metamorphic and sedimentary rocks.

Drill hole derived annealing temperatures for fluorapatite indicate that it is effectively totally annealed (yield zero age) at temperatures that range from about 105°C for relatively long term heating of ~100 Ma duration to 150°C for ~100,000 years heating (Naeser, 1981). This temperature-time correlation agrees reasonably well with the extrapolated laboratory annealing data. However, the annealing behaviour of fission tracks in apatite is also influenced by its anionic composition and the crystallographic orientation of the track (Crowley et al., 1991; Donelick, 1991). Fission tracks parallel to the c-axis are more resistant against annealing than tracks perpendicular to c-axis. As far as the effect of apatite's chemical composition is concerned, it is the Cl/F ratio which governs the annealing temperature. The tracks in Cl rich apatite are more resistant to annealing than tracks in fluorapatite. The **closure temperature** used in the present study is **120 ± 20°C.**

4.4.2 Annealing of Fission Tracks in Zircon

The fission track annealing behaviour of zircon is comparatively less well known. Although it is well established that FT retention is higher in zircon than in apatite, the various estimates for closure temperatures in zircon range widely from about 175° (Harrison et al., 1979) to 300°C (Krishnaswami et al., 1974). The potential difficulty in understanding the annealing behaviour of FT in zircon appears to be the role of accumulated radiation damage from the α-decay of uranium and thorium. According to Kasuya and Naeser (1988), the thermal stability of FT in zircon is inversely proportional to the density of accumulated alpha recoil damage within the zircon grains. On the other hand, Carter (1990) found no real correlation between uranium concentration and zircon fission track ages and suggested that differential annealing of FT in zircon might be rather a function of mineral chemistry similar to the one observed in apatite (Green et al., 1989).

The closure temperature of zircon appeared to be varied from 210° to 260°C for different cooling rates ranging from 1°C/Ma to 100°C/Ma (Brandon and Vance, 1992). Hurford's (1986) estimate of T_{zc}=240 ± 50°C for a cooling rate of 15°C/Ma from cooling history of Lepontine Alps based on a variety of isotopic data, is in good agreement with those predicted by Brandon and Vance (1992). In the present study we have used **240 ± 25°C** as the **closure temperature** of zircon.

4.5 FISSION TRACK STUDY RESULTS

4.5.1 Zircon FTD

The selected samples include mainly the Lower Cenozoic stratigraphic units and were collected from the units bounded by the MBT and the Nahan Thrust. FT method was used for 23 sandstone samples of the Cenozoic sediments including 5 from the Subathu, 5 from the Dagshai, 10 from the Kasauli, and 3 from the Lower Siwalik formations. Sample locations are given in Figure 2.3.

In the present study, the samples which were in close vicinity to each other, have been clubbed as per details given in Tables 4.3. FT analytical data of individual zircon grains are not included in the thesis due to its bulk and available with the author. However, the range of ages of individual grains and the number of grains analysed are given in the Table 4.3 and the composite probability density plot and histogram of zircon grain ages in general clubbed samples of different formations are given in Figure 4. 9.

4.5.2 Apatite FTD

FT age data of apatite samples is very limited as this mineral was not available in sufficient quantities in many samples. FT apatite ages are available from one sample of Kasauli Formation and two samples of Siwaliks. The analytical data of apatite samples are indicated in Table 4.4. The composite probability density plots of those samples are shown in figure 4. 10.

Table 4.3– Peak summary of zircon fission track age data of Cenozoic foreland sediments of NW Himalaya , India

FORMATION	Clubbed Sample	Age Range (Ma)	Deposit. Age (Ma)	Gaussian Best Fit Peaks			
				P_0	P_1	P_2	P_3
Lower Siwalik	**Siw2** (2, 5)	298-9 N_t = 64 U=513-29	14.3 (a) 18.5-10.5 (b) 10.8/8.2 (c)	13.9 N_f=25 π_f=38 % W=29	26.1 N_f=34 π_f=53 %	43.2 N_f=2 π_f=4 %	———
	Siw1 (1)	363-15 N_t=24 U=358-13		20.5 N_f=10 π_f=43 % W=30	24.3 N_f=6 π_f=29 %	93.7 N_f=5 π_f=22 %	314.0 N_f=3 π_f=12 %
Kasauli	**K3** (56, 58, 26, 27,40)	510-12 N_t=168 U=304-15	23.8 (d)	26.0 N_f=81 π_f= 48 % W=26	45.8 N_f=36 π_f= 22 %	180.0 N_f=13 π_f= 8 %	320.5 N_f=35 π_f= 21 %
	K2 (11, 17)	522-15 N_t=61 U=279-14		28.9 N_f=37 π_f= 61 % W=26	93.9 N_f=16 π_f= 26 %	348.1 N_f=4 π_f= 7 %	———
	K1 (51, 53, 54)	529-16 N_t = 98 U=191-12		31.1 N_f=40 π_f= 41 % W=26	76.4 N_f=15 π_f= 15 %	154.6 N_f=5 π_f=5 %	324.5 N_f=37 π_f= 38 %
Dagshai	**D2** (6, 9, 23, 42)	488-16 N_t=124 U=273-13	35.5 (e) <28- <25 (f)	25.0 N_f=46 π_f=37 % W=25	45.1 N_f=27 π_f=22 %	194.5 N_f=21 π_f=17 %	339.9 N_f=29 π_f=23 %
	D1 (33)	515-19 N_t=77 U=160-12		29.7 N_f=38 π_f= 50 % W=28	76.6 N_f=14 π_f= 18 %	272.1 N_f=14 π_f= 18 %	447.4 N_f=12 π_f= 15 %
Subathu	**S2** (33, 61)	555-144 N_t=36 U= 105-5	62-40 (g)	———	131.1 N_f=2 π_f=6 % W=19	241.1 N_f=8 π_f=22 %	389.1 N_f=27 π_f=74 %
	S1 (64, 32, 28)	557-42 N_t=90 U=125-10		40.7 N_f=3 π_f=4 % W=21	91.4 N_f=7 π_f=7.4 %	217.4 N_f=29 π_f=32 %	393.5 N_f=51 π_f=57 %

The depositional age value are adopted from: (a) Johnson et al. (1985); (b) Sangode et al. (1996); (c) Harrison et al. (1993); (d) Arya (1998); (e) Najman et al. (1994); (f) Najman et al. (1997); and (g) Mathur (1978) .The used symbols are N_t = Total number of grains, N_f = Grain number fraction which is composed the peak, π_f =Proportion of total % of grains, W= Peak width. The sample no. referred to the Figure 2.3.

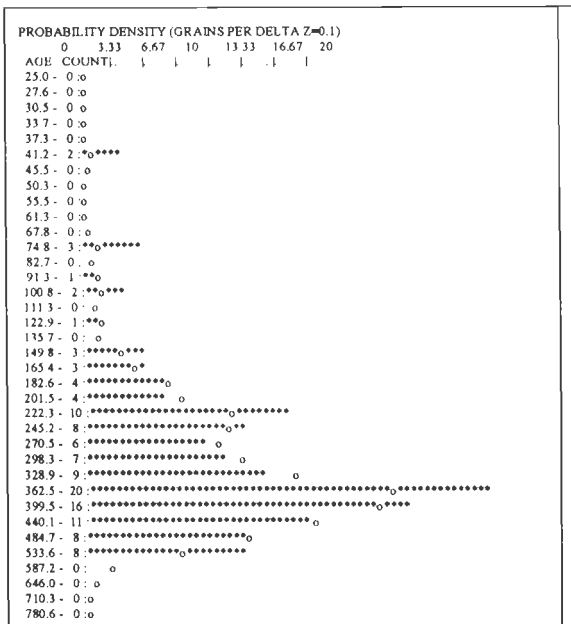

Subathu Formation

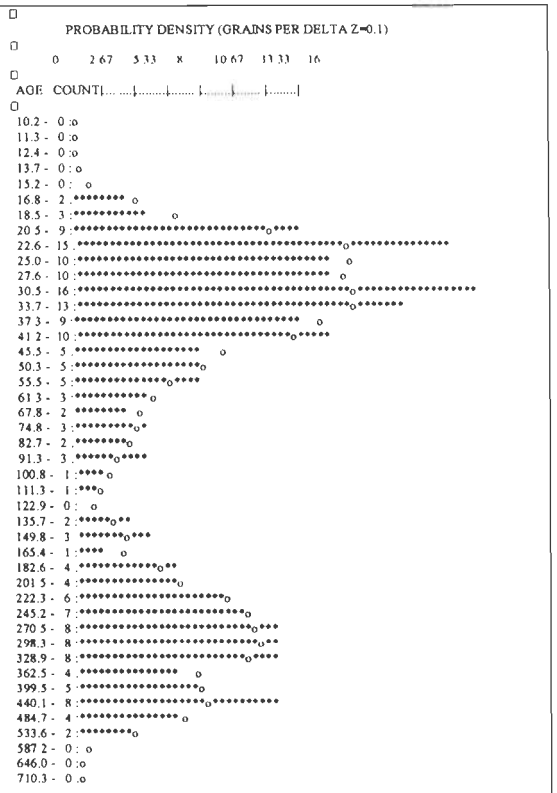

Dagshai Formation

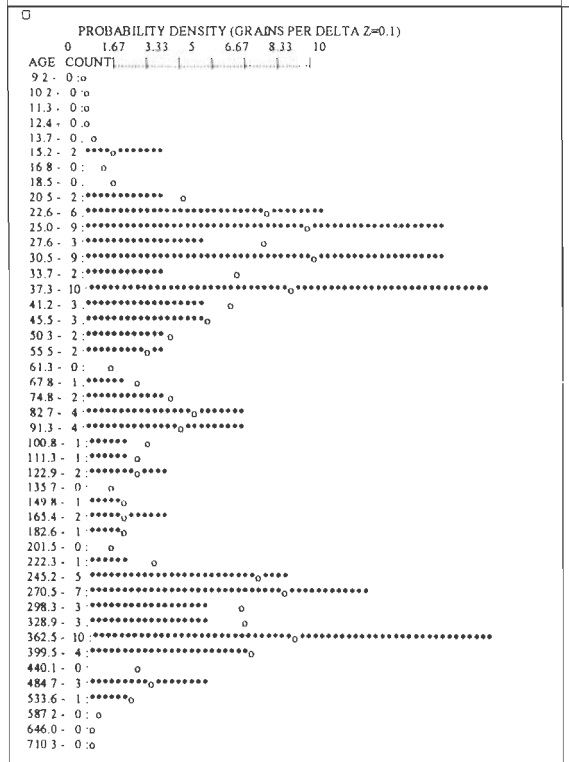

Kasauli 1

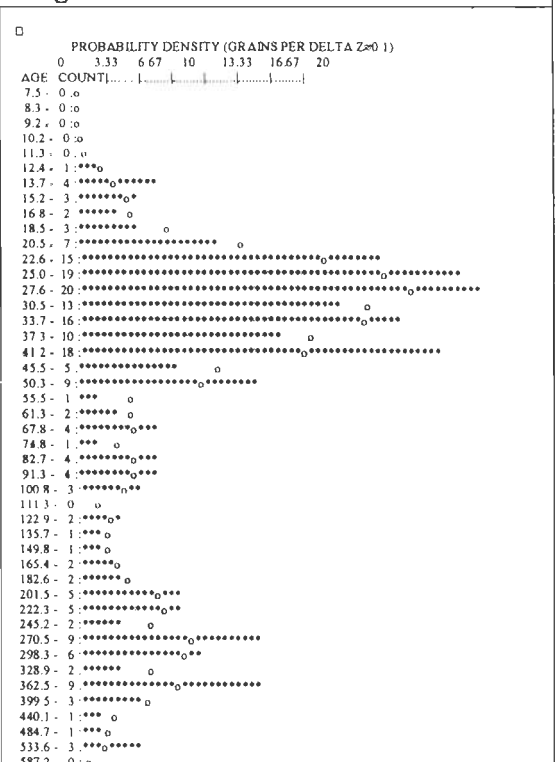

Kasauli 2

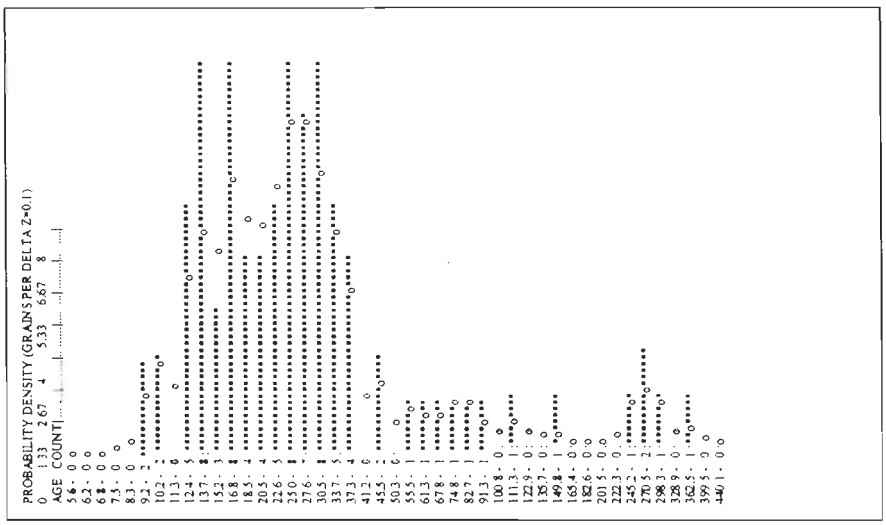

(Lower Siwalik Formation)

Figure 4.9- Composite probability density plot and histogram of zircon FT ages of general clubbed samples of Subathu, Dagshai, Kasauli (Kasauli 1= lower part and Kasauli 2= upper part), and Lower Siwalik (=Nahan) formations.

Table 4.4 Fission Track Analytical Data of Apatite

Sample Code	Lab Code	Number of Crystals	Track Densities		$P(\chi^2)$ % age	Glass Dosimeter ρ_d (N_d)	Age (Ma)	Weighted Mean Age (Ma)
			Spontaneous ρ_s (N_s)	Induced ρ_i (N_i)				
Siw1	SWAP2	2	0.625 (20)	4.375 (140)	30	0.5634 (5634)	11.94±2.86	9.96 ± 0.99
Siw1	SWAP1	19	0.2170 (94)	1.900 (823)	80		9.55±1.05	
KAS 37	KASAP1	14	0.2204 (54)	1.363 (334)	7		13.51±1.99	13.51± 1.99

4.6 DISCUSSION

While assigning any meaning to the FT data of individual mineral (apatite and zircon) grains from the sediments, three possible situations need to be considered.

1 If the sediments have remained at temperatures well above the closure temperature of apatite since deposition, the grain ages of both the detrital minerals will remain unreset and their FT ages would reflect the thermal history of the source region. The individual grain ages under such conditions will be greater than (or at the most comparable) the depositional age.

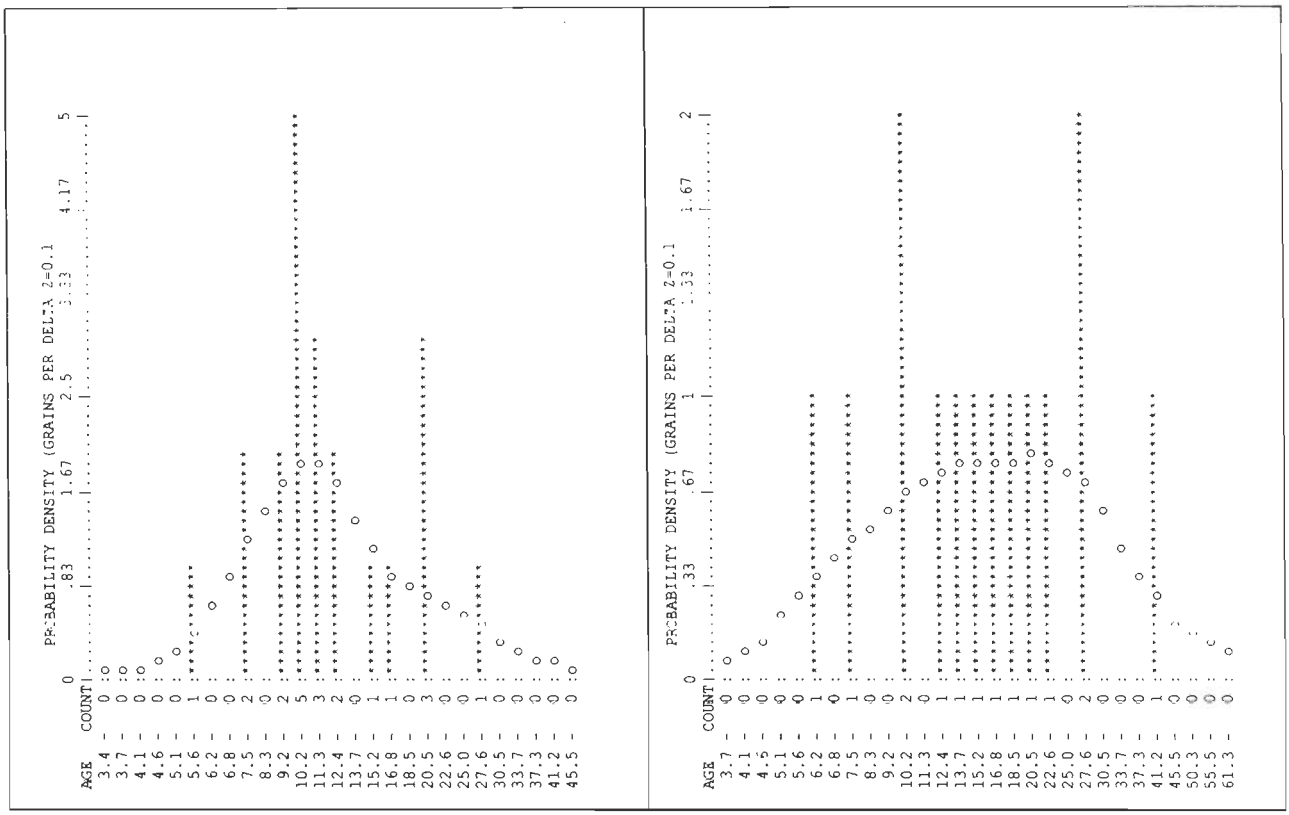

Lower Siwalik Formation **Kasauli Formation**

Figure 4.10- Composite probability density plot and histogram for apatite ages of Lower part of Lower Siwalik (=Nahan) sample from Nahan area, and upper part of Kasauli Formation (Kasauli area)

2 If the sediments were buried to a depth with temperature conditions below the closure temperature of apatite but well above that of zircon, the apatite grain ages will be reset while zircon ages will still remain unreset. Under such conditions the individual apatite grain ages shall be lower than depositional ages of the sediments and shall reflect the post-depositional thermal/exhumation history of the sediments. On the other hand, the situation of zircon grain ages will be similar to the one mentioned in (1) above.

3 If the post-depositional temperature conditions in sediments were well below the closure temperatures of zircon, the individual grain ages of both the cogenetic minerals will be reset and reflect the thermal/exhumation history of the sediments.

The present FT ages of individual grains of zircon and apatite appears to corroborate with the second possibility and is discussed below. Since the zircon age data represent the unreset grain-age distribution, it will be apposite to mention some of the salient features of the general principles involved in the interpretation of such distribution.

4.7 MEANING OF THE UNRESET-GRAIN AGE DISTRIBUTION: GENERAL PRINCIPLES

An unreset grain-age distribution can be viewed as a mixture of component populations, with each component derived from a specific FT source terrain (Brandon, 1992). The term FT source terrain refers to a discrete area in the general source region that yields zircons of a characteristic FT age (Brandon and Vance, 1992). (The American spelling for "terrain" is used to avoid confusion with the term "tectonic terrain" and to emphasized that the zircons are derived from surface outcrops and are not necessarily representative of the subsurface geology.) In reality, a given source region is probably capable of delivering a range of FT grain ages, but it is anticipated that a few dominant component populations will account for the bulk of the ages.

One problem in dating unreset detrital zircons is that the individual grain ages usually have fairly low precision, with an average relative standard error of about 13%. As a result, it is necessary to find related groups of grain ages in order to improve the precision of the age estimates. Brandon (1992) introduced two methods for identifying component population in a mixed population of grain ages. The first decomposition method, the χ^2age method, isolates the youngest fraction of "Plausibly related" grain ages and assigns an age to this fraction, called the χ^2age. This age estimate is useful in that it provides a maximum limit for the depositional age of the sandstone sample. The second method, the Gaussian peak-fitting method decomposes the entire grain distribution into a finite set of component Gaussian distributions, each of which is defined by a unique mean age, a relative standard deviation, and the size of the component distribution relative to the total distribution. Through a series of simulation experiments (Brandon, 1992) and a practical application (Brandon and Vance, 1992), it has been shown that

both of these methods can produce satisfactory results given a sufficient number of grain ages for each peak and adequate separation between adjacent peaks.

The Gaussian peak-fit method directly decomposes the grain-age spectrum into a series of component Gaussian populations or peaks. Each peak is defined by the mean age, the width of the Gaussian relative to mean age (W_f, equivalent to standard deviation divided by the mean age), and the size of the Gaussian relative to the total size of the grain age distribution (π_f). According to Garver and Brandon (1994) a peak should ideally correspond to a single-age population of FT grain ages. Because the relative standard deviation, W, of a single age peak does not change significantly with age, then it is expected that W should remain approximately the same for all peaks. Because few parameters are included in the solution, this modification tends to enhance the resolution and stability of the peak-fitting calculation. Following this approach, peak fitting in the present data has been done by estimating a common value of W for all peaks in the distribution rather than fitting a separate W for each peak.

FT source terrains can be divided into three types:

(1) a synorogenic source terrain, where the FT age of the source terrain is the result of cooling by erosion and/or extensional faulting of synorogenic topography;

(2) a post-orogenic source terrain, where the FT age of the source terrain is the result of cooling during post-orogenic erosion and/or gravitation collapse of mountains topography;

(3) a volcanic source terrain, where the characteristic FT age is a result of volcanism and near-surface magmatism. A volcanic FT source terrain might include a wide range of rock units, such as volcanic flows and pyroclastic deposits, hypabyssal intrusions and dikes, and thermally reset country rock, all of which would be related by a common FT age corresponding to the time of volcanism.

These various types of source terrains can be distinguished but only on the basis of indirect evidence. A general clue is provided by the petrology of the framework grains: metamorphic detritus would imply a synorogenic or post-orogenic source terrain, whereas volcanic detritus would imply a volcanic source terrain. The introduction of metamorphic detritus into a basin might reflect the initiation of a synorogenic source terrain, whereas a post-

orogenic source terrain might be characterized by a decreasing proportion of metamorphic detritus with time.

Another useful diagnostic measure is the lag time which is defined as the time between the cooling of FT source terrain, as indicated by the FT age of detrital zircons derived from the terrain, and the time of deposition of the zircons, as indicated by stratigraphic age of the sandstone that hosts the zircons. The lag time represents the age of the Gaussian peak at the time of deposition and it represents the total time required to bring rocks to the surface from the zircon annealing zone. Lag time, therefore, can be related to the denudation rate in a source region. A short lag time would be expected for volcanic source terrains and a variable lag time for orogenic source terrains. Unfortunately, the lag times that characterize these different types of settings are not always easily distinguished. Some tectonically active mountain belts have source terrains with lag time as 1 Ma (e.g., Cerveny et al., 1988), and some volcanic terrains may be denuded very slowly, resulting in long lag times, perhaps an order of tens of Ma.

In FT stratigraphy, where a series of stratigraphically-related age distributions are evaluated, two types of peak ages can be identified: 'moving peaks', defined by a peak age that gets progressively younger or older up-section, and 'static peaks', where, the peak age remains relatively constant up-section. A useful measure of the movement of peaks is the lag time, defined as the peak age minus the depositional age. Forward moving peak which get progressively younger up-section, can be produced by a source terrain characterized by either constant volcanic activity or the steady denudation of a source terrain. FT stratigraphy characterized by forward moving peaks generally represents first cycle detritus. Backward-moving peaks, which get progressively older up-section, are probably less common. However, erosion of a basin containing first cycle detritus could produce FT stratigraphy with backward-moving peaks, which would be indicative of recycled sediments.

Summarized here are some general guidelines for characterizing a source terrain: (1) a volcanic source terrain is probably best indicated when a zircon FT peak has a short lag time (<~5 Ma) and the sandstone contains a significant fraction of primary volcanic detritus, (2) an orgogenic source terrain is probably best indicated when a peak makes up a significant proportion of the total grain age distribution (π_f > ~20%), the lag time for the peak is >5 to 10

Ma, and the sandstone contains a significant fraction of metamorphic detritus, (3) an orogenic source terrain might also be inferred for those peaks where the lag time is short (<10Ma), but the sandstone has little or no volcanic detritus, (4) a confident interpretation is probably not possible for those minor peaks (π_f < ~20%) with relatively long lag times (>10 Ma), and (5) changes in provenance with stratigraphic level can be used to distinguish between syn-orogenic and post-orogenic source terrain. A syn-orogenic source terrain might be distinguished by the following changes up-section: the introduction of metamorphic detritus and the simultaneous appearance of a young FT peak, followed by a systematic decrease in the lag time of that peak as the rate of denudation accelerated toward a steady state condition. A post-orogenic source terrain might be distinguished by an up-section decrease in metamorphic detritus and an increase in the lag time for the relevant FT peak, reflecting a decreasing rate of denudation as topography becomes more subdued.

4.8 ANALYSIS OF THE PRESENT DATA

4.8.1 Zircon

The Gaussian peak fitting programme developed by Brandon and his group was run using the FT zircon grain data of each sample. The peak age values and all other peak parameters of each sample as obtained from Brandon's computer programme are indicated in Table 4.3. The grain age distributions of all samples contain 3-4 resolvable peaks.

The distribution width (W) of all samples are higher than 19%. The population of zircons derived from a single-age FT source is estimated to have W ≈16.3%. Such an inference has been drawn by investigating the grain age distribution of unreset volcanic zircons of tuff samples (Brandon and Vance, 1992). The values of W for all the samples in the present study (Table 4.3) which fall between 25-30 percent suggest that zircons within all the sediment samples were derived from a complex FT source terrain.

(i) Estimation of depositional age

Due to the very limited data (biostratigraphy, magnetostratigraphy and isotopic dating methods) the depositional ages of various sedimentary formations in the Himalayan foothill are not precisely constrained. However, if we go by the general inferences of the FT age data

discussed in the preceding pages and some limited available data regarding the depositional ages, the youngest age peak of all the samples given in Table 4.3 can be used for estimation of depositional age of different formations.

Subathu Formation- The depositional ages of this Formation are not well constrained. Depositional ages varying from 40 to 60 Ma has been proposed for this Formation (Mathur, 1978). In the present study only one sample i.e. S1(Table 4.3) has shown a peak at 40.7 Ma which falls very close to the lowest limit of this range. However this is not a dominant peak as the fraction of grains in this peak is very small. The youngest peak in white quartzite (sample S1) which forms the key bed at the upper part of Subathu Formation, was not recorded in the FT age data of this sample. The overall lack of grains in the youngest peak P_o of the Subathu Formation could arise due to several reasons. There is a possibility though with very small probability, that only very limited grains belonging to youngest fraction might have been included during mounting. Another reason for lack of low FT ages zircon grains in the Subathu Formation can be either low erosional rate during the early stages of Himalayan orogeny or very limited source region responsible for contributing the detritus affected by the Himalayan orogeny.

Dagshai Formation – Due to lack of fossils, all attempts are now focused to other dating methods to determine the age of deposition of the Dagshai Formation. On the basis of paleomagnetic study, Najman et al. (1994) proposed the depositional age of this Formation as 35.5±6.7 Ma. However due to large error associated with this age, Najman et al. (1997) determined K-Ar ages of detrital muscovites and proposed ≈28 Ma as the age of deposition.

In the present study the sample D1 from the lower part of Dagshai and D2 from the upper part indicate 29.7 Ma and 25.0 Ma as the youngest Gaussian peak ages respectively. These ages appear to represent the depositional age of Dagshai. The proportion of grains in the youngest peak has increased to 10-15 times in comparison to the Subathu Formation. This increase suggest that by the starting of deposition of Dagshai Formation, the erosional rate (which implies uplift of the rocks) and/or the extent of the provenance affected by the Himalayan orogeny increased sufficiently. Tectonic activity, therefore, increased during the Dagshai time and, so provided new sources with younger ages.

Kasauli Formation- There is practically no study reported in the literature about the depositional age of this formation. Arya (1998) on the basis of paleontology study has assigned an age of 23.8 Ma to the lower Kasauli. FT age data of zircons separated from the Kasaulis indicate the youngest peak at 31.1, 28.9, and 26.6 Ma respectively for the lower, middle and upper parts of this Formation. These ages appear to represent at least the upper limit of the deposition time of these rocks.

However, the overlapping ages of youngest peaks in Kasauli and Dagshai indicate that either these formations are not distinct as far as their deposition time frame is concerned. Or if they are distinct, then the ages given by the youngest peaks in various horizons of Kasauli are higher than their actual depositional ages. Such a situation could mean that exhumation of Kasauli was comparatively slow than during the Dagshai.

Lower Siwalik Formation- In these rocks the ages of youngest peaks in the zircon age distributions are 20.5 and 13.9 Ma respectively for the lower and upper parts of the formation. These ages appear to be consistent with the depositional ages estimated by Sangode (1997) using paleomagnetic stratigraphy.

(ii) Older peaks

Older peaks especially P_2 and P_3 are dominant in the Subathus. The fraction of grains in the older peaks of Subathus is very high while it decreases as we go up section towards the Siwaliks. On the other hand, fraction of grains in youngest peaks of the Siwaliks is very high in comparison to that of Subathus. Such a trend of distribution of grain ages certainly speaks something about the provenance. It appears that extent of the older detritus contributing to the Subathus was much larger than the orogeny affected-detritus implying thereby a very limited effect of the Himalayan orogeny both in terms of areal extent and uplift of the rocks during the time Subathus were deposited. During the time of deposition of the Dagshais and Kasaulis, the grain age distribution is biased towards younger ages. This means that the effect of the Himalayan orogeny during this time increased tremendously. In the lower part of the Lower Siwaliks, the amplitude of the P_3 and P_2 peaks is very small and is almost insignificant in the upper part of the Lower Siwaliks. If we assume that by Siwalik 's time all the source rocks were

affected by the Himalayan orogeny, then the higher ages peaks present in the Siwaliks could come from the recycled material i.e. from the Subathu, Dagshai, and Kasaulis etc. The presence of the Kasauli sandstone pebble (Fig. 4.11) within the Siwaliks give further configuration to such a possibility.

Thus, we find that peak ages within each group appear to vary with the depositional time. This is also evident from Figure 4.12, which is a composite probability density plot obtained by clubbing all the grain ages of individual formations (Table 4.5). The figure clearly depicts the shifting of peaks towards younger ages with the decrease in depositional ages. Such a feature indicates that the source is continuously rising and feeding the material to the sedimentary basin.

(iii) Erosional Model of the Source Rocks

The zircon fission track data show ages significantly older than any records within the Himalayan crystalline rocks exposed to the north of the foreland sediments. One possible explanation which can be invoked for this apparent anomaly is that the samples with older zircon ages were derived from the structurally highest part of the proto-Himalayan rocks that have now been removed by denudation. The process by which this is achieved is described below and illustrated in Figure 4.13.

Figure 4.11- Kasauli sandstone pebble in the upper part of Lower Siwalik (Nahan area)

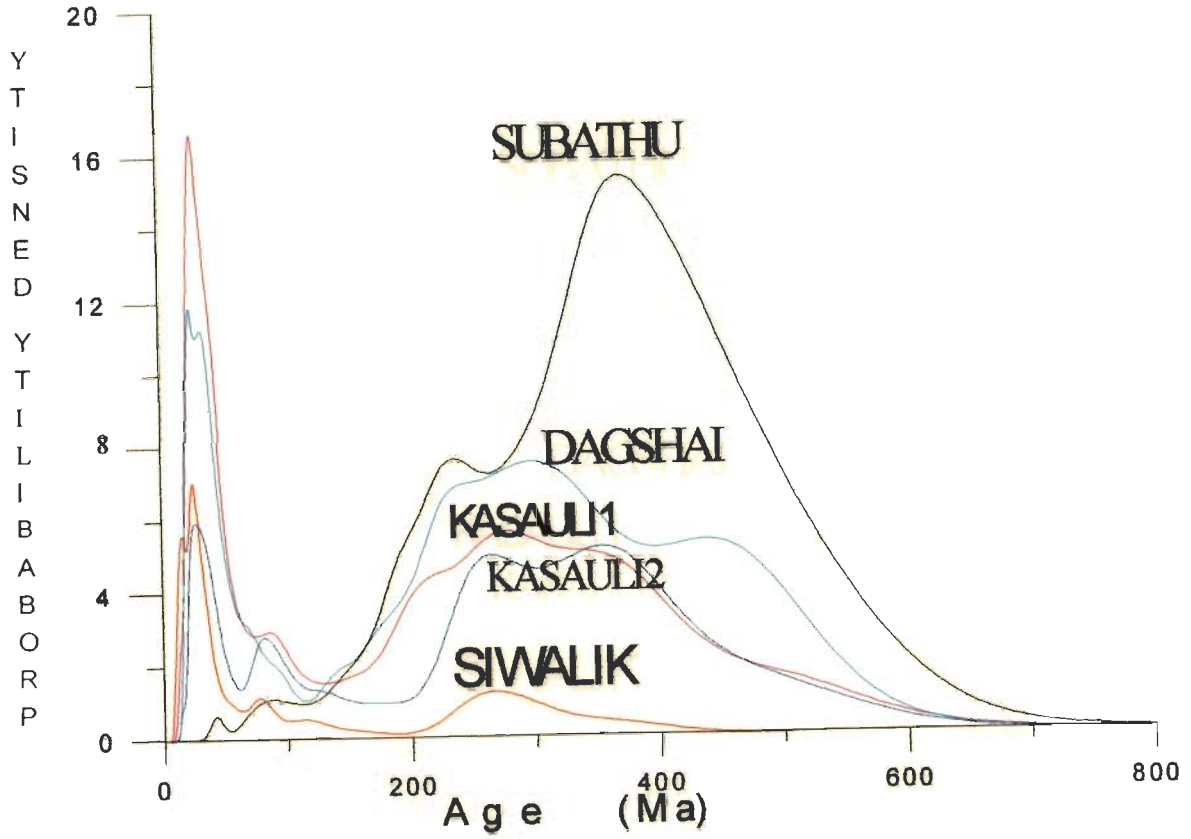

Figure 4.12 The general clubbing of zircon FT results of the Cenozoic samples.

It appears that as a result of collision between India and Eurasia around 55-40 Ma, the crystalline basement rocks underwent uplift resulting into sufficient topography to cause erosion/denudation. Prior to this, basement rocks that lay above the zircon partial annealing zone (<150° C) would have zircon FT ages related to a previous thermal history. If such rocks from the Subathus could be separated and analysed today, they would give zircon FT ages well in excess of 55-40 Ma. With the initiation of accelerated denudation rates at ca. 55-40 Ma, these rocks would have been the first to be removed by erosion and deposited at the base of the Subathus. With continued erosion and sufficient topography, the zircon partial annealing zone that existed prior to 55-40 Ma becomes a fossil zircon partial annealing zone exposed at the surface. Detritus derived from this zone will have reduced zircon FT ages, although if analysed today, they will still give ages in excess of 55-40 Ma. Before 55-40 Ma rocks below the zircon partial annealing zone of temperatures greater than 225° -240° C would not have retained

any rocks in zircon. With the initiation of accelerated denudation these rocks would pass through the isotherm corresponding to FT zircon closure temperature i.e. ~240°±25°C. Further denudation will result in these rocks being exposed at the surface. If these rocks were then eroded and re-deposited in the foreland sediments, they would yield zircon FT ages today of ≤55-40 Ma close to the age of deposition of Subathus.

With the continued collision, the limited extent of the Himalayan orogeny during the Subathus further extended to larger areas during the Dagshais which were not affected by the Himalayan orogeny during Subathu time and the source rocks continued eroding in a similar mechanism as discussed above and thus contributed older zircons to the sediments. The similar erosional phenomenon continued in the Kasaulis and Siwaliks.

Table 4.5- Summary of zircon FT results of bulk samples of the Cenozoic formations

FORM-ATION	Age Range (Ma)	χ^2-age (Ma)	Gaussian Best Fit Peaks				
			P1	P2	P3	P4	P5
Lower Siwalik	363-9 N_t = 88 U=470-12	9.7 N_f=4 π_f=4	14.6 N_f=31 π_f=35 W= 29	27.3 N_f=43 π_f=49	66.6 N_f=5 π_f=6	99.6 N_f=3 π_f=4	285.2 N_f=5 π_f=6
Kasauli (b)	523-12 N_t=218 U=281-13	14.2 N_f=7 π_f=3	15.2 N_f=10 π_f=5 W= 26	27.5 N_f=100 π_f=46	44.3 N_f=41 π_f=19	97.3 N_f=18 π_f=8	293 N_f=46 π_f=21
Kasauli (a)	529-15 N_t = 109 U=219-13	22.2 N_f=18 π_f=17	25.2 N_f=25 π_f=23 W= 26	36.1 N_f=26 π_f=24	85.1 N_f=16 π_f=15	153.2 N_f=4 π_f=4	324.8 N_f=37 π_f=34
Dagshai	515-16 N_t=201 U=241-11	26.2 N_f=84 π_f=42	25.1 N_f=67 π_f=33 W= 26	40.3 N_f=45 π_f=23	80.4 N_f=15 π_f=8	226.5 N_f=36 π_f=18	381.7 N_f=37 π_f=19
Subathu	557-42 N_t=126 U=118-9	58.8 N_f=6 π_f=5	39.1 N_f=4 π_f=3 W =21	84.5 N_f=6 π_f=4	144.3 N_f=6 π_f=5	229.6 N_f=35 π_f=28	393.4 N_f=77 π_f=61

Kasauli (a) indicating the clubbed samples no. 51, 54, 11, 53, and Kasauli (b) is: 56, 58, 40, 27, 26, and 17. The location of these samples is in Figure 2.3.

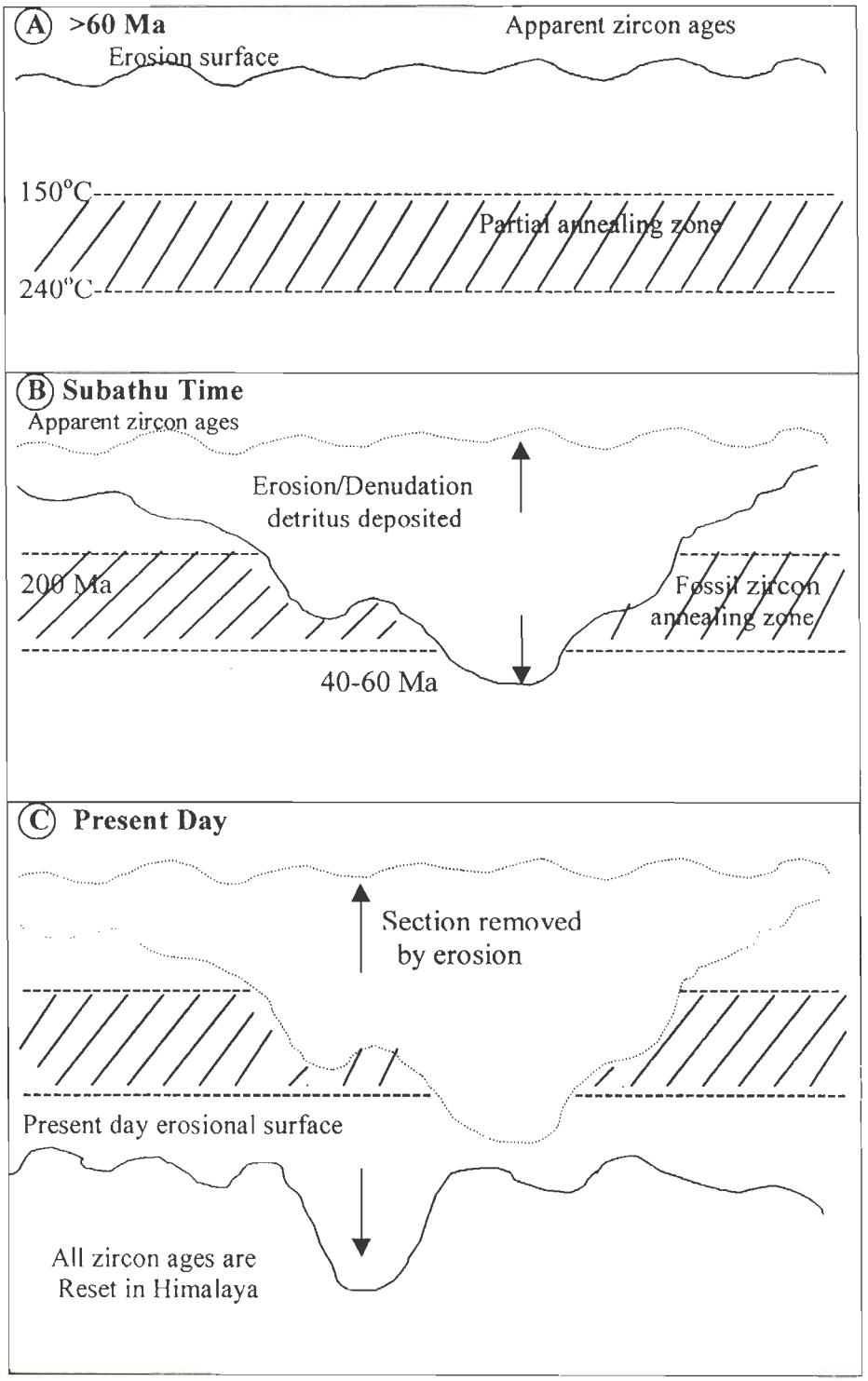

The schematic relation between erosion surface and partial annealing zone of zircon to the observed distribution of zircon FT grain ages in the Cenozoic Himalayan foreland sediments.

The second possibility for the source of old zircon grains is the Lesser Himalayan sedimentary basin. In general, data from the Himalaya strongly support at least an earlier mid-Paleozoic (600-500 Ma) diastrophism (Caledonian) which was later superimposed by the Cenozoic Himalayan orogeny. It is logic to suppose that these old sediments were eroded off and detritus transported and deposited in the pre-Cenozoic/Cenozoic basins in southern parts before starting of collision and ubiquitous effects of Himalayan orogeny on sediments. Therefore, it can be considered that at least, a fraction of the present old zircon FTD ages supplied by this type of source.

Based on paleocurrent directions (Figs. 2.5, and 2.6) it is considered that the Himalayan terrain, which has been active continuously from ~50 Ma to present time, incorporating also the Krol basin located in the northern adjacent part of the Cenozoic foreland basin probably plays an important role to supply the old grains.

4.8.2 Apatite

The resetting of apatite ages from the Kasauli and Siwalik sediments indicate that the Cenozoic sediments subsided to a depth corresponding to the closure temperature of apatite, i.e. 100°-120° C. Assuming the normal geothermal gradient of 30° C/km in the area, it can be inferred that these sediments were buried to a depth of ~ 4 km. In addition, Mehta (1995) calculated apatite ages for Dagshai Formation around Mandi around 8 Ma.

4.9 CONCLUDING REMARKS

The present work consists of more than 750 zircon and apatite FT grain ages from 23 sandstone samples collected from Nahan-Subathu-Solan-Kalka area. Unreset FT zircon ages and their distribution and reset apatite ages leads to the following conclusions.

(i) The thermal conditions in the Cenozoic sediments were below the closure temperature of apatite (120°±20° C) but much above the closure temperature of zircon (240°± 25° C), i.e. the conditions were favourable for organic matter maturation.

(ii) The areal extent of the Himalayan orogeny appears to continuously increasing after the collision of the Indian Plate with the Eurasian Plate.

(iii) In general, pattern of zircon FT ages from the foreland Cenozoic sediments (Table4.5) have shown χ^2-ages of 58.8 Ma, 26.2 Ma, 22.2-14.2 Ma, and 9.7 Ma from the Subathu to the Lower Siwalik formations, respectively.

(iv) The youngest age peak of all the FTD samples can be used for estimation of depositional age of different formations.

(v) The presence of old zircon FT peaks in pre-Siwalik sediments indicates that the uplift rate in the source area is not uniform. Such that, the zircon grains in the youngest peaks are supplied from the area with the high rate of uplift, and those of consists the oldest peaks came from the area with very low uplift rate as discussed earlier by Cerveny et al. (1988) for the northern part of Pakistan.

(vi) There are three possibilities for the source of the old grain ages: a) the veneer within the Himalaya, with their characteristics inherited from the proto-Himalayan tectonic events and unaffected by the young Himalayan thermal events, b) the old Cenozoic sediments of the foreland basin itself may be involved as an additional source of the old grains into the younger formations. The existence of sedimentary lithic fragments in the Cenozoic formations could be considered as a document of this point and c) the old basins such as Krol basin located in the northern adjacent part of Cenozoic foreland basin may have an important role in the supply of the grains.

vii) The resetting of apatite ages from the Kasauli and Siwalik sediments indicate that Cenozoic sediments subsided to a depth of ~ 4 km corresponding to the closure temperature of apatite.

CHAPTER- 5

PETROLEUM SOURCE ROCK EVALUATION

5.1 INTRODUCTION

It is believed that the hydrocarbon prospects and productivity of a sedimentary basin depends mainly on the quantity, quality, degree of thermal maturity of organic matter, areal extent and thickness of source rock (Bray and Evans, 1961; Philippi, 1965; Welte, 1965; Tissot, 1971; Tissot and Welte, 1978; Hunt, 1979; Hedberg, 1982; Waples, 1985). The term *source rock* is generally used for fine grained sedimentary rock that has generated or capable of generating petroleum hydrocarbon. A potential source rock is a unit of rock that has the capacity to generate oil and gas in sufficient quantity to form commercial accumulation, but has not done yet, because of insufficient thermal maturation (Dow, 1977). An effective petroleum source rock may be defined as a fine grained sediments, in their natural setting, which have generated and released enough hydrocarbon to form a commercial accumulation of oil and gas (Hunt, 1979).

In the present study the argillaceous sediments found in the type-sections of the Subathu, Dagshai, Kasauli and Nahan (= Lower Siwalik) formations in Nahan, Subathu, Kalka and Solan areas of the Himachal Pradesh, have been evaluated for petroleum source rock.

Source rock in a sedimentary basin are evaluated in terms of the following three factors:

(i) The abundance of organic matter in a source sedimentary

(ii) The nature of the sedimentary organic matter

(iii) The maturity level or stage of evolution of the kerogen, which is governed by its thermal exposure.

The principles and methodology of evaluating these factors are discussed below.

5.1.1 Abundance of Organic Matter

The quantity of hydrocarbons generated from the biogenic source depends on the amount of organic matter preserved in the fine grained sediments. Therefore, the abundance of organic

matter in sediments is an important parameter of a source rock. Higher the amount of organic matter, higher is the total organic carbon content in the sediments. Therefore, the total organic carbon (TOC) is considered as an indicator of organic matter content of the sediments.

For a sedimentary rock to generate and expel hydrocarbons in commercial quantity, it should have adequate amount of organic matter above a minimum level. A large variety of sediments from different geological provinces, including the best sequences which are proved to have generated petroleum hydrocarbons, have been analysed for TOC by a number of researchers such as Philippi (1965), Welte (1965), Tissot and Welte (1978), Hunt (1979), Kraus and Parker (1979), Waples (1981), and Barker (1989). Although some of them have organic carbon content of 10% and above, most of the source rocks have carbon content ranging from 0.5 to 2% (Hunt, 1979).

On the basis of these observation, it has been found that the non-reservoir shale and calcareous sediments should contain in general, total organic carbon content more than 0.5% and 0.3% respectively (Tissot, 1984). In fact, whatever the nature of organic matter, an original organic carbon content of lower than 0.5% in argillaceous fine-grained sediments is likely to produce insufficient amounts of liquid petroleum with respect to the adsorption properties of the source rock and to the necessary pressure building for the expulsion of oil (Tissot, 1984).

The following classification is made for the organic mater richness in terms of organic carbon concentration (TOC) in shale (Ower, 1980).

Richness Rating	**Organic Carbon Concentration (TOC)%**
Poor	< 0.5
Moderate	0.5 - 1.0
Good	1.0 - 2.0
Rich	2.0 - 10.0

In order to determine the total organic carbon content of a rock, analysis is performed on ground rock which is treated with hydrochloric acid to remove the carbonates as potential source

of carbon dioxide. Then, it is burnt in an atmosphere of oxygen, in Hosthoff Carmograph. The amount of carbon dioxide generated by combustion is measured and thus provides the carbon content of the rock by weight. Flow chart of the procedure to determine TOC is given in appendix-II.

5.1.2 Quality of Organic Matter

Even if the TOC of shale is more than 0.5%, the rock may not generate petroleum hydrocarbons commercially. The type or quality of organic matter in the sedimentary rocks plays very important role in the hydrocarbon generation. The right type of organic matter is capable of yielding large amount of oil and gas on its optimal maturation.

Kerogen is a variety organic matter which generates petroleum hydrocarbons. Originally, Kerogen was referred to as the organic matter in the oil shale that yielded oil on heating. In the recent years it has been defined as all the disseminated organic matter of sedimentary rock, insoluble in non-oxidizing acids, bases and organic solvents (Durand, 1980).

Kerogen, which is the precursor of most oil and gas, has three sources namely; (i) marine, (ii) terrestrial and (iii) recycled organic matter.

The quality of kerogen, therefore, depends on the type of organic source material and the early diagenetic history (Tissot and Welte, 1978). The determination of the type of organic matter is assessed by several techniques, which can be grouped into:

i) Chemical methods which include rock eval pyrolysis, elemental analysis of kerogen, carbon isotopic studies and analysis of bitumen. Rock eval pyrolysis is a very fast and cheap method of evaluating and screening of large number of samples.

ii) Optical methods, includes observation and measurement on organic matter by transmitted and reflected light microscopy.

(i) Rock Eval Pyrolysis

The isolation of kerogen from mineral matrix and the determination of its elemental composition for assessing the quality of organic matter, is time consuming and costly affair. To get around this disadvantage and other drawbacks, a faster and more flexible method of analysis

was developed by Espitalie et al. (1977). It is now widely accepted for source rock characterization (Cleamentz et al., 1979; Espitalie et al., (1980).

The method consists of programmed temperature heating (25°C/minute on an average) in an inert atmosphere to pyrolise a small quantity of rock sample of about 100 milligram to determine quantitatively the following parameters:

i) The amount of hydrocarbon already present in the rock "S_1"

ii) The remaining generation potential of the rock "S_2"

iii) Measure of oxygen content of the kerogen "S_3" and

iv) Maturation index "T_{max}°C".

In rock eval pyrolysis, the type of kerogen is characterized by two indices called Hydrogen Index (HI=S_1/total organic carbon) and Oxygen Index (OI=S_3/total organic carbon). These indices are independent of the abundance of organic carbon and are strongly related to the elemental composition of kerogen (Espitalie et al., 1980).

These indices are plotted on a modified van-krevelen diagram (Fig. 5.1) in which each kerogen type follows an independent path, with OI decreasing at the onset of maturation, followed by a decrease in the HI during hydrocarbon generation (Cleamentz et al., 1979).

HI has been used as an indicator of source rock potential of the kerogen (Waples, 1985). Hydrogen indices below 150 mg CO_2/g TOC, indicate the absence of significant amounts of oil generative lipid materials suggesting the kerogen as mainly of type-III. Those with HI between 150 and 300 mg CO_2/gTOC contain more of type-III kerogen than type-II and therefore, have marginal to fair potential for liquid hydrocarbon. Kerogens with hydrogen indices above 300 mg CO_2/gTOC contain substantial amounts of type-II organic matter and thus, are considered to have good source potential for liquid hydrocarbons. Kerogens with hydrogen indices above 600 mg CO_2/g TOC usually consist of nearly pure type-I kerogen. They have excellent potential to generate liquid hydrocarbons. The source rock potential based on HI is given in the Table 5.1.

5.1.3 Maturation of Organic Matter

It is well known that the oil and gas are formed from disseminated organic matter in sedimentary rocks by a complex reaction of over all first order kinetics, at a rate which depends

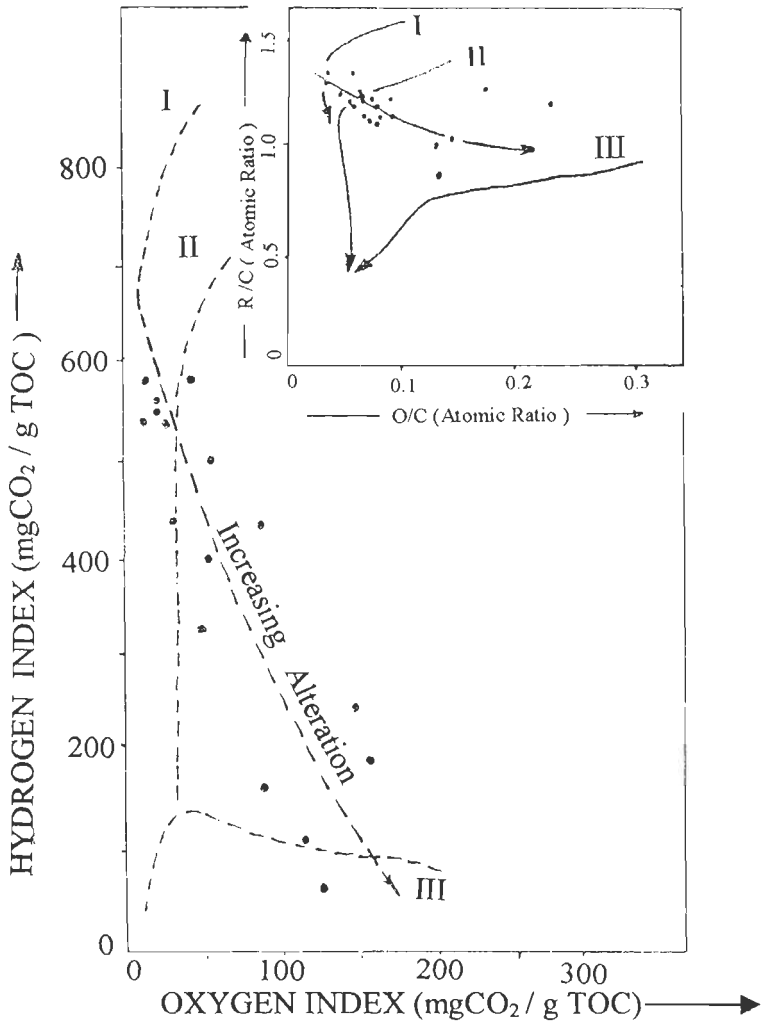

Figure 5.1- Modified Van Krevelen diagram for kerogen characterization (Tissot and Welte, 1978). Inset- Van Krevelen diagram.

Table 5.1 Source Rock Potential of Kerogen Based on HI (Waples, 1985)

Hydrogen Index (mg CO_2/g TOC)	Principal Product	Relative Concentration Potential
< 150	Gas	Small
150 – 300	Oil + Gas	Small
300 – 450	Oil	Moderate
450 – 600	Oil	Large
> 600	Oil	Very Large

primarily on temperature and duration of heating (Tissot and Espitalie, 1975; Dow, 1978: Tissot and Welte, 1978; Tissot, 1984; Waples, 1985). Incipient oil generation begins at approximately

65°C and both oil and gas are generated between 120°C and 175°C, and only dry gas is generated at temperature of more than 175°C (Hunt, 1979). Most of the hydrocarbons in the sedimentary rocks are believed to be generated within a temperature range of 80°C and 150°C.

The stage of thermal maturation of organic matter can be assessed by a number of methods (Tissot et al., 1987):

(a) Organic Matter Based Method

(1) Optical method such as vitrinite reflectance (VR_o), and thermal alteration index (TAI)

(2) Physico-chemical method such as T_{max}

(b) Inorganic Method

Diagenesis of minerals related method such as illite crystallinity which is based on progressive conversion of clay minerals from smectite to mixed layer, smectite/Illite (S/I) and finally to illite, or fission track dating method (Gleadow et al., 1983; Storzer and Selo, 1984).

(i) Organic Matter Based Techniques

(a) Optical method: The most commonly used optical indicator of maturity is vitrinite reflectance.

Vitrinite Reflectance (VR_o)- Vitrinite reflectance the most widely used method of measurement of organic diagenesis (Bustin, 1989). The monotonic increase in the intensity of vitrinite reflectance through the entire range of thermal maturation has found immense use in geological studies. Some of them are: 1) semi-quantitative reconstruction of the burial and temperature histories sequences (e.g. Kalkreuth and Mc Mechan, 1984), 2) tectonic studies (Unomah and Ekweozor, 1993), thermal history of source rock (Dow, 1977), 3) tectonic evolution and hydrocarbon potential (Johnson et al., 1993), 4) exploration of oil and gas (e.g. Hunt, 1979; Waples 1981; Tissot and Welt, 1984; Alizadeh-Shahzaidy and Awasthi, 1996), 5) estimation of maximum temperatures attained by sedimentary rocks (Barker et al., 1986; Barker, 1983, 1989; Bostick and Pawlewicz, 1984; Daniel and Cole, 1983), 6) evaluate the extent of

thermal alteration of sedimentary rocks (Katz et al., 1988), 7) as an absolute paleogeothermometer independent of burial history (Price, 1983) from 20°C to at least 400°±20° C, 8) as an indicator of heat flow (Lerche et al., 1984; Guidish et al., 1985), 9) thermal maturation (Daniel and Cole, 1983), 10) the degree of organic metamorphism (Hood et al., 1975; Middleton, 1982; Price, 1982), 11) as an indicator of the degree of organic matter diagenesis and maturation of hydrocarbon (Shibaoka et al., 1973; Dow, 1977; Kantsler et al, 1978), 12) an indicator of paleo and in-situ stresses in coal and coal-bearing strata (Ting, 1982) and metallic mineral exploration (Duba and William-Jones, 1983).

Temperature and duration of heating are the most important factors which affect the vitrinite reflectivity (Tan, 1965; Hood et al., 1975; Tissot and Welte, 1978; Bostick, 1979; Waples, 1980; Middleton, 1982; Suggate, 1982; Barker, 1983; Mc Kenzie and Mc Kenzie, 1983; Lerche and Kendall, 1985; Barker, 1991, 1993 a, 1993 b). With increasing temperature, the reflectivity increases.

Organic maturity indicators such as vitrinite reflectance or rock eval pyrolysis are commonly used to determine the thermal history of sedimentary basins (Tilley et al., 1989; Heroux et al., 1979).

Evaluation of vitrinite under the microscope involves comparison of intensity of a narrow light beam reflected vertically from the polished surface of vitrinite particles, with that from a surface of known reflectance. The intensity is generally measured by a photo multiplier and expressed as percentage VR_o.

The vitrinite reflectance has been related in terms of petroleum generative capacity by Tissot and Welte (1978), as below:

VR_o%	Rating
less than 0.5	Immature
0.5 to 1.30	Oil Window
1.30 to 2.00	Zone of wet gas and condesates
more than 2.00	Dry gas zone

(b) Physico-chemical method: This method consists of analysing the sample by an equipment known as rock eval pyrolysis. Pyrolysis temperature is frequently used as a maturity parameter (Espitalie et al., 1977). The parameter 'T_{max}' i.e. the temperature at which maximum amount of hydrocarbon are pyrolysed (at the peak of S_2 obtained by REP has proved to be a reliable method of characterizing thermal evolution (Tissot, 1984). T_{max} increases with increasing maturity (Barker, 1979). The value of T_{max} depends on the amount of energy required to break the chemical bonds in the kerogen (Espitalie et al., 1977). In an immature state, the kerogen has lot of side chains which can be easily broken as the bond energy between the side chain and the macro molecule kerogen is weak. However, in the highly matured kerogen, the chemical bonds that persist are the ones requiring the most energy during pyrolysis to be broken. Hence, T_{max} increases in the matured organic matter.

The following ratings have been used for determining maturity in the present study.

Rating	T_{max} °C Range
Immature	less than 435
Mature	435-470 i) 435-450, initial stage of maturation ii) 450-470, main stage of maturation
Over mature	more than 470

(ii) Inorganic methods: In the absence of organic indicator (e.g. vitrinite reflectance), inorganic indicators can be used quantitatively to estimates levels of thermal maturity and cautiously to approximate hydrocarbon generation preservation stages of potential source rocks (Guthrie et al., 1986). The most important of these indicators are illite-crystallinity and fission track formed by radioactive constituent in certain minerals. These are discussed below:

(a) Illite- crystallinity index: As already discussed in Chapter 3, temperature is the principal factor controlling illite crystallinity but, the crystallinity of illite is also dependent on other factors such as, the composition of the sediment and the fluid phase, porosity and

permeability. The relation between illite crystallinity, vitrinite reflectance and temperature is discussed in section 5.2.3 (ii, a).

(b) Fission Track: Fission tracks are linear damage features produced in a crystal lattice by nuclear fragments from the spontaneous fission of ^{238}U. Once formed, these tracks begin to anneal in a process that appears to be of first order. It is a function of temperature and time (Green et al., 1989; Weaver, 1989). Tracks in apatite and zircon crystals will be annealed in the temperature range of 120° ±20° C and 240°±25° C, respectively. Therefore fission track studies can be used in reconstruction of paleotemperature in sedimentary basin, and to find the maturity of organic matter. The stability temperature range of tracks in apatite and zircon are in the temperature range of oil (100–150°C) and gas (150-220°C) formation (Quigley and Mc Kenzie, 1988). Figure 5.2, shows the relationship between fission track annealing in apatite and zircon, temperature and generation of petroleum hydrocarbons with depth.

5.2 SOURCE ROCK STUDIES OF CENOZOIC SEDIMENTS

The Cenozoic sediments of the area are mainly the shale and sandstone. The shale has been evaluated in terms of the abundance of organic matter and quality of organic matter and the maturity of organic matter.

5.2.1 Abundance of Organic Matter

For hydrocarbon generation in commercial quantity, the organic matter must be preserved in sufficient amount in sediments (Demaison and Moor, 1980). Since carbon is an integral part of organic matter, total organic carbon content (%TOC) is directly related to it. Hence % TOC in sediments is universally considered as a measure of abundance of organic matter.

The total organic carbon content (%TOC) for shale samples were determined using Hoshoff Carmograph. The results of the analysis are presented in Table 5.2. The perusal of the Table 5.2, indicates that the TOC values in Subathu vary between 0.09% - 0.3% with the average of 0.2%. The Subathu samples in comparison with other samples, uniformly have higher amounts of TOC%. Dagshai shale indicates variation in TOC from 0.09 to 0.36% with the average of 0.15%. Kasauli shale have a range of 0.05 to 0.6% with the exception of a bituminum

sample (near Kumarhatti) which has higher value of TOC (31.31%). In this formation, however, the horizons with some richness of organic matter are observed, but TOC% is low. Lower Siwalik samples also show variation in TOC value from 0.06 to 0.17% with the average of 0.12%.

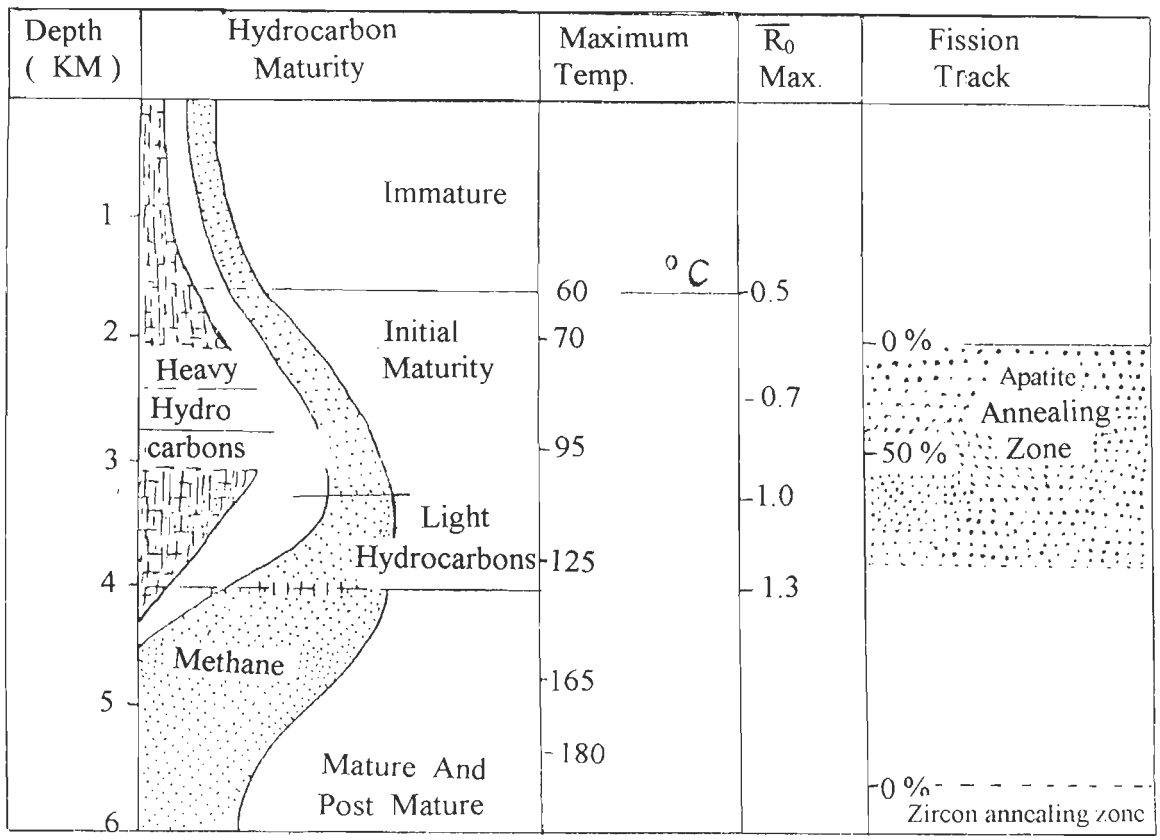

Figure 5.2- The relationship between the fission-track annealing zone in apatite (and zircon), temperature and hydrocarbone maturity (Gleadow et al., 1983).

5.2.2 Quality of Organic Matter

The quality and amount of hydrocarbon, generated from a source rock depend largely on the type and quality of the organic matter which produced it (Barker, 1979). The kerogen of type-III (mainly terrestrial) is gas prone, whereas kerogen of type-I and type-II are mainly oil prone (Tissot and Welte, 1978). In view of this it is important not only to know the amount of organic matter, but also the type of organic matter found in the sediments, to evaluate their source rock potential in terms of oil and gas proneness. An attempt has, therefore, been made to

evaluate the quality of organic matter in Cenozoic sediments, by using the chemical approach based on whole rock pyrolysis.

Table 5.2 Total Organic Carbon Content (TOC) in the Sediments (Shales)

Stratigraphic Unit	Sample no.	TOC%	CO_2%	Average TOC
Lower Siwalik (Middle Miocene-Late Miocene) (15-10.4 Ma)	100	0.17	7.8	0.1
	4	0.06	8.0	
	10	0.05	8.5	
Kasauli (Early Miocence – MiddleMiocene) (23-15 Ma)	14	0.05	5.7	0.2
	15	0.18	13.6	
	16	0.63	16.7	
	50	31.31	46.4	
	38	0.09	16.3	
Dagshai (Late Eocene-Early Miocene) (40-23.7 Ma)	7	0.09	6.0	0.15
	8	0.09	3.4	
	18	0.21	4.3	
	20	0.08	3.2	
	22	0.09	5.1	
	34	0.07	12.4	
	41	0.36	3.4	
	52	0.22	8.1	
Subathu (Late Palcocene-Middle/Late Eocene) (62-52/40 Ma)	29	0.23	26.1	0.2
	30	0.3	28.7	
	36	0.09	3.4	
	43	0.15	19.0	
	59	0.25	25.4	
	60	0.25	16.1	
	63	0.15	26.0	

Note: Sample No. 50 is a bituminum seam. Therefore it is not counted in the average of TOC.

(i) Quality of Organic Matter Using Whole Rock Pyrolysis: Pyrolysis of whole rock in an inert atmosphere using rock eval technique developed by Espitalie et al. (1977) has made major contribution to systematic analysis of kerogen (Cleamentz et al., 1979). These samples which had shown higher TOC% were selected to determine the quality of organic matter present in them. For the quality of kerogen, the hydrogen index (HI) and oxygen index (OI) of these samples were plotted on an modified Van Krevelen diagram (Fig. 5.3). The other available data is also plotted and considered for comparison purposes (Fig. 5.3 and Table 5.3). A perusal of

Table 5.3, and Figure 5.3, shows that hydrogen indices are below than ~150 mg CO_2/gTOC. It indicates that the kerogen is as mainly of type-III.

Table 5.3 Rock–Eval Data of Outcrop Samples from Himalayan Foreland Basin

S. No	Area	Formation	TOC	S1	S2	S3	HI	OI	T_{max}
1	Tauapani	Subathu	4.85	0.00	0.60	0.00	12.00	-	517.00
			4.25	0.06	0.00	5.20	-	-	-
2	Kalakot Tawi Harbal Nar	Subathu	5.26	0.06	1.66	0.54	31.00	10.00	525.00
			2.37	0.16	0.78	1.10	32.00	46.00	514.00
			1.20	0.09	0.26	0.10	21.00	8.00	499.00
			80.33	1.96	15.08	0.77	19.00	-	506.00
			21.07	0.03	2.14	0.36	10.00	-	514.00
3	Triyath Nala Mahogla-Babbiangala	Subathu	1.74	0.00	0.00	0.42	-	-	-
			46.58	1.61	23.82	3.13	50.00	-	489.00
			7.27	0.00	0.00	0.40	-	-	-
			21.60	0.10	13.20	10.30	61.00	47.00	522.00
			9.36	0.06	2.40	0.13	2.00	1.00	515.00
			1.06	0.00	0.02	0.27	2.00	25.00	-
			1.16	0.00	0.00	0.33	-	-	-
4	Seogali-Ujh	Murree	41.87	1.40	69.0	6.29	164.00	14.00	436.00
			0.87	0.02	0.08	0.17	9.00	19.00	-
5	Najot Ant.	Murree	1.02	0.02	0.11	0.48	10.00	42.00	438.00
6	Dhar-Naini Khad Road Traverse	Dharmsala	0.54	0.03	0.07	0.22	12.00	40.00	-
7	Bilaspur-Ghagus	Subathu	2.13	0.00	0.00	0.62	-	-	-
8	Bilaspur	Siwalik	0.69	0.02	0.00	0.57	-	-	-
9	Dharampur-Dagshai	Subathu	7.20	0.03	0.06	0.10	0.80	2.00	-
10	Deothal-Nainatikkar	Subathu	1.78	0.02	0.00	0.03	-	-	-
			6.62	0.00	0.00	0.00	-	-	-
11	Jahar-Pashog	Subathu	1.99	0.00	0.00	0.00	-	-	-
12	Dharampur	Subathu (60)	0.25	0.01	0.00	0.10	0.00	40.00	-
		(30)	0.30	0.00	0.00	0.12	0.00	40.00	-
13	Kalka-Kasauli	Dagshai (41)	0.36	0.04	0.00	0.02	0.00	5.00	-
14	Kumarhatti	Dagshai (52)	0.22	0.00	0.00	0.00	0.00	0.00	-
		Kasauli (50)	31.31	0.00	10.72	3.22	34.00	10.00	489.00
15	Sarahan	Kasauli (16)	0.63	0.01	0.04	0.11	6.00	17.00	432.00
16	Nahan	Lower Siwalik (100)	0.17	0.00	0.00	0.06	0.00	35.00	-

NOTE: 1-11 data from Samanta et al. (1994). The numbers in the parenthesis show number of sample.

5.2.3 Thermal Maturation of Organic Matter

As mentioned earlier, to find the maturation stage of organic matter in the present study, the organic and inorganic methods were utilized.

(i) Organic Methods

(a) Vitrinite Reflectance: The sample crushed, sieved, mounted in epoxy, grinded, polished (appendix-III) and analysed using reflected light microscopy. VR_o were performed on randomly oriented grain using conventional microphotmetric methods. Reflectance was measured under illumination on a zeiss universal microscope fitted with a MPM-01 microphotometer system. In the present case study due to very low organic matter, measurement could only be done on a few particles.

The VR_o result of the present work has shown in the Table 5.4. These values indicate that organic matter in the all formations is in the mature stage (oil window).

In the Kasauli Formation, the measurement of VR_o% was done on a bituminum seam (Just after Kumarhatti). Using Bertrand and Heroux (1987) approach [$R_{vitrinite} = 0.618 \times R_{bituman} + 0.4$], vitrinite reflectivity (VR_o) was estimated. Vitrinite-temperature-time nomogram (Fig. 5.4) of Middleton (1982), was used to estimate paleotemperatures of the Cenozoic formations. The paleotemperatures thus worked out are given in Table 5.4. Considering the thickness of the Cenozoic sediments and the temperature gradient 20°C/km, the estimated paleotemperature may be around 100°C-120°C for Lower-Siwalik, 120°C-130°C (Kasauli) and 130°C-140°C for Dagshai and 140°C-160°C for Subathu corroborating the paleotemperature estimated earlier through the Middleton's (1982) approach.

(b) Rock Eval T_{max} Value: Pyrolysis temperature T_{max} is frequently used as a maturity parameter because of the case with which it is measured during the pyrolysis of rock sample to determine the quality of organic matter. Since, T_{max} value is measured on whole rock basis on entire organic matter, T_{max} values are taken as a reliable maturity parameter and are discussed below.

Table 5.4 The Values of VR_o % of Cenozoic Shale Samples.

Formation	Approximate Age (Ma)	VR_o %	Temperature (T°C)**
Lower Siwalik	15-10	0.8	100-120
Kasauli	23-15	0.9	120-130
Dagshai	40-23	~1*	130-140*
Subathu	60-40	1.2	140-160

*- Estimated value.

**- Temperature estimated, using Middleton's nomogram (1982)

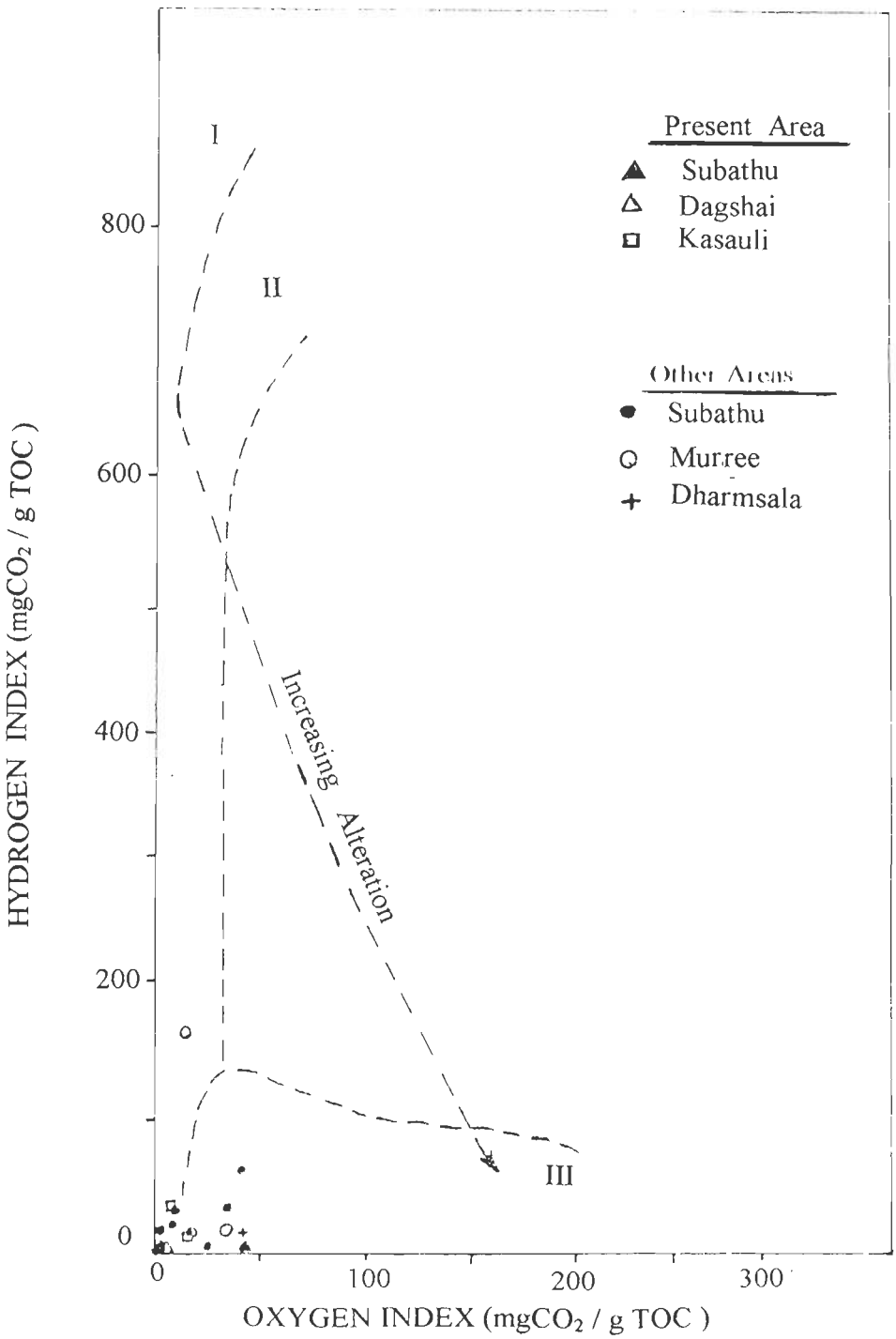

Figure 5.3- Plot of samples on the modified Van Krevelen diagram for kerogen characterization (Tissot and Welte, 1978).

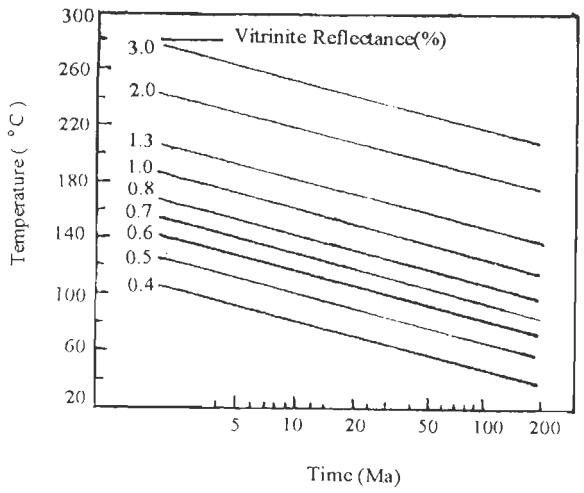

Figure5.4- The vitrinite reflectance-temperature-time nomogram (Middleton, 1982). It is a combination of the Shibaoka and Bennett (1977) nomogram, with the LOM-vitrinite reflectance correlation and the LOM nomogram of Hood et al. (1975).

In the present study T_{max} has been used to determine the degree of maturity of organic matter. The Subathu shale with the T_{max} >470°C, indicate over maturation stage, the Dagshai Formation with T_{max} of 450° C and the Kasauli (Murree) sediments with T_{max} between 450°–430°C indicate initial to middle stage (catagenetic) of maturation of organic matter; and the Lower Siwalik Formation with T_{max} 445°C (estimated) indicates that it is in the gas stage catagenetic maturation to generate petroleum hydrocarbons. These results and also the vitrinite reflectivity indicate that the shales of the Cenozoic sediments are maturated to generate petroleum hydrocarbons.

(ii) Inorganic Methods

(a) Illite Crystallinity Index (I.C.I. or K.I.): Illite crystallinity index is controlled by the same geologic agent that control vitrinite reflectance (Guthrie et al., 1986). Therefore, in the absence of vitrinite, Illite-crysallinity can be used quantitatively to estimate levels of thermal maturity. The estimated values of VR_o based on the relation of the variation of Illite crystallinity index and VR_o-measurements, are presented in the Table 5.5. The values obtained by these equations:

$$VR_o\% = \frac{SR-1.16}{1.2}$$

$$VR_o\% = \frac{6.4-C.I.\ (mm)}{2}$$

Table 5.5 Estimated VR_o% Using Illite Crystallinity Index

Stratigraphic Unit	Illite Crystallinity Index (Kubler Index)	Estimated VR_o%
Lower Siwalik	5.7	0.7
Kasauli	5.0	0.9
Dagshai	4.6	1.0
Subathu	4.3	1.1

The paleotemperature was estimated by using the VR_o values which were measured and estimated with the help of time-temperature nomogram of Middleton (1982) and diagram of Gleadow et al. (1983). The maximum temperature to which Cenozoic sediments were subjected to are 100–120°C (110°C) for Lower Siwalik, 120-130°C (125°C) for Kasauli, 130–140°C (135°C) for Dagshai and 140–160°C (150) for Subathu formations. These are the temperatures under which petroleum hydrocarbons were generated from the organic matter found in the these formations.

(b) Fission Track Study: Analysis of fission track on apatite and zircon crystals, separated from sandstones of different formations of the Cenozoic basin (see, FTD results, Chapter 4), indicate that the paleotemperature during the deposition of the Subathu Formation due to unreset of zircon crystals, could not more than 215°C. But all sediments due to resetting of apatite ages, seems to be reached at 100°C isotherm which is necessary to reset of tracks in apatite crystals.

Paleotemperature attained by Cenozoic sediments, based on FT data, 100°C-215°C, caused the maturity of organic matter. In the youngest sediments, organic matter is in initial to middle stage and in the oldest one is in end of maturity. This point also supported by other maturity indicators, namely vitrinite reflectance and illite crystallinity.

5.3 TIME OF PETROLEUM GENERATION

Maturation/subsidence curve of the Subathu sediments as the base of the Cenozoic sediments, was constructed (Fig. 5.5) using paleotemperature and time-stratigraphic data of the area under study (see Chapter-6). This figure indicates that the Subathu sediments, as a potential source rock, are within the "oil window zone". However, in some part of Cenozoic basin such as Tauapani and Kalalbot Tawi area (Table 5.3) based on T_{max} values (>470°C) the Subathu sediments are in "gas-zone". The petroleum generation was started at ~25 Ma (Middle Miocene) when Subathu reached a burial depth of ~2500 m and continued till ~13 Ma when these sediments reached a depth ~4500 m. From >13 Ma to present time the sediments have undergone the process of uplift. (The uplift/exhumation history of the Cenozoic sediments will be discussed in detail in the next Chapter.) Since the kerogen in these sediments is mainly of type-III, the hydrocarbons generated would be mainly gaseous.

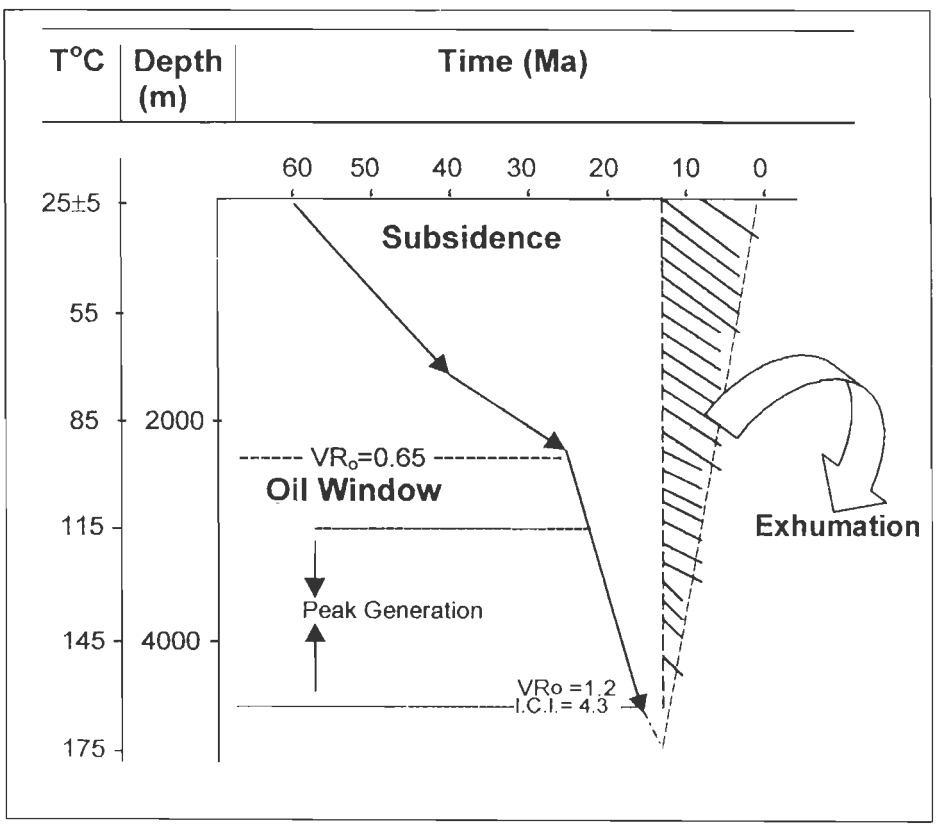

Figure 5.5- Subsidence and exhumation curve of Subathu sediments. The uplift should start ~ >13 Ma, based on apatite reset ages on the Kasauli Formation.

The kerogen type-III also indicates that the principal organic matter is prone to gas generation. The source rock of the Cenozoic sediments are thus, maturated to generate gas. These results are supported by the gas seepage and live oil shows found in the Siwalik foreland basin. However, since the TOC is generally less than 0.5% the chance of generation of commercial quantities of petroleum hydrocarbons are less, and it is important to note in this regard that the exploration efforts of Oil Natural Corporation for decades have not met with success as yet.

5.4 CONCLUDING REMARKS

The present study on petroleum source rock potential of the Cenozoic sediments indicates the following results:

(i) TOC% in the shales varies from 0.09 to 0.3 in Subathu, 0.07 to 0.36 in Dagshai, 0.05 to 0.63 in Kasauli, 0.06 to 0.17 in Lower Siwalik formations. The Siwalik and Kasauli formations (Upper Murree/Upper Dharmsala) therefore, do not have adequate organic carbon content and as such do not have adequate source rock potential for generation of petroleum hydrocarbon commercially.

(ii) VR_o % in all sediments is greater thsn 0.6%. It suggests that the organic matter in the sediments has undergone adequate thermal degradation (100°-150°C) to generate petroleum hydrocarbons. Since most of the kerogen is of type-III, the hydrocarbons generated are mostly the gaseous.

(iii) Thermal maturity, based on VR_o data and T_{max} data suggest that Subathu as base of Cenozoic sediments has reached the late stage of maturation (R_o% =1.2 and T_{max}= >470°C). Illite crystallinity, sharpness ratio and apatite and zircon fission track studies also indicate that the Dhagshai sediments have passed only the threshold temperature of annealing of fission tracks in apatite (120±20°C). Therefore, the temperature which Subathu sediments were subjected to, should be higher, but not more than 215°C.

(iv) The estimated maximum paleotemperature attained by Cenozoic sediments are 100–120°C for Lower Siwalik, 120-130°C for Kasauli, 130–140°C for Dagshai and 140–160°C for Subathu formations.

(v) The Subathu shale with the T_{max} >470°C and VR_o=1.2 have reached to late stage of metagenesis, whilst the Dagshai Formation (T_{max} of 450° C and VR_o=1), the Kasauli (Murree) Formation (T_{max} between 450°–430°C and VR_o= 0.9) and the Lower Siwalik Formation (T_{max} 445° C and VR_o= 0.8) are in initial to middle stage (catagenetic) of maturation of organic matter to generate petroleum hydrocarbons.

(vi) The organic matter present in these sediments is mainly the kerogen of type-III which indicates that the principal products of hydrocarbons generated are gaseous material.

(vii) The petroleum generation was started at ~25 Ma (Middle Miocene) when Subathu reached a burial depth of ~2500 m and continued till ~13 Ma when these sediments reached a depth ~4500 m. From >13 Ma to present time the sediments have undergone the process of uplift.

(viii) The above results indicate that the Cenozoic sediments are matured to generate petroleum hydrocarbon-mainly the gas. These results are supported by the gas seepage and live oil shows found in the Siwalik foreland basin. However, since the TOC is generally less than 0.5%, the chance of generation of commercial quantities of petroleum hydrocarbons is less, and it is important to note in this regard that the exploration efforts of Oil and Natural Corporation for decades have not met with success as yet.

CHAPTER-6

PALEOTEMPERATURE, SUBSIDENCE AND EXHUMATION HISTORY

6.1 BACKGROUND

Subsidence is sinking or downwarping of sediments in a basin whereas uplift is the gradual upheaval of sediments by positive movements in the crust. Processes of subsidence and uplift cause thermal changes in the sediments. Subsidence results in rise of temperature and uplift results in drop of temperature in the sediments. These thermal changes are recorded in inorganic/organic components of the sediments as thermal indicators. Therefore, a study of these thermal indicators can help in understanding the paleothermal history of the rocks and also be used to interpret the subsidence/uplift history of the basin. The thermal regime of the sediments also affects the petroleum potential of the source rock.

6.2 PALEOTEMPERATURE

Amongst the various methods, the following approaches have been made to decipher the paleotemperature history of the study area.

-Fission track

-Illite crystallinity

-Vitrinite reflectance

6.2.1 Fission Track Method

In a sedimentary basin, the ages of FT preserved in the mineral grains can be indicative one of the following modes in the sediments. (i) FT ages>depositional age indicates that the sediments have never been subjected to temperatures higher than the annealing temperature of the FT, i.e. it gives unreset FT ages. (ii) FT ages=the stratigraphic age indicates rapid uplift of

source and quick and short distance transportation of sediments before deposition. (iii) FT ages < the stratigraphic age indicates resetting of the FT clock, i.e. the sediments, at least once, were subjected to temperatures higher than the annealing temperature of the fission tracks.

Amongst the minerals, the analysis of naturally-occurring radiation damage in the form of fission track in detrital grains of apatite and zircon in sediments allows determination of the timing and the magnitude of paleotemperatures up to a maximum limit of around 120° ± 20°C for apatite (Duncan et al., 1998), and 240° ±25° C for zircon (Brandon, 1992). Whereas the fission tracks in apatite are annealed at temperatures above 100° C, the ones in zircon get annealed at temperatures at least 215° C or above.

In view of above considerations, estimation of fission track ages and the stratigraphic age of the sedimentary unit is important to work out thermal events of the depositional basin.

As already discussed in Chapter 4, FT ages in apatite grains from the Cenozoic sediments indicate resetting while zircon ages are still unreset. It indicates that the paleotemperature of these sediments were more than the annealing temperature of apatite, i.e. 120°±20° C and less than that of zircon, i.e. 240° ±25° C (Table 6.1). It implies that the Cenozoic basin has undergone subsidence to a minimum depth range between 2.5 to 4.0 km, as calculated from apatite annealing temperatures, and maximum depth of 6 to 8 km, based on zircon annealing temperatures.

Table 6.1 Summary of Fission Track Results and Estimated Paleotemperature (° C) and Depth (km)

Formation	Depositional Ages (Ma) *	F T Results (Ma)		Estimated Temp. (° C)	Estimated Depth (km)
		Apatite	Zircon		
Lower Siwalik	10 –15	10	363-9	>120±20 <240±25	Min. 2.5-4 Max. 6-8
Kasauli	15 – 24	13	529-12		
Dagshai	24 – ~30	8	515-19		
Subathu	40 – 60	------	557-42		

* The depositional age values are adopted from: Johnson et al. (1985) for the Lower Siwalik, Arya (1998) for the Kasauli, Najman et al. (1997) for the Dagshai, and Mathur (1978) for the Subathu formations.

6.2.2 Illite Crystallinity

Illite crystallinity has been used to study the burial diagenesis. With increasing burial, temperature increases and causes a decrease in the illite crystallinity indices and an increase in

the illitization of illite-smectite (mixed layer) fractions. With this premise illite crystallinity can be used to estimate maximum temperature (Duba and William-Jones, 1983; Pollastro and Barker, 1986; Pollastro, 1990; Akande and Viczian, 1998).

As worked out in Chapter 5, the illite crystallinity indices in the Cenozoic sediments of study area varies from about 0.53 to 0.37 2θ (Table 6.2). It is lowest 0.37 in the oldest sediments (Subathu Formation) and increases upwards continually through Dagshai (0.42), Kasauli (0.44) and is highest (0.53) in the Lower Siwaliks. This systematic decrease in the illite crystallinity index from the Lower Siwalik to Subathu formations is attributed to increasing temperature with burial of sediments. Following Weaver (1989) these values of illite crystallinity index (Kubler Index) indicate that the pre-Siwalik sediments are in the end of middle or early late stage of diagenesis, but the Lower Siwalik is in the early middle stage. In view of this, late stage of diagenesis takes place at about 180°-200° C (Winkler, 1979). Therefore, the paleotemperature could not be more than 180°-200° C (Table 6.2). The sediments of the Lower Siwalik, Kasauli, Dagshai, and Subathu have undergone early middle, late middle, late middle, and early late stage of the diagenesis respectively. Following the relation between I.C.I., VR_o and temperature as discussed in Chapter 5, the maximum temperature have been estimated to be about 100° for the Lower Siwaliks, 120° for Kasauli, 130° for Dagshai and 150° for Subathu formations. These inferences are in conformity with the inference drawn from the FT approach.

Table 6.2 Summary of Illite Crystallinity Indices and Estimated Paleotemperature

Formation	Illite Cryst. Index (Kubler Index) (2θ)	Estimat. Temp. (° C)
Lower Siwalik	0.53	100
Kasauli	0.44	120
Dagshai	0.42	130
Subathu	0.37	150

6.2.3 Vitrinite Reflectance

Vitrinite reflectance is a reliable optical technique for estimating the level of maximum thermal maturity of sedimentary organic matter (Tissot and Welte, 1978; Stach et al, 1982).

Vitrinite reflectivity commonly increases with depth in response to heat flux and is not reversible with a subsequent drop in temperature (Bostick, 1973; Dow, 1977; Tissot and Welte, 1978). The reflectivity is primarily affected by maximum temperature attained by the sediments (Staplin, 1969; Connan, 1974; Hood et al., 1975). Observations have shown that maximum reflectance is set by the maximum burial temperature, and reaction duration has relatively little influence on the degree of maturation of organic matter (Barker, 1983; Price, 1983).

As discussed in Chapter 5, the vitrinite reflectance decreases continually from 1.2 % in the oldest Subathu to 0.8 % in the Lower Siwalik formations (Table 6.3). Vitrinite reflectance is directly related to temperature. Middleton (1982) has given a time-temperature nomogram to estimate maximum temperature. Using this nomogram the maximum paleotemperature of the sediments has been estimated to be ~120°-100°C for the Lower Siwalik, ~130°–120°C for the Kasauli, ~ 140°-130° C for the Dagshai and about 160°-140° C for the Subathu formations (Table 6.3).

The maximum paleotemperature, obtained from these Cenozoic sediments, using VR_o are in good agreement with those estimated from fission track analysis and Kubler Index values for crystallinity of illite.

Table 6.3 VR_o Results and Estimated Paleotemperature

Formation	VR_o %	Temp. * (°C)
Lower Siwalik	0.8	120-100
Kasauli	0.9	130-120
Dagshai	1.0	140-130
Subathu	1.2	160-140

*- Based on time-temperature nomogram of Middleton (1982).

Inference- As mentioned above, the paleotemperatures estimated through FT, I.C.I, and VR_o methods are summarized in Tables 6.1, 6.2, 6.3. The paleotemperature estimates are comparable and average maximum paleotemperature estimated for the Lower Siwalik, Kasauli, Dagshai, and Subathu formations are 110°, 125°, 135°, 150°C respectively (Table 6.4).

Table 6.4 Paleotemperature Results, Diagenesis Stages and Estimated Burial Depth (km)

Formation	Average Temperature (°C)	Diagenesis Stage	Depth (km) *
Lower Siwalik	110	Early Middle	2.5-3.0
Kasauli	125	Late Middle	3.0-3.5
Dagshai	135	Late Middle	3.5-4.0
Subathu	150	Early Late	4.0-4.5

* Thermal gradient in this area is 3° C/100 m and surface temperature = 25° ± 5°C

6.3 BURIAL AND EXHUMATION HISTORY OF SEDIMENTS

Analysis of fission tracks on zircon using External Detector Method (EDM) indicates that sediments of all the formations of the Cenozoic foreland basin have not subsided to the depth level corresponding to the closure temperature of zircon (240° ±25°C). The basin subsided to the depth level corresponding to maximum temperatures of the order of 160° C, as determined from vitrinite reflectance (Table 6.3). The fission tracks in the apatite grains in sandstone of various formations, thus, got completely annealed which is also indicated by the ages of FT in apatite. These apatite ages are 8 Ma for the Dagshai, 13 Ma for the Kasauli and 10 Ma for the Lower Siwalik Formations and distinctly younger than the depositional ages of the respective formations (Table 6.1). In this basin, the Subathu sediments may have been uplifted to about 2 km to reach the temperature zone, which is necessary to start the FT clock in apatite grains, assuming a temperature gradient of 30° C per km.

If the apatite FT ages estimate the uplift of the complete Cenozoic sequence in a part of basin, then the AFT ages must continually increase towards the youngest sediments in the stratigraphic column. The present AFT ages indicate that there is a change in the expected trend of the AFT ages between the Kasauli and the Lower Siwalik formations. This indicates (a) normal exhumation of Kasauli at one place, and (b) since the FT ages in the Lower Siwalik are lower than that of the Kasauli, the Siwalik sequence must have existed over the Kasauli during upliftment and must have been tectonically transported from adjoining southern part of the basin. In this connection this is important to note that Siwalik has thrust contact with the pre- Siwalik

sediments and it may, thus, be inferred that the burial history of the pre-Siwalik sediments in northern part of the foreland basin is different from that of the Siwalik sediments (Table 6.5) in the southern part of it.

Assuming a thermal gradient of 30° C/km, surface stratigraphy (Table 6.5) has been used to draw subsidence and exhumation history curve of the Subathu Formation in the present area under study (Fig. 5. 5).

Table 6.5 Time-Stratigraphic Data of the Present Study

Formation	Age (Ma)	Thickness (m)
Lower Siwalik	15-10	1700
Kasauli	24-15	2100
Dagshai	40-24	600
Subathu	60-40	1500

Thrust

Drill-hole data (Figs. 6.1-6.3), as reported by Biswas (1994) and Agarwal et al. (1994), indicate that (i) the subsidence rate in all parts of the Cenozoic basin has not been uniform, and varies from place to place, and (ii) there are breaks in the patterns of subsidence at places like Suruinsar, Jammu hills from 40-23 Ma, and 6.5 -5 Ma in the same area (Fig. 6.3). Therefore, it may be inferred that the thickness of sediments and the subsidence rate in different parts of the Cenozoic basin were variable. According to these changes, different subsidence phases are recognizable. For example, these phases are 50 Ma, 22 Ma, 17 Ma and 5 Ma for Surinsar, Jammu Hills (Fig. 6.3); 20 Ma, 17 Ma, 10 Ma and 6 Ma for Mohand area (Fig. 6.2 A); and 10 Ma, 6 Ma for Jammu area (Fig. 6.2 B).

In the present area also, the subsidence is not continuous (Fig. 5.5). Subsidence started with the deposition of the Subathu Formation (60-40 Ma). From 40 Ma to around 13 Ma, the Dagshai and Kasauli formations were deposited with continuous of subsidence. This part of the foreland basin started uplifting around 13 Ma.

Exhumation- Displacement of rocks with respect to the ground surface defines as exhumation, and therefore, related to uplift process (England and Molnar, 1990), as:

Exhumation = uplift of rocks – surface uplift

Therefore, the rate of exhumation is simply the rate of erosion or the rate of removal of overburden by tectonic processes.

Time elapsed since the formation of FT just below the annealing temperature of a fission tracked mineral is termed as the cooling age of the mineral. Each mineral has its own annealing temperature and therefore, the cooling ages are specific to specific mineral in a given terrain. The cooling age of a mineral should record the time at which it became cool enough to retain the fission tracks or the daugther products produced by the decay of radioactive isotopes. Inferences of exhumation rates from fission tracks and radiometric ages are one of major advances in geochronology over the past 20 yr (e.g. Clark and Jager, 1969). With an assumed thermal profile, the rate of exhumation can be calculated.

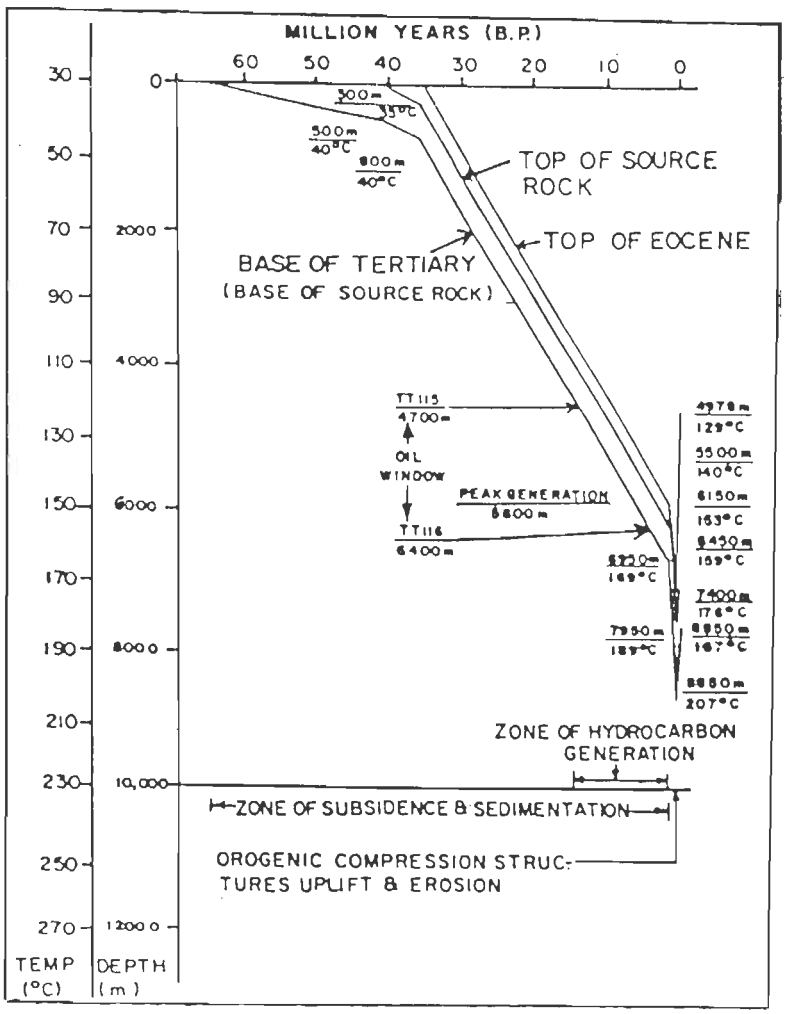

Figure 6.1 –Subsidence history curve of well JM1–B,Jawalamukhi (Biswas, 1994)

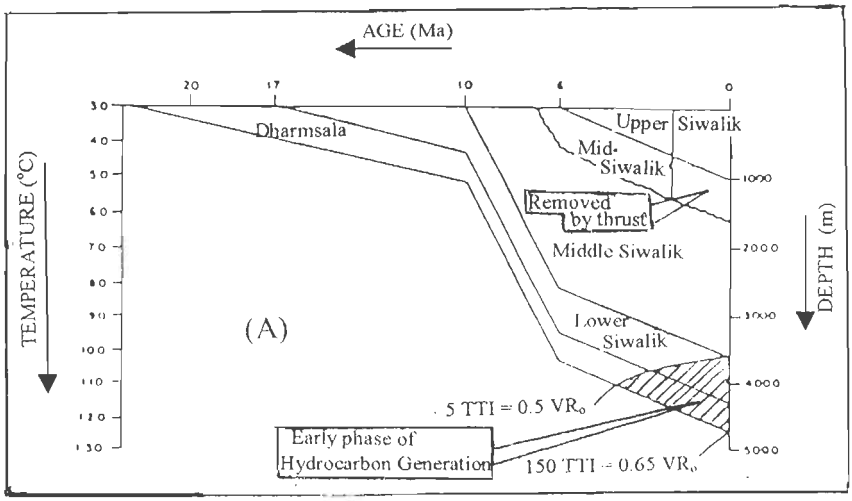

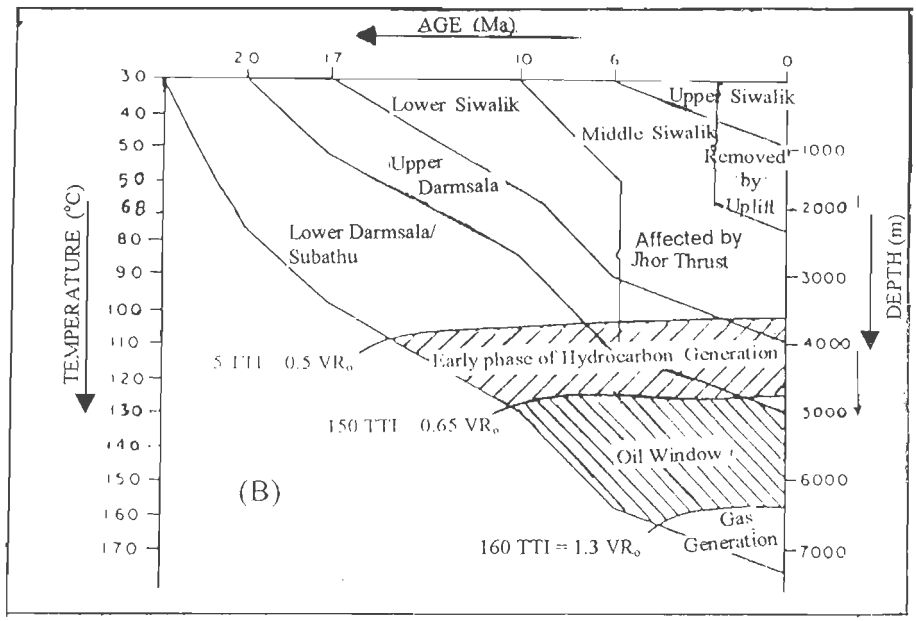

Figure 6.2– Maturation history of the sediments (A) Mohand –1 well, Dehra Dun, (B) JMI-B well, Jawalamukhi (Agarwal et al., 1994).

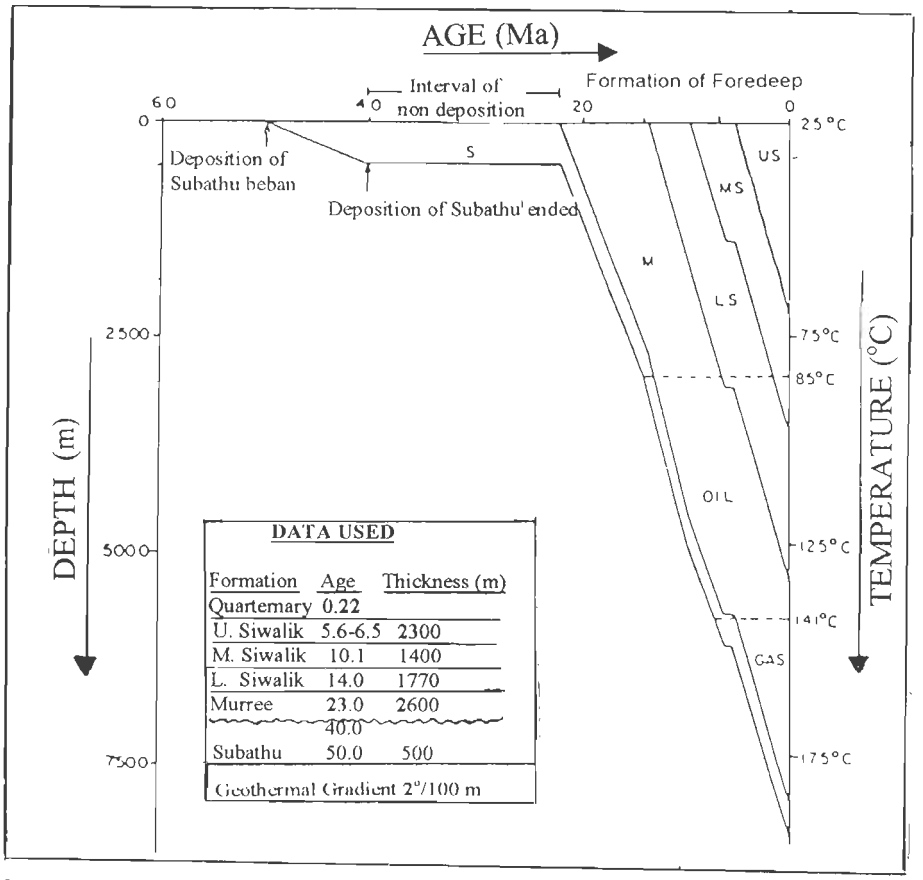

Figure 6.3– Subsidence curve in the region of Surinsar, Jammu hills (Agarwal et al., 1994).

As mentioned in the Section 6.2.1, all apatite FT ages (8 Ma in Dagshai, 13 Ma in Kasauli, 10 Ma in Lower Siwalik sediments) are less than the depositional ages of the sediments. Hence, we can estimate the extent of exhumtion/uplift to reach adequate temperature to start the FT clock. As already discussed, VR_o data indicated that the Kasauli sediments have reached a maximum temperature of 125°C. Assuming geothermal gradient of 30° C/km, it is estimated that the Cenozoic sediments were exhumed/uplifted about 1km since 13 Ma to attain annealing temperature of apatite i.e. at least 100° C. This age is recorded by apatite FT clock in the Kasauli Formation. The Dagshai Formation with AFT age of 8 Ma (Mehta, 1995), and the estimated

maximum paleotemperature of 130°-140°C indicates that the foreland sediments exhumed ~1.5 km till 8 Ma. Therefore, the Cenozoic sediments exhumed about 0.5 km (1.5–1 km= 0.5 km) in time span of 13-8 Ma. Thus, the rate of exhumation is estimated to be 0.1 km/Ma (0.5 km/5 Ma).

The available basic information, therefore, helps us to extract the total exhumation of sediments in the foreland basin (Fig. 5.5). Since 8 Ma to present time, the sediments have been exhumed to about 2.5 to 3 km in the present area, i.e. 0.3-0.4 km/Ma (the maximum burial depth of the Subathu sediments is estimated to be 4.0-4.5 km as shown in Fig. 5.8). Thus, the rate of exhumation of foreland basin from early to end of Middle Miocene (from 13-8 Ma) is very low (0.1 km/Ma) but from the Upper Miocene to present is high (~0.3-0.4 km/Ma).

6.6 CONCLUDING REMARKS

i) By combination of fission track analysis, illite crystallinity indices and vitrinite reflectance data, the maximum paleotemperatures of various Cenozoic formations are estimated to be ~120°-100°C (Lower Siwalik), ~130°-120°C (Kasauli), ~ 140°-130°C (Dagshai) and ~160°- 140°C (Subathu).

ii) Rate of subsidence in all parts of the foreland Cenozoic basin has not been uniform both spatially and temporally. Subsidence history shows breaks between 40-30 Ma and 6.5-5 Ma in the continuous trend in the region of Surinsar, Jammu hills, whilst these gaps are not observed in other places.

iii) The Kasauli sediments (125°C) exhumed 1 km before 13 Ma. The Dagshai Formation since 13 to 8 Ma at least 0.5 km exhumed, i.e. 0.1 km/Ma. The exhumation of sediments in the foreland basin since 8 Ma to present time estimated to be about 2.5 to 3 km in the present area, i.e. 0.3-0.4 km/Ma. Thus, the total exhumation of the sediments is around 4-4.5 km since the starting of exhumation. Thus the rate of exhumation of foreland sediments from early to end of Middle Miocene (from 13-8 Ma) is very low (0.1 km/Ma) but from the Upper Miocene to present is high (~0.3-0.4 km/Ma).

CHAPTER-7

SUMMARY AND CONCLUSIONS

The Himalaya is geodynamically active youngest mountain belt on the surface of the earth. The Cenozoic Sub-Himalayan foreland basin occupying the southern parts, forms an important sedimentary basin of this mountain belt. Subsidence–uplift history of a sedimentary basin affects the thermal maturation of organic sediments to generate petroleum hydrocarbons. Accordingly, the Early to Late Cenozoic sediments, occurring to the south of Main Boundary Thrust (MBT), formed the object of present study. This study is based on the Subathu, Dagshai, Kasauli and Lower Siwalik formations encountered along the traverses in areas of Nahan-Sarahan, Kalka- Kasauli-Dharampur, Dharampur-Subathu, Dharampur-Kumarhatti and Kumarhatti-Solan of Himachal Pradesh (H. P.).

Geologically, the sediments encountered along these traverses belong to the oldest Subathu Formation (Paleocene-Late Eocene), Dagshai (Late Eocene-Early Oligocene), Kasauli (Middle Oligocene-Early Miocene), and the Lower Siwaliks formations (Middle Miocene). The Subathu Formation forms 1500 m thick sequence of shale, siltstone and limestone with minor intraformational conglomerate, and quartz arenite. It is abruptly overlain by the Dagshai Formation which consists of 600 m thick sequence of gray and purple claystone/shale alternating with fine grained, greenish, hard, and impure sandstone. The overlying Kasauli Formation is marked by 2100 m thick sediments, characterized by massive pale gray to buff coloured micaceous sandstone alternating with the purple and gray shale. The Kasauli Formation is thrust over the Lower Siwalik Formation which comprises of 1700 m thick sequence of alternating sandstone-shale/siltstone with minor amount of conglomerate.

The Main Boundary Thrust (MBT) has played an important role in juxtaposing the different stratigraphic horizons. In the present area, it is manifested as a zone of thrusting, as various other thrusts in the area terminate at MBT.

Estimates of the maximum thickness of various formations of the Sub-Himalayan foreland basin provides different depositional rates. These are 75 m/Ma (1500/20 Ma) for the Subathu, 100 m/Ma (600 m/6 Ma) for the Dagshai, 300 m/Ma (2700 m/9 Ma) for the Kasauli and ~340 m/Ma (1700 m/5 Ma) for the Lower Siwalik formations. Thus, depositional rates have increased with decreasing age of stratigraphic formations.

The depositional environment of the Subathu Formation varies from shallow marine to marginal marine. Overlying the Subathu Fromation are the dominant continental sediments of the Murree/Dharmsala Formation (Dagshai-Kasuli formations). The Siwalik sediments are continental fluvial deposits and characterized by typical fining upwards cycles of deposition. The major trends of the paleo-current patterns of pre-Siwalik and Siwalik formations have been from north to south and also from northeast to southwest. However, a few subsidary paleocurrents from south to north trend have also been recognized during pre-Siwalik period, but these trends have not been observed / reported during the Siwalik time.

The **petrographic studies** were carried out on sandstone samples. The results of the modal analysis of sandstones of various stratigraphic units are presented in the Table given below.

Parameters		**Stratigraphic Units**			
		Subathu	**Dagshai**	**Kasauli**	**Lower Siwalik**
Light Minerals	**Q %**	96	76	68	67
	F %	1	3	4	7
Lithic Fragments%		3	21	28	26
Heavy minerals		Tourmaline, zircon, Oxide	Tourmaline, zircon, oxide, apatite	Garnet, Tourmaline, zircon, oxide, apatite	Garnet, sphene, staurolite, tourmaline, zircon, oxide, apatite
Rock fragments		Plutonic, metamorhic (low grade), and re-cycled rocks	Plutonic, metamorhic (low grade), and re-cycled rocks	Plutonic, metamorhic (low-medium grade), and re-cycled rocks	Plutonic, volcanic, metamorhic (low-high grade), and re-cycled rocks
Cement %		Trace to 29	1-16	1 - 4	Trace to 28
Matrix %		8-15	22-32	11-34	Trace to 24

Q= Total quartz, F= feldspars

Light minerals- Quartz is the most dominant constituent of all sandstone samples. Both monocrystalline and polycrystalline varieties of grains are found. The monocrystalline quartz is the major component which at times is replaced by calcite. It varies from 49% to 86% in the Subathu, 44% to 55% in Dagshai, 37 to 53% in Kasauli, 34 to 52% in Lower Siwalik formations.

Plagioclase varies from trace to 1.3% (An=18%), trace to 3.1% (An=18%), 1.7 to 3.4% (An = 16%), 5 to 8% (An=18-23%) in the Subathu to Lower Siwalik formations respectively. Orthoclase is the prominent variety of potash feldspar. Microcline is found to be in very small amounts.

Amongst the other constituents, mica, biotite and muscovite, chlorite are found in general. The main source of chlorite is due to alteration of biotite. Serpentine and glauconite are found in the Subathu and Kasauli formations.

Heavy minerals- Amongst the heavy minerals, zircon, tourmaline, and oxides (mainly magnetite) are the main constituents. Zircon and tourmaline occur both as euhedral to rounded grains. The other minerals are apatite (not found in the Subathu formation), garnet (in the Kasauli and Lower siwalik formations) and sphene, staurolite (only in the Lower Siwalik Formation), and epidote (in the Subathu, Dagshai and Lower Siwalik formations).

Rock fragments include fine to coarse grained lithic fragments. Fine grained lithic fragments are both the metamorphic lithics (slate and phyllite) and the sedimentary lithics (as chert). The metamorphic lithics with medium to high grade (garnet mica schist, and gniess) are found in the Kasauli and Lower Siwalik formations. The coarse grained lithic fragments are quartzite and metamorphic lithic in general. The percentage of the sedimentary fragments increase towards. Volcanic fragments showing needle form of plagioclase in the glass mass are also present in the Lower Siwalik Formation. The percentage of lithic fragments varies from 3.4 in the Subathu, 21 in Dagshai, 28 in Kasauli and 26 in Lower Siwalik formations.

The **matrix** generally consists of clay, sericite and quartz. It varies from less than 15% in Subathu, 22-30% in Dagshai, 12 to 30% in Kasauli, up to 24% in Lower Siwalik formations.

The **cement** in these sandstones is mainly siliceous and calcitic (sparite) forming negligible to about 29% in Subathu, 1% to 16% in Dagshai, up to 4% in Kasauli, and 28% in Lower Siwalik formations of the bulk composition. There appears to be a definite order in which

different types of cement were formed. Silica was initially precipitated, followed by ferruginous (in Dagshai and Kasauli formations), siliceous (chert) and calcite cements, respectively.

Based on light minerals of the sandstones, it is observed that the quartz percentage forms 2/3 or more of the bulk and continually decreases upwards from the Subathu to Lower Siwalik. Unlike quartz, feldspar and lithic fragments increases upwards.

Further analysis of these data bring out an (a) upward decrease in the amount of monocrystalline quartz, (b) upward increase though small, of detrital feldspar and polycrystalline quartz, (c) upward increase of lithic constituents (metamorphic, igneous and sedimentary) and (d) upward increase in higher grade metamorphic rock fragments. These patterns indicate relatively quiet tectonic conditions with very low rate of erosion and uplift during the deposition of Subathu Formation. After the Subathu time, continual increase in lithic fragments in the sandstones suggests relatively higher uplift rates in younger rocks and diversity of sources of these sediments. The present data plotted in the QFL diagram support that the Cenozoic sediments had source from the recycled orogenic materials. In the early stage of basin formation, detritus was largely derived from sedimentary and very low grade metamorphic rocks of mainly Late Protrozoic to Cambrian from the proto-Himalaya reliefs (supracrustal Indian margin rocks).

In the present study, Folk's (1980) classification of sandstone was used. This classification utilizes only three major framework constituents as the basis for assigning clan names. These constituents are Quartz (Q), Feldspar (F), and Rock Fragments (RF). Accordingly, sandstones are classified mainly as quartzite–sublitharenite for the Subathu Formation, sublitharenite-litharenite for the Dagshai Formation, and litharenite for the Kasauli and Lower Siwalik formations. However, considering framework constituents and matrix classification (Pettijohn, 1975), sandstone samples may be classified as: quartz arenite, sublitharenite (Subathu), lithic graywacke (Dagshai), lithic graywacke and litharenite (Kasauli and Lower Siwalik formations).

The **X-ray** studies indicate that the dominant clay minerals in shales and matrix of sandstones based on Weir's parameters (1975) are illite, kaolinite, mixed layer, chlorite, vermiculite and montmorillonite in order of decreasing abundance. The illite peaks (8.8°, 17.7°, and 26.75° 2θ in untreated samples with no change in ethylene glycol and intense in heated

samples) are sharp and well defined. The percentage of illite varies from 50 to 82 in Subathu, 73 to 99 in Dagshai, 77 to 89 in Kasauli and 67 to 70 in the Lower Siwalik shales. The percentage of kaolinite (with peaks of 12.38°, 24.94° 2θ in untreated samples, no change in ethylene glycol and collapse and absence in heated samples) varies from 14 to 28% in Subathu, 8 to 26% in Dagshai, 6 to 19% in Kasauli and 24 to 28% in the Lower Siwalik shale samples. The percentage of chlorite in shales (with peaks of 6.3°, 12.62°, 18.92°, 25.45° 2θ in untreated samples, no change in ethylene glycol and intensified in heated samples) is in the range from 20 to 30% in Subathu, 1 to 7% in Dagshai, 4 to 6% in Kasauli formations. In montmorillonite, peaks of 6.8° to 5.89° 2θ (13-15 A°) in untreated samples increase to 5.2° 2θ (17 A°) in ethylene glycol and collapse to 9.83°-8.84° 2θ (9-10 A°) in heated samples. Percentage is very less (<9.5) and only presents in the younger sediments. The clay matrix of sandstone samples shows the same variations as shale samples.

Kubler index, sharpness ratio and Jacob's crystallinity index were determined to find illite and other clay mineral crystallinity. It was observed that Kubler index (illite crystallinity index) increases from Subathu to Lower Siwalik formations. However, Jacob's crystallinity index showed the least crystallinity of illite and kaolinite for Subathu, but the mean of illite intensity ratio from Lower Siwalik to Subathu formations generally shows little recrystallization of illite. The crystallinity of illite decreases with younging of sediments. The relation of sharpness ratio and illite crystallinity index (I.C.I) in pre-Siwalik and Lower Siwalik sediments is uniform and linear.

Numerous studies have confirmed that the shape and width of the 10A° illite-mica peak changes with increased depth of burial and grade of metamorphism (Weaver, 1989). Thus, the illite crystallinity index is one of the principal parameters used in assessing the conditions of burial from diagenesis to low–grade metamorphism. Diagenesis is generally considered to include all changes which affect minerals. The boundary between diagenesis and metamorphism is a controversial problem, but commonly the boundary occurs at ~200°C when recrystallization of clay minerals occurs. The temperature at which the boundary changes occur, varies with grain size. In order to standardize the boundary between diagenesis and very low grade metamorphism, it is best to use the <2 μm fraction (Weaver, 1989). The variations of sharpness

ratio and crystallinity values to identify the boundary between diagenesis, very low grade (anchizone) and low grade metamorphism (epizone; Weaver, 1989). Weaver (1989) indicated that the diagenetic stage is characterized by sharpness ratio less than 2.3, and illite crystallinity index (Kubler Index) more than 3 (mm) or 0.42 (2θ). The sharpness ratio for anchizone should be between 12.1 and 2.3, whilst the illite crystallinity index will be between 3.0 to 1.50 (mm) or 0.42 and 0.25 (2θ).

The mean 2θ values of I.C.I. (Kubler Index) showed that the Subathu (0.37) and Dagshai (0.42) formations are both at the same stage of "late diagenesis", the Kasauli Formation (0.44) is at the "lower stage of middle diagenesis", and the Lower Siwalik Formation (0.53) is at the "middle stage" of diagenesis.

Based on genesis of clay minerals and their occurrences in the Cenozoic Himalayan foreland sediments, it is evident that the depositional environment changed from epineritic (Subathu Formation) to continental fluvial regime (younger formations).

Fission Track Analysis- The studies of the effects of various environmental parameters on **track stability** in different mineral and glasses (see Fleischer et al., 1975; Wagner and Van Den Haute, 1992), indicate that ordinarily it is the temperature which has the predominant effect on fission track. Under geological conditions, fading of fission tracks is a common phenomenon and the resulting loss of fission tracks tends to lower the apparent FT age. In that case, the time at which the FT clock was turned on and the time that is given by the clock is no longer the same. The apparent FT mineral ages lowered by partial or complete track fading have resulted in understanding the insights of the thermal history of the host rock.

Fission track studies were carried out on the zircon and apatite grains (>750 total grains) of selected sandstone samples, using External Detector Method (EDM). In the present study, the samples which were in close vicinity to each other, have been clubbed together. The range of ages of individual zircon grains, the number of grains analyzed, youngest Gaussian age peak in clubbed samples (A) and general bulk of each formation (B), older peacks (B), and χ^2 ages are given below:

Parameters		Stratigraphic Units			
		Subathu	Dagshai	Kasauli	Lower Siwalik
Number of Grains		126	201	327	88
Age Range (Ma)		557-42	515-16	281-13	363-9
Youngest Gaussian age peak (Ma)	A	41	30-25	31-26	20-14
	B	39	25	25-15	15
Older peaks (Ma)	B	84, 144, 229, 393	40, 80, 226, 382	U. part = 27, 44, 97, 293 L. part= 36, 85, 153, 324	27, 66, 99, 285
χ^2 –ages (Ma)		58.8	26.2	22.2-14.2	9.7
Peak Width (W)	A	19, 21	25, 28	26	29, 30

FT age data of apatite samples is very limited as this mineral was not available in sufficient quantities in many samples. FT apatite ages are available from one sample of Kasauli Formation and two samples of Siwaliks. The analytical data of **apatite** samples are indicated below:

Stratigraphic Units	Sample	Number of Crystals	P (χ^2) % age	Age (Ma)	Weighted Mean Age (Ma)
Lower Siwalik	Upper part	2	30	11.94±2.86	9.96 ± 0.99
	Lower part	19	80	9.55±1.05	
Kasauli	Upper part	14	7	13.51±1.99	13.51± 1.99

The zircon FT results have shown very wide age range with the Gaussian peak width "W" 19 to 30. These data suggest that (a) the FT in zircon grains are unreset, implying thereby that the FT in the zircon grains could not have been annealed, and FT ages reveal the characteristics of the provenance before the onset of the major thermal events associated with the Himalayan orogeny, and (b) the zircon grains were derived from multiple FT sources. The fission tracks preserved in the **apatite** grains in the sandstone of various formations appear to be reset. This resetting is also indicated by the ages of FT in apatite, which are younger than their depositional ages (8 Ma in Dagshai, 13 Ma in Kasauli and 10 Ma in Lower Siwalik formations). The Dagshai apatite data is from Mehta (1995). The thermal conditions in the Cenozoic sediments were, therefore, below the closure temperature of apatite (120°±20° C) but much above the closure

temperature of zircon (240°±25°C), i.e. the conditions were favourable for organic matter maturation.

The Gaussian peak-fit method directly decomposes the grain-age spectrum into a series of component Gaussian populations or peaks. Each peak is defined by the mean age, the width of the Gaussian relative to mean age (W_f, equivalent to standard deviation divided by the mean age), and the size of the Gaussian relative to the total size of the grain age distribution (π_f).

In FT stratigraphy, where a series of stratigraphically-related age distributions are evaluated, two types of peak ages can be identified: 'moving peaks', defined by a peak age that gets progressively younger or older up-section, and 'static peaks', where the peak age remains relatively constant up-section. The grain age distributions of all samples using Gaussian peak fitting programme developed by Brandon and his group, contain 3-4 resolvable peaks.

The distribution width (W) of all samples are higher than 19%. The population of zircons derived from a single-age FT source is estimated to have W ≈16.3%. Such an inference has been drawn by investigating the grain age distribution of unreset volcanic zircons of tuff samples (Brandon and Vance, 1992).

In the present zircon FT results, there are two distinct Gaussian age peaks, youngest and older, are summarized below.

(i) Youngest peak ages- The youngest age peak of all the samples can be used for **estimation of depositional age** of different formations. The youngest zircon Gaussian peak age becomes dominant upward the stratigraphic section and estimates the upper limit of deposition. These ages in clubbed nearest samples are: 40.7 Ma (Subathu); 29.7-25.0 Ma (Dagshai); 31.1, 28.9, 26.0 Ma (Kasauli); and 20.5-13.9 Ma (Lower Siwalik), and in general clubbing of individual formations, are determined as: Subathu ca. 39.1 Ma, Dagshai ca. 25.1 Ma, Kasauli ca. 25.2-15.2 Ma and Lower Siwalik ca. 14.6 Ma. These ages are consistent with the ages determined by biostratigraphy (Arya, 1998), magnetostratigraphy (Sangode, 1997) and argon-argon methods (Harrison, 1992; Najman, 1997). In general, pattern of zircon FT ages from the foreland Cenozoic sediments have shown χ^2-ages of 58.8 Ma, 26.2 Ma, 22.2-14.2 Ma, and 9.7 Ma from the Subathu to the Lower Siwalik formations, respectively.

In the present study, only one sample of Subathu Formation, i.e. S1 (Table 4.3) has shown a peak at 40.7 Ma. However, this is not a dominant peak as the fraction of grains in this peak is very small. The youngest peak in white quartzite (sample S2) which forms the key bed at the upper part of Subathu Formation, was not recorded in the FT age data of this sample. The overall lack of grains in the youngest peak of the Subathu Formation could arise due to several reasons. There is a possibility though with very small probability, that only very limited grains belonging to youngest fraction might have been included during mounting. Another reason for lack of low FT ages zircon grains in the Subathu Formation can be either low erosional rate during the early stages of Himalayan orogeny or very limited source region responsible for contributing the detritus affected by the Himalayan orogeny.

In the present study the sample D1 from the lower part of Dagshai and D2 from the upper part indicate 29.7 Ma and 25.0 Ma as the youngest Gaussian peak ages respectively. These ages appear to represent the depositional age of Dagshai. The proportion of grains in the youngest peak has increased to 10-15 times in comparison to the Subathu Formation. This increase suggest that by the starting of deposition of Dagshai Formation, the erosional rate (which implies uplift of the rocks) and/or the extent of the provenance affected by the Himalayan orogeny increased sufficiently. Tectonic activity, therefore, increased during the Dagshai time and, so provided new sources with younger ages.

FT age data of zircons separated from the Kasaulis indicate the youngest peak at 31.1, 28.9, and 26.6 Ma respectively for the lower, middle and upper parts of this Formation. These ages appear to represent at least the upper limit of the deposition time of these rocks.

However, the overlapping ages of youngest peaks in Kasauli and Dagshai indicate that either these formations are not distinct as far as their deposition timeframe is concerned. Or if they are distinct, then the ages given by the youngest peaks in various horizons of Kasauli are higher than their actual depositional ages. Such a situation could mean that exhumation of provenance for Kasauli was comparatively slow than during the Dagshai.

In the Lower Siwalik samples, the ages of youngest peaks in the zircon age distributions are 20.5 and 13.9 Ma respectively for the lower and upper parts of the formation. These ages

appear to be consistent with the depositional ages estimated by Sangode (1997) using paleomagnetic stratigraphy.

(ii) Older peaks- The fraction of grains in the older peaks of Subathus is very high while it decreases as we go up section towards the Siwaliks. On the other hand, fraction of grains in youngest peaks of the Siwaliks is very high in comparison to that of Subathus. Such a trend of distribution of grain ages certainly speaks about the provenance. It appears that extent of the older detritus contributing to the Subathus was much larger than the orogeny affected-detritus implying thereby a very limited effect of the Himalayan orogeny both in terms of areal extent and uplift of the rocks during the time Subathus were deposited. During the time of deposition of the Dagshais and Kasaulis, the grain age distribution is biased towards younger ages. This means that the effect of the Himalayan orogeny during this time increased tremendously. In the lower part of the Lower Siwaliks, the amplitude of the P_3 and P_2 peaks is very small and is almost insignificant in the upper part of the Lower Siwaliks. If we assume that by Siwalik's time all the source rocks were affected by the Himalayan orogeny, then the older ages peaks present in the Siwaliks could come from the recycled material, i.e. from the Subathu, Dagshai, and Kasaulis etc. The presence of the Kasauli sandstone pebble within the Siwaliks further support such a possibility.

The general zircon FT clubbing of Cenozoic formations clearly depicts the shifting of peaks towards younger ages with the decrease in depositional ages. Such a feature indicates that the source is continuously rising and feeding the material to the sedimentary basin.

The FT older ages of zircon grains could be derived from (a) the veneer part of the Lesser Himalaya with traces of older pre-Himalayan thermal events, (b) Late Proterozoic-Early Paleozoic sedimentary basin such as Krol basin, and (c) the old Cenozoic sediments of the foreland basin itself may be involved as an additional source of the old grains into the younger formations. The existence of sedimentary lithic fragments in the Cenozoic formations could be considered as a document of this point.

As a general trend in the bulk samples, all observed zircon peak ages are moving and becoming younger towards the Cenozoic stratigraphic column. The percentage of old zircon FT ages continually decreases upwards and the younger FT ages continually increase upwards from

the oldest Subathu Formation to the Lower Siwalik Formation indicating continual rising up of the source (Himalaya) which contributed the sediments to this Cenozoic foreland basin. The absence of regular pattern in the age distribution of Gaussian zircon peaks may be related to the recycling of sediments which is also corroborated by petrographic evidences in the form of sedimentary lithics, abraded quartz overgrowth, and rounded zircon, tourmaline and garnet found in these sediments. The youngest peak ages may be derived from the source with the high rate of uplift and the old ages may have come from the source with the low rate of uplift. These Gaussian peak ages and their " peak width " in zircon grains in various formations of the Cenozoic sediments show (i) the non-uniform uplift in the provenance, such that the zircon grains in the youngest peaks are supplied from the area with the high rate of uplift, and those consisting of the oldest peaks came from the area with very low uplift rate as discussed earlier by Cerveny et al. (1988) for the northern part of Pakistan, and (ii) the areal extent of the Himalayan orogeny appears to continuously spreading after the collision of the Indian Plate with the Eurasian Plate.

Analysis of fission tracks on **zircon** and **apatite**, therefore, indicates that sediments of all the formations of the Cenozoic foreland basin have not subsided to the depth level corresponding to the closure temperature of fission tracks in zircon (240°±25°C). The resetting of apatite ages from the Kasauli and Siwalik sediments indicates that Cenozoic sediments subsided to a depth of ~ 4 km corresponding to the closure temperature of apatite ($120^0 \pm 20$°C).

The shales from various stratigraphic units were subjected to **petroleum source rock evaluation**. The studies were carried out to estimate abundance of organic matter in terms of Total Organic Carbon (TOC) content, quality of organic matter in terms of kerogen and the thermal maturation of organic matter to generate the hydrocarbons.

Quantity of organic matter- Since carbon is an integral part of organic matter, total organic carbon content (%TOC) is directly related to it. Hence % TOC in sediments is universally considered as a measure of abundance of organic matter. The TOC in shales found in the area of study, varies from 0.09% to 0.3% (mean 0.2%) in the Subathu Formation, 0.07% to

0.37% (mean 0.15%) in the Dagshai Formation, 0.09% to 0.6% (mean 0.2%) in the Kasauli Formation and 0.06% to 0.17% (mean 0.1%) in the Lower Siwalik Formation.

Quality of organic matter- The quality and amount of hydrocarbon, generated from a source rock depend largely on the type and quality of the organic matter which produced it (Barker, 1979). The kerogen of type-III (mainly terrestrial) is gas-prone, whereas kerogen of type-I and type-II are mainly oil-prone (Tissot and Welte, 1978). Pyrolysis of whole rock in an inert atmosphere using rock eval technique developed by Espitalie et al. (1977) has made major contribution to systematic analysis of kerogen (Cleamentz et al., 1979). Those samples which had shown higher TOC% were selected to determine the quality of organic matter present in them. The hydrogen index (HI) and oxygen index (OI) of these samples are below ~150 and ~40 mg CO_2/gTOC respectively. These data were plotted on an modified Van Krevelen diagram. It indicates that the kerogen is as mainly of type-III with major terrestrial component. This type of kerogen which is prone to generate mainly gas but little oil, is found in all formations.

Thermal maturation of organic matter- The level of thermal maturity of organic matter found in the sediments, has been determined using organic and inorganic methods such as vitrinite reflectance (VR_o), T_{max} obtained by pyrolysis, illite crystallinity index (Kubler index), and fission track analysis.

Vitrinite reflectance (VR_o)- The mean values of vitrinite reflectance (VR_o) are 1.2% for Subathu, 0.9% for Dagshai, 0.7% for Kasauli and 0.8% for the Lower Siwalik formations, indicating thereby that organic matter is matured to various levels to generate petroleum hydrocarbons. The Subathu sediments have reached peak stage of maturity for generation of petroleum.

In the present study, T_{max} has been used to assess the degree of maturity of organic matter. The Subathu shale with the T_{max} >470°C, indicates maturation to early metagenetic stage, the Dagshai Formation with T_{max} of 450° C and the Kasauli (Murree) sediments with T_{max} between 450°–430°C indicate initial to middle stage (catagenetic) of maturation of organic matter; and the Lower Siwalik Formation with T_{max} 445° C (estimated) indicates that it is in the gas stage catagenetic maturation to generate petroleum hydrocarbons. These results and also the

vitrinite reflectivity indicate that the shales of the Cenozoic sediments have maturated to generate petroleum hydrocarbons.

Illite crystallinity index (I.C.I. or K.I.): illite crystallinity index is controlled by the same geologic agent that control vitrinite reflectance (Guthrie et al., 1986). Therefore, in the absence of vitrinite, illite-crysallinity was used quantitatively to estimate levels of thermal maturity as diagenesis indicator or estimation of paleotemperature using relevant equation with vitrinite reflectance. Illite crystallinity index (Kubler Index) revealed that all the Cenozoic sediments are in the diagenesis stage. Therefore, the paleotemperature attained by sediments would not be more than 180°- 200°C (the boundary between diagenesis and very low grade metamorphism).

Fission Track Study- As already mentioned that analysis of fission track on apatite and zircon crystals indicate that the paleotemperature during the deposition of the Subathu Formation due to unreset of zircon crystals, could not more than 180°C. But all sediments due to resetting of apatite ages, seems to be reached 120° ±20° C isotherm which is necessary to reset of tracks in apatite crystals. Paleotemperature attained by Cenozoic sediments (100°-215°C) caused the maturity of organic matter. In the youngest sediments, organic matter is in initial to middle stage and in the oldest one it is at the end of maturity. This point is also supported by other maturity indicators, namely vitrinite reflectance and illite crystallinity.

The **paleotemperature** was estimated by using the VR_o values which were measured and estimated with the help of time-temperature nomogram of Middleton (1982) and diagram of Gleadow et al. (1983). The maximum temperature to which Cenozoic sediments were subjected to be 100–120°C (110°C) for Lower Siwalik, 120-130°C (125°C) for Kasauli, 130–140°C (135°C) for Dagshai and 140–160°C (150°C) for Subathu formations. With regards to the temperature limit of petroleum hydrocarbons generation between 60°–180° C and the peak oil generation at a temperature of the order of 120° C, it is apparent that the Cenozoic sediments are in oil window.

Based on paleotemperature data and surface stratigraphy, an attempt was worked out to reconstruct the **subsidence and uplift** history of the Cenozoic Himalayan foreland basin in the present area. According to the paleotemperature, and observed geothermal gradient of 30° C/km in the Cenozoic basin, it is estimated that the shales of the Cenozoic sediments are maturated to

generate petroleum hydrocarbons. In the Cenozoic Himalayan foreland basin, the petroleum hydrocarbon generation started at ~25 Ma (Middle Miocene) when the Subathu reached a burial depth of 2500 m and continued subsiding till to about 13 Ma when these sediments reached a depth ~4500 m. The Cenozoic sediments were exhumed/uplifted to about 1km before 13 Ma to attain the annealing temperature of apatite (120°±20°C). This age is recorded by apatite FT clock in the Kasauli Formation. The Dagshai Formation with AFT age of 8 Ma (Mehta, 1995), and the estimated maximum paleotemperature of 130°-140°C indicate that the foreland sediments exhumed ~1.5 km till 8 Ma. Therefore, the Cenozoic sediments exhumed to about 0.5 km (1.5–1 km= 0.5 km) in time span of 13-8 Ma. Thus, the rate of exhumation is estimated to be 0.1 km/Ma (0.5 km/5 Ma). Since 8 Ma to present time, it is estimated to be about ~2.5 to 3 km in the present area, i.e. 0.3-0.4 km/Ma. Thus, the total exhumation of the sediments is around 4.0-4.5 km since the beginning of exhumation of the Cenozoic sediments. Thus, the rate of exhumation of foreland sediments from early to end of Middle Miocene (from 13-8 Ma) is very low (0.1 km/Ma), but from the Upper Miocene to present is appreciably high (~0.3-0.4 km/Ma).

These data along with the published drill-hole data show that subsidence in all parts of the foreland Cenozoic basin has not been uniform in rate, spatially and temporally. Subsidence history shows breaks (40-30 Ma and 6.5-5 Ma) in the continuous trend in the region of Surinsar, Jammu hills.

Therefore, the following salient conclusions are drawn:

(i) The collision of Indian plate with the Asian plate has resulted in subsidence-uplift phenomenon in the Himalaya. Subsidence in all parts of the foreland Cenozoic basin has not been uniform in rate. Subsidence history shows breaks in the continuous trend during the periods of 40-30 Ma and 6.5-5 Ma (in the region of Surinsar, Jammu hills).

(ii) The exhumation of sediments started at about 13 Ma. This may be related to the activation of the Main Boundary Thrust (MBT).

(iii) The exhumation has also not been uniform through time. The total exhumation of the sediments is around 4.0-4.5 km since the start of exhumation. Thus, the rate of exhumation of foreland sediments from early to end of Middle Miocene (from 13-

8 Ma) is very slow (0.1 km/Ma) but from the Upper Miocene to present is fast (~0.3-0.4 km/Ma).

(iv) For all formations, TOC% is generally low, and the hydrogen (HI) and oxygen (OI) indices are below ~150 and ~ 40 mg CO_2/g TOC respectively. These data indicate the kerogen mainly of type-III having low prospects of liquid hydrocarbon. The Subathu shales with the T_{max}>470°C and VR_o%=1.2 (early metagenetic stage); the Dagshai Formation with T_{max} of 450° C and VR_o%=0.9, the Kasauli (Murree) sediments with T_{max} between 450°-430°C and VR_o%=0.7 indicate initial to middle stage (catagenetic) of maturation of organic matter; and the Lower Siwalik Formation with T_{max} 445°C and VR_o%=0.6, indicates that it is in the gas stage catagenetic maturation to generate petroleum hydrocarbons.

(v) On the basis of fission track analysis, illite crystallinity index and vitrinite reflectance data, the maximum paleotemperature of the Lower Siwalik estimated to be ~100°-120°C, Kasauli ~ 120°-130°C, Dagshai is ~ 130°-140°C and about Subathu Formation is 140°-160°C.

(vi) The Cenozoic sediments have right type of kerogen (type-III) which has undergone adequate thermal maturation for generation of petroleum hydrocarbons. However, the quantity of organic matter in the sediments is generally low < 0.5%. Hence, the possibility of generation of petroleum hydrocarbons in commercial quantity is low. This appears to be one of the major reasons why the exploration efforts of the Oil & Natural Gas Corporation for the last three decades or so have not been successful to locale any commercial find of oil/gas in this basin.

REFERENCES

Abid, A. I., Abbasi, I. A., Khan, M. A., and Shah, M. T., Petrography and geochemistry of the Siwalik sandstone and its relationship to the Himalayan orogeny. Geol. Bull. Univ. Peshawar, Vol. 16, P.65-83, 1983.

Agarwal, R. d., Prasad, D. N., Samanta, U., Berry, C. M., and Sharma, J., Hydrocarbon potential of Siwalik basin. Him. Geol., Vol. 15, P. 301-320, 1994.

Allegre, C. J., Courtilot, V., Tapponier, P., Hirn, A., Mattauer, M., Coulon, C., Jaeger, J. J., Achache, J., Scharer, U., Marcocux, J., Burg, J. P., Girardeau, J., Armijo, R., Gariepy, C., Gopel, C., Tindong, Li, Xuchang, X., Chenfa, C., Guangqin, Li, Baoyu, L., Jiwen, T., Naiwen, W., Guoming, C., Tonglin, H., Xibin, W., Wanming, D., Huaibin, S., Yougong, C., Ji, Z., Hongrong, Q., Peisheng, B., Songchan, W., Bixiang, W., Yaoxiu, Z., and Xu, R., Structure and evolution of the Himalaya Tibet orogenic belt. Nature, Vol., 307, P. 17-22, 1984.

Akande, S. O., and Viczian, B. D., Burial metamorphism (thermal metamorphism) in Cretaceous sediments of the Southern Benue Trough and Anambra basin, Nigeria. AAPG Bull., Vol. 82, No. 6, P.1191-1206, 1998.

Alizadeh-Shahzaidi, B., and Awasthi, A. K., Spectral signatures of Barakar shales as maturity indicator of organic matter. National Conference on Evolution of Gondwanic Crust, Alligarh Muslim University, P.33-34, 1996.

Appeal, E., Rosler, W., and Corvinus, G., Magnetostratigraphy of the Miocene-Pleistocene Surai Khola Siwaliks in west Nepal. Geophys. J. Inter., Vol.105, P. 191-198, 1991.

Armijo, R., Tapponier, P., Merceier, J. L., and Han, T. L., Quaternary extension in Southern Tibet: Field observations and tectonic implications. J. Geophy. Res., Vol. 91, P.13803-13872, 1986.

Arya, R., and Awasthi, N., A new species of Bauhinia from the Kasauli Formation (Lower Miocene), Kasauli, Himachal Pradesh. Geophytology, Vol. 24, No.1, P. 59-62, 1994.

Arya, R., Biotic and abiotic changes at Oligocene/Miocene boundary in Northweatern Indian Himalayas: Paleoecology and paleobiogeographic implications. Workshop Himalayan foreland basin with special reference to pre-Siwalik Tertiaries, Jammu, March, 16-19, P. 12-14, 1998.

Auden, J. B., Traverses in the Himalaya, India. Geol. Surv. Records, Vol. 66, P. 461-471, 1935.

Awasthi, A. K., Sedimentoogical studies of the Jodhpur Group in the Districts of Jodhpur and Nagpur, Rajastan, India. Ph. D. Thesis, Roorkee Univ., India, 314 P, 1979.

Babu, S. K. and Dehadrai, P. V., Petrological investigations of the rocks of Mohand near Dehra Dun. Curr. Sci., VOL. 27, P. 168-170, 1958.

Bagati, T. M., and Kumar, R., Clay mineralogy of the Middle Siwalik sequence in the Mohand area, Dehra Dun: Implications for climate and source area. Him. Geol., Vol. 15, P. 219-228, 1994.

Baldwin, S. L., and Harrison, T.M., Fission track dating of detrital zircon from the Scotland Formation, Barbados, W.I. (Abs.). Nuclear Tracks, Vol. 10, P. 402, 1985.

Baldwin, S. L., Harrison, T. M., and Burke, K., Fission track evidence for the source of accreted sandstones, Barbados. Tectonics, Vol.5, P.457-468, 1986.

Baranowski,J., Armbruster, J., Seeber, L. and Molnar, P., Focal depths and fault plane solutions of earthquakes and active tectonics of the Himalaya. J.Geophys. Res., Vol.89, P.8918-8928, 1984.

Barker, C., Organic geochemistry in petroleum. AM. Assoc. Pet. Geol. Bull., Memoir., Continuing Education Course note Series, P. 10-15, 1979.

Barker, C. E., Influence of time on metamorphism of sedimentary organic matter in liquid-dominated geothermal systems, western North America. Geology, Vol. 11, P.384-388, 1983.

Barker, C.E., Temperature and time in the thermal maturation of sedimentary organic matter, in: N.D, Naeser and T.H. Mc Culloh, (eds.), Thermal history of sedimentary basins- methods and case histories. New York, Springer-verlag, P. 75-98, 1989.

Barker, C.E., Implications for organic maturation studies of evidence for a geologically rapid increase and stabilization of vitrinnite reflectance at peak-temperature: Cerro Prieto geothermal system, Mexico. AAPG. Bull., Vol. 75, No. 12, P. 1852-1863, 1991.

Barker, C.E., Reply to discussion of Sweeny and Burnham on the paper of Barker, 1991: Implications for organic maturation studies of evidence for a geologically rapid increase and stabilization of vitrinnite reflectance at peak-temperature: Cerro Prieto geothermal system, Mexico (AAPG. Bull., Vol. 75, P. 1852-1863). AAPG Bull., Vol.77, No.4, P.668-669, 1993 a.

Barker, C.E., Reply to disscussion of Bostick, N.H., on the Barker's Paper, 1991 (see ref.). AAPG. Bull., Vol. 77, No.4, P. 673-678, 1993 b.

Barker, C.E., Crysdale, B.L., and Pawlewicz, M.J., The relstionship between vitrinite reflectance, metamorphic grade and temperature in the Cerro Prieto, Salton Sea, and East Mesa geothermal system. Salton trough, United States and Mexico in: F.A., Mumpton, ed., Study in diagenesis. U.S.G.S., Bull,. 1578, P.83-95, 1986.

Barry, J. C., Lindsay, E. H., and Jacob, L. L., A biostratigraphic zonation of the Middle and Upper Siwaliks of the Potwar Plateau of Northern Pakistan. Palaeo. Palaeo. Palaeo., Vol. 37, P. 95-130, 1982.

Batra, R. S., A reinterpretation of the geology and biostratigraphy of the lower tertiary formations exposed along the Bilaspure-Simla Highway, Himachal Pradesh, India. J. Geol. Soc. India, Vol. 33, P.503-523, 1989.

Berry, C. M., Hydrcarbon potential of the Siwalik and pre-Siwalik sediments in Himachal Pradesh and jammu- Kashmir areas-A palynological prospects. Him. Geol., Vol. 15, P. 321-328, 1994.

Bertrand, R. and Heroux, Y., Chitinozoan, graptotite, and scoledont reflectance as an alternative to vitrinite and pyrobitumen reflectance in Ordovician and Silurian strata, Anti Costi Island, Quebec, Canada. AAPG Bull., Vol.1, No.8, P.951-957, 1987.

Besse, J., Courtillot, V., Pozzi, J.P., Westphal, M., and Zhou, Y.X., Paleomagnetic estmates of crustal shortening in the Himalayan-thrusts and Zangbo suture. Nature, Vol. 311, P. 621-626, 1984.

Bhattacharya, N., Clay mineralogy and trace element geochemistry of Subathu, Dharmsala and Siwalik sediments in Himalayan foothills of North Western India. J. Geol. Soc. India, Vol. 11, No.4, P.309-332, 1970.

Bhattacharya, N., and Raiverman, V., Clay mineral distribution of Dharmsala sediments in NW-India. J. Geol. Soc. India. Vol., 14, No.1, P. 71-78, 1973.

Bhushan, B., On the Uper Muree-Lower Siwalik Provenance. J. Geol. Soc. India, Vol. 14, P. 186-189, 1973.

Bigazi, G., The problem of decay constant of ^{238}U. Nucl. Tracks, Vol. 5, P. 35, 1981.

Biscay, P. E., Mineralogy and sedimentation of recent deep sea clays in the Atlantic Ocean and adjacent seas and oceans. Geol. Soc. Am. Bull., Vol. 76, P. 803-832, 1965.

Biswas, S. K., Study of exploration for hydrocarbns in Siwalik basin of India and future trends. Himal. Geol., Vol.15, P.283-300, 1994.

Bordet, P., Recherches geologifues dans 1' Himalaya du Nepal, Region du Makalu, editions Centre, National Dela Research Scientifice, Paris, 275 P, 1961.

Bostick, N. H., Time as a factor in thermal metamorphism of phytoclasts (coaly particles). Congress Internationale Stratigraphie, Geologie Carbonifere Compte Rendu 7th Session, Vol. 2, P. 183-193, 1973.

Bostick, N. H., Microscopic measurement of the level of categenesis of solid organic mater in sedimentary rocks to aid exploration for petroleum and to determine former burial temperatures–A review, in P.A.Scholle and P.R. Schluger, (edits.) Aspects of

diagenesis.Society of Economic Paleonto. and Mineral. special publication , 26 , P.17-44, 1979.

Bostick, N. H. and Pawlewicz, M. J., Paleotemperatures based on vitrnite reflectance of shales and limestones in igenous dike aureoles in the Upper Cretaceous Pierre shale, Walsenburg, Colorado, in J. Woodward, F. F. Meissner and J. L. Clayton. Eds., Hydrocarbon source rocks of the Greater Rocky mountain region: Denver. Rocky Mountain Association of Geologists, P.387-392, 1984.

Bradley, W. F., and Grim, R. E., Mica clay minerals. In: The x-ray identification and crystal structures of clay minerals, edit. G. Brown, P. 208-241. Mineralogical Socity London, 1961.

Brandon M. T., Decomposition of fission-track grain age distributions. Am. J. Sciences, Vol. 292, P. 535-564, 1992.

Brandon, M. T. and Vance, J. A., Tectonic evolution of the Cenozoic Olympic subduction complex, Washington State. As deduced from FT age for detrital zircons. Am. J. Sciences, Vol. 292, P. 565-636, 1992.

Bray, E. E., and Evans, E. D., Distribution of n-paraffins as a clue to recognition of sorce rock beds. Geochim. Cosmochim. Acta., Vol. 2, P. 2-15, 1961.

Bray, R.J., Green, P.F. and Duddy, I.R., Thermal history reconstruction in sedimentary basins using AFTA and vitrinite reflectuance: A case study from the East Middlands of England and Southern North seas, submitted to Geological Society of London, Conference proceeding special publications, Vol. 67, P.3-26, in Hardman, R.F.P.(ed.). Exploration Britain into the next decade, 1992.

Brindley, C. W., Kaoline, serpentine and kindred minerals. In: Brown, G. (edit.), The X-ray identifications and crystal structure of clay minerals. Min. Soc. London, 544 P., 1961.

Brookfield, M.E., Comment and Reply on "Thrust tectonics and the deep structure of the Pakistan Himalaya". Geology, Vol. 14, P. 364-365, 1986.

Burbank, D. W., and Johnson, G. D., The late Cenozoic chronologic and stratigraphic development of the Kashmir intermountain basin, Northwestern Himalaya, Palaeo. Palaeo. Palaeo., Vol. 43, P. 205-232, 1983.

Burchfiel, B.C. and Royden, L.H., North-South extension within the convergents Himalayan region. Geology, Vol. 13, P.679-682, 1985.

Bustin, R.M., Diagenesis of kerogen. In: I.E. Hutcheon (edit.), short course in burial diagenesis. Mineralogical Association of Canada Short Course Handbook, Vol. 15, P.1-15, 1989.

Carrol, D., Clay minerals; A guide to their X-ray identification. Geol. Soc. Am. Spec. Pap. 126, 1970.

Carter, A., The thermal history and annealing effects in zircons from the Ordivician of North Wales. Nucl. Tracks. Rad. Meas., Vol.17, P.309, 1990.

Cerveny, P.F., Uplift and erosion of the Himalaya over the past 18 million years- evidence from fission track dating of detrital zircons and heavy mineral Analysis. M.S., Thesis, Dartmouth College, Hanover, New Hampshire, 198 P, 1986.

Cerveny, P. F., Naeser, N. D. Naeser, C. W. and Johnson, N. M., Uplift and erosion of Himalayas during the past 18 million years: Evidence from fission track dating of detrital zircon in Siwalik Group sediments (Abs.). Symposium on New Perspectives in basin Analysis Abstracts, no page number is available, 1986.

Cerveny, P. F., Naeser, N. D., Zeitler, P. K., Naeser, C. W. and Johnson, N. M., History of uplift and relief of the Himalaya during the past 18 million years: Evidence from fission track ages of detrital zircons from sandstones of the Siwalik Group, in Kleinsphen, K.L. and Paola, C., (edits): New Perspective in Basin Analysis, New York, Springer-Verlag, P.43-61, 1988.

Chakraborty, A., Mitra, R. N. and Sastry, C. V. S., Some Tertiary conglomerates and grits of NW Himalayan foothills. Geological Survey. India, Vol. 15, P.111-116, 1963.

Chakraborty, A., Venkataraman, S., and Kumar, S. P., Report on the Geology of parautochton belt in Hatkot-Kasauli-Subathu area in Mahasu District, H. P., and Patiala and Ambala Districts, Punjab, Field season 1961-1962, Rept. Oil Nat. Gas Comm. (Unpublished), 1962.

Chaudhri, R.S., Geology of the Lower Tertiary rocks of Simla Hills. Doctorate thesis, Punjab University, Chandigarh, 1966 a.

Chaudhri, R.S., Complexometric determination of iron in the Dagshai rocks. Indian Mineralogist, Vol. 7, P.71-73, 1966 b.

Chaudhri, R.S., Stratigraphy of the Lower Tertiary formations of Punjab Himalayas. Geol. Mag., Vol. 105, P.421-430, 1968.

Chaudhri, R. S., Sedimentology of the Lower Tertiary rocksof the Punjab Himalayas. Res. Bull. (N. S.) of the Punjab University, Vol. 20, Parts I-II, P. 229-238, 1969 a.

Chaudhri, R.S., Some leaf impressions from the Kasauli Series of the Simla Hills, Curr. Sci., Vol. 38, P. 95-97, 1969 b.

Chaudhri, R. S., Environments of deposition of the Lower Tertiary rocks of Punjab Himalayas. J. Geol. Soc. Univ. Saugar, Vol.5, P.71-77, 1969 c.

Chaudhri, R.S., Provenance of the Lower Tertiary sediments of northwestern Himalayas. Bull. Ind. Geol. Assoc., Vol. 2, P. 51-56, 1969 d.

Chaudhri, R.S., Metasediments of Kasauli Series and kinematic metamorphism. J. Ind. Geosci. Assoc., Vol. 10, P. 59-62, 1969 e.

Chaudhri, R.S., Sedimentary structures from the Lower Tertiary rocks of Punjab Himalayas. Proc. 57th Ind. Sci. Congr., P.207, 1970 a.

Chaudhri, R.S., Heavy minerals from the Lower Tertiary sediments. Ind. Mineralogist, Vol. 11, P. 47-54, 1970 b.

Chaudhri, R.S., Petrology of the Siwalik Formation of northwestern Himalayas. Bull. Ind. Geol. Assoc., Vol. 3, P. 19-25, 1970 c.

Chaudhri, R.S., Nahan- a problematical horizon of northwestern Himalayas. J. Geol. Soc. India, Vol. 12, P. 373-377, 1971 a.

Chaudhri, R. S., Petrogenesis of Cenozoic sediments of NW-Himalayas. Geol. Mag., Vol. 108, No.1, P. 43-48, 1971 b.

Chaudhri, R.S., Vol. P. Petrology of the Lower Tertiary formations of northwestern Himalayas. Bull. Ind. Geol. Assoc., Vol. 4, P. 45-53, 1971 c.

Chaudhri, R.S., Heavy minerals from the Siwalik Formation of northwestern Himalayas. Sed. Geol., Vol.8, P.77-82, 1972 a.

Chaudhri, R.S., Development in sediments of northwestern Himalayas. Bull. Ind. Geol. Assoc., Vol. 5, P. 23-32, 1972 b.

Chaudhri, R.S., Vol. P. Petrogenesis of the Siwalik sediments of northwestern Himalayas. J. Geol. Soc. India, Vol. 13, P. 399-402, 1972 c.

Chaudhri, R. S., Tertiary sediments of NW-Himalayas – A critique. Punjab Univ. Res. Bull. (Sci.), Vol.23, P.83-90, 1972 d.

Chaudhri, R. S., Sedimentology and genesis of the Cenozoic sediments Dharmsala, North Western Himalaya (India). Sounder Druck aus der Geologischem Rudschau Band, Vol. 64, P. 958-977, 1975.

Chaudhri, R. S., Paleocene-Eocene sequence of Northwestern Himalayas - A product of rhytmic sedimentation. Geol. Soc. India , Bangalore, Vol. 17, No. 1, P. 67-72, 1976.

Chaudhri, R. S., and Gill, G. T. S., Clay mineralogy of the Siwalik Group of Simla hills, North Western Himalaya. J. Geol. Soc. India, Vol.24, No.3, P.159-165, 1983.

Clark, S. P., and Jager, E., Denudation rates in the Alps from Geochronological and heat flow data. Am. J. Sci., Vol. 267, P. 1143-1160, 1969.

Cleamentz, D. M., Demaison, G. J., and Daly, A., Welsite geochemistry by programmed pyrolysis. O. T. C., Paper No. 3410, 1979.

Condie, K. C., Plate tectonics and crustal evolution, Fourth edition, printed and bound in Great Britain by the Bath Press, Bath, 282 P, 1997

Connan, J., Time-temperature relation in oil genesis. AAPG Bull.,Vol. 58, P. 2516-2521, 1974.

Copeland, P., Harrison, T. M., Hodges, K. V., Maruejol, P., Lefort, P., and Pecher, A., An early Pliocene thermal disturbance of the Main Central Thrust, Central Nepal: Implications for Himalayan tectonics. J. Geophy. Res., Vol. 96, No. B5, P.8475-8500, 1991.

Critelli, S. and Garzanti, E., Provenance of the Lower Tertiary Muree Red Beds (Hazara-Kashmir syntaxis Pakistan) and initial rising of the Himalayas. Sedim. Geology, Vol. 89, P. 265-284, 1994.

Crowley, K. D., Cameron, M., and Schaefer, R. L., Experimental studies of annealing of etched fission tracks in fluoraptite. Geochim. Cosmochim. Acta, Vol. 55, P. 1449, 1991.

Cummins, W. A., Graywacke in Lower Siwaliks, Simla Hills. Nature, Vol. 196, P. 1085, 1962.

Daniel, J. A., and Cole, G. A., VR of coals from the Heat Formation, Central Montana (Abst.). AAPG Bull., Vol. 67, P.1333, 1983.

Dass, B. K., Vanshnarayan, Nahan sandstones and its exfoliation, Nainital Distt., U.P., India. Geol. Mag., Vol. 108, P. 229-234, 1971.

Datta, A. K., Some observations on sedimentological and paleontological aspects of the Subathu and Lower Dharmsala sediments in the Simla Hils area and their bearing on the tectonic evolution of the foothill belt. Proc. 4th Sem. Him. Geol., Pub. Ctr. Adv. Stdy. Geol., Vol. 7, P. 23-30, 1970.

Dayal, R., and Chaudhri, R. S., Dicotyledonous leaf impressions from the Nahan Beds, North-west Himalayas. Cur. Sci.,Vol.36, P.181-182, 1967.

Demaison, G., and Moore, G. T., Anoxic environments and oil source bed genesis. Am. Assoc. Pet. Geol. Bull., Vol. 64, No. 8, P. 1179-1209, 1980.

Demaison, G. and Murns, R. J., Pertoleum geochemistry and basin evaluation. Am. Assoc. Pet. Geol. Memoir, 35, 426 P, 1984.

Dewey, J. F., Cande, S. and Pitman, W.C., Tectonic evolution of the India/Eursia collission zone. Ecol. Geol. Helv., Vol. 82, P. 717–734, 1989.

Dodson, M. H., Closure temperature in cooling geochronological and petrological systems. Contrib. Mineral. Petrol., Vol. 40, P. 259-274, 1973.

Dodson, M. H., Theory of cooling ages. In: E. Jager and J. C. Hunziker (eds.). Lectures in isotope geology, P. 194-202, 1979.

Dodson, M. H., Thermochronology. Nature, Vol. 293, P.606, 1981.

Dodson, M. H., and Mc Celland-Brown, Isotopic and paleomagnetic evidence for rates of cooling, uplift and erosion. In: N. J. Snelling (ed.)- The chronology of the geological record. Geol. Soc. Lond. Mem., Vol. 10, P. 315-325, 1985.

Doglioni, C., Foredeeps versus subduction zones. Geology, Vol. 22, P.271-274, 1994.

Donelick, R.A., Crystallographic oreientiation dependence of mean etchable fission track length in apatite; an impirical model and experimental observations. Am. Mineral., Vol. 76, P.83-91, 1991.

Dow, W. G., Kerogen studies and geological interpretation. J. Geochem. Exploration, Vol. 7, P.79-99, 1977.

Dow, W. G., Petroleum source beds on continental slopes and rises. Am. Assoc. Pet. Geol. Bull., Vol. 62, P. 1584-1606, 1978.

Duba, D., and William-Johnes, A. E., The application of illite crystallinity, organic matter reflectance and isotopic techniques to mineral exploration: A case study in Southwestern Gaspe, Quebec. Econ. Geol. ,Vol. 78, P. 1350-1363, 1983.

Duddy, I. R. and Gleadow, A. J. W., and Keene, J. B., Fission track dating of apatie and sphene from Paleogene sediments of Deep Sea Drilling Prject Leg 81, Site 555. In: Initial Reports of the Deep Sea Drilling Project, D. G. Roberts et al., (US Gov. Printing Office, Washington D. C.), Vol. 81, P. 725-729, 1984.

Duddy, I. R., Green, P. F. Hagerty, K. A., and Bray, R., Reconstruction of thermal history in basin modelling using apatite F-T-A. What is reall possible?. Exploration, 49-62, 1991.

Duddy, I. R. and Green, P. F., A thermal and structural framework for the Otway basin, S.E. Australia: An integrated kinetic approach using AFTA and vitrinite reflectance. AAPG Bull., Vol. 76, No. 17, P. 1098, 1992.

Duncan, W., Green, P. F., and Duddy, I. R., Source rock burial history and seal effectiveness: Key facets to understanding hydrocarbon exploration potential in the East and Central Irish Sea basins. AAPG Bull., Vol. 82, No. 7, P. 1401-1415, 1998.

Dunoyer De Segonzac, G., The transformation of clay minerals during diagenesis and low grade metamorphism. Sedimentology, Vol. 15, P. 281-348, 1970.

Durand, B., Kerogen-insoluble organic matter from sdimentary rocks, Ed. Technip, Paris, 519 P., 1980.

Durani, S. A., and Bull, R. K., Solid state nuclear track detection, Pergamon press, Oxford, 304 P., 1987.

Edelman, S. H., A critical review of tectonic process of continental margin oroges. Tectonophys. ,Vol. 91, P. 199-212, 1991.

England, S. P., and Molnar, P., Surface uplift, uplift, uplift of rocks, and exhumation of rocks. Geology, Vol. 18, P. 1173-1177, 1990.

Espitalie, J., Leporte, J. L., Madec, M., Marquis, F., Leplat, P., Poulet, T., and Boutefeu, A., Rapid method for source rock characterization and for evaluating their petroleum potential and their degree of evolution. Institute Francais du Petrole and Labofina S. A., Vol. 32, P. 13-34, 1977.

Espitalie, J., Madec, M., and Tissot, B., Role of mineral matrix in kerogen pyrolysis influenceof petroleum generation and migration. Am. Assoc. Petr. Geol. Bull.,Vol. 64, P. 55-66, 1980.

Esquevin, J., Influence de la composition chimique des illites sur leur crystallinite. Bull. Centre Rech. Pan, Vol. 3, P. 147-154, 1969.

Fiestmantel, O., Note on the remains of Palm leaves from the Tertiary Muree and Kasauli Beds in India. Record. Geol. Sur. India , Vol. 15, P. 51-53, 1982.

Fleischer, R. L., and Hart, H. R. Jr., Fission-rack dating: Techniques and problems in: W.W. Bishop, D.A., Miller and S. Cole (Eds). Proc. Burg Wartenstein Conf. on calibration of hominoid evolution, Scott. Acad. Press, Edinburg, P. 135-170, 1972.

Fleischer, R. L. and Price, P. B., Techniques for geologic dating of minerals by chemical etching of fission fragment tracks. Geochim. Cosmochim. Acta., Vol. 28, P. 1705-1714, 1964.

Fleischer, R. L., Price, P. B. and Walker, R. M., Tracks of charged particles in solid. Science, Vol. 149, P. 383-393, 1965 a.

Fleischer, R.L., Price, P.B. and Walker, R.M., Effects of temperature, pressure and ionization on the formation and stability of fission tracks in minerals and glasses. J. Geophys. Res., Vol.70, P.1497-1502, 1965 b.

Fleischer, R. L., Price, P. B., and Walker, R. M., Nuclear tracks in solids. Principles and applications, University of California Press. Berkely, 605 P, 1975.

Folk, R. L., and Ward, W. C., Brazose River bar: A study in the significance of grain size parameters. J. Sed. Petrology, Vol. 27, P. 3-26, 1957.

Folk, R. L., Perology of sedimentary rocks, Hemphil's Austin, Tex., 170 P., 1980.

Ganju, P. N., and Srivastava, V. K., Petrology of Dagshai sandstones near Barog (Simla Hills). Mahadevan Commomeration Volume, P. 138-147, 1961.

Ganju, P. N., and Srivastava, V. K., Occurenc of graywacke in the Lower Siwalik, Simla Hills. Nature,Vol. 194, P. 566-567, 1962.

Gansser, A., The geology of the Himalayas. Wiley-Inter Science, New York , 289 P., 1964.

Gansser, A., Ideas and problem on Himalayan geology. Proc. Seminar on geodynamics of the Himalay region, N.C.R.I., Hyderabad, P.97-103, 1973.

Gansser, A., The significance of the Himalayan suture zone. Techonophysics, Vol. 62, P. 37-52, 1980.

Garver, J. I., and Brandon, M. T., Erosional deposition of the British Columbia Goast ranges as determined from fission-track ages of deterital zircon from the Tofino basin, Olympic Peninsula, Washington. Geol. Soc. Am. Bull. ,Vol. 106, P. 1398-1412, 1994.

Gentner, W., Kleinmann, B., and Wagner, G. A., New K-Ar and fission track ages of impact glasses and tektites. Earth. Planet. Sci. Lett., Vol. 2, P. 83-86, 1967.

Gibbs, R. G., The geochemistry of the Amazon River system: Part I, the factors that control the salinity and the composition and concentration of the suspended solids. Geo. Soc. Am. Bull., Vol. 78, P. 1203-1232, 1967.

Gilbert, C. M., Sedimentary rocks in petrography by Williams, H., F. G. Turner and C. M. Gilbert, Freeman and Co., San Francisco, Calif., 406 P., 1955.

Gleadow, A. J. W., Anisotropic and variable track etching characteristics in natural sphene. Nucl. Track. Detection, Vol. 2, P. 105-118, 1978.

Gleadow, A. J. W., Fission track age of the KBS tuff and associated hominid remains in Northern Kenya. Nature, Vol. 284, P. 225-230, 1980.

Gleadow, A. J. W., Fission-track dating methods: What are the real alaternatives?. Nucl. Tracks., Vol. 5, No. ½, P.3-14, 1981.

Gleadow, A. J. W, and Duddy, I. R., Fission track dating and thermal history analysis of apatites from wells in the northwestern Canning basin. In: Purcell, P. G. (Ed.). the Canning basin Perth. Geological Society of Australia and the Petroleum Exploration Society of Australia, 377 P, 1984.

Gleadow, A. J. W., Duddy, I. R., and Lovering, J. F., Fission track analysis: A new tool for the evaluation of thermal histories and hydrocarbon potential. Aus. Petrl. Explor. Assoc. J., Vol. 23, P. 93-102, 1983.

Gleadow, A. J. W., Duddy, I. R., Green, P. F., and Lovering, J. F., Confined fission track lengths in apatite: A diagnostic tool for thermal history analysis. Contrib. Mineral. Petrol., Vol. 94, P. 405-415, 1986.

Gleadow, A. J. W., Hurford, A. J., and Quaife, R. D., Fission track dating of zircon: Improved etching techniques. Earth Planet. Sci. Lett., Vol. 33, P. 273-276, 1976.

Gleadow, A. G. W., and Lowering, J. F., Geometry factor for external detectors in fission track dating. Nucl. Track Detect., Vol. 1, P. 99-106, 1977.

Gopel, C., Allegre, C. J. and Hua-Xu, R., Lead isotopic study of the Xigatse ophiolite (Tibet): The problem of the relationship between migmatites (gabbros, dolerite, lavas) and tectonics (harzbrgites). Earth. Planet. Sci. Lett., Vol. 69, P. 301-310, 1984.

Green, P. F., Comparison of zeta calibration baselines for fission track dating of apatite, zircon, and sphene. Chem. Geol. (Isot. Geosc. Sect.), Vol. 58, P. 1-22, 1985.

Green, P. F., Duddy, I. R, Gleadow, A. J. W., and Lovering, J. F., Apatite fission-track analysis as a paleotemperature indicator for hydrocarbon exploration. In: N.D., Naeser and T.H., Mc. Cullon (Eds.), Thermal History of Sedimentary Basins- Methods and Case Histories. New York Springer-Verlag, P. 181-195, 1989.

Green, R. F., Duddy, I. R., and Bray, R. J., Early Tertiary heating in North West England: Fluids or buarial (or both), extended extract from Geofluids, 93, Held at Torque, England, May 4-7, P. 1-5, 1993.

Griffin, G. M., Regional clay facies- products of weahering, intensity, and current distribution in the Northeastern Gulf of Mexico. Geol. Soc. Am. Bull., Vol. 73, P. 737-768, 1962.

Grim, R. E., Dietz, R. S., and Bradley, W. F., Clay mineral composition of some sediments from the Pacific ocean of the California coast and the Gulf of California. Geol. Soc. Amer. Bull., Vol.60, P. 1785-1808, 1949.

Guidish, T. M., Kandell, C. G. St. C., Lerche, I., Toth, D. J., and Yarzab, R. F., Basin evolution using burial history, an overview. AAPG Bull., Vol. 69, No. 1, P. 92-105, 1985.

Guthrie, J. M., Houseknecht, D. W., and Johns, W. D., Relationships among vitinite reflectance, illite crystallinity and organic geochemistry in Carboniferous strata, Ouachita mountains, Oklahoma and Arkanzas. AAPG Bull., Vol. 70, No. 1, P. 26-33, 1986.

Hamet, J., and Allegre, C. J., Rb-Sr, systematics in granite from Central Nepal (Manaslu): Significance of the Oligocene age and high $^{87}Sr/^{86}Sr$ ratio in Himalayan orogeny. Geology,Vol. 4, P. 470-472, 1976.

Harlan, R. W., A clay mineral study of recent and Pleistocene sediments from Sigsbee Deep, Gulf of Mexico, Thesis, A and M Univ. of Texas, 40 P., 1966.

Harrison, T.M., Armstrong, R.L., Naeser, C.W., and Harakal, J.E., Geochronolgy and thermal history of the Coast Plutonic Complex, near Prince Rupert, British Columbia. Cand. J. Earth Sci., Vol. 16, P. 400-410, 1979.

Harrison, M., Copeland, P., Hall, S. A., Quade, J., Burner, S., Ojha, T. P., and Kidd, W. S. F., Isotopic preservation of Himalayan, Tibetan uplift, denudation, and climatic histories of two molase deposits. J. Geology, Vol. 101, P. 157-175, 1993.

Harrison, T.M., Copeland, P., Kidd, W. and An, Y., Rising Tibet. Science, Vol. 255, P.1663-1670, 1992.

Hedberg, H. D., Significanceof high wax oils with respect to genesis of petroleum. Am. Assoc. Pet. Geol. Bull., Vol. 52, P. 736-750, 1982.

Heim, A., and Gansser, A., Central Himalaya geological observations of Swiss Expedition, 1936, Mem. Soc. Helve. Sci. Nat., Gebruder Fretz, Zurich, Vol. 73, No.1, P.245, Repr. Hindustan Pub. Corp., Delhi, 1939.

Heroux, Y., Chagnon, A., and Bertrand, R., Compilation and correlation of major thermal maturation indicator. AAPG Bull., Vol. 63, No. 12, P. 2128-2144, 1979.

Hinckley, D. N., Variability in "crystallinity" values among the kaolin deposits of the Coastal Plain of Georgia and South Carolina. In: Clays, Clay Min. Proc. 11th Conf. (Edit. by E. Ingerson), P. 229-235, Pergamon Press, Oxford, 1963.

Hodges, K., Burchfiel, B. C., Chen, Z., Housch, T., Lux, D., Parrish, R., and Royden, L.H., Rapid Early Miocene tectonic unroofing of the metamorphic core of the Himalaya: Evience for the Qomolangma (Everest) region-Tibet. VII, Himalayan Workshop, Oxford, Abstr. P. 39-40, 1992.

Hodges, K. V., Hubbard, M. S., and Silverberg, D. S., Metamorphic constraints in the thermal evolution of the Central Himalayan orogen. Phil. Trans. Roy. Soc. Lond., A326, P. 257-280, 1988.

Hood, A., Gutjahr, C. C. M., and Heacock, R. L., Organic metamorphism and the generation of petroleum. AAPG Bull., Vol. 59, No. 6, P. 986-996, 1975.

Hunt, J. M., Petroleum geochemistry and geology, James Gilluy (edit.), P.328-369, W.H., Freeman and Company, 617 P, 1979.

Hurford, A. J., Cooling and uplift patterns in the Lepontine Alps South Central Switzerland and an age of vertical movement on the insubric fault line. Contrib. Miner. Petrol., Vol. 92, P. 413-427, 1986.

Hurford, A. J., Fitch, F. J., and Clark, A., Resolution of the age structure of the detrital zircon populations of two Lower Cretaceous sandstones from the Weld of England by fission track dating. Geol. Mag., Vol. 121, P. 269-277, 1984.

Hurford, A. J., and Gleadow, A. J. W., Calibration of fission track dating parameters. Nucl. Track detect., Vol. 1, P. 41-48, 1977.

Hurford, A. J., and Green, P. F., The zeta age calibration of fission tack dating. Isot. Geosc., Vol. 1, P. 285-317, 1983.

Hurford, A. J., and Hammerschmidt, K., Ar/ Ar and K/Ar dating of the Bishop and Fish Canyon tuffs: a calibration ages for fission track standards. Chem. Geol., (Isot. Geosc. Sect.), Vol. 58, P. 23-32, 1985.

Hurford, A. J., Hammerschmidt, K., Green, P. F., Carter, A., and Lux, D., Age of the Tardree rhyolite, co. Antrim: evidence for the timing of Lower Tertiary magmatism in northern Ireland (Unpublished manuscript).

Hurford, A. J., and Watkins, R. T., Fission track age of the tuffs of the Buluk Member, Northern Kenya: A suitable fission track age standard. Chem. Geol., (Isot. Geosc. Sect.), Vol. 66, P. 209-216, 1987.

Hurly, P. M., Heezen, B. C., Pinson, W. H., and Fairbairn, H. W., K-Ar age values in plagic sediments of the North Atlantic. Geochem. et Cosmochem. Acta., Vol. 27, P. 393-399, 1963.

Ingersoll, R. V., Bullard, T. F., Ford, R. L., Grimm, J. P., Pickle, J. D., and Saves, S. W., The effects of grain size on detrital modes: Test of the Gazzi-Dickinson point- counting method. J. Sedim. Petrol., Vol. 54, No. 1, P. 103-116, 1984.

Ingersoll, R. V., and Suczek, C. A., Petrology and provenance of Neogene sand from Nicobar and Bengal fans, DSDP sites 211and 218. J. Sed. Petrol. ,Vol. 49, P.1217-1228, 1979.

Ismail, F.T., Role of ferrous-iron oxidationin the alteration of biotite and its effects on the type of clay mineral formed in soils of arid and humid regions: Am. Mineral. Vol.54, P.1460-1466, 1969.

Jacob, M. B., Clay mineral changess in Antarctic deep sea sediments and Cenozoic climatic events. J. Sed. Petrology, Vol. 44, P. 1079-1086, 1974.

Jain, A. K., and Manickavasagam, R. M., Inverted metamorphism in the intra continental ductile shear zone during Himalayan collision tectonics. Geology, Vol. 21, P. 407-410, 1993.

Jain, A. K., and Manickawasagam, R. M., Reply to comment of Searle, M. P., Dransfield, M.W., and Johnson, M. R. W., On inverted metamorphismin the intracontinental ductile shear zone during Himalayan collision. Geology, Vol. 22, P. 91-92, 1994.

Johns, W. D., Grim, R. E., and Bradley, W. F., Quantitative estimation of clay minerals by diffraction methods. J. Sedim. Petrol., Vol. 24, P. 242-251, 1954.

Johnson, S. Y., Stratigraphy, age and paleogeography of the Eocene Chuckanut Formation, North West Washington. Cand. J. Earth Sci. , Vol., 21, P. 92-106, 1984.

Johnson, M. J., Howell, D. G., and Bird, K. J., Thermal maturity patterns in Alaska: Implications for tectonic evolution and hydrocarbon potential. AAPG Bull., V. 77, No. 11, P. 187-1903, 1993.

Johnson, N. M., Opdyke, N. D., Johnson, G. D., Lindsay, E. H., and Tahirkheli, R. A. K., Magnetic polarity stratigraphy and ages of Siwalik Group rocks of the Potwar Plateau, Pakistan. Palaeo. Palaeo. Palaeo.,Vol. 37, P. 17-42, 1982 a.

Johnson, G. D., Zeitler, P., Naeser, C. W., Johnson, N. M., Summers, D. M., Fost, C. D., Opdyke, N. D., and Tahirkheli, R. A. K.: The occurrence and fission track ages of late Neogene and Quaternary volcanic sediments, Siwalik Group, Northern Pakistan. Palaeo. Palaeo. Palaeo.,Vol. 37, P. 63-93, 1982 b.

Johnson, G. D., Opdyke, N. D., Tandon, S. K., and Nanda, N. C., The magnetic polarity stratigraphy of the Siwalik Group at Haritalyangar (India) and a new last appearance datum for Ramaphithecus and Sivapithecusin Asia. Palaeo. Palaeo. Palaeo., Vol. 44, P. 223-249, 1983.

Johnson, N. M., Stix, J., Tauxe, L., Cerveny, P. F., and Tahirkheli, r. A. K., Paleomagnetic chronology, fluvial process, and tectonic implications of the Siwalik deposits near Chinji village, Pakistan. J. Geol., Vol. 93, P. 27-40, 1985.

Kalkreuth, W., and Mc Mechan, M. E., Regional pattern of thermal maturation as determined for coal rank studies Rocky mountain foothills and front. Ranges North of Grand Cache, Alberta-Implications for petroleum exploration. Bull. of Canadian Petroleum Gelogy, Vol. 32, P. 249-271, 1984.

Kantsler, A. J., Smith, J. C., and Cook, A. C., Lateral and vertical rank variation: Implication for hydrocarbon exploration. APEA J., Vol. 18, P. 143-156, 1978.

Kasuya, M., and Naeser, C. W., The effect of a alpha damage on fission track annealing in zircon. Nucl. Tracks. Rad. Meas., Vol. 14, P.477-4 80, 1988.

Katz, B. J., Phelter, R. N., and Schunk, D. J., Interpretation of discontinuous VR-profiles. AAPG Bull., Vol. 72, No. 8, P.926-931, 1988.

Keller, W. D., Diagenesis in clay minerals- a review. In: Bradley, W. F., clay and clay minerals. Proc. Nat. Conf. New York, Macmillan Co., Vol.11, P. 136-157, 1963.

Keller, W. D., Environmental aspects of clay minerals. J. Sed. Pet. ,Vol. 40, P. 785-813, 1970.

Khan, I. B., Bridge, J. S., Kappelman, J., and Wilson, R., Evolution of Miocene fluvial environments, Eastern Potwar Plateau, N- Pakistan. Sedimentology, Vol. 44, P. 221-251, 1997.

Kharkwal, A. D., Ocurrence of coquinite in the Subathu Beds. Curr. Sci., Vol. 33, P. 750, 1964.

Kharkwal, A. D., Glauconite in the Subathu Beds (Eocene) of the Simla Hills of India. Nature, Vol. 211, P. 615-616, 1966.

Kharkwal, A. D., Petrological study of the Upper Siwalik near Chandigarh. Indian Mineralogist, Vol.10, P. 210-221, 1969.

Klootwijk, C.T., Sharma , M. L., Gergan, J., Tirkey, B., Shah, S. K., and Agarwal, V., The extent of greater India, II- Paleomagnetic data from the Ladakh intrusives at Kargil. Northwetern Himalaya. Earth. Planet. Sci. Lett., Vol. 44, P. 47-64, 1979.

Klootwijk, C.T., Conaghan, P.J., and Powell, C. Mc. A., The Himalaya arc: Large scale continental subduction, oroclinal bending and back arc spreading: Earth. Planet. Sci. Lett., Vol.75.P. 167-183, 1985.

Knuze, G.W., and Scafe, D. W., A clay mineral investigation of six cores from Gulf of Mexico. Marine Geology, Vol. 10, P. 69-85, 1971.

Kowallis, B. J., and Heaton, J. S., FT dating of bentonites and bentonitic mudstones from he Morrison Formation in Centeral Utah. Geology, Vol. 15, P. 1138-1142, 1987.

Kowallis, B. J., and Heaton, J. S., and Bringhunt, K., Fission track dating of volcanically derived sedimentary rocks. Geology, Vol. 14, P. 19-22, 1986.

Kraus, G. P., and Parker, K. A., Geochemical evaluation of petroleum source rock in Bonapart Gulf Timor Sea Regions, northwestern Australia. Am. Assoc. Pet. Geol. Bull., Vol. 63, P. 2021-2041, 1979.

Krishnan, M. S., Geology of India and Burma, Higginbothams (private) ltd., Madras, 604 P., 1960.

Krishnan, M.S., Geology of India and Burma. 6th edition, Published by Satish Kumar Jain for CBS Publishers and Distributors, 536 P, 1982.

Krishnaswamy, V. S., Jalot, S. P., and Shome, S. K., Recent crustal movements in the NW Himalaya and the Gangetic foredeep, and related pattern of saismisity. Proc. 4th Symp. Earthquake Engeering, Roorkee Univ., ROORKEE, India, P.414-439, 1970.

Krishnaswami, S., Lal, D., Prabhu, N., and Mac Dougall, D., Characteristics of fission tracks in zircon:applications to geochronology and cosmology. Earth Planet. Sci. Lett., Vol. 22, P. 51-59, 1974.

Krynine, P. D., Petrography and genesis of the Siwalik Series. Amer. J. Sci., Vol. 34, P. 422-446, 1937.

Krynine, P. D., Petrology and genesis of the Third Bradford Sand. Bull. Mineral Industries. Expetl. St. 29. Penn. State College, 1940.

Krynine, P. D., The tourmaline group in sediments. J. geology, Vol. 54, P. 65-87, 1946.

Krynine, P. D., The megascopy study and field classification of sedimentary rocks. J.Geol. Vol. 56, P. 130-165, 1948.

Kubler, B., La crystallinite de illite et les zones tout a fait superieres du metamorphisme. In: Etages tectoniques, a la Baconniere, Nenchatel, Suisse, 105-121, 1967.

Kubler, B., Evaluation quantitative du metamorhisme par la crystallinite de l'illite. Bull.Centre Rech. Pan. SNPA. 2, P. 385-397, 1968.

Kulbicki, G., and Millot, G., Diagenesis of clays in sedimentary and petroliferous series. Proc. of the Tenth National Conf. on clays and clay minerals, (ed. A. Swineford), 10, 329. Pergamon Press. London, 1963.

Kumar, K., Paleontological investigation of Subathu Vertebrates from Jammu and Kashmir, Gharwal Synform, Uttar Pradesh, India. J. Paleont. Soc. India, Vol. 28, P. 106-111, 1982.

Kumar, R., Fundamentals of historical geology and stratigraphy of India, Willey Eastern Limited Publication, third reprint, 254 P, 1992.

Kumar, D., Fission track zircon-apatite ages and exhumation of the Himalayan metamorphic belt (HMB) along Beas-Sutlej valleys, Himachal Pradesh, Unpublished Ph. D. thesis, Kurukshetra University, Kurukshetra (India), 86 P, 1999.

Kumar, R., Ghosh, S. K., Virdi, N. S., and Phadtare, N. R., Excursion guide: The Siwalik foreland basin (Dehra Dun-Nahan sector). Sp.Pub. No. 1, Wadia Institute of Himalayan Geology, Dehra Dun, 61 P, 1991.

Kumar, K., and Loyal, R. S., Eocene ichthyofauna from the Subathu Formation, NW Himalaya, India. J. Palaeontology Soci. India, Vol. 32, P. 60-84, 1987.

Kumar, K., and Loyal, R. S., and Srivastava, R., Eocene rodents from new localities in Himachal Pradesh, NW Himalaya, India: Biochronologic implications. J. Geol. Soci. India, Vol. 50, No.4, P. 461-474, 1997.

Lal, N., Solid state nuclear track detectors I: Track characteristics and formation mechanisms. Phy. Edu., Vol. 7, No. 4, P. 289-299, 1991.

Lal, N., Solid state nuclear track detectors II: Various sub-fields. Phy. Edu., Vol. 8, No.3, P. 311-319, 1992 a.

Lal, N., Solid state nuclear track detectors III: Applications in science and technology. Phy. Edu., Vol. 8, No. 4, P. 359-366, 1992 b.

Le Fort, P., Himalaya: the collided range present knowledge of the continental arc. Am. J. Sci., Vol. 275, P 1-44, 1975.

Le Fort, P., The Himalayan orogenic segments. In: A.M.C., Sengor (Edit.), Tectonic evolution of the Tethyan region, P. 289-386, 1989.

Lerche, I., and Kendall, C. G. St. C., Reply to discussion of Reaves, C.M., and Von Rosenberg, D.U. on the paper of Lerche et al., 1984 (see ref.). AAPG Bull., Vol. 60, No. 12, P. 2148-2149, 1985.

Lerche, I., Yarzab, R. F., and Kendall, C. G. St. C., Determination of paleoheat flux from VR data. AAPG. Bull., Vol. 68, No. 11, P. 1704-1717, 1984.

Lindholm, R. C., A practical approach to sedimentology, Allen & Unwin Inc., 277 P, 1987.

Lonergan, L., and Johnson, C., Reconstruction orogenic exhumation histories using synorogenic detrital zircons and apatites: an example from the Betic Cordillera, SE Spain. Basin Research, Vol. 10, P. 353-364, 1998.

Lyon-Caen, H., and Molnar, P., Gravity anomalies, flexural of Indian plate, and structure, support and evolution of Himalaya and Ganga basin. Tectonics, Vol. 4, P. 513-538, 1985.

Mahandroo, M. P. S., Geology of the Lower Tertiary rocks of Mandi-Sarkagat-Sundernagar near region (N.W. Himalaya). Doctorate thesis, Punjab Univ., Chandigarh, 1972.

Mathur, N. S., Biostratigraphy of the Subathu Beds (Eocene), Simla Hills. Unpublished Ph. D. thesis, Punjab Univ., Chandigarh, 314 P, 1969.

Mathur, N. S., Biostratigraphical aspects of the Subathu Formation, Kumaun Himalayan. Recent Researches in Geology, Vol. 5, P. 96-112, 1978.

Mc Bride, E. F., A classification of common sandstone classification. J. Sed. Petrology, Vol. 33, P. 664-669, 1963.

Mc Dougall, I., and Watkins, R.T, Age of hominoid-bearing sequence at Buluk, Northern Kenya. Nature, Vol. 318, P. 175-178, 1985.

Mc Dowell, F. W., and Keizer, R. P., Timing of Mid Tertiary volcanism in the Sierra Madre occidental between Durango City and Mazatlan, Mexico. Geol. Soc. Am. Bull., Vol. 88, P. 1479-1487, 1977.

Mc Kenzie, A. S., and Mc Kenzie, D., Isomerization and aromatization of hydrocarbony in sedimentary basins formed by extension. Geol. Mag., Vol. 120, No. 5, P. 417-470, 1983.

Mc Mahon, C. A., On the microscopic structure of some Sub-Himalayan rocks of Tertiary age. Rec. Geol. Surv. India, Vol. 16, No. 4, 1883.

Medlicott, H. B., On the geological structure and relations of the Southern portion of the Himalayan ranges between the rivers Ganges and Ravee. Mem. Geol. Surv. India, Vol.3, Part 2, P.11, 1864.

Mehta, Y. P., Thakur, A. K., Nand Lal, Shukla, B., and Tandon, S. K., 1993, Fission track age of zircon separates of tuffaceous mudstoness of the Upper Siwalik subgroup of jammu-Chandigarh sector of the Panjub Sub-Himalaya. Cur. Sci., Vol. 64, No. 7, P. 519-521, 1993.

Mehta, Y. P., Exhumation history of Mandi-Dalhouse-Bandal regions, NW Himalaya, Himachal Pradesh- A fission track study. Doctorate thesis, Kurukshetra Univ., 134 P, 1995.

Meigs, A. J., Burbank, D. W., and Beck, R. A., Middle Late Miocene (ca.10 Ma) formation of the Majn Boundary Thrust in the Weatern Himalaya. Geology, Vol. 23, P. 423-426, 1995.

Middleton, M. F., Tectonic history from vitrinite reflectance. Geophys. J.R. Astr. Soc., Vol. 68, P. 121-132, 1982.

Miller, D. S., Duddy, I. R., Green P. F., Hurford, A. J., and Naeser, C. W., Results of inter laboratory comparison of fission track age standards. Fission Track Workshop–1984. Nucl. Tracks,Vol. 10, No. 3, P. 383-391, 1985.

Misra, K.S., Himalayan transverse faults and folds and their parallelism with subsurface structure of North Indian Plains. Discussion. Tectonophys. , Vol. 56, P. 299-302, 1979.

Misra, R. C, and Vadiya, K. S., Petrography and sedimentation of the Siwaliks of the Tanakpur area, District Nainital, U. P., India. Indian Mineralogist, Vol 2, P. 7-35, 1961.

Molnar, P., Inversion of profiles of uplift rates for the geometry of dipslip faults at depth, with example from the Alps and the Himalaya. Ann . Geophy, ,5B, P. 663- 670, 1987.

Murray, H. H., Genesis of clay minerals in some Pennsylvanian shales of Indiana and Illinois: Proc. of the second national conference of clays and clay minerals. A. Swinefod (ed.): Nat. Acad. Sci. Nat. Res. Council, Washington, D. C., Publ. 327, P. 47-67, 1954.

Naeser, C. W., Thermal history of sedimentary basins: Fission track dating of subsurface rocks. In: P.A. Scholle and P.R., Schluger (eds.): Aspects of diagenesis. SEPM special Publication, Vol. 26, P. 109-112, 1979.

Naeser, C. W., The fading of fission tracks in the geologic environment-data from deep drill holes (Abs.). Nucl. Tracks, Vol. 5, P. 248-250, 1981.

Naeser, C. W., and Fliescher, R. L., The age of the apatite at Cerro de Mexico: a problem for fission track annealing corrections. Geophys. Res. Lett., Vol. 2, P. 67-70, 1975.

Naeser, C. W., and Forbes, R. B., Variation of fission track ages with depth in two deep drill holes. Eos.Trans.AGU, Vol. 57, P. 1-353, 1976.

Naeser, C. W., Izett, G. A., and Obradovich, J. D., Fission track and K-Ar ages of natural glasses. U. S. Geol, Surv. Bull., Vol. 1489, P. 1-31, 1980.

Naeser, C. W., Zimmerman, R. A., and Cebula, G. T., Fission track dating of apatite and zircon: an interlaboratory comparison. Nucl. Track., Vol. 5, P. 65-72, 1981.

Naeser, C. W., and Naeser, N. D., Fission track dating of Quaternary events. In: D.J. Easterbrook (ed.), Dating Quaternary Sediments. GSA Sepcial Paper, 227, P. 1-11, 1988.

Naeser, N. D., Naeser, C. W., and Mc Culloh, T. H., The application of fission track dating to the depositional and thermal history of rocks in sedimentary basins. In: N.D. Naeser and T.H., Mc Calloh (eds.), Thermal history of basins: methods and case histories: Berlin, Springer-Verlag, P. 157-180, 1989.

Naeser, N. D., Naeser, C. W., and Mc Culloh. T.H., Thermal history of rocks in Southern San Joaquin Valley, California: Evidence from fission track analysis. AAPG Bull., Vol. 74, No. 1, P. 13-29, 1990.

Najman, Y., Clift, P., Johnson, M. R. W., and Robertson, A. H. F., Early stage of foreland basin evolution in the Lesser Himalaya, N-India. In: Himalayan tectonics from Treloar, P.J. and Searle, M.P. (eds.). Geol. Soc. Sp. Publ., No. 74, P. 541-558, 1993.

Najman, Y. M. R., Enkin, R. J., Johnson, M. R. W., Robertson, A. H. F., and Baker, J., Paleomagnetic dating of the earliest continental Himalayan foredeep sediments: Implications for Himalayan evolution. Earth. Plant. Sci. lett., Vol. 128, P. 713-718, 1994.

Najman, Y. M. R., Pringle, M. S., Johnson, M. R. W., Robertson, A. H. F., and Wijbrans, J. R., Laser $^{40}Ar/^{39}Ar$ dating of single detrital muscovite grains from early foreland basin sedimentary deposits in India: Implications for early Himalayan evolution. Geology, Vol. 25, No. 6, P. 535-538, 1997.

Nakata, T., Active faults of Himalaya of India and Nepal. In: Tectonics of the Western Himalayas. L.L.,Malin Conico, and R.J., Lihic (eds.), Sacc. Pap. Geol. Soc. Am., Vol. 232, P. 243-264, 1989. In: Copeland et al., 1991, an Early Pliocene thermal distrubance of the Main Central Thrust, Centra Nepal, implications for Himalayan tectonics: J. Geophy. Res., Vol. 96, No.B5, P.8475 – 8500.

Nossin, J. J., Outline of the geomorphology of the Doon Valley, Northern U. P., India. Zeitschrift fur Geomorphologie, Vol. 12, P. 18-50, 1971.

Opdyke, N. D., Lindsay, E. H., Johnson, G. D., Johnson, N. M., Tahirkheli, R. A. K., and Mirza, M. A., Magnetic polarity stratigraphy and vertebrate paleontology of the Upper Siwalik subgroup of northern Pakistan. Palaeo. Palaeo. Palaeo., Vol. 27, P. 1-34, 1979.

Ower, J., Elements of geochemistry in petroleum exploration, North Wales. Robersten Research Institute, London, 1980.

Parkash, B., Sharma, R. P., and Roy, A. K., The Siwalik Group (molosse)-sediments shed by collision of continental plates. Sediment. Geol., Vol. 25, P. 127-159, 1980.

Patrait, P., and Achache, J., Indian Eurasia collision chronlogy has implications for crustal shortening and driving mechanism of plates. Nature, Vol. 31,P. 615-621, 1984.

Pettijohn, F. J., Sedimentary rocks, 3rd edition, Harper and Row, New York, 1975.

Philippi, G. T., On the depth, time and mechnism of petroleum generation. Geochim. Cosmochim. Acta., Vol. 29, P. 1021-1049, 1965.

Pollastro, R. M., and Barker, C. E., Application of clay mineral, vitrinite reflectance and fluid inclusion studies to the thermal and burial history of the Pinedale anticline, Green River Basin, Wyoming. SEPM Special Publication, 28, P. 73-83, 1986.

Pollastro, R. M., Clays. In: L. B. Morgan, ed., The petroleum system-status of research and methods. U.S. Geology Survey Bull., 1912, P. 28-31, 1990.

Price, L. C., Time as factor in organic metamorphism and use of VR as an absolute paleogeothermometer. AAPG Bull., Vol.66, P.519-520, 1982.

Price, L. C., Geologic time as a parameter in organic metamorphism and vitrinite reflectance as an absolute paleogeothermometer. J. Petrol. Geol., Vol. 6, P. 5-38, 1983.

Price, P. B., and Walker, R. M., Fossil tracks of charged particles in mica and the age of minerals. J. Geophy. Res., Vol. 68, No.16, P. 4847-4863, 1963.

Quigley, T. M., and Mc Kenzie, A. S., The temperature of oil and gas formation in sub-surface. Nature, Vol. 333, P. 549-552, 1988.

Rai, H., Geological evidence against the Shyok paleosuture, Ladakh, Himalaya: Nature, Vol. 297, P. 142-144, 1982.

Raiverman, V., Clay sedimentation in Subathu-Dharmsala Group of rocks in the foothills on NW-Himalays. Bull. Oil & Natural Gas Commission, Vol. 1, P. 27-35, 1964.

Raiverman, V., Petrography of the Tertiary sediments of Sarkaghat anticline in the Himalayan foothills of Himachal Pradesh, Pub. Ctr. Adv. Stdy. Geol., Vol. 5, P. 39-52, 1968.

Raiverman, V., Time series and stratigraphic correlation of Cenozoic sediments in foothills of Himachal Pradesh, Himalaya. Geology, Vol.2, P. 82-11, 1972.

Raiverman, V., Chakraborty, A., Goswami, V. N., and Kumar, S. P., Report on the geology of parts of Mandi, Bilaspur and Mehasu Districts, H. P., Field season 1960-1961, Rept. Oil Nat. Gas Comm. (Unpublished), 1961.

Raiverman, V., Kunte, S. V., and Mukerjea, A., Basin geometry, Cenozoic sedimentation and hydrocarbon prospects in North Western Himalaya and Indo-Gangetic plains. Petrol. Asia J., P. 67-92, 1983.

Raiverman, V., and Raman, K. S., Facies relations in the Subathu sediments, Simla hills, NW-Himalaya, India. Geol. Mag., Vol. 108, No. 4, P. 329-341, 1971.

Raiverman, V., and Seshavataram, B. T. V., On mode of deposition of Subathu and Dharmsala sediments in the Himalayan foothills in Punjab and Himachal Pradesh: Reprinted from Dr. D. N., Wadia,Commemorative Volume, Book of Geology, 833 P, Mining and Metalurgical Institute of India, P. 556-573, 1970.

Raiverman, V., Srivastava, A K., and Prasad, D. N., Structural style in Northern Himalayan foothills. Him. Geol., Vol. 15, P. 263-280, 1994.

Raju, A. T. R., Observations on the petrography of Tertiary clastic sediments of the Himalaya foothills of North India. Bull. Oil. Nat. Gas Comm., Vol. 4, P. 5-15, 1967.

Raju, A. T. A. and Dehadrai, P. V., Note on heavy mineral classification of Siwalik from Jammu and Punjab (India). Curr. Sci. Vol. 31, P. 378, 1962 a.

Raju, A. T. A. and Dehadrai, P. V., Clastic deposition of Siwalik sediments. Curr. Sci., Vol. 31, P. 494-495, 1962 b.

Raju, A. T. A. and Dehadrai, P. V., Upper Siwalik sedimentation in parts of Punjab. Quart. J. Geol. Min. Met. Soc. India, Vol. 34, P. 1-7, 1962 c.

Raman, K. S., and Ravi Shankar, Geology of parts of Ambala and Simla Districts, Punjab and Sirmur Districts, H. P., Field season 1962-1963, Rept. Oil Nat. Gas Comm. (Unpublished), 1963.

Rao, A. R., Neogene-Quaternary boundary in the Siwalik of Northwestern Himalayan foothills, India. J. Geol. Soc. India, Vol. 33, P. 95-103, 1989.

Sahni, B., Angiosperm leaf impressions from the Kasauli Beds, N.W., Himalaya. Palaeobotanis, Vol. 2, P. 83-87, 1953.

Sahni, An Eocene mammal from the Subathu-Dagshai transition zone, Dharampur, Simla Hills. Bull. Indian Geologists Assoc., Vol. 12, No. 2, P. 259-262, 1979.

Sahni, A., Bhatia, S. B., Hartenberger, J. L., Jager, J.J., Kumar, K., Sudre, J., and Vianey-Liaud, M., Vertebrate from the Subathu Formation and coments on thebiostratigraphy of Indian subcontinent during the Early Paleogene. Bull. Geol. Soc. Of France, Vol. 23, No. 6, P. 689-695, 1981.

Sahni, M. R., and Mathur, L. P., Stratigraphy of the Siwalik Group. Proc. Intl. Geol. Cong. 22nd Session (India), 1964.

Samanta, U., Baruah, A. K., and Mehrotra, L., Hydrocarbon potential of the Siwalik and Ganga basins- geochemists view. Himal. Geol.,Vol. 15, P. 329-333, 1994.

Sangode, S. J., Kumar, R., and Ghosh, S. K., Magnetic polarity stratigraphy of the Siwalik sequence of Haripure area (H. P.), NW Himalaya. J. Geol. Soci. India, P. 683- 704, 1996.

Sangode, S. J., Magnetostratigraphy and sedimentation history of the Siwalik foreland basin in Dehra Dun sector. NW Himalaya. Doctorate thesis, Wadia Institute of Himalayan Geology, Dehra Dun, 150 P, 1997.

Saxena M. N., Bhatia, S. B., and Pande, I. C., The Lower Siwaliks and the Graywacke problem. Res. Bull. Pb. Univ. N. S., Vol. 19, P. 255-259, 1968.

Schultz, L. G., Quantitative X-ray determination of some aluminous clay minerals in rocks. In: Clays, clay minerals. Proc. 7th Nat. Conf., Edit by E. Ingerson, PP. 216-224, Pergamon Press Oxford, 1960.

Schultz, L. G., Quatitative interpretation of mineralogical composition from X-ray and chemical data for the Pierre Shale. U. S. Geol. Surv., Prof., Pap. 391 C, 31 P, 1964.

Searle, M. P., Windley, B. F., Coward, M. P., Cooper, D. J. W., Rex, A. J., Tinglong, Li., Xuchang, Y., Jan, M. Q., Thakumr, V. C., and Kumar, S., The closing of Tethys and the tectonics of the Himalaya. Geol. Soc. Am. Bull.,Vol. 98, P. 678-701, 1987.

Sen, D. P., Early Tertiary deltaic sedimentation around Kalka and Nahan, Punjab Himalaya, India. Sedimentary Geology, Vol. 30, P. 291-310, 1981.

Shibaoka, M., and Benett, A. J. R., Patterns of diagenesis in some Australian sedimentary basins. APEA J., Vol. 17, P. 58-63, 1977.

Shibaoka, M., Benett, A. J. R., and Gould, K. W., Diagenesis of organic matter and occurrence of hydrocarbons in some Australian sedimentary basins. APEA J., Vol. 13, P. 73-80, 1973.

Shukla, S. D., and Verma, V. K., Sedimentological studies in a part of the Doon Valley, Garhwal Himalaya (U.P.). Him. Geol., Vol. 6, P. 338-364, 1976.

Sikka, D. B., Saxena M. N., Bhatia, S. B., and Jain, S. P., Ocurrence of Graywacke in the Lower Siwalik, Simla Hills. Nature, Vol. 192, P. 61, 1961.

Singh, H. N., Geology of the Simla Hills, Edit. Roy, B. C., and Jhingram, A. G., 17 P, 1964.

Singh, B. P., and Singh, H., Diagenetic influence and porosity pattern in the sandstones of Murree Group, Jammu Himalaya. Him. Geol., Vol. 15, P. 205-217, 1994.

Sinha, R. N., Heavy mineral investigation in the Siwaliks of Mohand, Distt. Saharanpur, U. P. J. Geol. Soc. India, Vol. 11, P. 163-177, 1970.

Srikantia, S. V., and Bhargava, O. N., Kakara Series- A new Paleocene Formation in Simla Hills. Bull. Geol. Soc. India, Vol. 4, No. 4, P. 114-116, 1967.

Srivastava, V. K., and Casshyap, S. M., Evolution of pre-Siwalik Tertiary basin of Himachal of Himalaya. J. Geol. Soc. India, Vol. 24, No. 3, P. 134-148, 1983.

Stach, D., Mackowsky, D. M. Th., Teichmuller, M., Taylor, G.H., Chandra, D., Teichmuller, R., Stach's text-book of coal petrology. Translation and english revision by Murchison, D.G.,Taylor, G.H. and Zierke, F., Published by Gebruder Borntraeger, Berlin, Stuttgart, 535 P, 1982.

Staplin, F. L., Sedimentary organic matter, organic metamorphism, and oil and gas occurrence. Bull. Cand. Pet. Geol., Vol. 17, P. 47-66, 1969.

Staudacher, Th., Jassberger, E. K., Dominik, B., Kirsten, T., and Schaeffer, O.A., $^{40}Ar/^{39}Ar$ ages of rocks and glasses from the Nordlinger ries crater and the temperature history of impact breccias. J. Geophys., Vol. 51, P. 1-11, 1982.

Steiger, R. H., and Jager, E., Subcommision on geochronology: Convention on the use of decay constant in geo-cosmochronology. Earth Planet. Sci. Lett., Vol. 36, P. 359-362, 1977.

Steven, T. A., Mehnert. H. H., and Obradovich, J.D., Age of volcanic activity in the San Juan mountains, Colorado. U.S. Geol. Surv. Prof. Papers, 575-D, P.D47-D55, 1967.

Storzer, D., and Selo, M., Toward a new tool in hydrocarbon resource evaluation: the potential of the apatite fission track chronothermometer, in B. Durand, Ed., Thermal phenomena in sedimentary basins, Paris, P. 89-110, 1984.

Suggate, R. P., Low rank sequence and scales of organic metamorphism. J. Petrol. Geol., Vol. 4, P. 377-392, 1982.

Sumii, T., Tagami, T., and Nishimura, S., Anisotropic etching character of spontaneous fission tracks in zircon, Nucl. Track Radiat. Meas., Vol. 13, P. 275-277, 1987.

Sweeney, J. J., and Burnham, A. K., Evaluation of a simple model of vitrinite reflectance based on chemical kinetics. AAPG Bull., Vol. 74 , No. 10, P. 1559-1570, 1990.

Tagami, T., Lal, N., Sorkhabi, R. B., Ito, H., and Nishimura, S., Fission track dating using external detector method: A laboratory procedure. Memoirs of the Faculty of Science, Kyoto University, Series of Geol. Mineral., Vol.L III, No.1& 2, P. 1-30, 1988.

Tan, Li-Ping, The metamorphism of Taiwan Miocene coals: Geol. Survey of Taiwan Bull., Vol.16, 44P, 1965.

Tandon, S. K., Pebble and grain fabric analysis of the Siwalik sediments around Ramnagar, Kumaun Himalayas. Him. Geol., Vol. 1, P.59-74, 1971.

Tandon, S. K., Mechanical analysis of Middle Siwalik sandstones from Ramnagar, Nainital Distt., Kumaun Himalayas. J. Geol. Soc. India, Vol. 13, P. 51-58, 1972 a.

Tandon, S. K., Observation on the matrix of Siwalik sediments of a part of Kumaun himalayas. Curr. Sci. Vol. 41, P. 192.193, 1972 b.

Tapponnier, P., et al. (29 authors), The subsidence of the India and Eurasia collision: Nature, Vol. 294, P. 405-410, 1981.

Tauxe, L., and Opdyke, N. D., A time framwork based on magnetostratigraphy for the Siwalik sedments of the Khaur area, Northern Pakistan. Palaeo. Palaeo. Palaeo., Vol. 37, P. 43-61, 1982.

Teichmuller. M., Teichmullerm, R. M., and Weber, K., Inkohlung und illite-kristallinite (vergleichende untersuchungen im Mesozo-ikum und Palaozoikum Von West Fallen). Fortschr. Geol. Rheint. West Fal., 27, P. 201-276, 1979.

Thakur, V., Physics and chemistry of the earth, Vol. 19, Parts I-VI, Geol.Western Himalaya, Pergamon Press Ltd., P. 1-366, 1993.

Thakur, A. K., and Lal, N., Determination of Zeta calibration factor for fission track dating of apatite, sphene and zircon. Ind. J. Pure appl. Phys., Vol. 31, P.241-250, 1993.

Theil, K., and Herr, W., The ^{238}U spontaneous fission decay constant redetermined by fission tracks. Earth Plant, Sci, Lett., Vol. 30, P. 50-56, 1976.

Tilley, B. J., Nesbitt, B. E., and Longstaffe, F. J., Thermal history of Alberta deep basin: Comparative study of fluid inclusion and VR data. AAPG Bull., Vol. 73, No. 10, P. 1206-1222, 1989.

Ting, F. T. C., Use of optical axis of vitrinite as an indicator of paleo and in-situ stresses in coal and coal-bearing strata. AAPG Bull., Vol. 66, P. 1176, 1982.

Tissot, B., The application of the results of organic geochemical studies in oil and gas exploration in g. B. Hobson, (Ed.), Development in petroleum geology-I, Applied Science, London, 335 P, 1971.

Tissot, B. P., Recent advances in petroleum geochemistry, applied to hydrocarbon exploration. AAPG Bull.,Vol. 68,No. 5, P. 545-563, 1984.

Tissot, B. P., and Espitalie, J., Thermal evolution of organic material in sediments: Application of a mathematical simulation. Revue De L' Inst. Fr. Pet., Vo. 30, P. 743-777, 1975.

Tissot, B.P., Pelet, R., and Ungerer, Ph., Thermal history of sedimentary basins, maturation indices and kinetics of oil and gas generation. AAPG Bull.,Vol. 71, No. 12, P. 1445-1466, 1987.

Tissot, B. P., and Welte, D. H., Petroleum formation and occurrence. New York, Springer, Verlag, 538 P, 1978.

Tissot, B. P., and Welte, D. H., Petroleum formation and occurrence. New York, Springer-Verlag, P. 601-604, 1984.

Todd, T. W., Petrology of Pennsylvanian rocks, Bighorn basin, Wyoming. Bull. Am. Assoc. Petrol. Geologists, Vol. 48, P. 1063-1090, 1964.

Treloar, P. J., and Coward, M. P., Indian plate motiona and shape: Constraints on the geometry of the Himalayan orogen. Tectonophys., Vol. 191, P. 189-198, 1991.

Tripathi, C., and Saxena S. P., Siwalik and origin of the Main Boundary Fault in relation to Tertiary orogeny. Proc, Nat. Sem, Tert, Orogeny, P. 137-152, 1987.

Unomah, G. I., and Ekweozor, C. M., Application of vitrinite reflectance in reconstruction of tectonic features in Anambra basin, Nigeria: Implication for petroleum potential. AAPG Bull., Vol. 77, No. 3, P. 436-451, 1993.

Valdiya, K. S., Himalayan transverse faults and folds and their parallelism with subsurface structure of North Indian plains, reply to S. Sinha Roy. Tectoniphysics, Vol. 56, P.299-303, 1979 a.

Valdiya, K. S., Himalayan transverse faults and folds and their parallelism with subsurface structures of North Indian plains- reply to S. Misra. Tectonophysics, Vol. 59, P. 302-303, 1979 b.

Valdiya, K. S., The two intracrustal boundary thrusts of the Himalaya. Tectonophysics, Vol. 66, P. 323-348, 1980.

Vemuri R., Practical notes on the semiquantitative analysis of clay minerals in sediments. Tech. Memo., Mc Master Univ., Canada, Tech. Memo. P. 67-69, 1967.

Verma, R. K., Mukhopahdya, M., and Roy, B. N., Seismotectonics of the Himalaya and continental plate convergence. Tectonophys., Vol. 42, P. 319-335, 1977.

Virdi, N. S., The floor of the Tertiary basin of Northwest India, Control of basement highs and paleo topogaphy on the basin evolution. Himal. Geol.,Vol. 15, P. 231-244, 1994.

Wadia, D. N., Geology of India. The English Language Book Society and MacMillan & Co. ltd., London, 532 P, 1966.

Wagner, G. A., Altershestimmungen an tektiten und undern naturlichen glasern mittels spuren der spontanen kernspaltung des Uran^{238} (fission track method). Z. Naturforschung, Vol. 21 a, P. 733-745, 1966.

Wagner, G. A., and Van Den Haute, P., Fission track dating. Published by Ferdinand Enke, Verlag, 285 P, 1992.

Walker, G. F., Vermiculities. In: J.W. Gieseking (Editor), Soil component. Vol.2, Inorganic Components, Springer-Verlag, P. 155-190, 1975.

Waples, D. W., Time and tempeature in petroleum formation: Application of Lopatin's method to petroleum exploration. AAPG Bull., Vol. 64, No. 6, P. 916-926, 1980.

Waples, D. W., Organic geochemistry for exploration geologists. Minneapolis, Minesota, Murgess Publishing, 151P, 1981.

Waples, D. W., Geochemistry in petroleum exploration, Ed., International Human Research Development Corporation, Boston, 232 P, 1985.

Weaver, C. E., Geological interpretation of argillaceous Sediments, Pt, I: Origin and significance of clay minerals in sedmentary rocks. Bull. Amer. Assoc. Petrol. Geol., Vol. 42, P. 254-271, 1958.

Weaver, C. E., Possible use of clay minerals in search for oil. Amer. Assoc. Pertol. Geol. Bull., Vol. 44, P. 1505-1518, 1960.

Weaver, C. E., Clay minerals of the Ouactita structural belt and adjacen foreland: The Ouachita system. Flawn, P.T. Goldstein, Jr.A., Kindg,P.B.,and Weaver,C.E., U.S. Texas, Pub., No. 6120, P. 147-162, 1961.

Weaver, C. E., The sinificance of clay minerals in sediments. In: Fundamental aspects of petroleum geochemistry, Elsevier Publ. Co. Amsterdam, P. 37-76, 1967.

Weaver, C. E., and Associates, Developments in petrology, 10: Shale-slate meramorphism in Southern Appalachians, Elseiver Publication, 238 P, 1984.

Weaver, C. E., Developments in sedimentology, 44: Clays, muds and shales, Elsevier Science Publisher B.V., 819 P, 1989.

Weir, A. H., Ormerod, E.C., and El-Mansey, M. I., Clay mineralogy of sediments of the western Nile Delta. Clay Mineralogy, Vol. 10, P. 369-386, 1975.

Welte, D. H., Relationship between petroleum and source rock. Am. Assoc. Pet. Geol. Bull., Vol. 49, P. 2246-2268, 1965.

Williams. I.S., Tetly, N. W., Compston, W., and Mc Dongall, I., A comparison of K-Ar and Rb-Sr ages of rapidly cooled igneous rocks: Two points in the Paleozoic time scale re-evaluated. J. Geol. Soc. Lond., Vol.139. P.557-568, 1982.

Winkler, H.G.F, Petrogenesis of metamorphic rocks, Springer-Verlag, N.Y., 348 P, 1979.

Yim, W. W. S., Gleadow, A. J. W., and Van Moort, J. C., Fission track dating of alluvial zircons and heavy mineral provenance in Northeast Tasmania. J. Geol. Soc. Lond. ,Vol. 142, P. 351-356, 1985.

Zaleh, M.J., Fluvial and lacustrine paleoenvironments of the Miocene Siwalik Group, Khaure area, Northern Pakistan. Sedimentology, Vol. 44, P. 349-368, 1997 a.

Zaleh, M.J., Intra and extrabasinal controls on fluvial deposits in the Indo-Gangetic foreland basin, Northern Pakistan. Sedimentology, Vol. 44, P. 369-390, 1997 b.

Zietler, P. K., Johnson, N. M., Naeser, C. W., and Tahir Kheli, R. A. K., Fission track evidence for Qaternary uplift of the Nanga Parbat region, Pakistan. Nature, Vol. 298, P. 255-257, 1982.

Zeitler, P. K., Johnson, N. M., Briggs, N. D., and Naeser, C. W., Uplift history of the NW Himalaya as recorded by fission track ages on detrital Siwalik zircons. In: H. Jiqing, Ed.: Symposium on Meassoic and Cenozoic Geology Proceedings, Beijing, China; Geological Publishing Houses, P. 481-494, 1986.

Zimmermann, R. S., The interpretation of apatite fission track ages with an application to study of uplift since the Cretaceous in Eastern North America. Ph.D., Dissertation, 146 P. Univ. of Pennsylvania , Philadelphia, 1977.

Zimmermann, R. A., and Gains, A. M., A new approach to the study of fission track fading. In: R.E. Zartman (edit.), Short Papers of the Fourth Intern.Conf. on Geoch., Cosmoch., and Isotopgeol. USGS Open file Report, 78-701, P. 467-468, 1978.

Appendix

Appendix-I

Clay mineral difractograms of shales and sandstone's matrix of various Cenozoic sediments of the present area. Symbols are such as text. O-ordinary, G-glycolated, H-heated mounts. A-Subathu shale (A_s for sandstone), B-Dagshai (B_s for sandstone), C-Kasauli shale (C_s for sandstone), D-Lower Siwalik shale (D_s for sandstone) samples. Numbers are sample reference no.

Appendix-II

Flow chart of TOC determination

Appendix-III

The procedure of preparation of samples for Vitrinite Reflectance (VR_o) study

Appendix-I: clay mineral difractograms

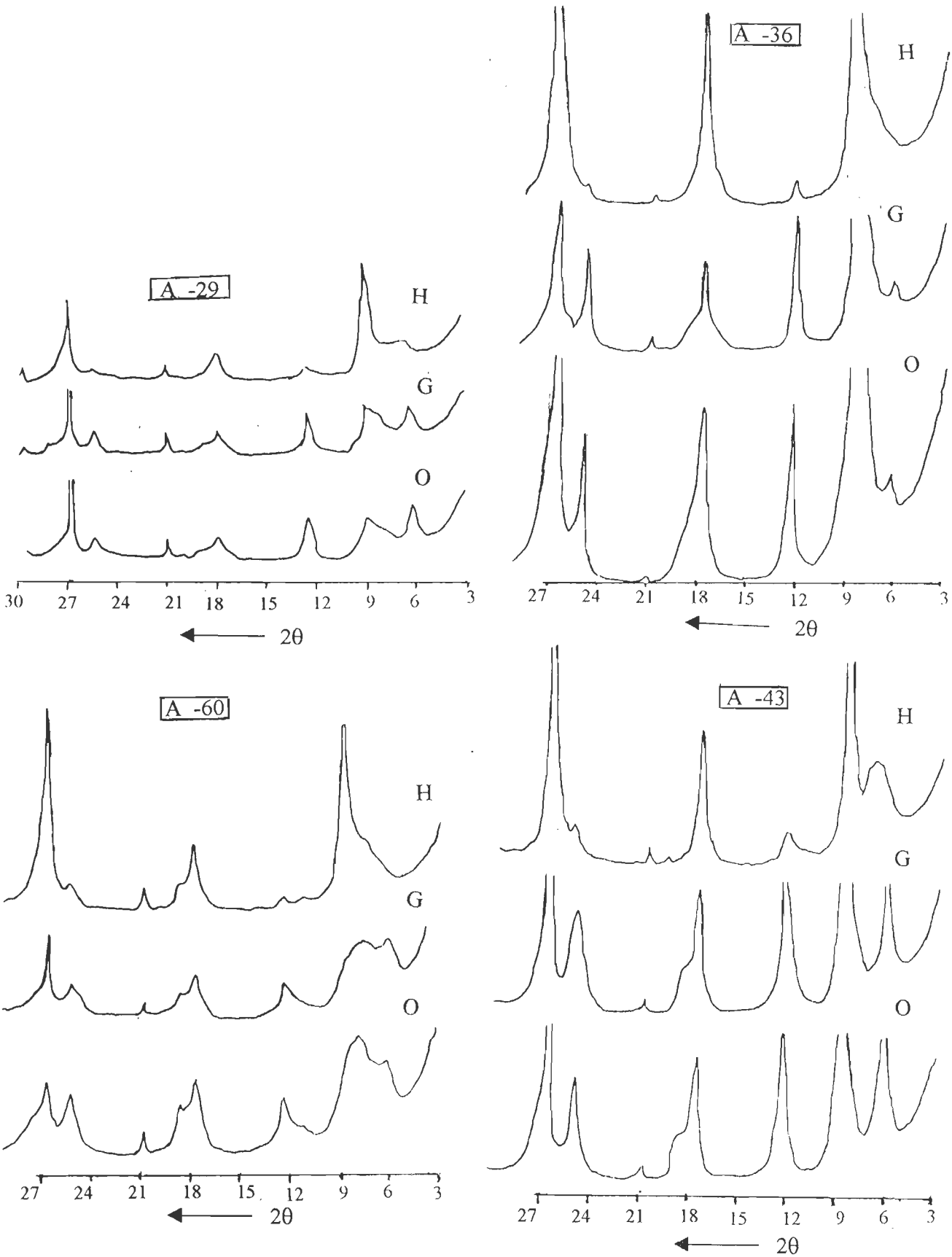

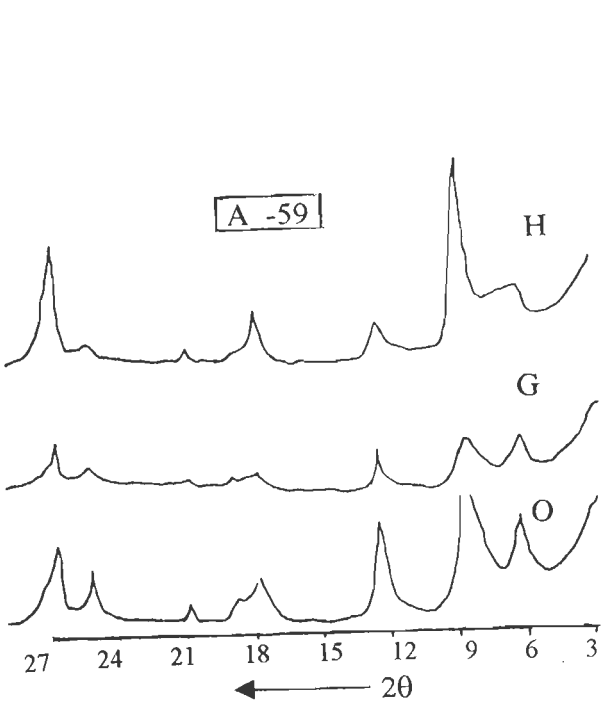
A -59
H
G
O
27 24 21 18 15 12 9 6 3
2θ

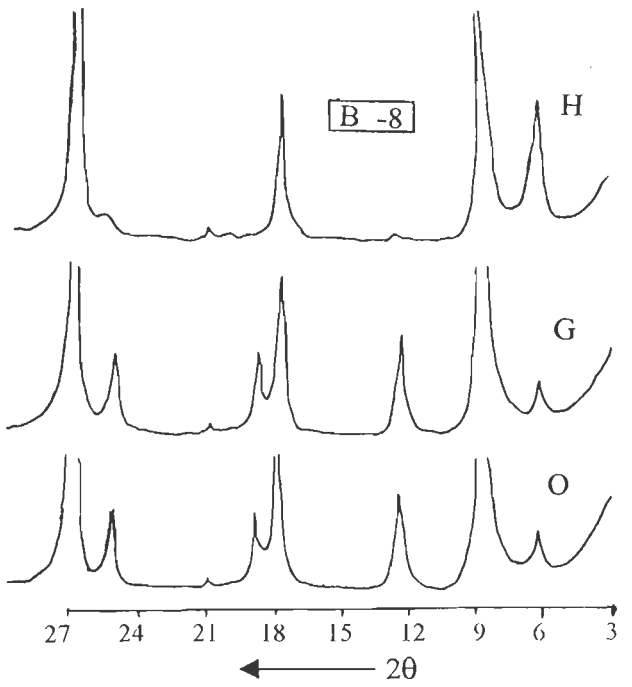
B -8
H
G
O
27 24 21 18 15 12 9 6 3
2θ

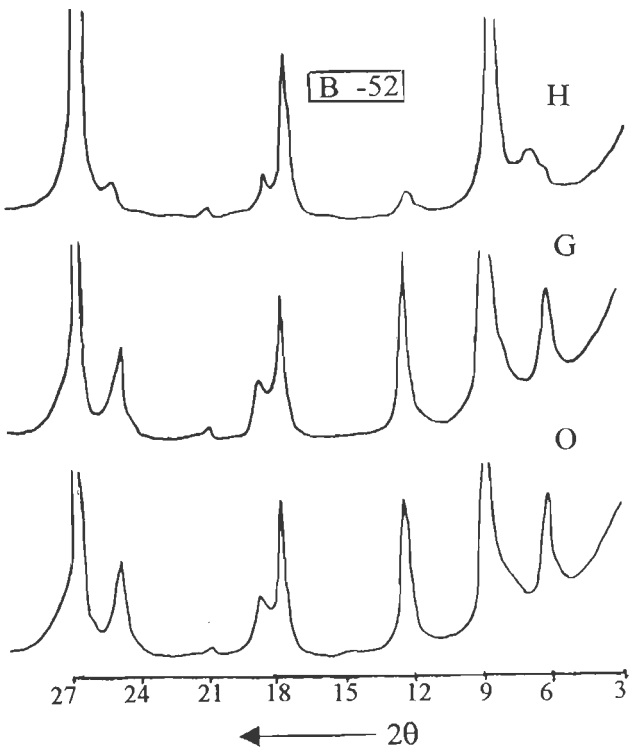
B -52
H
G
O
27 24 21 18 15 12 9 6 3
2θ

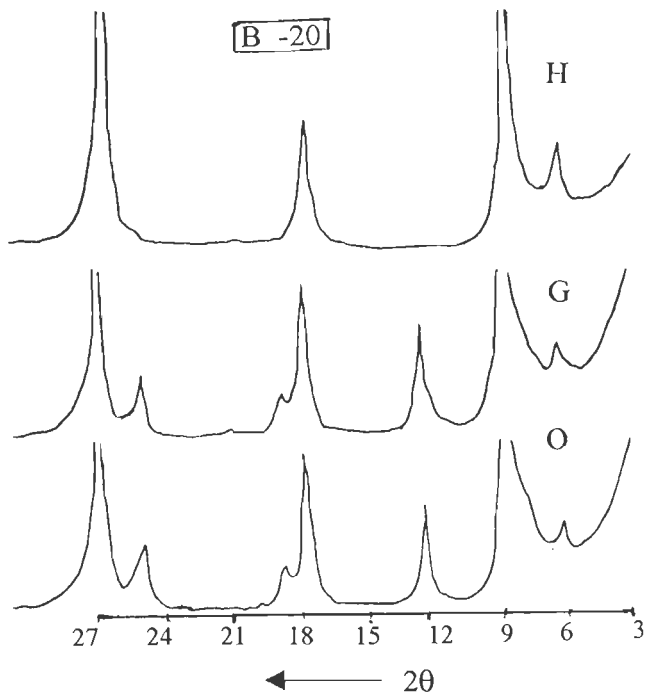
B -20
H
G
O
27 24 21 18 15 12 9 6 3
2θ

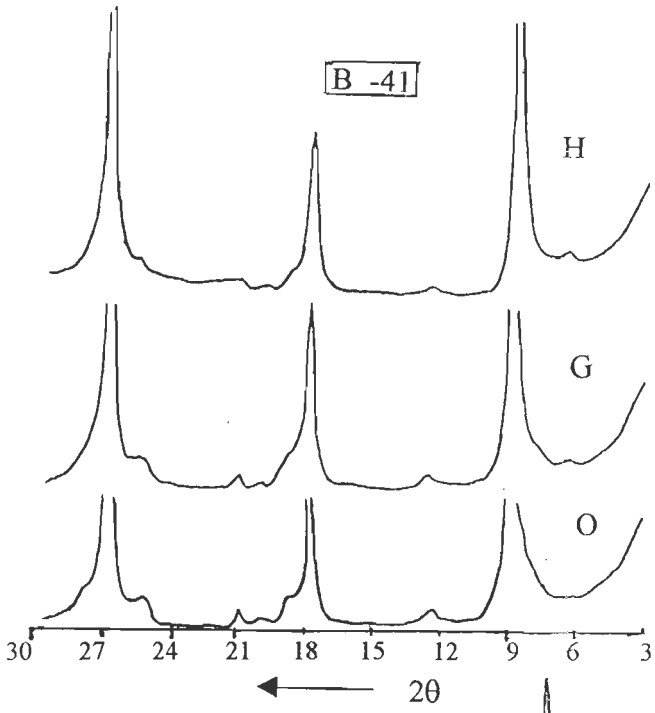
B -41
H
G
O
30 27 24 21 18 15 12 9 6 3
2θ

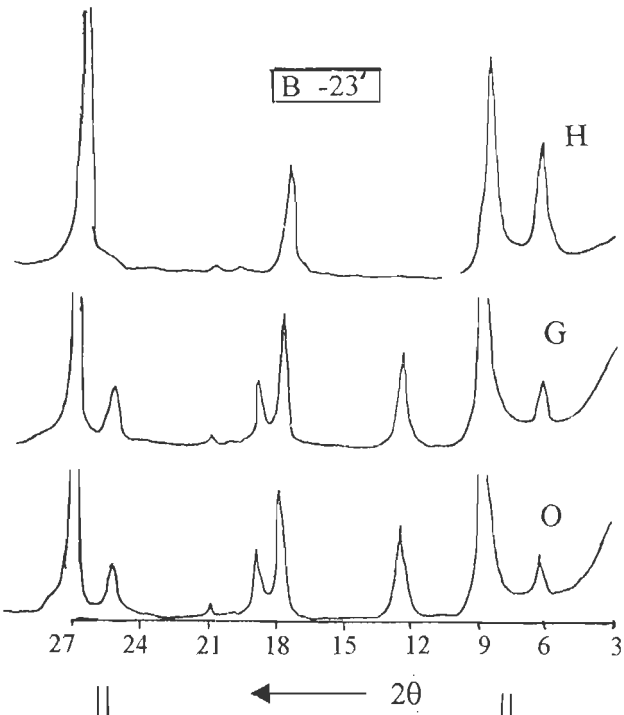
B -23'
H
G
O
27 24 21 18 15 12 9 6 3
2θ

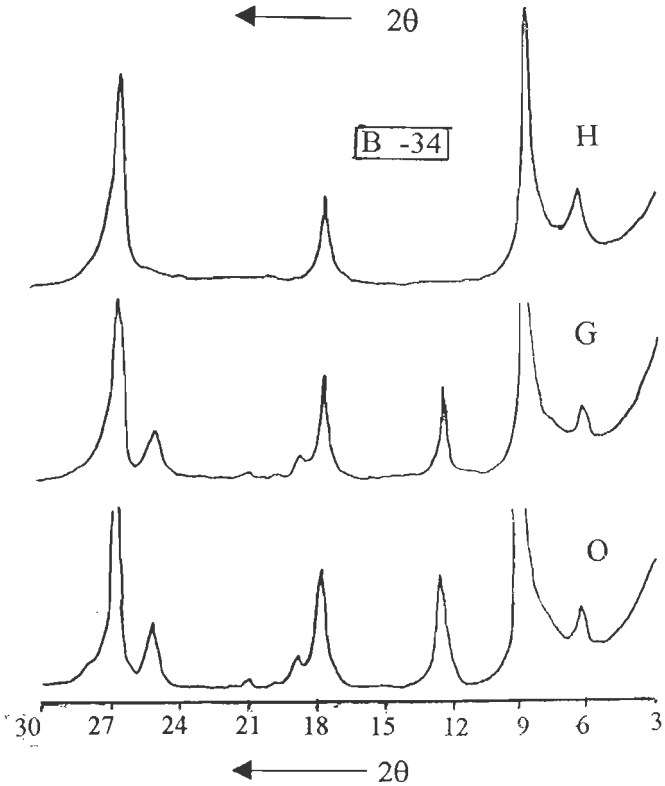
B -34
H
G
O
30 27 24 21 18 15 12 9 6 3
2θ

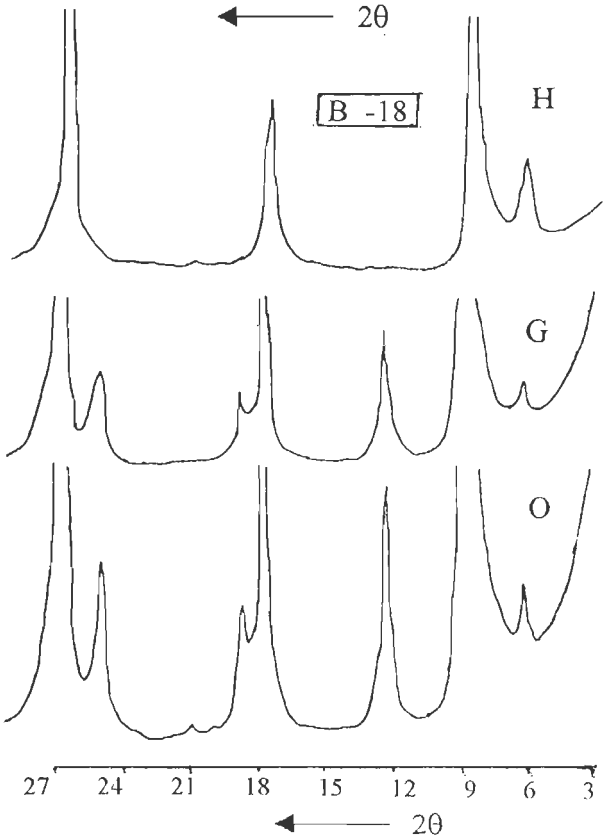
B -18
H
G
O
27 24 21 18 15 12 9 6 3
2θ

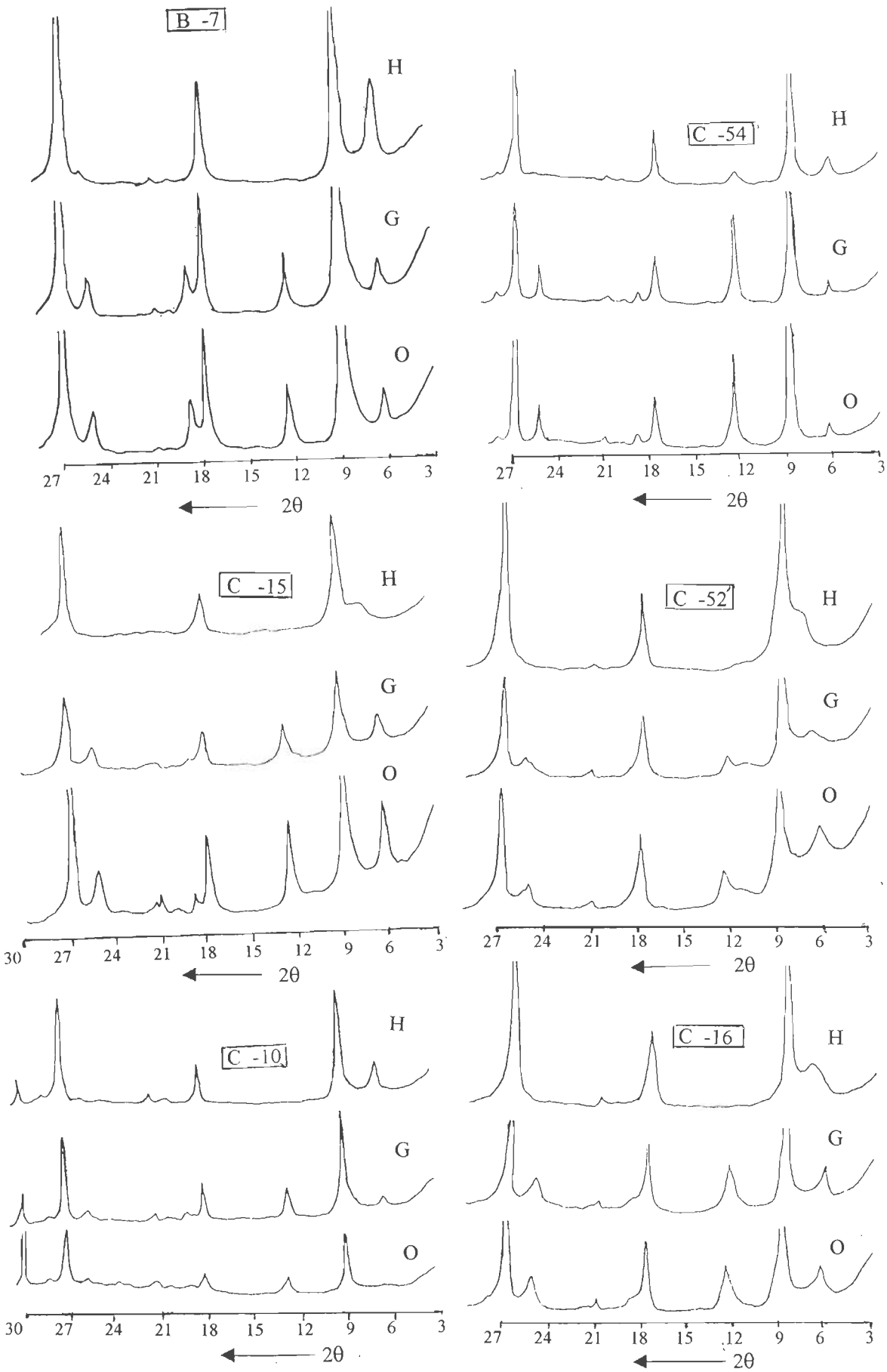
B -7
H
G
O
27 24 21 18 15 12 9 6 3
2θ
C -54
H
G
O
27 24 21 18 15 12 9 6 3
2θ
C -15
H
G
O
30 27 24 21 18 15 12 9 6 3
2θ
C -52
H
G
O
27 24 21 18 15 12 9 6 3
2θ
C -10
H
G
O
30 27 24 21 18 15 12 9 6 3
2θ
C -16
H
G
O
27 24 21 18 15 12 9 6 3
2θ

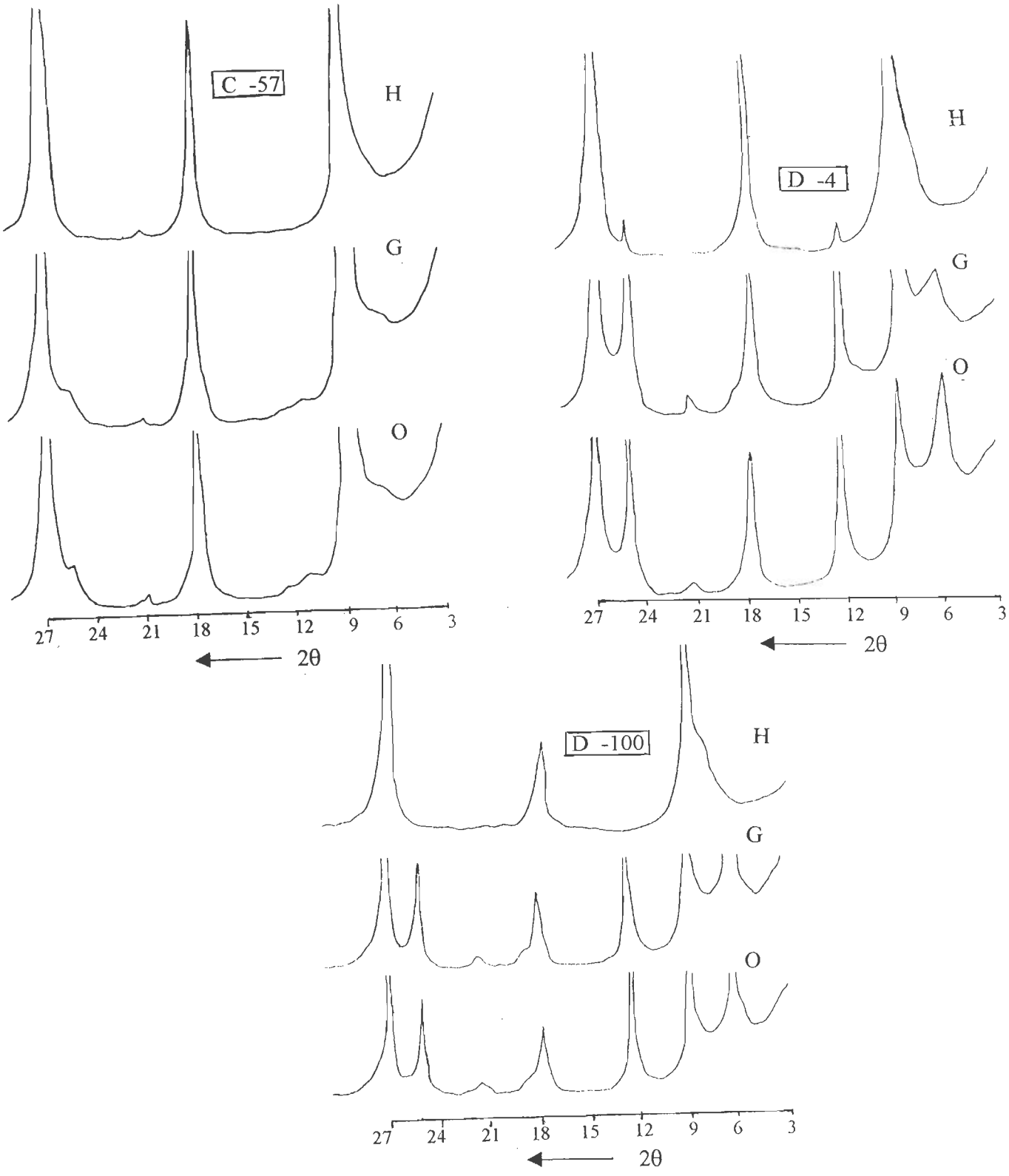
C -57
H
G
O
27 24 21 18 15 12 9 6 3
2θ
D -4
H
G
O
27 24 21 18 15 12 9 6 3
2θ
D -100
H
G
O
27 24 21 18 15 12 9 6 3
2θ

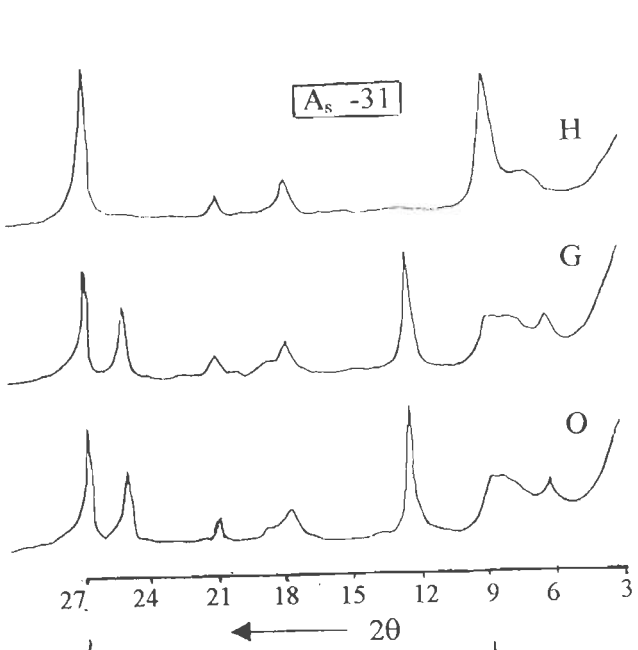
As -31
H
G
O
27 24 21 18 15 12 9 6 3
2θ

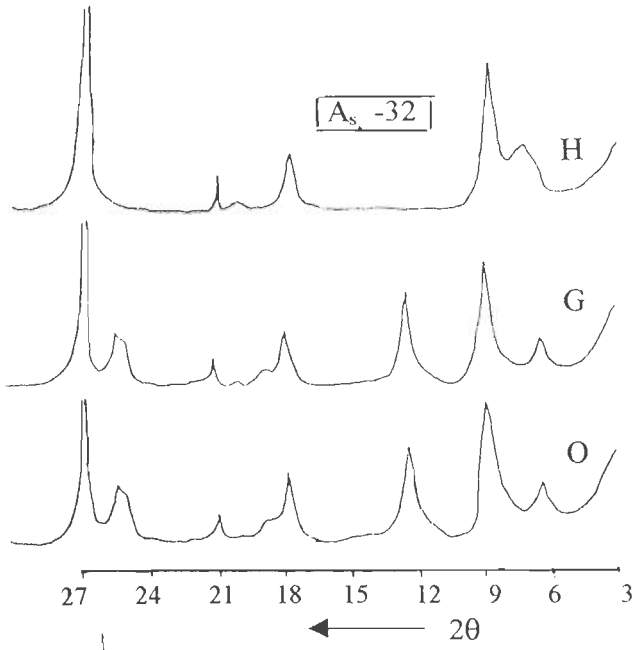
As -32
H
G
O
27 24 21 18 15 12 9 6 3
2θ

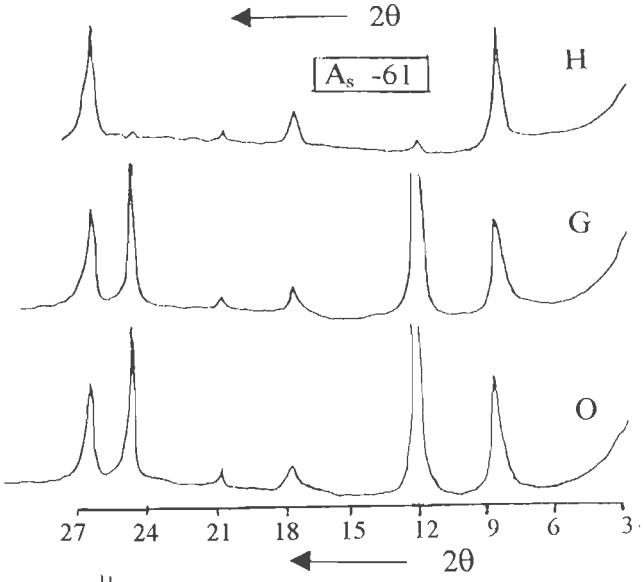
As -61
H
G
O
27 24 21 18 15 12 9 6 3
2θ

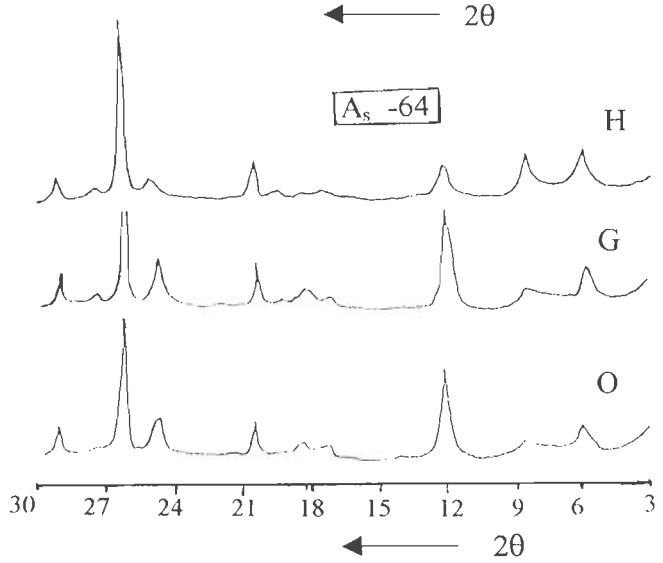
As -64
H
G
O
30 27 24 21 18 15 12 9 6 3
2θ

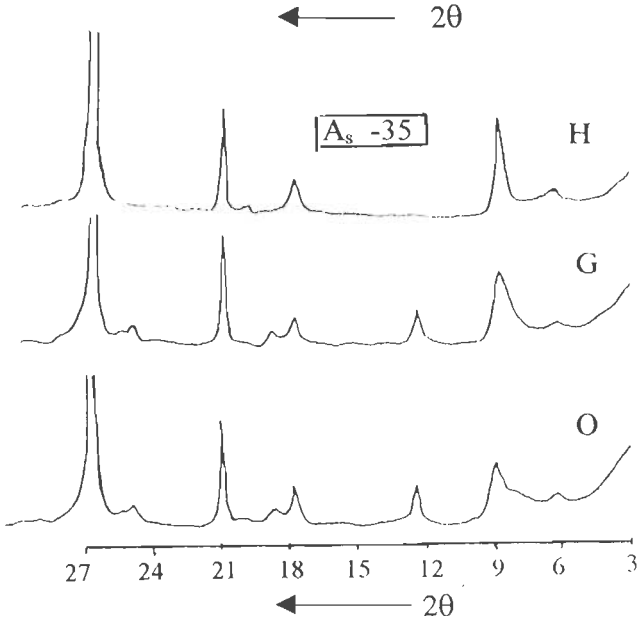
As -35
H
G
O
27 24 21 18 15 12 9 6 3
2θ

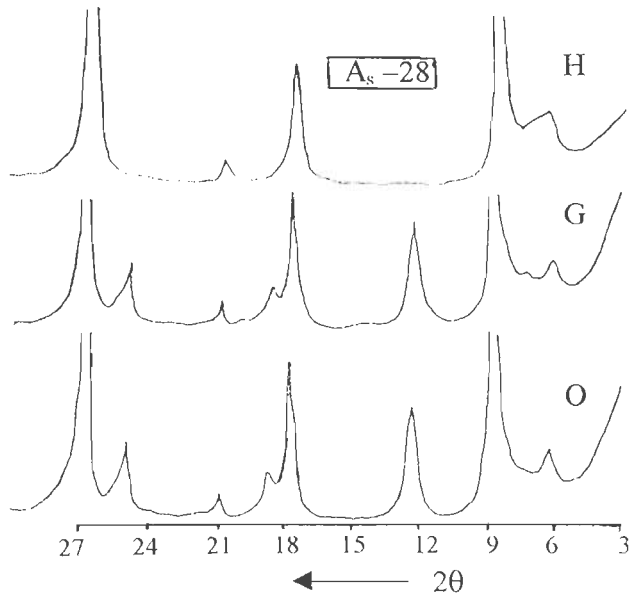
As -28
H
G
O
27 24 21 18 15 12 9 6 3
2θ

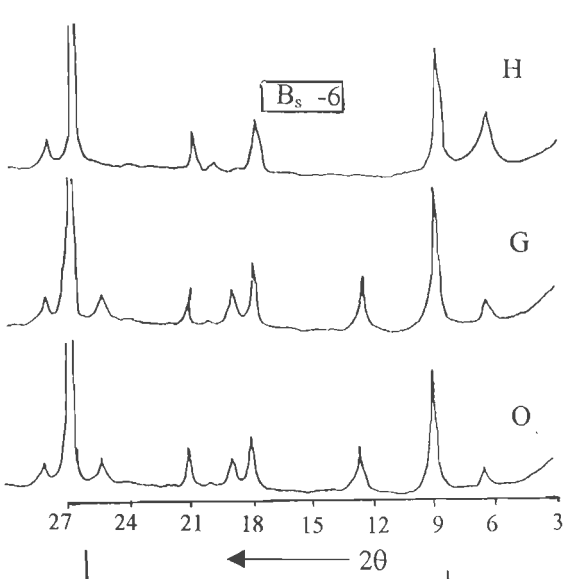
Bs -6
H
G
O
27 24 21 18 15 12 9 6 3
2θ

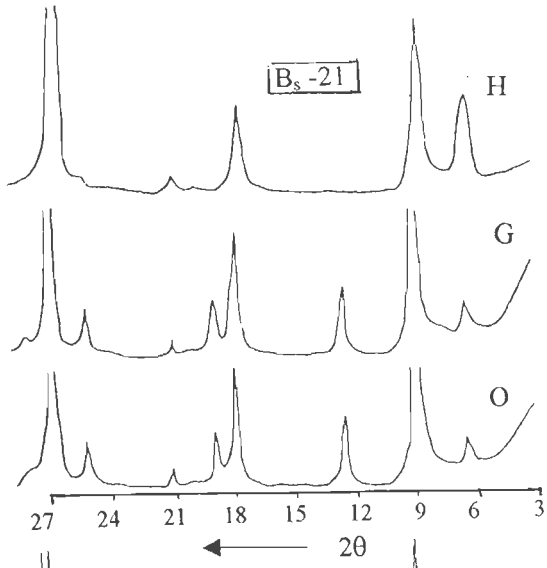
Bs -21
H
G
O
27 24 21 18 15 12 9 6 3
2θ

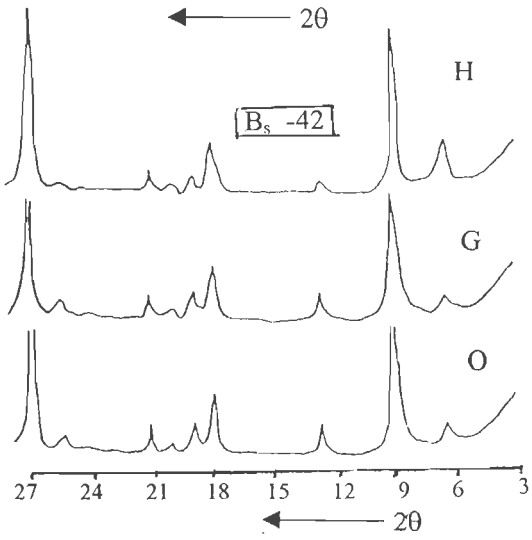
Bs -42
H
G
O
27 24 21 18 15 12 9 6 3
2θ

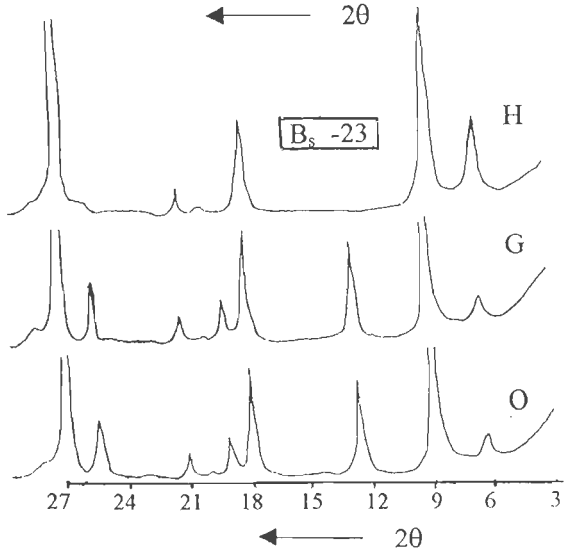
Bs -23
H
G
O
27 24 21 18 15 12 9 6 3
2θ

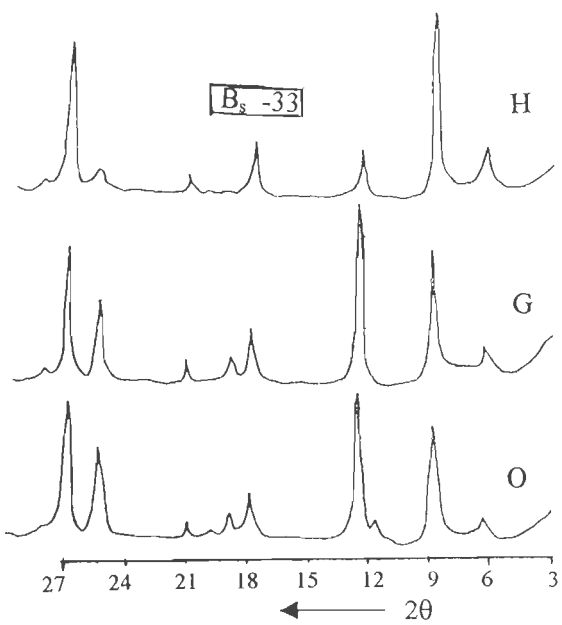
Bs -33
H
G
O
27 24 21 18 15 12 9 6 3
2θ

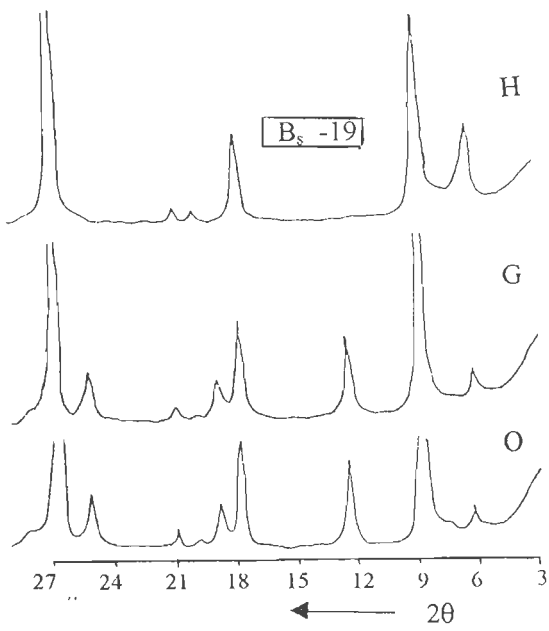
Bs -19
H
G
O
27 24 21 18 15 12 9 6 3
2θ

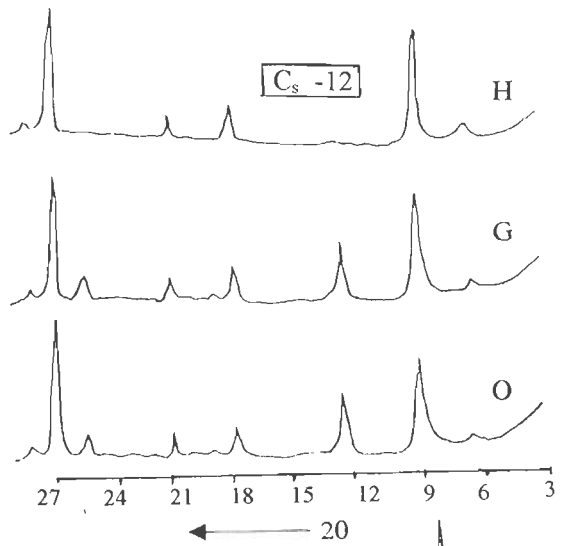
Cs -12
H
G
O
27 24 21 18 15 12 9 6 3
2θ

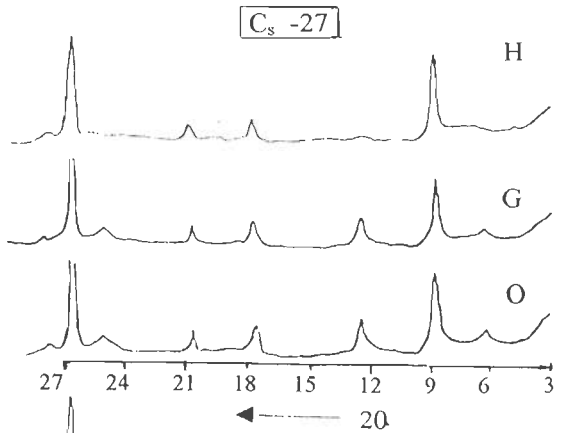
Cs -27
H
G
O
27 24 21 18 15 12 9 6 3
2θ

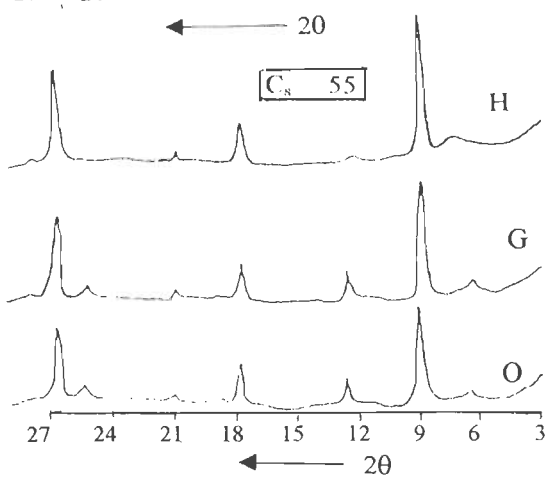
Cs 55
H
G
O
27 24 21 18 15 12 9 6 3
2θ

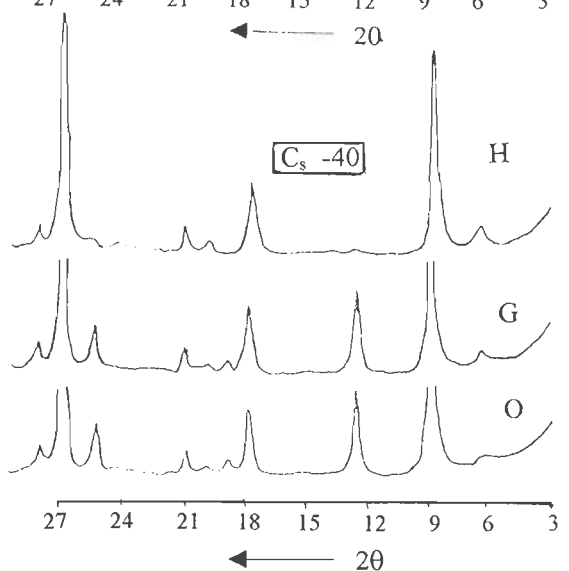
Cs -40
H
G
O
27 24 21 18 15 12 9 6 3
2θ

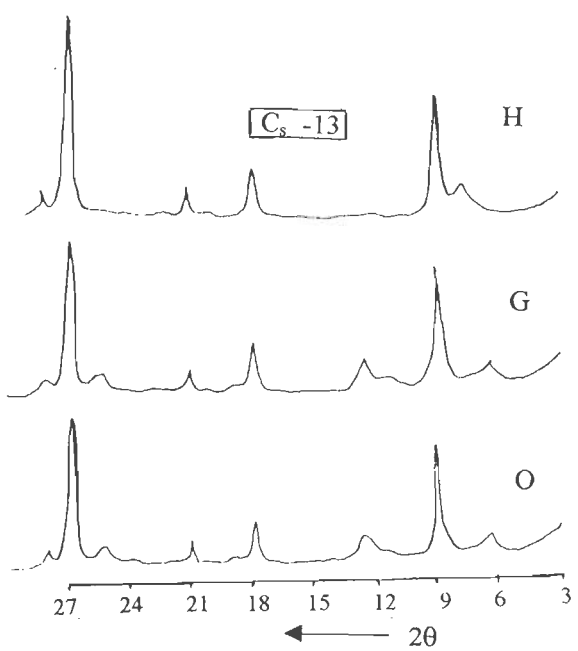
Cs -13
H
G
O
27 24 21 18 15 12 9 6 3
2θ

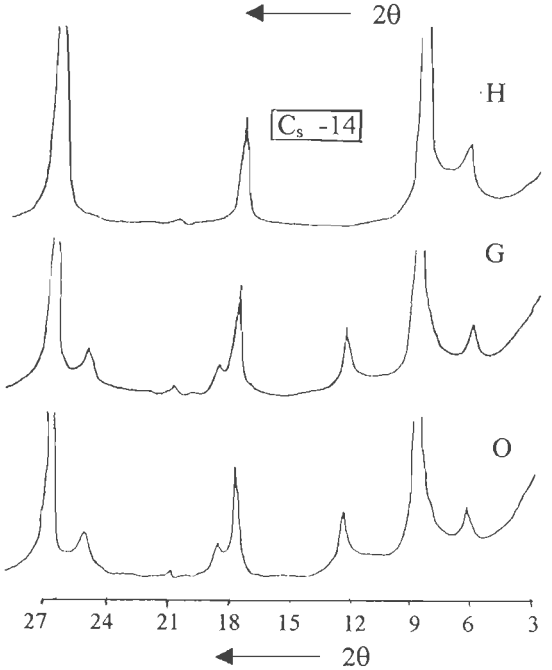
Cs -14
H
G
O
27 24 21 18 15 12 9 6 3
2θ

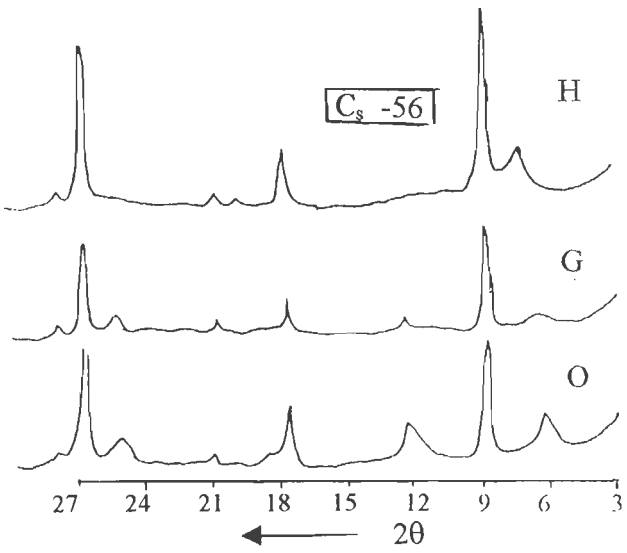
Cs -56
H
G
O
27 24 21 18 15 12 9 6 3
2θ

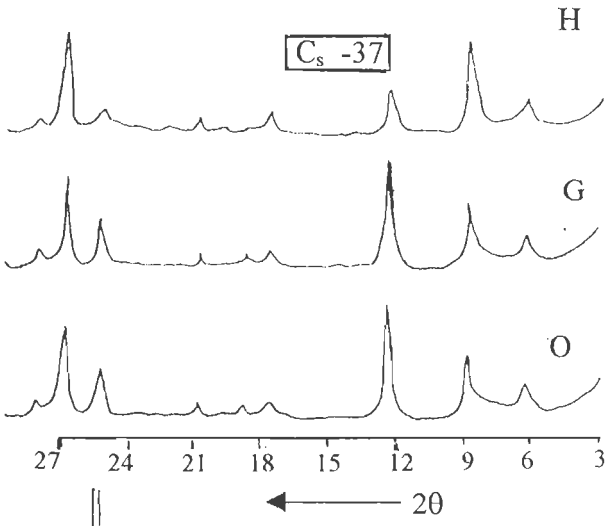
Cs -37
H
G
O
27 24 21 18 15 12 9 6 3
2θ

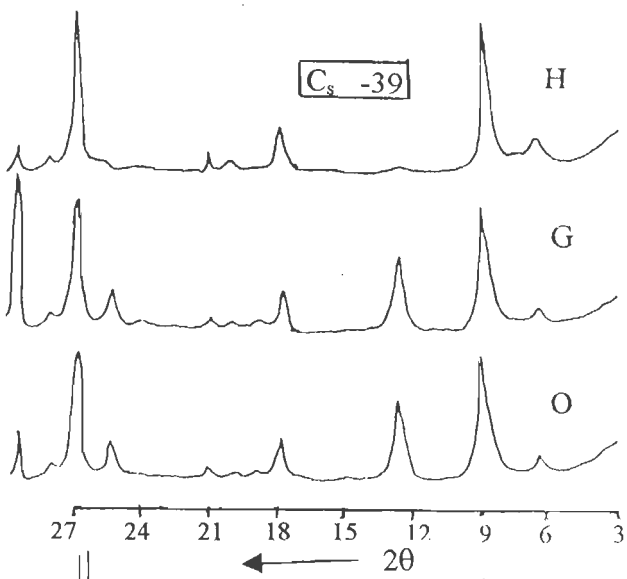
Cs -39
H
G
O
27 24 21 18 15 12 9 6 3
2θ

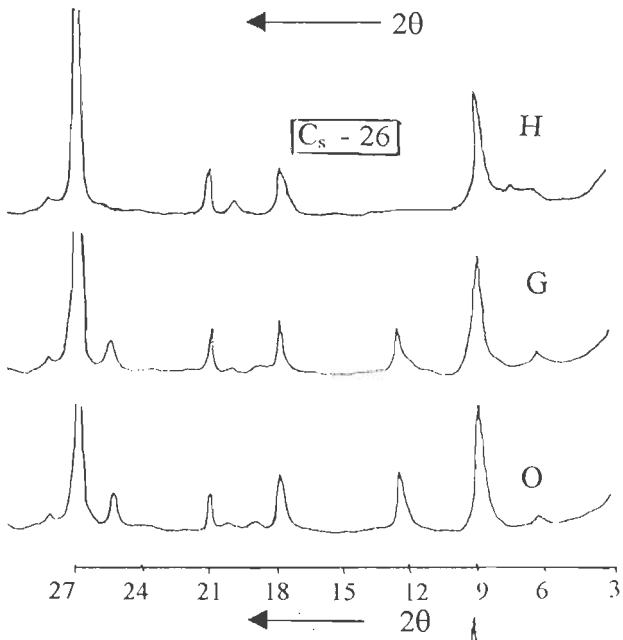
Cs - 26
H
G
O
27 24 21 18 15 12 9 6 3
2θ

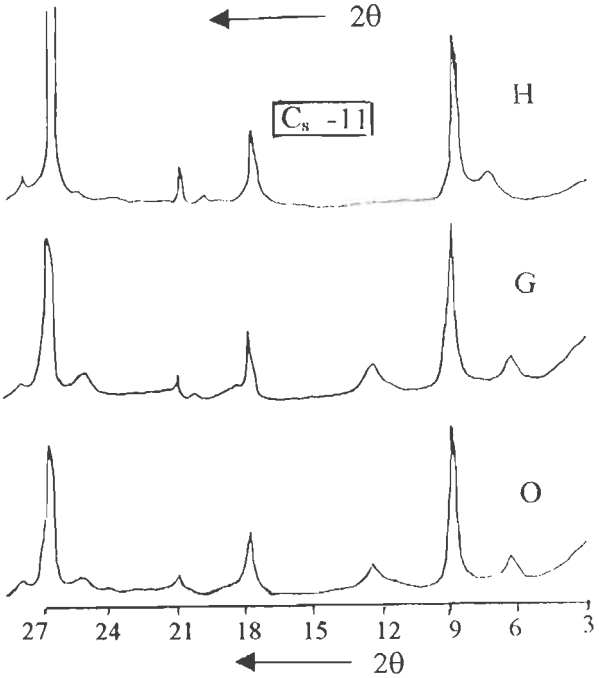
Cs -11
H
G
O
27 24 21 18 15 12 9 6 3
2θ

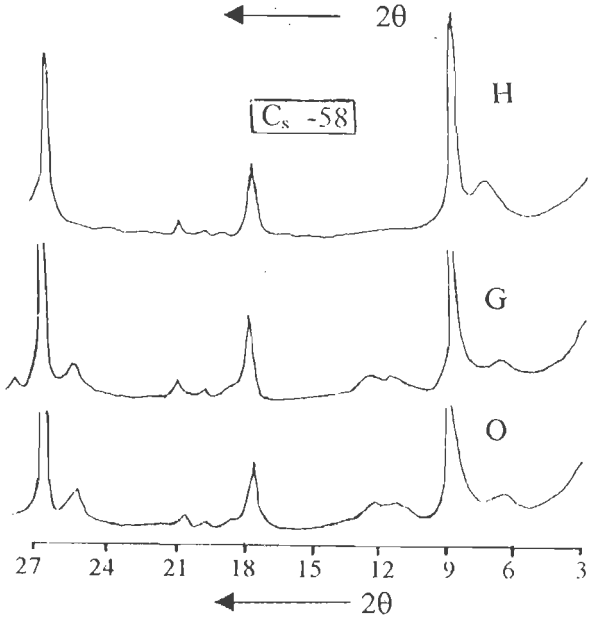
Cs -58
H
G
O
27 24 21 18 15 12 9 6 3
2θ

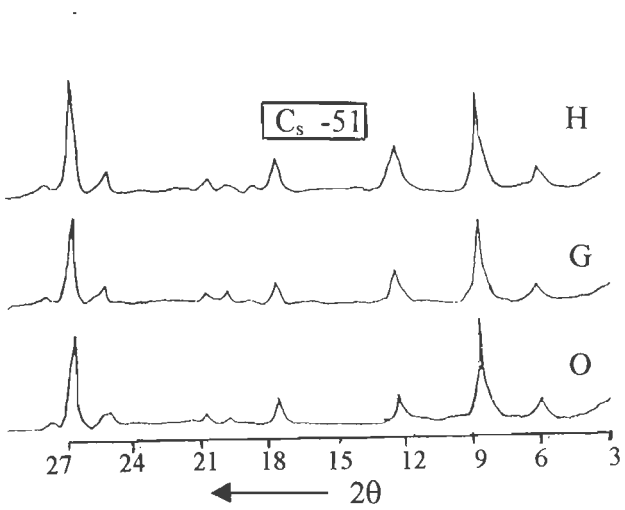
Cs -51
H
G
O
27 24 21 18 15 12 9 6 3
2θ

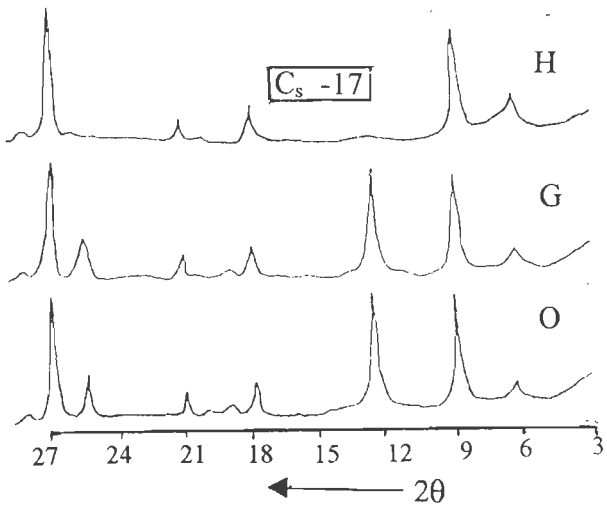
Cs -17
H
G
O
27 24 21 18 15 12 9 6 3
2θ

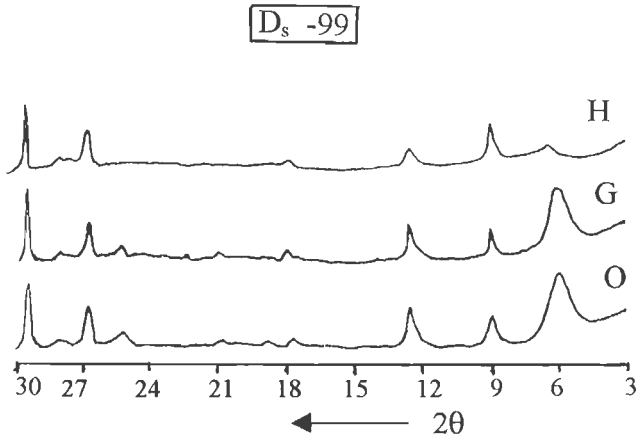
Ds -99
H
G
O
30 27 24 21 18 15 12 9 6 3
2θ

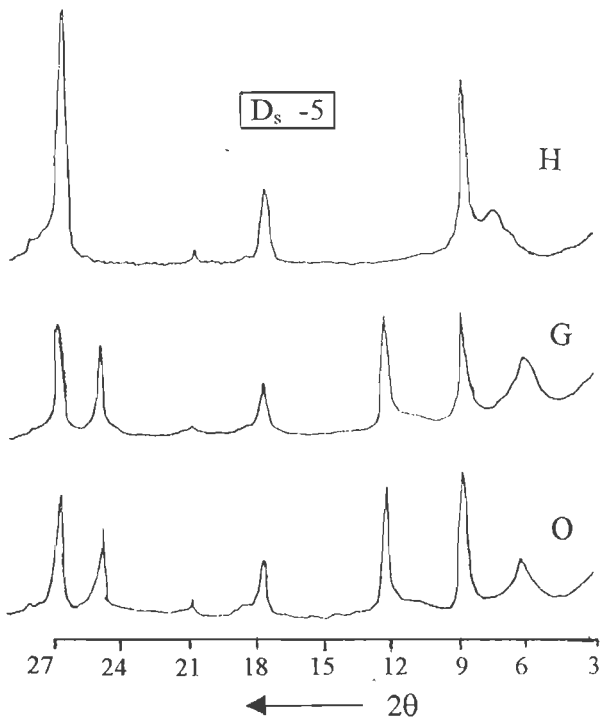
Ds -5
H
G
O
27 24 21 18 15 12 9 6 3
2θ

Appendix-II: TOC determination chart

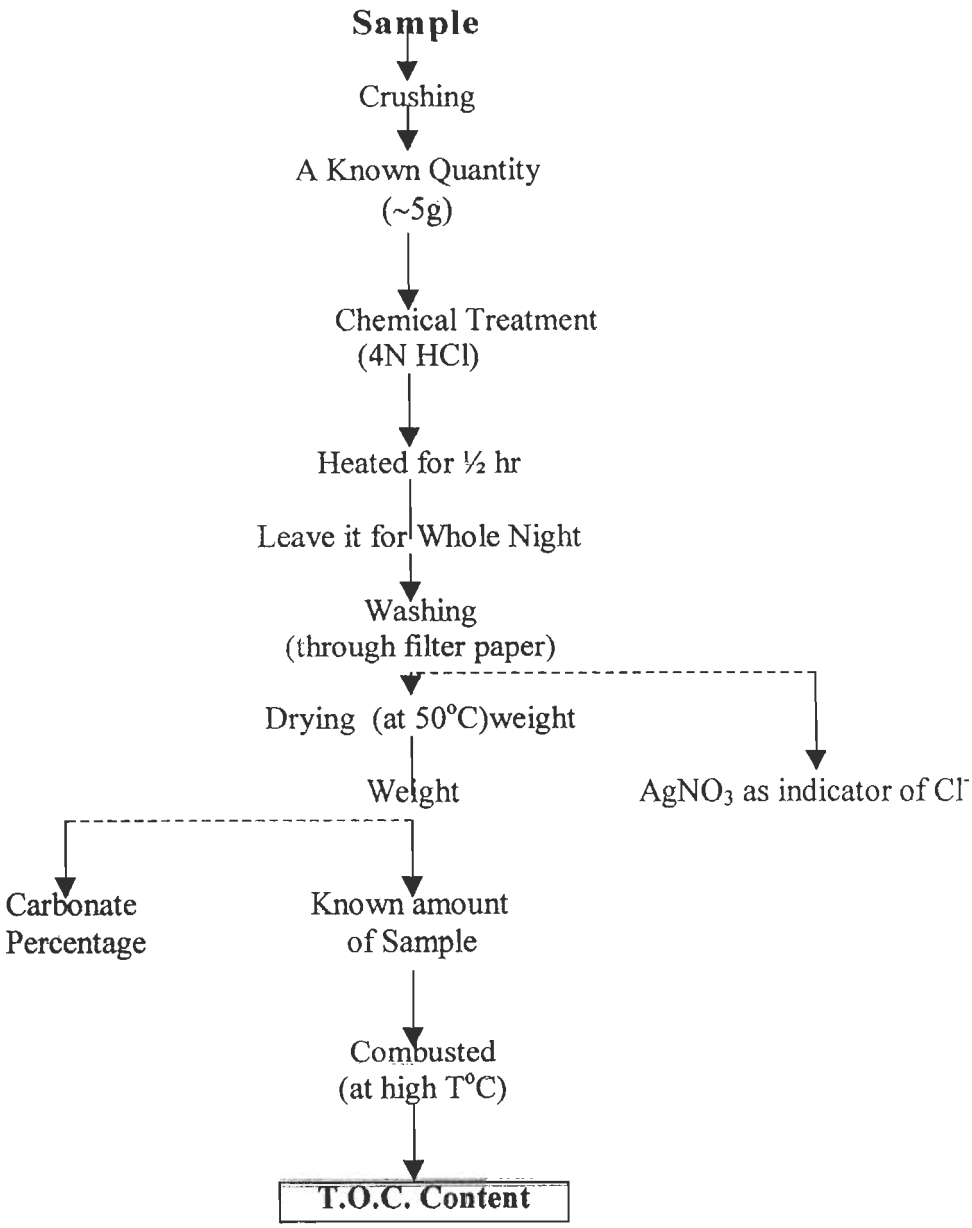

Appendix-III:

The procedure of preparation sample for Vitrinite Reflectance (VR_o) analysis (Stach et al., 1982)